

Journal of Polymer Science

PART A-1: POLYMER CHEMISTRY

Volume 4, 1966

Board of Editors: H. MARK • C. G. OVERBERGER • T. G. FOX

Advisory Editors: R. M. FUOSS • J. J. HERMANS • H. W. MELVILLE • G. SMETS

Editor: C. G. OVERBERGER Assistant Editor: E. M. PEARCE

Advisory Board:

T. ALFREY, JR.
Midland, Mich.

W. O. BAKER
Murray Hill, N. J.

D. BALLANTINE
Upton L. I.

H. BENOIT
Strasbourg

J. C. BEVINGTON
Lancaster

G. BIER
Köln

F. BOVEY
Murray Hill, N. J.

J. W. BREITENBACH
Vienna

A. M. BUECHE
Schenectady, N. Y.

G. B. BUTLER
Gainesville, Fla.

T. W. CAMPBELL
Waynesboro, Va.

E. F. CASASSA
Pittsburgh, Pa.

F. DANUSSO
Milano

F. R. EIRICH
Brooklyn, N. Y.

E. M. FETTES
Monroeville, Pa.

P. J. FLORY
Stanford, Calif.

H. N. FRIEDLANDER
Durham, N. C.

J. FURUKAWA
Kyoto

G. GEE
Manchester

H. D. KEITH
Murray Hill, N. J.

A. KELLER
Bristol

W. KERN
Mainz

O. KRATKY
Graz

H. MARKOVITZ
Pittsburgh, Pa.

C. S. MARVEL
Tucson, Arizona

G. NATTA
Milano

S. OKAMURA
Kyoto

A. PETERLIN
Durham, N. C.

P. PINO
Pisa

C. C. PRICE
Philadelphia, Pa.

B. G. RÄNBY
Stockholm

C. SADRON
Strasbourg

J. K. STILLE
Iowa City, Iowa

W. H. STOCKMAYER
Hanover, N. H.

M. SZWARC
Syracuse, N. Y.

A. V. TOBOLSKY
Princeton, N. J.

L. A. WALL
Washington, D. C.

F. H. WINSLOW
Murray Hill, N. J.

K. WOLF
Ludwigshafen

INTERSCIENCE PUBLISHERS

Copyright © 1966, by John Wiley & Sons, Inc.

Statement of ownership, management, and circulation (Act of October 23, 1962: Section 4369, Title 39 United States Code)

1. Date of filing: September 30, 1966
 2. Title of Publication: JOURNAL OF POLYMER SCIENCE
 3. Frequency of issue: monthly
 4. Location of known office of publication: 20th and Northampton Streets, Easton, Pennsylvania 18042
 5. Location of headquarters of general business offices of publisher: 605 Third Avenue, New York, New York 10016
 6. The names and addresses of publisher, editor, and managing editor:
Publisher: Eric S. Proskauer, John Wiley & Sons, Inc., 605 Third Avenue, New York, New York 10016
Editor: Herman Mark, Charles G. Overberger, Polytechnic Institute of Brooklyn, 333 Jay Street, Brooklyn, New York 11201 and T. G. Fox, Mellon Institute, Pittsburgh, Pennsylvania 15213
Managing Editor: None
 7. Owner: John Wiley & Sons, Inc., 605 Third Avenue, New York, New York 10016
Stockholders owning or holding 1 per cent or more of total amount of stock as of September 30, 1966: Cynthia W. Darby, 23 Farrington Street, Newburgh, N. Y.; Maurits Dekker, 511 West 232nd Street, Bronx, N. Y.; Rozetra S. Dekker, 511 West 232nd Street, Bronx, N. Y.; Ulia W. Gilbert, Box 1191, Carmel, California; Edward P. Hamilton, % John Wiley & Sons, Inc., 605 Third Avenue, New York 16, N. Y.; W. Bradford Wiley and Francis Lobdell, Trustees of Elizabeth W. Hamilton Trust, dated 12/23/52, % John Wiley & Sons, Inc., 605 Third Avenue, New York 16, N. Y.; I. M. Kolthoff, University of Minnesota, School of Chemistry, Minneapolis, Minnesota; Willy Levinger, 336 Central Park West, New York, N. Y.; R. R. Pennywitt, Box 211, Mantaloking, N. J.; C. R. Runyon, Jr., 130 East End Avenue, New York 28, N. Y.; Francis Lobdell and William J. Seawright, Trustees f/b/o Deborah Elizabeth Wiley, u/a dated 6/2/58, % John Wiley & Sons, Inc., 605 Third Avenue, New York 16, N. Y.; Francis Lobdell and William J. Seawright, Trustees f/b/o Peter Booth Wiley, u/a dated 6/2/58, % John Wiley & Sons, Inc., 605 Third Avenue, New York 16, N. Y.; Francis Lobdell and William J. Seawright, Trustees f/b/o William Bradford Wiley, 2nd, u/a dated 6/2/58, % John Wiley & Sons, Inc., 605 Third Avenue, New York 16, N. Y.; Adele E. Windheim, 8 Dundee Road, Larchmont, N. Y.; W. Bradford Wiley and E. P. Hamilton, Trustees for Edward P. Hamilton Foundation, u/a dated 12/23/57, % John Wiley & Sons, Inc., 605 Third Avenue, New York 16, N. Y.; Reing & Co., P. O. Box 491, Church Street Station, New York 8, N. Y.; Eric S. Proskauer and Charles H. Lieb, as Trustees u/a dated 11/27/62, 220 Central Park South, New York 19, N. Y.; Edward P. Hamilton, as Executor of the Will of Elizabeth Wiley Hamilton, dec'd.; Cynthia Darby and Julia Wiley Gilbert as Executors of the Will of Kate R. Q. Wiley; Edward Hamilton and Cynthia Wiley Darby as Trustees under Will of William Q. Wiley; American Growth Fund Limited, 7 King Street, E., Toronto, Ontario, Canada.
 8. Known bondholders, mortgagees, and other security holders owning or holding 1 per cent or more of total amount of bonds, mortgages, or other securities: None
 9. Paragraphs 7 and 8 include, in cases where the stockholder or security holder appears upon the books of the company as trustee or in any other fiduciary relation, the name of the person or corporation for whom such trustee is acting, also the statements in the two paragraphs show the affiant's full knowledge and belief as to the circumstances and conditions under which stockholders and security holders who do not appear upon the books of the company as trustees, hold stock and securities in a capacity other than that of a bona fide owner. Names and addresses of individuals who are stockholders of a corporation which itself is a stockholder or holder of bonds, mortgages or other securities of the publishing corporation have been included in paragraphs 7 and 8 when the interests of such individuals are equivalent to 1 per cent or more of the total amount of the stock or securities of the publishing corporation.
 10. This item must be complete for all publications except those which do not carry advertising other than the publishers own and which are named in Sections 132.231, 132.232, and 132.233, Postal Manual (Sections 4355a, 4355b, and 4356 of Title 39, United States Code)
- I certify that the statements made by me above are correct and complete:

Eric S. Proskauer
Publisher

CONTENTS

Vol. 4, Issue Nos. 1-12

Journal of Polymer Science
Part A-1: Polymer Chemistry

ISSUE NO. 1, JANUARY

Editorial	1
Information for Contributors	3
PETER KOVACIC and LI-CHEN HSU: Polymerization of Aromatic Nuclei. VIII. Molecular Weight Control in Benzene Polymerization	5
P. COLOMBO, L. E. KUKACKA, J. FONTANA, R. N. CHAPMAN, and M. STEINBERG: Co^{60} γ -Radiation-Induced Copolymerization of Ethylene and Carbon Monoxide	29
J. G. COLSON, R. H. MICHEL, and R. M. PAUFLER: Polybenzoylenebenzimidazoles	59
R. A. WALLACE and K. L. HADLEY: Kinetics of Styrene Homogeneous Polymerization to Atactic Polypropylene	71
KYOICHI SHIBAYAMA and MINEKAZU KODAMA: Effects of Concentration of Urethane Linkage, Crosslinking Density, and Swelling upon the Viscoelastic Properties of Polyurethanes	83
YOSHIO TANAKA and HIROSHI KAKIUCHI: Epoxy Compounds. VIII. Stereoregular and Stereorandom Polymerization of Phenyl Glycidyl Ether with Tertiary Amines, and Infrared Spectra of Poly(phenyl Glycidyl Ether)	109
JAMES E. FEARN, DANIEL W. BROWN, and LEO A. WALL: Polymers and Telomers of Perfluoro-1,4-pentadiene	131
SHIGEO TAZUKE and SEIZO OKAMURA: Effect of Metal Salts on Polymerization. Part I. Polymerization of Vinylpyridine Initiated with Cupric Acetate	141
YOSHIO IWAKURA, MUNENORI SAKAMOTO, and MICHIO YONEYAMA: Polyaddition Reactions of Bisethyleneureas and 1,1,3,3-Diethyleneurea with Polymethylene Dimercaptans in LiCl -Dimethylformamide	159
J. G. HENDRICKSON and J. C. MOORE: Gel Permeation Chromatography. III. Molecular Shape versus Elution	167

ROGER S. PORTER: Characterization of Ethylene-Propylene Block Copolymers by Proton Magnetic Resonance.....	189
TOSHIKAKI TAKAMATSU and KENICHI SHINOHARA: Radiation-Induced Graft Polymerization of Styrene to Poly(vinyl Chloride).....	197
R. D. BUSHICK and R. S. STEARNS: Relationship between the Ionic Nature of Some Organoaluminum-Transition Metal Catalysts and the Rate of Polymerization.....	215
PRONAY K. CHATTERJEE and CARL M. CONRAD: Investigation by Infrared Absorption of the By-Products of the Cyanoethylation of Cotton Cellulose.....	233

Notes

S. KOBAYASHI, Y. KATO, H. WATANABE, and A. NISHIOKA: NMR Spectra of Propylene-Styrene Copolymers.....	245
MARIO RUSSO, LUIGI MORTILLARO, LINO CREDALI, and CARLO DE CHECCHI: New Crystalline Modification of Polyselenomethylene by Polymerization of 1,3,5,7-Tetraselenocane.....	248
D. T. TURNER, GEORGE F. PEZDIRTZ, and GEORGE D. SANDS: Influence of Dose Rate on Radiation-Induced Network Formation in Polyethylene Terephthalate.....	252
ZIGMOND W. WILCHINSKY: Relationship Between Orientation Parameters in Biaxially Oriented Polymers.....	255

ISSUE NO. 2, FEBRUARY

YUZURU FUJIWARA, SHIZUO FUJIWARA, and KIYOSHI FUJII: NMR Study of Model Compounds of Vinyl Polymers.....	257
F. S. ARIMOTO: Polymerization with Organoboron Compounds.....	275
SUEO MACHI, TAKASHI TAMURA, MIYUKI HAGIWARA, MASAO GOTODA, and TSUTOMU KAGIYA: Short-Chain Branching in γ -Radiation-Induced Polymerization of Ethylene.....	283
TSUTOMU KAGIYA, SHIZUO NARISAWA, TAIZO ICHIDA, KENICHI FUKUI, HISAO YOKOTA, and MASATSUNE KONDO: Alternative Copolymerization of Aziridines and Carbon Monoxide by γ -Ray Irradiation.....	293
HISAYA TANI and TUYOSHI KONOMI: Polymerization of Five-, Six-, and Seven-Membered Ring Lactams by Using Metallic Potassium or Metallic Aluminum Alkylate as Catalyst and Certain <i>N</i> -Acyl Lactams or Diphenyl Ketene as Initiator.....	301
J. W. BEGLEY: The Role of Diffusion in Propylene Polymerization	319
JUERG-HEINRICH KALLWEIT: Relationship between Viscosity and Direct Current Conductivity in PVC.....	337
L. A. WALL, S. STRAUS, and R. E. FLORIN: Pyrolysis of Vinyl and Vinylidene Fluoride Polymers: Influence of Prior γ -Irradiation	349

Z. ZLÁMAL, A. KAZDA, and L. AMBROŽ: Donor-Acceptor Interaction in Cationic Polymerization. VI. Influence on the Molecular Weight of Polyisobutylene of Some Anions Derived from the Complexes of Aluminum Trichloride with Some Electron Donors	367
K. JIJIE, M. SANTAPPA, and V. MAHADEVAN: Vinyl Polymerization by Cobaltic Ions in Aqueous Solution. Part I. Polymerization of Methyl Methacrylate.....	377
K. JIJIE, M. SANTAPPA, and V. MAHADEVAN: Vinyl Polymerization by Cobaltic Ions in Aqueous Solution. Part II. Polymerization of Acrylonitrile and Methyl Acrylate.....	393
P. HOWARD and R. S. PARIKH: Solution Properties of Cellulose Triacetate. I. Fractional Precipitation.....	407
R. C. POTTER, C. L. JOHNSON, D. J. METZ, and R. H. BRETTON: γ -Radiation-Induced Ionic Polymerization of Pure Liquid Styrene	419

Notes

C. GEACINTOV, R. B. MILES, and H. J. L. SCHUURMANS: On the Form III Transformation of Polybutene-1.....	431
PRINOY K. CHATTERJEE and DAVID J. STANONIS: Furoylation of Cellulose.....	434
H. G. GILCH: Preparation and Properties of Poly($\alpha,\alpha',\alpha',\alpha'$ -Tetrachloro- <i>p</i> -xylylene) Films.....	438
D. F. LONCRINI, W. L. WALTON, and R. B. HUGHES: Aromatic Polyesteramideimides.....	440
WILLIAM A. KRINER: Catalytic Polymerization of 1,3-Disilacyclobutane Derivatives.....	444
WILLIAM H. STUBBS, CHRISTOPHER ROBERT GORE, and C. S. MARVEL: α,ω -Glycols from Polyisobutylene.....	447

ISSUE NO. 3, MARCH

F. LEONARD, G. A. HANKS, and R. K. KULKARNI: Polymerization in Liquid Ammonia: Acrylate Esters and Vinyl Thiolaacetate..	449
PRINOY K. CHATTERJEE and CARL M. CONRAD: Kinetics of Heterogeneous Cellulose Reactions. I. Cyanoethylation of Cotton Cellulose.....	459
RODNEY E. HARRINGTON and P. GARTH PECORARO: Precise Molecular Weight Distributions of High Polymers by Semiautomatic Solvent Extraction.....	475
RODNEY E. HARRINGTON: Degradation of Polymers in High Speed Rotatory Homogenizers: A Hydrodynamic Interpretation.....	489
A. F. SHEPARD and B. F. DANIELS: Interfacial Anodic Polymers from Benzene in Hydrogen Fluoride.....	511
JOHN G. ERICKSON: Polymers from the Iterated Addition of Hydrogen Sulfide to Diolefins.....	519

J. PRESTON: New High Temperature Polymers. I. Wholly Aromatic Ordered Copolyamides.....	529
E. A. S. CAVELL and I. T. GILSON: Increased Rates of Initiation of Polymerization by 4-4'-Dicyano-4-4'-azopentanoic Acid in the Presence of Ferric Salts.....	541
J. K. STILLE and F. E. ARNOLD: Polyquinoxalines. III.....	551
JITSUO TSURUGI, TSUGIO FUKUMOTO, MASAYUKI YAMAGAMI, and HIROSHI ITATANI: Radiation-Induced <i>cis-trans</i> Isomerization of Polyisoprenes and Temperature Dependence of Equilibria..	563
SELWYN H. ROSE and B. P. BLOCK: Inorganic Coordination Polymers. VII. Zinc(II) Dimethyl-, Methylphenyl-, and Diphenylphosphinates.....	573
SELWYN H. ROSE and B. P. BLOCK: Inorganic Coordination Polymers. VIII. Cobalt(II) and Zinc(II) Phosphinate Polymers and Copolymers.....	583
J. D. WELLS and V. STANNETT: Permeation, Sorption, and Diffusion of Water in Ethyl Cellulose.....	593
GLENN D. COOPER and JOHN R. ELLIOTT: Promotion of Base-Catalyzed Siloxane Rearrangements by Dimethyl Sulfoxide.....	603
S. D. BUROW, D. T. TURNER, GEORGE F. PEZDIRTZ, and GEORGE D. SANDS: γ -Irradiation of Poly(ethylene Terephthalate). I. Yields of Gas and Carboxyl Groups.....	613
ROBERT K. TUBBS: Sequence Distribution of Partially Hydrolyzed Poly(vinyl Acetate).....	623
KOICHI ITO and YUYA YAMASHITA: Triad Distribution of 1,1-Diphenylethylene-Methyl Acrylate Copolymer Determined from NMR Study.....	631
F. S. MODEL, G. REDL, and E. G. ROCHOW: Internal Motion in Organosilicon Polymers. I. Linear Dimethylpolysilazane...	639
H. N. FRIEDLANDER, H. E. HARRIS, and J. G. PRITCHARD: Structure-Property Relationships of Poly(vinyl Alcohol). I. Influence of Polymerization Solvents and Temperature on the Structure and Properties of Poly(vinyl Alcohol) Derived from Poly(vinyl Acetate).....	649
H. E. HARRIS, J. F. KENNEY, G. W. WILLCOCKSON, R. CHIANG, and H. N. FRIEDLANDER: Structure-Property Relationships of Poly(vinyl Alcohol). II. The Influence of Molecular Regularity on the Crystallization-Dissolution Temperature Relationships of Poly(vinyl Alcohol).....	665
J. F. KENNEY and G. W. WILLCOCKSON: Structure-Property Relationships of Poly(vinyl Alcohol). III. Relationships between Stereoregularity, Crystallinity, and Water Resistance in Poly(vinyl Alcohol).....	679
J. F. KENNEY and V. F. HOLLAND: Crystallization and Dissolution Temperatures of Poly(vinyl Alcohol) Crystal Lamellae.....	699
J. G. PRITCHARD, R. L. VOLLMER, W. C. LAWRENCE, and W. B. BLACK: Fluorine NMR Spectra of Poly(vinyl Trifluoroacetate)	707

Notes

JEAN-CLAUDE MILEO and LOUIS NICOLAS: Greffage de Méthacrylate de Méthyl sur la Cellulose au Moyen de Peracides, en Presence d'Ions Cu^{2+} et Fe^{3+} Comme Catalyseurs.	713
L. UTRACKI: On the Computation of Viscosity Measurements Data of Dilute Solutions of High Polymers.	717
S. M. COHEN and R. H. YOUNG: A Sulfone Polymer from Diphenyl Ether.	722
Y. ARIMATSU: Cyclic Trimer of 3,3-Bis(chloromethyl)oxacyclobutane.	728
TSUNEO MATSUDA, YOSHIO ONO, and TOMINAGA KEI: On the Activation of the Phillips Catalyst.	730
TAKAYUKI OTSU, TOSHIO ITO, and MINORU IMOTO: Further Correlations between the Reactivity and the Structure of Alkyl Acrylates and Methacrylates.	733

ISSUE No. 4, APRIL

A. EISENBERG and D. A. MCQUARRIE: Tailored Heterogeneity Indices in Anionic Polymerization.	737
YOSHIO IWAKURA, SHIN-ICHI IZAWA, and FUSAKAZU HAYANO: Polyoxazolidones Prepared from Bisurethans and Bisepoxides.	751
PAUL SIGAL, PHILIP MASCANTONIO, and PAUL FUGASSI: Catalytic Polymerizations of Nitrobenzene and Aniline.	761
ROBERT JENKINS: γ -Irradiation of Siloxane Polymers in Air and Vacuum at Several Temperatures.	771
H. M. ANDERSEN: Isothermal Kinetic Calorimeter Applied to Emulsion Polymerization.	783
STANLEY P. ROWLAND and EDWIN R. COUSINS: Periodate Oxidative Decrystallization of Cotton Cellulose.	793
M. E. MILBERG: Enhanced X-Ray Diffraction Patterns from Oriented Fibers.	801
S. P. MOULIK and D. K. MULLICK: Catalysis in the Polymerization of Silicic Acid.	811
SUEO MACHI, TAKASHI SAKAI, MASAO GOTODA, and TSUTOMU KAGIYA: Alternating Copolymerization of Ethylene with Maleic Anhydride.	821
K. C. STUEBEN: Cyclobutane Polymers from Acrylonitrile Dimer.	829
KENNETH A. KUN: Macroreticular Redox Polymers. II. Further Synthesis and Properties of Some Redox Polymers.	847
KENNETH A. KUN and ROBERT KUNIN: Macroreticular Redox Polymers. III. Characterization of Some Hydroquinone-Quinone Redox Polymers.	859
A. MIZOTE, T. TANAKA, T. HIGASHIMURA, and S. OKAMURA: Cationic Polymerization of Cyclic Olefins.	869
GEORGE A. MORTIMER: Chain Transfer in Ethylene Polymerization	881

BHAIIRAB CHANDRA MITRA, SUBHASH CHANDER CHADHA, PREMAMOY GHOSH, and SANTI R. PALIT: Studies on Some Radical Transfer Reactions. Part I. Hydrogen Atom Abstraction from Some Organic Substrates by OH Radicals.....	901
HIROSHI SUMITOMO and KAZUKIYO KOBAYASHI: Polymerization of β -Cyanopropionaldehyde.....	907
T. B. GIBB, JR., R. A. CLENDINNING, and W. D. NIEGISCH: Polymers from Aryl Glycidyl Ethers.....	917
Y. OHSUMI, T. HIGASHIMURA, and S. OKAMURA: Stereospecific Polymerization of α -Methylstyrene by Friedel-Crafts Catalysts....	923
THOMAS GILLESPIE and BILL M. WILLIAMS: Diffusion of Water Vapor Through a Hydrophilic Polymer Film.....	933
J. B. LANDO, H. G. OLF, and A. PETERLIN: Nuclear Magnetic Resonance and X-Ray Determination of the Structure of Poly(vinylidene Fluoride).....	941
MAURZYCY KALFUS and JAN MITUS: Application of the Flory-Mandelkern Equation to Individual Unfractionated Polymer Samples.	953

Notes

M. HIRAMI: X-Ray Scattering from Mixtures of Nylon 6 and <i>m</i> -Cresol.....	967
ZBIGNIEW WOJTCZAK: Interaction Between Alkaline Earth Metal Cations and Polymethacrylic Acid in Dilute Solutions. II. Potentiometric Titration.....	969
YOSHINOBU TAKEGAMI, TORU UENO, and RYUICHI HIRAI: The Polymerization of Tetrahydrofuran with Niobium Pentachloride and Tantalum Pentachloride.....	973
JOHN B. GARDNER and BILLY G. HARPER: Iodine Complex of Grafted Latex.....	975

ISSUE NO. 5, MAY

W. M. PEFFLEY, V. R. HONNOLD, and D. BINDER: X-Ray and NMR Measurements on Irradiated Polytetrafluoroethylene and Polychlorotrifluoroethylene.....	977
CAROLYN E. M. MORRIS, A. E. ALEXANDER, and A. G. PARTS: Polymerization of Methyl Acrylate in Aqueous Media.....	985
L. M. MINSK and K. R. DUNHAM: Stability of Styrene-Maleamic Acid Interpolymers.....	997
M. TASUMI, T. SHIMANOUCI, H. KENJO, and S. IKEDA: Molecular Vibrations of Irregular Chains. I. Analysis of Infrared Spectra and Structures of Polymethylene Chains Consisting of CH ₂ , CHD, and CD ₂ Groups.....	1011
M. TASUMI, T. SHIMANOUCI, and S. IKEDA: Molecular Vibrations of Irregular Chains. II. Configurations of Polydeuterioethylene.....	1023

ZOILA REYES, C. E. RIST, and C. R. RUSSELL: Grafting Vinyl Monomers to Starch by Ceric Ion. I. Acrylonitrile and Acrylamide.....	1031
GEORGE L. BRODE and JOHN WYNSTRA: Analysis of the Base-Catalyzed Phenol-Epichlorohydrin Condensation.....	1045
LEON B. LEVY and GENE J. FISHER: Efficiencies of Some Ethyl Acrylate Chain Terminators.....	1057
K. SHIINA and Y. MINOURA: Reaction of <i>n</i> -Butyllithium with Poly(vinyl Chloride).....	1069
N. NAGY KOVACS, A. D. DELMAN, and B. B. SIMMS: Silicon-Containing Schiff Base and Benzimidazole Derivatives.....	1081
W. CONTI and I. GIGLI: Non-Newtonian Behavior of Polymers with Log-Normal Molecular Weight Distribution.....	1093
MITSUZO SHIDA and HARRY P. GREGOR: Oleophilic Ion-Exchange Resins. IV. Swelling of Quaternary Ammonium Polymers in Mixed Solvents.....	1113
KUNIHARU KOJIMA, N. YODA, and C. S. MARVEL: Base-Catalyzed Polymerization of Maleimide and Some Derivatives and Related Unsaturated Carbonamides.....	1121
ROBERT ROSEN and HERBERT A. POHL: Some Polymers of High Dielectric Constant.....	1135
BEN-AMI FEIT, ERI HELLER, and ALBERT ZILKHA: Anionic Heterogeneous Polymerization of Methacrylonitrile by <i>n</i> -Butyllithium.....	1151
JOGINDER LAL: Polymerization of Olefin Oxides and of Olefin Sulfides.....	1163
R. A. WALLACE and D. G. YOUNG: Graft Polymerization Kinetics of Acrylamide Initiated by Ceric Nitrate-Dextran Redox Systems.....	1179
WASABURO KAWAI: Polymerizations of Some Diene Monomers. Preparations and Polymerizations of Vinyl Methacrylate, Allyl Methacrylate, <i>N</i> -Allylacrylamide, and <i>N</i> -Allylmethacrylamide.....	1191
ROBERT E. CUNNINGHAM: Vanadium- or Vanadylacetylacetonate as a Cocatalyst for the Terpolymerization of Ethylene, Propylene, and Dicyclopentadiene.....	1203
J. P. ALLISON: Photodegradation of Poly(methyl Methacrylate).....	1209
J. E. GLASS and N. L. ZUTTY: Investigation of Autoacceleration Effects during the Solution Polymerization of Styrene.....	1223
S. BURCKHARDT, K.-H. REICHERT, and K. HAMANN: Untersuchung der Bildung von Polyesteramiden aus Dicarbonsäure-anhydriden und Oxazolidinonen-2.....	1245
STANLEY R. SANDLER and FLORENCE R. BERG: Room Temperature Polymerization of Glycidol.....	1253
ROY L. WHISTLER and PAUL A. SEIB: Polymerization of 1,2:5,6-Di- <i>O</i> -Isopropylidene- α -D-Glucofuranose and 1,2- <i>O</i> -Isopropylidene- α -D-Glucofuranose.....	1261

A. D. DELMAN, J. KELLY, J. MIRONOV, and B. B. SIMMS: Studies on Poly(aquahydroxychromium Diphenylphosphinate).....	1277
AKIRA SHIMIZU and KOICHIRO HAYASHI: Radiation-Induced Solid-State Copolymerization of Maleic Anhydride and Acenaphthylene.....	1291
KAZUO SAOTOME and KENICHIRO SATO: Polyamides from α,ω -Oxalkanedioic Acid Having Long Methylene Chain Units.....	1303

Notes

JAN F. RABEK: Thiobenzophenone—A New Sensibilizer for the Photodegradation of Diene Polymers in Solutions by Visible and Ultraviolet Light.....	1311
H. YASUDA and WILLIAM STONE, JR.: Permeability of Polymer Membranes to Dissolved Oxygen.....	1314
HOWARD C. HAAS: Phthalaldehydic Acid-Glycol Reactions.....	1317
DANIEL E. GEORGE, ROBERT E. PUTNAM, and STANLEY SELMAN: The Synthesis of Polymeric Ylids.....	1323
TADAO KATAOKA and SHIGEYUKI VEDA: A Note on the Capillary Flow of Polydimethylsiloxane.....	1326
J. W. BREITENBACH and H. DWORAK: Crosslinking in Popcorn Polymers.....	1328

ISSUE No. 6, JUNE

IVO KÖSSLER and HELENA KRAUSEROVÁ: Continuous Fractionation of Polymers in Solution by Thermal Diffusion.....	1329
H. G. GILCH and W. L. WHEELWRIGHT: Polymerization of α -Halogenated <i>p</i> -Xylenes With Base.....	1337
H. G. GILCH: Preparation of Poly- <i>p</i> -Xylylenes by Electrolysis.....	1351
NAOYA OGATA, TOMOHIKO ASAHARA, and SYUNROKU TOHYAMA: Polymerization of Lactam Ethers.....	1359
S. ENOMOTO, M. ASAHINA, and S. SATOH: Spectroscopic Studies Poly(vinyl Chloride) and Its Deuterated Derivatives.....	1373
J. A. GERVAZI and A. B. GOSNELL: Synthesis and Characterization of Branched Polystyrene. Part I. Synthesis of Four- and Six-Branched Star Polystyrene.....	1391
A. B. GOSNELL, J. A. GERVAZI, and A. SCHINDLER: Synthesis and Characterization of Branched Polystyrene. Part II. Fractionation.....	1401
YASUAKI ABE, MITSUO TASUMI, TAKEHIKO SHIMANOUCI, SHIROH SATOH, and RICHIRO CHŪJŌ: NMR Spectra of Model Compounds of Poly(vinyl Chloride).....	1413
H. L. BROWNING, JR., HAZEL D. ACKERMANN, and H. W. PATTON: Electron Paramagnetic Resonance of Ultraviolet-Irradiated Polyolefins.....	1433

PETER KOVACIC and ROGER J. HOPPER: Polymerization of Aromatic Nuclei. X. Polymerization of Benzene to <i>p</i> -Polyphenyl Oligomers by Nitrogen Dioxide-Aluminum Chloride.....	1445
KAZUO SAOTOME and HIROSHI KOMOTO: Polyamides Having Long Methylene Chain Units.....	1463
KAZUO SAOTOME and HIROSHI KOMOTO: Isomorphism in Copolyamides of Long Repeating Chain Units Containing Oxa- and Thia-Alkylene Linkages.....	1475
K. JESCH, J. E. BLOOR, and P. L. KRONICK: Structure and Physical Properties of Glow Discharge Polymers. I. Polymers from Hydrocarbons.....	1487
BEN-AMI FEIT, ERI HELLER, and ALBERT ZILKHA: Anionic Oligomerization of Methacrylonitrile.....	1499
M. BERGER and T. A. MANUEL: Chemistry of Polybutadiene-Iron Carbonyl Systems.....	1509
SUEO MACHI, MIYUKI HAGIWARA, MASAO GOTODA, and TSUTOMU KAGIYA: Initiation and Propagation in γ -Radiation-Induced Polymerization in Ethylene.....	1517
D. F. LONCRINI: Aromatic Polyesterimides.....	1531
C. R. BOSS and J. C. W. CHIEN: Oxygen Diffusion Limitation in Autoxidation of Polypropylene.....	1543
GÁBOR KOVÁCS, ESZTER KOVÁCS, and HERBERT MORAWETZ: Polymerization in the Crystalline State. VIII. Polymerization in <i>N</i> -Carboxy Anhydrides of γ -Benzyl Glutamate, γ -Methyl Glutamate, and ϵ -Carbobenzoxylysine.....	1553
R. D. LUNDBERG, F. E. BAILEY, and R. W. CALLARD: Interactions of Inorganic Salts with Poly(ethylene Oxide).....	1563
TAKAYUKI OTSU, AKIHIKO SHIMIZU, and MINORU IMOTO: Polymerization of Butene-2 with Isomerization to Butene-1.....	1579
GUNTHER E. MOLAU and HENNO KESKKULA: Heterogeneous Polymer Systems. IV. Mechanism of Rubber Particle Formation in Rubber-Modified Vinyl Polymers.....	1595
R. J. KERN and J. D. CALFEE: Stereoregular Polymerization of Methyl Vinyl Ether with Fluoro Aluminum Initiators.....	1609
STELVIO PAPETTI, B. B. SCHAEFFER, A. P. GRAY, and T. L. HEYING: A New Series of Organoboranes. VII. The Preparation of Poly- <i>m</i> -carboranylenesiloxanes.....	1623

Notes

JOGINDER LAL and WILLIAM M. SALTMAN: Reaction of Dichlorocarbene with <i>cis</i> -1,4-Polyisoprene.....	1637
M. M. ZWICK: The Blue Complexes of Iodine with Poly(vinyl Alcohol) and Amylose.....	1642
G. F. L. EHLERS and J. D. RAY: Preparation and Properties of a New Poly- <i>s</i> -Triazinylene Imide.....	1645

Errata

RALPH W. MAGIN, C. S. MARVEL, and EDWARD F. JOHNSON: Terpolymers of Ethylene and Propylene with <i>d</i> -Limonene and β -Pinene (article in <i>J. Polymer Sci. A</i> , 3 , 3815, 1965).....	1647
ROBERT S. MOORE: Ringed Spherulites and Multiple-Order Light Scattering from Ringed Spherulites (article in <i>J. Polymer Sci. A</i> , 3 , 4093, 1965).....	1647
R. H. MARCHESSAULT, H. CHANZY, S. HIDER, W. BILGOR, and J. J. HERMANS: Studies on Alcohol-Modified Transition Metal Polymerization Catalysts. I. Infrared Studies (article in <i>J. Polymer Sci. A</i> , 3 , 3713, 1965).....	1647
GEORGE B. BUTLER and RADHAKRISHNA B. KASAT: Studies in Cyclopolymerization. II. Relative Rates of Addition in the Copolymerization of Acrylonitrile with Certain 1,4-Dienes (article in <i>J. Polymer Sci. A</i> , 3 , 4205, 1965).....	1648
ISSUE NO. 7, JULY	
A. H. FRAZER and I. M. SARASOHN: Thermal Behavior of Polyhydrazides and Poly-1,3,4-oxadiazoles.....	1649
YUJI MINOURA, TAKESHI HANADA, TOSHIYUKI KASABO, and YUKIO UENO: Cationic Graft Copolymerization of Styrene onto Chlorinated Butyl Rubber.....	1665
MASAHIDE YAMAMOTO and GERALD OSTER: Zinc Oxide-Sensitized Photopolymerization.....	1683
D. R. ANDERSON and JOHN M. HOLOVKA: Thermally Resistant Polymers Containing the <i>s</i> -Triazine Ring.....	1689
P. ROSENBLUM, A. S. TOMBALAKIAN, and W. F. GRAYDON: Homogeneous Ion-Exchange Membranes of Improved Flexibility....	1703
D. W. AUBREY and A. BARNATT: Polymerization of <i>n</i> -Octadecene-1 with Catalysts Derived from Titanium Tetrachloride and Triethylaluminum.....	1709
ED VANZO: Ordered Structures of Styrene-Butadiene Block Copolymers.....	1727
KOICHI TAKAKURA, KOICHIRO HAYASHI, and SEIZO OKAMURA: Polymerization of Cyclic Ethers in the Presence of Maleic Anhydride. Part I. Polymerization of Trioxane and 3,3-Bis(chloromethyl)oxetane by γ -Rays, Ultraviolet Light, and Benzoyl Peroxide.....	1731
KOICHI TAKAKURA, KOICHIRO HAYASHI, and SEIZO OKAMURA: Polymerization of Cyclic Ethers in the Presence of Maleic Anhydride. Part II. Investigation of the Polymerization Mechanism....	1747
I. J. WAHBA and L. M. MASSEY, JR.: Degradation of Pectin by γ -Radiation under Various Moisture Conditions.....	1759
MASAO KATO and HIROYOSHI KAMOGAWA: Studies on Polymers Containing Functional Groups. II. Polymerization Behavior of <i>o</i> -Hydroxystyrene.....	1773

Z. ZLÁMAL and A. KAZDA: Donor-Acceptor Interactions in Cationic Polymerization. VII. Relationship between the Degree of Dissociation of Complex and the Molecular Weight of Polyisobutylene Formed in the Presence of Some Complexes of Aluminum Trichloride with Electron Donors.....	1783
CAROLYN P. HANEY, F. A. JOHNSON, and M. G. BALDWIN: Polymerization of Complex Systems. A Study of the System Methyl Methacrylate-Vinyl Isobutyl Ether-Maleic Anhydride by Means of an NMR Technique.....	1791
A. B. DESHPANDE, R. V. SUBRAMANIAN, and S. L. KAPUR: Polymerization of Styrene with Chromium Acetylacetonate and Triethylaluminum and Diethylaluminum Bromide.....	1799
G. J. BLAKE and A. M. CARLSON: Low-Temperature Polymerization of Isobutyl Vinyl Ether.....	1813
N. GRASSIE and E. M. GRANT: Bulk Polymerization of α -Chloroacrylonitrile.....	1821
ADRIAN A. CARACULACU: Macromolecular Models for Branched PVC. I. Copolymer of Vinyl Chloride with Isopropenyl Chloride.....	1829
ADRIAN A. CARACULACU: Macromolecular Models for Branched PVC. II. Reactivity of Chlorine Bound to a Tertiary Carbon Atom in the Copolymer Vinyl Chloride-Isopropenyl Chloride..	1839
JAMES G. SMITH, CHARLES J. KIBLER, and BOBBY J. SUBLETT: Preparation and Properties of Poly(methylene Terephthalates)....	1851
J. BOOR, JR. and E. A. YOUNGMAN: Preparation and Characterization of Syndiotactic Polypropylene.....	1861

Notes

EUGENE F. LUTZ and GEORGE M. BAILEY: Selective Polymerization of 1-Pentene in the Presence of 2-Methyl-1-Butene....	1885
A. G. DAVIES and A. WASSERMANN: Proton Magnetic Resonance Spectra of Cyclopentadiene Polymers.....	1887
E. MERASKENTIS and H. ZAHN: Synthesis of Cyclic Tris(ethylene Terephthalate).....	1890
RICHARD H. WILEY and T. K. VENKATACHALAM: Sulfonation of Polystyrene Crosslinked with Pure <i>m</i> -Divinylbenzene.....	1892
GEORGE A. MORTIMER: Chain Transfer in Ethylene Polymerization. II.....	1895
WILLIAM H. STUBBS, CHRISTOPHER R. GORE, and C. S. MARVEL: α,ω -Glycols from Butadiene.....	1898

ISSUE NO. 8, AUGUST

L. A. M. RODRIGUEZ, H. M. VAN LOOY, and J. A. GABANT: Studies on Ziegler-Natta Catalysts. Part I. Reaction between Trimethylaluminum and α -Titanium Trichloride.....	1905
--	------

L. A. M. RODRIGUEZ, H. M. VAN LOOY, and J. A. GABANT: Studies on Ziegler-Natta Catalysts. Part II. Reactions between α - or β -TiCl ₃ and AlMe ₃ , AlMe ₂ Cl, or AlEt ₃ at Various Temperatures.....	1917
H. M. VAN LOOY, L. A. M. RODRIGUEZ, and J. A. GABANT: Studies on Ziegler-Natta Catalysts. Part III. Composition of the Nonvolatile Product of the Reaction between Titanium Trichloride and Trimethylaluminum or Dimethylaluminum Chloride..	1927
L. A. M. RODRIGUEZ and H. M. VAN LOOY: Studies on Ziegler-Natta Catalysts. Part IV. Chemical Nature of the Active Site.....	1951
L. A. M. RODRIGUEZ and H. M. VAN LOOY: Studies on Ziegler-Natta Catalysts. Part V. Stereospecificity of the Active Center....	1971
J. H. GRIFFITH, C. S. MARVEL, G. W. HEDRICK, and FRANK MAGNE: Preparation and Polymerization of Some Vinyl Ester Amides of Pinic Acid.....	1993
R. LIEPINS and C. S. MARVEL: Polymers from Vinyl Esters of Perhydrogenated Rosin.....	2003
AKIO TAKAHASHI and NORMAN G. GAYLORD: AlEt ₃ -Metal Soap Catalysts for the Polymerization of Epoxides.....	2015

Notes

G. RAUSA: Ultraviolet Spectrum of a Glass Resin.....	2021
G. M. BURNETT, J. M. PEARSON, and J. D. B. SMITH: Copolymerization of Methyl Methacrylate and Diethyl Fumarate and the Homopolymerization of Diethyl Fumarate.....	2024
J. B. LEWIS and G. W. HEDRICK: Vinyl Esters of Rosin.....	2026
KOZO TSUJI, KOICHI TAKAKURA, MASANOBU NISHII, KOICHIRO HAYASHI, and SEIZO OKAMURA: ESR Study on the Solid-State Polymerization of <i>N</i> -Vinylcarbazole Initiated by Electron Acceptors.....	2028

Erratum

M. V. RAMIAH and D. A. I. GORING: The Thermal Expansion of Cellulose, Hemicellulose, and Lignin (article in <i>J. Polymer Sci. C</i> , 11 , 27, 1965).....	2031
---	------

ISSUE NO. 9, SEPTEMBER

FRED W. ROWLAND and FREDERICK R. EIRICH: Flow Rates of Polymer Solutions through Porous Disks as a Function of Solute.	
I. Method.....	2033
N. SHAVIT, A. OPLATKA, and M. LEVY: Study of the Mechanism of Formation of Transparent Polyacrylonitrile.....	2041
R. MCGUCHAN and I. C. MCNEILL: Radiochemical Determination of Low Unsaturation in Polyisobutene.....	2051

Y. P. CASTILLE and V. STANNETT: Radiation-Induced Copolymerization of Formaldehyde and Styrene	2063
TSUTOMU KAGIYA, SHIZUO NARISAWA, KUNIYOSHI MANABE, MIKIO KOBATA, and KENICHI FUKUI: Preparation of Crystalline Polyamides by the Alternating Copolymerization of Aziridines and Cyclic Imides	2081
FRANK DOBINSON and J. PRESTON: New High-Temperature Polymers. II. Ordered Aromatic Copolyamides Containing Fused and Multiple Ring Systems	2093
SEYMOUR SIEGEL, ROBERT J. CHAMPETIER, and A. R. CALLOWAY: Quantum Efficiency of the 2537 Å. Photolysis of a Mixed Phenyl-Methyl Polysiloxane	2107
YUYA YAMASHITA, TETSUO TSUDA, MASAHIKO OKADA, and SHOUJI IWATSUKI: Correlation of Cationic Copolymerization Parameters of Cyclic Ethers, Formals, and Esters	2121
MIHIR K. SAHA, MANASI SEN, and DINABANDHU PRAMANICK: Studies in Some New Initiator Systems for Vinyl Polymerization. Part I. Molecular Halogens or Halates as One Component	2137
EBERHARD W. NEUSE and KAZUKO KODA: Ferrocene-Containing Polymers. XIII. Polymeric Compounds Possessing Carboxyphenyl Side Groups	2145
ROBERT K. JENKINS: Irradiation of Some Polysiloxanes in Various Gases	2161
TSUTOMU KAGIYA, SHIZUO NARISAWA, TAIZO ICHIDA, KENICHI FUKUI, and HISAO YOKOTA: Influence of Addition of Ethylene on the γ -Ray-Induced Alternating Copolymerization of Ethylenimine and Carbon Monoxide	2171
M. P. DREYFUSS and P. DREYFUSS: <i>p</i> -Chlorophenyldiazonium Hexafluorophosphate as a Catalyst in the Polymerization of Tetrahydrofuran and Other Cyclic Ethers	2179
F. DE SCHRIJVER and G. SMETS: Polymerization Kinetics in Highly Viscous Media	2201
S. BARZAKAY, M. LEVY, and D. VOFSI: Studies on Anionic Polymerization of Lactams. Part II. Effect of Cocatalysts on the Polymerization of Pyrrolidone	2211
E. URETA, J. SMID, and M. SZWARC: Anionic Copolymerization of Styrene and 1,1-Diphenylethylene	2219
R. E. LOWRY, D. W. BROWN, and L. A. WALL: Radiation-Induced Polymerization of Hexafluoropropylene at High Temperature and Pressure	2229
ISAO KAETSU, NORIO SAGANE, KOICHIRO HAYASHI, and SEIZO OKAMURA: Radiation-Induced Solid-State Polymerization in Binary Systems. II. Relationship between Polymerization Rate and Physical Structure of Binary Systems	2241

D. A. TOMALIA and D. P. SHEETZ: Homopolymerization of 2-Alkyl- and 2-Aryl-2-Oxazolines	2253
FLOYD L. RAMP, ELMER J. DEWITT, and LOUIS E. TRAPASSO: Hydroformylation of High Polymers	2267
HIROKO SUGIYAMA and HIROYOSHI KAMOGAWA: Studies on Polymers Containing Functional Groups. III. Charge-Transfer Interaction between Quinone and Aza Polymers	2281
R. E. PUTNAM and W. H. SHARKEY: Fluorodienes. V. Copolymerization of 1,1,4,4-Tetrafluoro-1,3-butadiene with Oxygen and Nitric Oxide	2289
R. C. POTTER, R. H. BRETTON, and D. J. METZ: γ -Radiation-Induced Ionic Polymerization of Pure Liquid Styrene. II	2295
A. D. DELMAN, A. A. STEIN, B. B. SIMMS, and R. J. KATZENSTEIN: Preparation and Thermal Stability of Organometallosiloxanes and Organometallic Compounds	2307

Notes

S. L. REEGEN and K. C. FRISCH: Catalytic Effect of Urethane Groups on Reaction of Alcohols and Isocyanates	2321
S. DILLI and J. L. GARNETT: A Charge-Transfer Theory for the Interpretation of Radiation-Induced Grafting of Monomers to Cellulose	2323
K. KOJIMA, C. R. GORE, and C. S. MARVEL: Preparation of Polysiloxanes Having Terminal Carboxyl or Hydroxyl Groups	2325
RALPH W. MAGIN and HARRY G. NUNNAMAKER: Improved Method of Polymer Purification	2328
N. S. MARANS and R. J. EHRIG: Solid-State Polymerization of Diacetone Acrylamide	2330
G. E. MOLAU and J. E. MASON: Anionic Polymerizations in Dimethyl Sulfoxide	2336
S. NISHIZAKI and A. FUKAMI: Aromatic Polyamides Containing the 4,4'-Oxydiphenylene Group	2337
PAUL M. HERGENROTHER and HAROLD H. LEVINE: Polybenzothiazoles. II. A New Synthetic Approach and Preliminary Stability Evaluation	2341

Errata

R. D. BUSHICK and R. S. STEARNS: Relationship Between the Ionic Nature of Some Organoaluminum-Transition Metal Catalysts and the Rate of Polymerization (article in <i>J. Polymer Sci. A-1</i> , 4 , 215-232, 1966)	2349
J. G. COLSON, R. H. MICHEL, and R. M. PAUFLER: Polybenzoylenebenzimidazoles (article in <i>J. Polymer Sci. A-1</i> , 4 , 59-70, 1966)	2349

ISSUE No. 10, OCTOBER

H. L. DOPPERT and A. J. STAVERMAN: Kinetics of Amylose Retrogradation.....	2353
H. L. DOPPERT and A. J. STAVERMAN: Polyelectrolytic Character of Amylose. I.....	2367
H. L. DOPPERT and A. J. STAVERMAN: Polyelectrolytic Character of Amylose. II.....	2373
ALAN R. MONAHAN: Photolysis of Poly(<i>tert</i> -butyl Acrylate) in the Region of the Glass Transition Temperature.....	2381
ALAN R. MONAHAN: Thermal Degradation of Polyacrylonitrile in the Temperature Range 280–450°C.....	2391
FRED W. ROWLAND and FREDERICK R. EIRICH: Flow Rates of Polymer Solutions through Porous Disks as a Function of Solute. II. Thickness and Structure of Adsorbed Polymer Films.....	2401
Fritz MARKTSCHEFFEL, A. F. TURBAK, and Z. W. WILCHINSKY: Crystalline Polymers of Bis(β -chloroethyl) Vinylphosphonate.....	2423
KAZUO SOGA and TOMINAGA KEI: Kinetic Studies of Polymerization of Propylene with Active $\text{TiCl}_3\text{-Zn}(\text{C}_2\text{H}_5)_2$	2429
YOSHIO ONO and TOMINAGA KEI: Electron Spin Resonance Studies on Ziegler-Natta Type Catalyst Systems.....	2441
TURNER ALFREY, JR. and CHARLES R. PFEIFER: Rates of Copolymerization of Acrylonitrile and Ethylenesulfonic Acid.....	2447
SHIGEO TAZUKE, NORITAKA SATO, and SEIZO OKAMURA: Effects of Metal Salts on Polymerization. Part II. Polymerization of Vinylpyridine Complexed with the Group IIb Metal Salts.....	2461
I. C. McNEILL: Thermal Volatilization Analysis: A New Method for the Characterization of Polymers and the Study of Polymer Degradation.....	2479
HERBERT MORAWETZ: Polymerization in the Crystalline State. IX. Relation between the Velocity of Radiation-Induced In-Source Polymerization and Post-Polymerization.....	2487
N. G. GAYLORD, B. MATYSKA, K. MACH, and J. VODEHNAL: Cyclo- and Cyclized Diene Polymers. XII. Cationic Polymerization of Isoprene.....	2493
A. SIMON, P. A. JAROVITZKY, and C. G. OVERBERGER: Kinetic Study of Heterogeneous Polymerizations of Styrene and/or $\beta,\beta\text{-d}_2$ -Styrene by Ziegler-Natta Catalysis.....	2513
MARTIN M. TESSLER: Theoretical Studies on the Degradation of Ladder Polymers.....	2521
A. RAVVE and C. W. FITKO: Graft Copolymers of Phenolic Novolacs on Polyamide Backbones.....	2533
G. M. BURNETT, J. M. PEARSON, and J. D. B. SMITH: Study of Crosslink Formation by Partial Conversion Properties. IV. Copolymerization of Styrene with Poly(ethylene Fumarate).....	2543
AJAIB SINGH and LEONARD WEISSBEIN: Kinetics of Urethane Cleavage in Crosslinked Polyurethanes.....	2551

H. W. COOVER, JR., RICHARD L. McCONNELL, F. B. JOYNER, D. F. SLONAKER, and R. L. COMBS: Costereosymmetric α -Olefin Copolymers	2563
H. W. COOVER, JR., J. E. GUILLET, R. L. COMBS, and F. B. JOYNER: Active Site Measurements in the Coordinated Anionic Polymerization of Propylene	2583
D. CAMPBELL, K. ARAKI, and D. T. TURNER: ESR Study of Free Radicals Formed by γ -Irradiation of Poly(ethylene Terephthalate)	2597
JOHN A. KREUZ, A. L. ENDREY, F. P. GAY, and C. E. SROOG: Studies of Thermal Cyclizations of Polyamic Acids and Tertiary Amine Salts	2607
A. L. BARNEY, J. M. BRUCE, JR., J. N. COKER, H. W. JACOBSON, and W. H. SHARKEY: Fluorothiocarbonyl Compounds. VI. Free-Radical Polymerization of Thiocarbonyl Fluoride	2617
A. G. PITTMAN, D. L. SHARP, and R. E. LUNDIN: Polymers Derived from Fluoroketones. I. Preparation of Fluoroalkyl Acrylates and Methacrylates	2637
YOSHIO IWAKURA, FUJIO TODA, and YOSHINORI TORII: Copolymerization of Isopropenyl and Isopropylidene Oxazolones with Styrene	2649
JOHN R. COSTANZA and JOSEPH A. VONA: Polymerization and Cross-linking Characteristics of a 3-Methoxybutyl Acrylate	2659
M. L. WALLACH and M. A. KABAYAMA: Poly(vinyl Fluoride) Solution Characteristics	2667
BHUPATI RANJAN BHATTACHARYYA and UMASANKAR NANDI: Studies on Addition Polymerization in Mixed Solvent System. Part I. Chain Transfer of Water in Polymerization of Methyl Methacrylate	2675
ANDREW A. KATAI and CONRAD SCHUERCH: Mechanism of Ozone Attack on α -Methyl Glucoside and Cellulosic Materials	2683

Notes

H. H. G. JELLINEK: Thermal Gradients in Degradation Reactions	2705
KEIJI TAKEDA, HIROSHI YOSHIDA, KOICHIRO HAYASHI, and SEIZO OKAMURA: Electron Spin Resonance Study of Radiation-Induced Solid-State Polymerization of Conjugated Dienes . .	2710
T. A. GARRETT and G. S. PARK: Reactivity Ratios for the Copolymerization of Vinyl Acetate with Methyl Acrylate	2714

Errata

T. B. GIBB, JR., R. A. CLENDINNING, and W. D. NIEGISCH: Polymers from Aryl Glycidyl Ethers (article in <i>J. Polymer Sci. A-1</i> , 4, 917-922, 1966)	2719
---	------

- PRONoy K. CHATTERJEE and CARL M. CONRAD: Kinetics of Heterogeneous Cellulose Reactions. I. Cyanoethylation of Cotton Cellulose (article in *J. Polymer Sci. A-1*, **4**, 459-474, 1966) . . . 2719

ISSUE No. 11, NOVEMBER

- YUJI MINOURA and TAKA AKI SUGIMURA: Effect of Thiourea on the Radical Polymerizations of Vinyl Monomers. Part II. Effect of Diphenyl Thiourea on the Polymerization of Methyl Methacrylate with Benzoyl Peroxide as Initiator. 2721
- TAKA AKI SUGIMURA and YUJI MINOURA: Effect of Thiourea on the Radical Polymerization of Vinyl Monomers. Part III. Effect of Diphenyl Thiourea on the Polymerization of Methyl Methacrylate with Various Organic Peroxides as Initiator. 2735
- TAKA AKI SUGIMURA, YAYOI OGATA, and YUJI MINOURA: Effects of Polysulfides on the Polymerization of Methyl Methacrylate. 2747
- YUJI MINOURA, YASUYUKI SUZUKI, YASUHIRO SAKANAKA, and HIROYUKI DOI: Copolymerization of Trialkylvinyltin Compounds. 2757
- MASAO KATO and HIROYOSHI KAMOGAWA: Studies on Polymers Containing Functional Groups. VI. Kinetics of the Polymerization and Copolymerization Behaviors of *o*-Hydroxystyrene. 2771
- A. K. INGBERMAN, I. J. LEVINE, and R. J. TURBETT: Mechanism of Stereospecific Polymerization of Propylene with Titanium Trichloride-Aluminum Alkyl Catalysts. 2781
- ICHIRO SAKURADA, NORIO ISE, YOSHINOBU TANAKA, and YUZURU HAYASHI: Ionic Polymerization Under an Electric Field. III. Cationic Polymerizations of α -Methylstyrene and Styrene. 2801
- VICTOR E. MEYER: Copolymerization of Styrene and Methyl Methacrylate. Reactivity Ratios from Conversion-Composition Data. 2819
- HANS JADAMUS, FRANZ DE SCHRYVER, WALTER DE WINTER, and C. S. MARVEL: Model Compounds and Polymers with Quinoxaline Units. 2831
- R. CHIANG and J. J. HERMANS: Influence of Catalyst Depletion or Deactivation on Polymerization Kinetics. II. Nonsteady-State Polymerization. 2843
- R. CHIANG and H. N. FRIEDLANDER: Influence of Catalyst Depletion or Deactivation on Polymerization Kinetics. III. Solution Polymerization of Acrylonitrile in *N,N*-Dimethylformamide at -30°C 2857
- B. L. FUNT, S. N. BHADANI, and D. RICHARDSON: Electrolytic Formation and Destruction of Living Anions. 2871
- GEORGE ADLER: Deviations from Topotaxy in Trioxane Polymerization. 2883
- E. J. GOETHALS and E. DU PREZ: Polymerization of Some Sulfur-Containing Oxetanes. 2893

Notes

- M. NEIMAN, A. BLUMENFELD, and B. KOVARSKAYA: Use of Labeled Oxygen ^{18}O in the Oxidation of Polyformaldehyde 2901
- R. H. SALLÉ, B. J. SILLION, and G. P. DE GAUDEMARI: A New Class of Heterocyclic Polymers: Polyhydantoins 2903
- C. H. H. NEUFELD and C. S. MARVEL: The Use of Dialysis in Polymer Purification 2907

Book Reviews

- Diffraction of X-Rays by Chain Molecules, B. K. Vainshtein, Ed. Reviewed by LUIS G. ROLDAN 2909
- Polymeric Sulfur and Related Polymers, Arthur V. Tobolsky and William J. MacKnight. Reviewed by E. R. BERTOZZI 2910

Erratum

- PETER KOVACIC, VINCENT J. MARCHIONNA, and JAN P. KOVACIC: Properties of *p*-Polyphenyl. Pellet Formation, Radiation Resistance, and Electrical Behavior (article in *J. Polymer Sci. A*, **3**, 4297-4298, 1965) 2911

ISSUE NO. 12, DECEMBER

- H. YASUDA, MICHAEL GOCHIN, and William STONE, JR.: Hydrogels of Poly(hydroxyethyl Methacrylate) and Hydroxyethyl Methacrylate-Glycerol Monomethacrylate Copolymers 2913
- YUJI MINOURA and SHIGEMITSU NAKAJIMA: Polymerization of Butadiene Sulfone 2929
- A. R. MATHIESON and R. T. SHET: Acid-Base Properties of Ion-Exchange Resins. Dissociation and Swelling of Resin Copolymers of Methacrylic Acid, Methyl Methacrylate, Divinylbenzene, and Ethylvinylbenzene 2945
- I. V. NICOLESCU and EM. ANGELESCU: Study of Hydrocarbon-Soluble Organometallic Catalysts. III. Investigations on the Activity and Electric Conductivity of $\text{Al}(\text{C}_2\text{H}_5)_3\text{-M}(\text{C}_5\text{H}_7\text{O}_2)_n$ Catalysts Employed in the Synthesis of Stereoregular Polyacetylene 2963
- KOICHI TADA, TAKAYUKI FUENO, and JUNJI FURUKAWA: Alternation Tendency in Copolymerization 2981
- KENICHI MURATA and AKIRA TERADA: Aminobutadienes. VI. Polymerization and Copolymerization of 2-Phthalimido-1,3-butadiene 2989
- LEWIS J. FETTERS, WALTER J. PUMMER, and LEO A. WALL: Monomer-Polymer Equilibria of Deuterated α -Methylstyrenes 3003
- C. L. LEE and O. K. JOHANNSON: Polymerization of Cyclosiloxanes. I. Kinetic Studies on Living Polymer-Octamethylcyclotetrasiloxane Systems 3013

WILLIAM F. GORHAM: A New, General Synthetic Method for the Preparation of Linear Poly- <i>p</i> -xylylenes.....	3027
L. STARR: Aromatic Polyamides of 2,6-Naphthalenedicarboxylic Acid.....	3041
K. G. MIESSEROV: Mechanism of Polymerization of α -Olefins on Oxide Catalysts.....	3047
CHARLES W. HOCK: How TiCl_3 Catalysts Control the Texture of As-Polymerized Polypropylene.....	3055
D. J. WILLIAMS and E. G. BOBALEK: Application of Molecular Weight and Particle Growth Measurements in Continuously Uniform Lattices to Kinetic Studies of Styrene Emulsion Polymerization.....	3065
J. A. BARRIE: Diffusion of Methanol in Polydimethylsiloxane.....	3081
R. CHIANG, J. H. RHODES, and R. A. EVANS: Solution Polymerization of Acrylonitrile Catalyzed by Sodium Triethylthioisopropoxyaluminate: A Polyacrylonitrile with High Structural Regularity.....	3089
C. G. OVERBERGER and NAOKI YAMAMOTO: Copolymerization of Styrene and Methyl Methacrylate with Lithium as Initiator..	3101

Notes

BROJA MOHAN MANDAL, UMASANKAR NANDI, and SANTI R. PALIT: On the Identification of the Radical $\cdot\text{S}-\text{C}(\text{NH})(\text{NH}_2)$	3115
JOHN D. COTMAN, JR.: Crosslinking in Lithium-Initiated Anionic Copolymerization of Methyl Methacrylate-Styrene.	3118

Erratum

PETER KOVACIC and LI-CHEN HSU: Polymerization of Aromatic Nuclei. VIII. Molecular Weight Control in Benzene Polymerization (article in <i>J. Polymer Sci. A-1</i> , 4 , 5-28, 1966)....	3123
Author Index, Volume 4.....	3125
Subject Index, Volume 4.....	3139

EDITORIAL

The first issue of a new year is perhaps the most propitious time for a publication to take stock of itself and to inform readers of any major plans in the offing. Certainly one of the notable developments of the past few years, as far as the *Journal of Polymer Science* is concerned, has been the great success we have achieved in attracting an increasing number of papers in the area of polymer physics. In the April, 1964, issue of the *Journal* we indicated editorially our plan to give stronger identification to the growing field of polymer physics. This plan was underscored at that time by the appointment of Dr. Richard S. Stein as one of the *Journal's* Editors (a post later taken by Dr. Thomas G. Fox, assisted by Dr. E. F. Casassa and Dr. H. Markovitz). Since then the influx of manuscripts in polymer physics has gained such momentum that the Editors and publisher of the *Journal* decided that the physical separation of such papers from the bulk of the material was both practical and desirable.

To implement this decision, we are undertaking a major change in the organization of the *Journal*: Commencing this year, Part A of the *Journal* (General Papers) is being divided into two separately published sections.

Part A-1 will comprise papers in polymer chemistry and will continue on a monthly basis.

Part A-2 will contain papers in polymer physics and polymer chemical physics and will be published on a bimonthly schedule.

The papers published in the chemistry section of the *Journal* (Part A-1) will deal with the synthesis of polymers, reaction mechanisms, kinetics, and other areas of the organic and physical organic chemistry of macromolecules. The physics section of the *Journal* (Part A-2) will include those papers dealing with macromolecules in solid state and solution. Specifically, they will deal with such topics as crystallization and crystallinity; polymer morphology; crystal physics; mechanical, optical, and other physical properties; molecular conformation; thermodynamics; and statistical thermodynamics.

Overall policy for the *Journal* will be the responsibility of a Board of Editors composed of Drs. H. Mark, C. G. Overberger, and T. G. Fox. R. M. Fuoss, J. J. Hermans, H. W. Melville, and G. Smets will serve as Advisory Editors. Dr. Overberger will act as the Editor for Part A-1, assisted by Dr. Eli Pearce of the J. T. Baker Company, Phillipsburg, New Jersey. Dr. Fox will act as the Editor for Part A-2, assisted by Drs. Casassa and Markovitz. A separate Advisory Board, representing all areas of polymer physics, will be appointed for Part A-2.

Publication Time-Lag Reduced

The Editors are also pleased to report that although the influx of manuscripts to Part A of the *Journal* has steadily increased during the 1964-1965 period, the time lag between receipt of manuscripts and actual publication has been substantially reduced. Whereas many articles appearing in the April, 1964, issue of the *Journal* had been received by the Editors 13 months previously, most manuscripts in the December, 1965, issue had been received only five months before. Because we are aware of the importance of speed in publication of scientific papers, both the Editors and the publisher give constant attention to this aspect of the *Journal*.

Editorial Policy

At a number of meetings of the *Journal's* Editorial Board the Editors have reviewed and discussed the overall editorial policy that guides them in evaluating manuscripts submitted for publication. It will undoubtedly be helpful to prospective authors to reiterate that policy here.

Naturally, the *Journal of Polymer Science* will at all times be selective in accepting contributions on the basis of merit and originality. The *Journal* is not intended as a repository for unevaluated data. Preference will be given to papers that contribute new concepts, new or more comprehensive interpretations, or novel experimental approaches and results.

When preparing a manuscript, please consider critically the following questions for they embody the criteria by which the Editors and referees will judge contributions.

Are the scientific problems clearly stated; are they significant?

Is the development of theoretical ideas logical and lucid? Are all quantities and symbols defined explicitly? Are all assumptions explicitly identified?

Are experimental data of an accuracy commensurate with the present development of technique, and do they elucidate the scientific problem? Are the experimental procedures and data given in sufficient detail to permit the reader to form a judgment of the work?

Are interpretations sound, and are the conclusions borne out by the evidence? Are tentative or speculative interpretations clearly labelled as such? Has full account been taken of pertinent earlier investigations?

Is the presentation clear, concise, and grammatical? Is the synopsis adequate; does it emphasize the important aspects of the problem, results, and conclusions?

In addition to meeting standards for excellence and significance, manuscripts for Part B (Polymer Letters) should exhibit a degree of novelty and timeliness that warrants speedy publication, even in preliminary form. Short communications, however meritorious, that do not meet this test can be considered for "Notes" in Parts A. The Notes are generally to be regarded as complete publications of limited scope, while Letters may sometimes deal with important material to be elaborated later in a full-length paper.

INFORMATION FOR CONTRIBUTORS

1. Manuscripts should be submitted to H. Mark, Polytechnic Institute of Brooklyn, 333 Jay Street, Brooklyn, New York 11201. In Europe, manuscripts may be submitted to Professor G. Smets, University of Louvain, Louvain, Belgium; and in the United Kingdom to Sir Harry W. Melville, Department of Scientific and Industrial Research, 5-11 Regent Street, London, S.W.1, England. Address all other correspondence to Periodicals Division, Interscience Publishers, John Wiley & Sons, Inc., 605 Third Avenue, New York, New York 10016.
2. It is the preference of the Editors that papers be published in the English language. However, if the author desires that his paper be published in French or German, it is necessary that a particularly complete and comprehensive synopsis be furnished.
3. Manuscripts should be submitted in triplicate (one *original*, two carbon copies), typed *double space* throughout and on one side of each sheet only, on a *heavy* grade of paper with margins of at least one inch on all sides.
4. A short synopsis (maximum length 200 words) is required for papers in Parts A. No synopsis is published for Part B or for "Notes" in Parts A. This synopsis should be carefully prepared, for it will appear in English, in French, and in German, and is automatically the source of most abstracts. The Synopsis should be a summary of the entire paper; not the conclusions alone.
5. The paper should be reasonably subdivided into sections and, if necessary, subsections. Please refer to any issue of this *Journal* for examples.
6. The references should be numbered consecutively in the order of their appearance and should be complete, including authors' initials and—for unpublished lectures or symposia—the title of the paper, the date, and the name of the sponsoring society. Please compile references on a separate sheet at the end of the manuscript. Abbreviations of journal titles should conform to the practices of *Chemical Abstracts*.
7. Please supply numbers and titles for all tables. All table columns should have an explanatory heading.
8. It is particularly important that all figures be submitted in a form suitable for reproduction. Good glossy photographs are required for halftone reproductions. For line drawings (graphs, etc.), the figures must be drawn clearly with India ink on heavy white paper, Bristol board, drawing linen, or coordinate paper with a very light blue background. The India ink lettering of graphs must be large, clear, and "open" so that letters and numbers do not fill in when reduced for publication. It is the usual practice to submit drawings that are twice the size of the final engravings; the maximum final size of figures for this *Journal* is $4\frac{1}{2} \times 7\frac{1}{2}$ inches. It is the author's responsibility to obtain written permission to reproduce material which has appeared in another publication. If in doubt about the preparation of illustrations suitable for reproduction, please consult the publisher at the address given above in paragraph 1 and ask for a sample drawing.
9. Please supply legends for all figures and compile these on a separate sheet.
10. Authors are cautioned to type—wherever possible—all mathematical and chemical symbols, equations, and formulas. If these must be handwritten, please print clearly and leave ample space above and below for printer's marks; please use only ink. All Greek or unusual symbols should be identified in the margin the first time they are used. Please distinguish in the margins of the manuscript between capital and small letters of the alphabet wherever confusion may arise (e.g., k, K, κ). Please underline with a wavy line all vector quantities. Use fractional exponents to avoid root signs. The nomenclature sponsored by the International Union of Chemistry is requested for chemical compounds. Chemical bonds should be correctly placed, and double bonds clearly indicated. Valence is to be indicated by superscript plus and minus signs.

JOURNAL OF POLYMER SCIENCE

11. Authors will receive 50 reprints of their articles without charge. Additional reprints can be ordered and purchased by filling out the form attached to the galley proof. Page proofs will not be supplied.
12. No manuscript will be returned following publication unless a request for return is made when the manuscript is originally submitted.

Manuscripts and illustrations not conforming to the style of the *Journal* will be returned to the author for reworking, thus delaying their appearance.

Polymerization of Aromatic Nuclei. VIII. Molecular Weight Control in Benzene Polymerization

PETER KOVACIC and LI-CHEN HSU, *Department of Chemistry, Case Institute of Technology, Cleveland, Ohio*

Synopsis

The molecular weight of *p*-polyphenyl prepared from benzene-aluminum chloride-cupric chloride, was affected by solvent, concentration, and temperature. Relative molecular weights were measured by polymer solubility in chloroform, and positions of the infrared *para* band and ultraviolet reflectance λ_{\max} . The order of effectiveness of the solvents in reducing molecular weight was: *o*-C₆H₄Cl₂ > 1,2,4-C₆H₃Cl₃ > SnCl₄ ~ CS₂ > [C₆H₆]. Degradative oxidation revealed that *o*-dichlorobenzene solvent was incorporated as an endgroup to only a minor extent. In general, the molecular weight of *p*-polyphenyl decreased with increasing temperature and with decreasing concentration. The theoretical aspects are treated.

Recently, a new polymerization method was developed in this laboratory whereby aromatic nuclei may be transformed in one step to homopolymers. For example, benzene was converted to *p*-polyphenyl under mild conditions on treatment with aluminum chloride-cupric chloride,^{1,2} molybdenum pentachloride,³ or ferric chloride.⁴ Aluminum chloride functions as the catalyst, and cupric chloride as the oxidant. The other metal halides apparently assume the dual role of catalyst and oxidant. An oxidative cationic mechanism has been postulated for this novel polymerization method.²⁻⁴ Unfortunately, extreme insolubility of the polymer precludes molecular weight determination by conventional solution methods. Previous work³ revealed that the polymers prepared from benzene-aluminum chloride by use of nitrogen oxides and *p*-quinones possessed relatively low molecular weights as evidenced by infrared spectroscopy. The results indicated that these oxidants also function as chain terminating agents.

Attention has been drawn to the similarities between the benzene transformation and the cationic polymerization of olefins.^{2,5-7} The literature contains a considerable number of reports dealing with molecular weight control in olefin polymerization by use of additives⁸⁻¹⁶ and variation in temperature⁸ or concentration.^{8,17} Included among the diverse types of terminating agents are aromatic compounds^{8,9} and various oxygen-containing substances.^{8,10-16}

The objective of this study was to effect molecular weight control in the polymerization of benzene to *p*-polyphenyl by varying the solvent, concentration, and temperature. Further elucidation of the mechanistic aspects was also desired.

RESULTS AND DISCUSSION

Analytical Methods

The molecular weight of *p*-polyphenyl prepared by reaction of benzene with aluminum chloride-cupric chloride in different kinds of solvents was found to vary with the nature of the solvent, concentration of the solution, and reaction temperature. Relative molecular weight data for the polymers were obtained primarily by use of the following techniques: solubility in chloroform, reflectance, and infrared spectroscopy. In certain cases it was possible to ascertain the molecular weight. Some insight concerning the structure was also gained from the elemental analyses.

Theoretically, the data from elemental analyses can provide information pertinent to the molecular weight problem. The C/H atomic ratio varies from 1.285 for *p*-terphenyl to a limiting value of 1.5 for an infinitely long *p*-polyphenyl chain. Practically, however, one finds that this approach has serious limitations, considering that a polyphenyl of quite low molecular weight ($n = 20$) possesses a C/H value, 1.46, which is experimentally indistinguishable from the limiting value. Since all of the polymers contained chlorine, usually in small amounts, the C/H ratio for the parent hydrocarbon was obtained from the expression, $C/(H + Cl)$. Inherent is the reasonable assumption that the chlorine is introduced by replacement of hydrogen.

Fractional extraction with media of varying solvent power has been employed to determine the molecular weight distribution of linear polymers.¹⁸ For comparing *p*-polyphenyls of greatly different molecular weights, chloroform was found to function as a useful solvent.

When ultraviolet transmittance measurements are extremely difficult or impossible to obtain, as in this case, because of strong sample absorption, the reflectance technique provides a possible alternative.^{19,20} The reliability was ascertained by examining anthracene and lower *p*-polyphenyls and then comparing the results with the published spectra obtained in solution (Table I).^{21,22}

The peak positions determined by the two methods were found to be in satisfactory agreement. It is apparent that the λ_{\max} of *p*-polyphenyls shifts to a shorter wavelength as the molecular weight is decreased.

TABLE I
Ultraviolet Spectroscopy by Solution and Reflectance Techniques

Compound	λ_{\max} , m μ	
	Solution	Reflectance
Anthracene	253,339,356,374	251,336,350,370
<i>p</i> -Terphenyl	380	286
<i>p</i> -Quaterphenyl	300	308
<i>p</i> -Quinquephenyl	310	317
<i>p</i> -Sexiphenyl	317.5	321

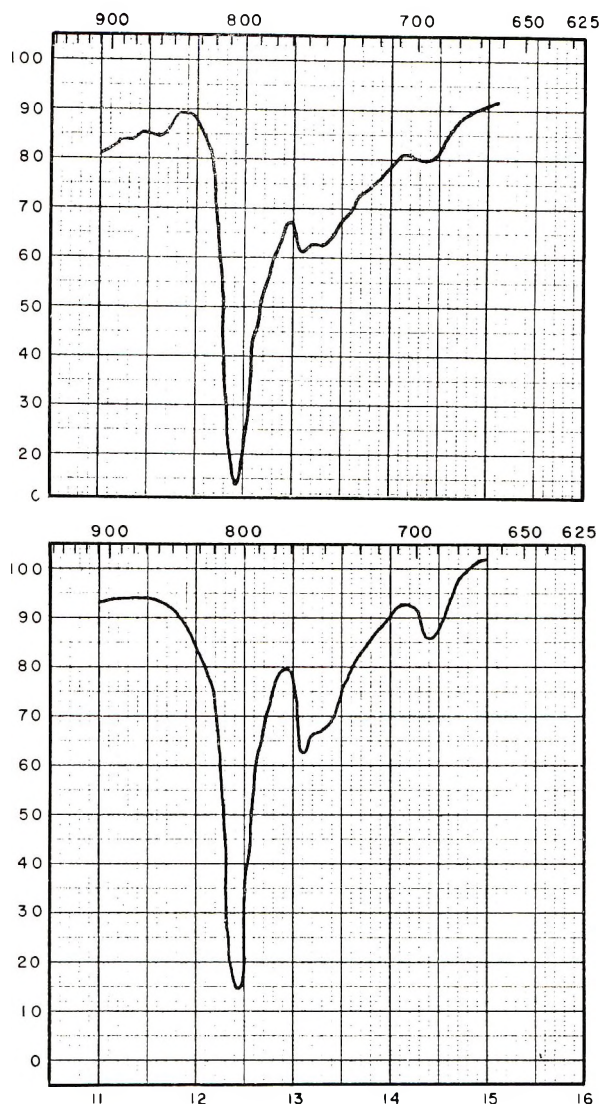


Fig. 1. Infrared spectra of *p*-polyphenyl: (top) before dechlorination; (bottom) after dechlorination. (Table III.)

The relation between the ultraviolet spectrum and molecular weight of *p*-polyphenyls has been discussed from the quantum mechanical viewpoint by Dewar²³ and Davydov.²⁴ Conjugation results in a bathochromic shift, with λ_{\max} increasing asymptotically to a limiting value as the number of aromatic nuclei increases.²⁵ From calculations based on Davydov's equation and λ_{\max} values (in solution) for the lower *p*-polyphenyls, Suzuki²⁵ reported 339 $m\mu$ as the peak position when n is infinity. In marked contrast, λ_{\max} experimental figures as high as 395 $m\mu$ have been obtained for *p*-polyphenyl prepared from neat benzene and in carbon disulfide. Al-

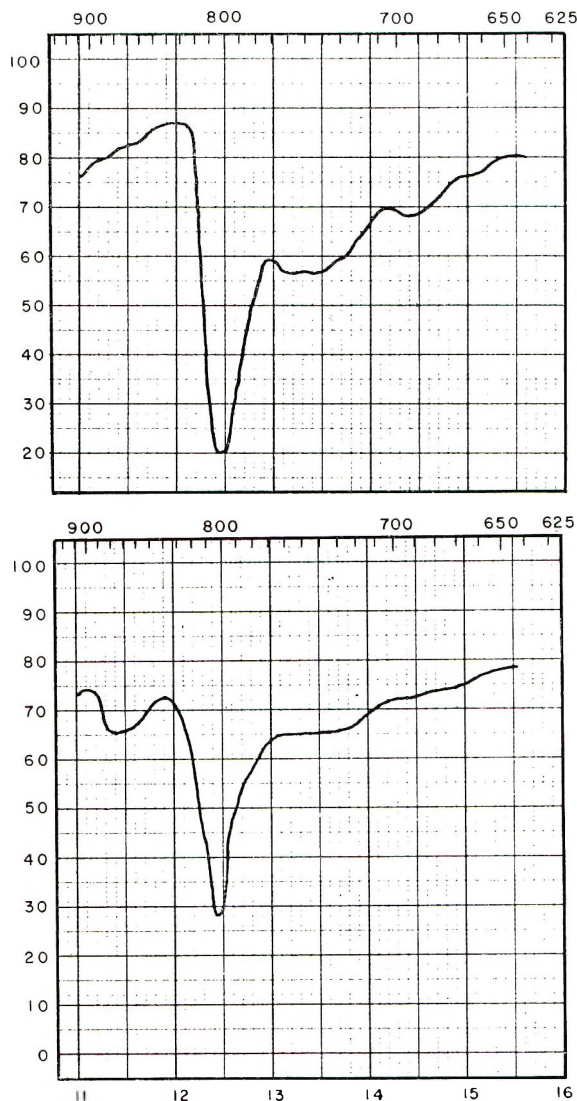


Fig. 2. Infrared spectra of *p*-polyphenyl: (top) before chlorination; (bottom) after chlorination (31% Cl, Table II).

though the correction factor is unknown, it appears unlikely that the discrepancy arises entirely from differences in the method of obtaining the spectra. Perhaps *p*-quinoid type linkages are present to some extent in the chains.

A shift of the infrared *para* band position to a lower wave number with increasing molecular weight in the *p*-polyphenyl series has been observed.^{5,20} Since the magnitude of the shift decreases with increasing molecular weight, the method is most applicable to lower molecular weight polymers and for

comparison of *p*-polyphenyls which differ widely in molecular weight. Valuable information was provided by this analytical approach.

The two mono bands, situated at 770–730 cm.^{-1} and 710–690 cm.^{-1} are derived from the terminal groups (Figs. 1 and 2). It is also evident that the ratio of the logarithm of the *para* band intensity to that of the summation of mono band intensities increases with increasing molecular weight.⁵ This technique then constitutes a type of endgroup analysis. Unfortunately, serious problems were encountered which severely limit the usefulness of this method. Of greatest concern was the presence of small quantities of chlorine in the polymer. Obviously, substitution of a halogen into a terminal phenyl nucleus would alter the infrared spectral pattern of the endgroup. As described in the subsequent section, efforts to resolve this difficulty were only partially successful.

In addition, in order to strive for completeness of critical evaluation, one should consider the question of the presence of small numbers of non-aromatic units in the polymer chains. Perhaps irregular structures of this type might be introduced by disproportionation of labile intermediates (cyclohexadiene units) during polymerization. Interruption of conjugation in this manner could have an important influence on the spectral analyses. At present, there is no definitive answer to this question.

Effect of Chlorine Content on Validity of the Analyses

Since the chlorine content of the polymers prepared in this study varied somewhat (2.3–14.8%), a series of experiments was carried out with the aim of determining the effect of change in per cent chlorine on solubility and ultraviolet and infrared analyses. Two methods of attack were used: (1) chlorination of *p*-polyphenyl after polymerization so as to provide polymers differing widely in halogen content; (2) dechlorination aimed at conversion to polymers completely devoid of substituents.

In the chlorination studies a relatively high molecular weight *p*-polyphenyl, prepared from neat benzene, was halogenated to various degrees

TABLE II
Effect of Chlorine Content on Polymer Properties

Cl, %	Benzene units/Cl	Color	C/(H + Cl), atomic ratio	Solubil- ity in CHCl ₃ , %	Infrared <i>para</i> band position, cm.^{-1}	Reflect- ance λ_{max} , $\text{m}\mu$
1.9 ^a	20	Brown	1.52	3.5	803	386
6.9 ^b	6	Dark brown	—	3.6	803	383
31.0 ^b	1	Brown- black	1.49	7.6	804	362

^a Prepared from neat benzene, $\text{C}_6\text{H}_6/\text{AlCl}_3/\text{CuCl}_2 = 12/1/0.5$ (molar ratio) at 32–35°C. for 2 hr.

^b From *p*-polyphenyl and antimony pentachloride (see Experimental).

by treatment with antimony pentachloride²⁶ in antimony trichloride (Table II). Increasing the chlorine content resulted in a darker color, but in no significant change in $C/(H + Cl)$.

An increase in chlorine from 1.9 to 6.9% produced essentially no change in chloroform solubility. A more drastic increase to 31% resulted in dissolution to the extent of 7.6%. Therefore the conclusion may be drawn that for this molecular weight level large variation in the per cent chlorine has relatively little effect on solubility. It might well be that for polymers possessing relatively short chains, solubility would be more drastically altered by similar changes in chlorine content. Kern and Wirth²⁷ made fairly extensive studies of the effect of substituents in *p*-polyphenyls on physical properties. The derivatives exhibited lower melting points and considerably enhanced solubility in comparison with the parent compounds.

The prior literature reveals, in general, a shift to longer wavelengths (bathochromic effect) in the ultraviolet λ_{\max} on introduction of a chlorine substituent into the aromatic nucleus. Also, compare biphenyl (λ_{\max} 246 $m\mu$) with 4,4'-dichlorobiphenyl (λ_{\max} 260 $m\mu$). The bathochromic effect presumably arises from the presence of an atom or group which donates electrons so as to increase the degree of conjugation.²⁸ In contrast, increase in the chlorine content of *p*-polyphenyl induced a shift to shorter wavelengths (Table II). The incremental change is about 0.8 $m\mu$ for each per cent increase in chlorine content. Perhaps the substituent on the polymer backbone sterically decreases the degree of coplanarity of the rings, thereby reducing resonance interaction of the aromatic nuclei. Support for this hypothesis is provided by spectral data reported for methylated biphenyls.²¹ *o*-Methylbiphenyl demonstrates a hypsochromic effect (λ_{\max} 237 $m\mu$ vs. λ_{\max} 246 $m\mu$ for biphenyl), whereas *p,p'*-dimethylbiphenyl falls in the bathochromic category (λ_{\max} 257 $m\mu$).

In relation to infrared analysis, the *para* band position remained essentially unchanged in the range, 1.9–31% chlorine (Table II). Therefore, the appears to constitute a valid criterion of molecular weight in the case of chlorinated *p*-polyphenyls. The mono substitution bands decreased and the isolated hydrogen band (860–900 cm.^{-1}) increased in intensity as the level of chlorination by antimony pentachloride increased (Fig. 2).

The pathway leading to chlorination of *p*-polyphenyl during polymerization remains to be elucidated. It seems reasonable to designate cupric chloride as the active species. Although this metal halide is a weak halogenating agent, aluminum chloride is known to exert a catalytic effect.²⁹ Furthermore, a small amount of the observed halogen might be incorporated by a termination reaction.

The principal objective of the dechlorination studies was to obtain the corresponding parent *p*-polyphenyl hydrocarbon to permit a valid end-group analysis. Sodium was used as the reagent at 160°C. with high-speed stirring. In most cases, less than 1% chlorine remained after treatment for 5 hr. Analytical data for the resultant polymers are summarized in Table III.

There was little or no change in *para* band position, reflectance λ_{\max} , solubility, and color. However, there occurred a marked decrease in intensity or complete loss of the band in the 860 cm.^{-1} region characteristic of an isolated hydrogen. This reflects the removal of backbone halogen. In addition, there was a considerable increase in mono band absorption, pointing to the loss of terminal chlorine (Fig. 1).

TABLE III
Comparison of Polymers Before and After Dechlorination

Polymer	Cl, %	Color	C/(H + Cl), atomic ratio	Solu- bility in CHCl ₃ , %	Infrared <i>para</i> band position, cm. ⁻¹	Infrared band intensi- ties, log (Σ mono)	Reflect- ance λ_{\max} , m μ
Prepared in <i>o</i> -C ₆ H ₄ Cl ₂ ^a	6.1	Dark brown	1.55	10	803.5	1.75	378
Same, after de- chlorination	0	Dark brown	1.50	9	804	1.57	375
Prepared in 1,2,4-C ₆ H ₃ Cl ₃ ^b	13.6	Black	1.87	11	804	1.97	380
Same, after de- chlorination	0.7	Black	1.53	12	804	1.36	375

^a *o*-C₆H₄Cl₂/C₆H₆ = 6, 80°C., 18 min.

^b 1,2,4-C₆H₃Cl₃/C₆H₆ = 12, 80°C., 18 min.

Regrettably two obstacles remained to obstruct the use of this technique. In some cases it was difficult to effect complete removal of halogen. Also dechlorination of a relatively low molecular weight polymer was apparently accompanied by reduction of aromatic nuclei as evidenced by a significant decrease in *para* band intensity.

Relative Molecular Weight

Solvent Effect. After establishing the validity and degree of applicability of the analytical methods for determining relative molecular weights we proceeded with a more detailed investigation of various solvents. Both inorganic and organic types were used, including carbon disulfide, stannic chloride, titanium tetrachloride, *o*- and *p*-dichlorobenzene, and 1,2,4-trichlorobenzene.

For each solvent, a control run was made under the most drastic polymerization conditions. With *o*- and *p*-dichlorobenzene, 1,2,4-trichlorobenzene, and carbon disulfide, benzene was not added. In the case of titanium tetrachloride and stannic chloride, aluminum chloride was omitted. No significant amount of solid organic product was obtained in any of these experiments. With the di- and trichlorobenzenes the reaction mixture after hydrolysis was also analyzed by gas chromatography and infrared

spectroscopy for possible isomerization and disproportionation. There was no evidence for the occurrence of such side reactions.

First, a comparison of the polymers prepared in the various solvents will be made based on the principal analytical methods. When the reactions were carried out at 35–40°C. for 18 min. at a solvent/benzene ratio of 12, products were obtained which displayed C/(H + Cl) ratios near 1.5 and low chlorine content (about 4%). Under these conditions no polymerization occurred in titanium tetrachloride, and *p*-dichlorobenzene was not investigated. The data (Table IV) point to the following order of effectiveness of the solvents in reducing molecular weight: *o*-C₆H₄Cl₂ > 1,2,4-C₆-H₃Cl₃ > SnCl₄ ~ CS₂ > (C₆H₆).

TABLE IV
Solvent Effect in the Polymerization of Benzene at 35–40°C.^a

Solvent	Cl, %	C/(H + Cl), atomic ratio	Solubility in CHCl ₃ , %	Infrared <i>para</i> band position, cm. ⁻¹	Reflectance λ _{max} , mμ
<i>o</i> -C ₆ H ₄ Cl ₂	4.1	1.46	20	804	385
1,2,4-C ₆ H ₃ Cl ₃	3.6	1.39	10	804	388
SnCl ₄	4.0	1.50	2.2	801	392
CS ₂	3.6	1.47	2.4	801.5	392
C ₆ H ₆	2.4	1.40	2.5	801.5	395

^a Solvent/C₆H₆/AlCl₃/CuCl₂ = 12/1/1/0.5 (molar), 18 min.

There is good agreement among the solubility, infrared, and reflectance analyses in relation to the relative changes in molecular weight. The following extremes were noted: solubility in chloroform (2.2–20%), infrared *para* band position (801–804 cm.⁻¹) and reflectance λ_{max} (395–385 mμ).

The same solvent order pertained to the studies carried out at 80°C. (Table V). It is interesting that similar results were obtained with the polymers prepared at the different temperatures, even though the products formed at 80°C. possessed somewhat greater structural irregularity. That is, the chlorine content was higher (4.1–13.6%) and with 1,2,4-trichlorobenzene and stannic chloride the C/(H + Cl) ratios were relatively high (1.78 and 1.86). This leads to the conclusion that these differences do not seriously affect the investigated properties. Titanium tetrachloride falls in a unique category since results from the three analytical methods were not in agreement. We surmise that in this case the infrared data constitute the most valid criterion of molecular weight. On this assumption, the following order of effectiveness in reducing molecular weight would pertain, *o*-C₆H₄Cl₂ > 1,2,4-C₆H₃Cl₃ > *p*-C₆H₄Cl₂ > TiCl₄ > SnCl₄ > (C₆H₆). The high C/(H + Cl) value, 1.95, for titanium tetrachloride points to the presence of polynuclear structures in appreciable amounts.⁶ Presumably this accounts for the unexpected λ_{max} figure, 370 mμ, since diffuse reflec-

TABLE V
 Solvent Effect in the Polymerization of Benzene at 80°C.^a

Solvent	Cl, %	C/(H + Cl) atomic ratio	Solubility in CHCl ₃ , %	Infrared <i>para</i> band position, cm. ⁻¹	Reflectance λ_{\max} , m μ
<i>o</i> -C ₆ H ₄ Cl ₂	8.0	1.58	26	806	366
1,2,4-C ₆ H ₃ Cl ₃	13.6	1.78	11	804	375
<i>p</i> -C ₆ H ₄ Cl ₂	8.4	1.62	3	804	377
TiCl ₄	6.6	1.95	2	802.5	370
SnCl ₄	5.5	1.86	2.6	801.5	385
(C ₆ H ₆)	4.1	1.48	2	801.5	388

^a Solvent/C₆H₆/AlCl₃/CuCl₂ = 12/1/1/0.5 (molar), 18 min.

tance cannot be measured accurately if the sample fluoresces,³⁰ as would be expected for polynuclear structures.

A polymer prepared in *o*-dichlorobenzene was fractionated and subjected to infrared analysis. The chloroform soluble portion exhibited strong mono bands and enhanced absorption derived from 1,2,4-trisubstitution (backbone halogen). In contrast, the reverse was true of the insoluble portion in comparison with the unfractionated material.

Degradative oxidation of several benzene polymers was carried out with chromic anhydride in order to obtain information concerning endgroup structure and chain regularity. After oxidation of a polymer prepared in *o*-dichlorobenzene, the product was esterified with diazomethane and analyzed by gas chromatography. The following components were identified: methyl benzoate, methyl *p*-chlorobenzoate, methyl 3,4-dichlorobenzoate, and dimethyl terephthalate. The qualitative and quantitative evidence points to the presence of three types of terminal structure in the indicated order of abundance, *p*-chlorophenyl > phenyl > 3,4-dichlorophenyl. Since the susceptibility to gross oxidation involving ring cleavage is in the order of phenyl > *p*-chlorophenyl > 3,4-dichlorophenyl, the actual ratio of the phenyl endgroup in the polymer would be greater than that found.

On the unlikely premise that the 3,4-dichlorophenyl endgroup arose from chlorination *in situ* of the *p*-chlorophenyl entity, oxidation of a polymer formed in another solvent (1,2,4-trichlorobenzene) was investigated in a similar manner. The following acids were detected, benzoic, *p*-chlorobenzoic, and terephthalic, but no 3,4-dichlorobenzoic. Therefore, confirmatory evidence is provided for covalent attachment of *o*-dichlorobenzene to the propagating species. These studies aid in the clarification of the problem concerning endgroup structure. Several conclusions may be put forth: (1) a principal mode of termination involves phenyl endgroup formation, apparently by loss of a proton from the propagating carbonium ion; however, this same terminal structure could result from initiation; (2) the *p*-chlorophenyl structure might arise by chlorination of the phenyl group; alternatively, there might be interaction of chloride

ion with the growing carbonium ion followed by oxidation with cupric chloride, (3) *o*-dichlorobenzene is incorporated as an endgroup to only a minor extent through the covalent attachment of *o*-dichlorobenzene to the propagating species.

An analogous situation relative to solvent effect is known to exist in polar polymerization of olefins. There is good evidence indicating incorporation of aromatic solvent as an endgroup.^{8,9,31a} Interestingly, Overberger and Endres⁸ found that this was not the exclusive termination route for styrene in the presence of various aromatic species.

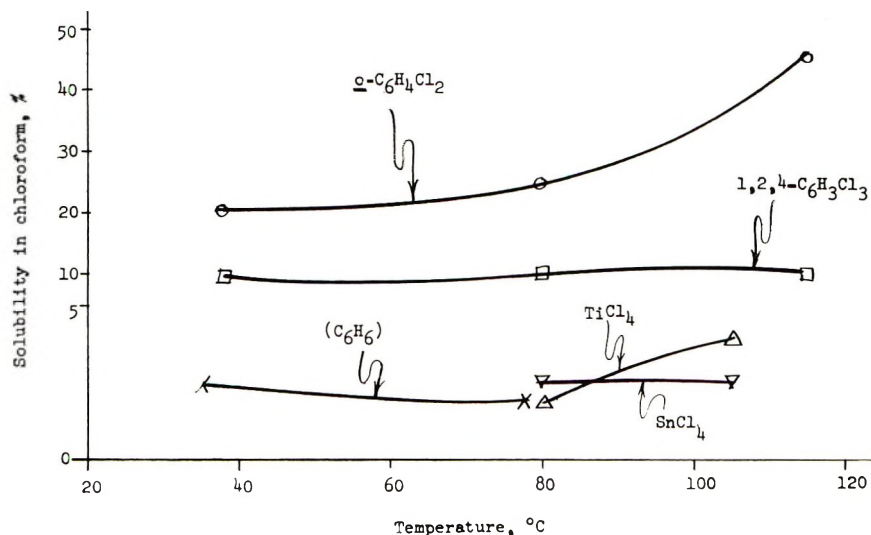


Fig. 3. Polymer solubility in chloroform vs. reaction temperature. Polymerization at solvent/C₆H₆ = 12 for 18 min.

In our studies there was no evidence for the presence of benzenedicarboxylic acids other than the *para* one. This provides additional support for the conclusion that the polymers possess essentially the *para* configuration. There may be small amounts of other structures (side chains, cross-links, and *meta* linkages), particularly in the polymers prepared under more drastic conditions.

There are detailed treatments dealing with the effect of physical properties of the medium on ionic polymerization of olefins.³¹ It is instructive to compare the solvent effect in benzene polymerization with the dielectric constant³²⁻³⁴ of the diluent, ϵ (20°C.): *o*-dichlorobenzene, 7.5; 1,2,4-trichlorobenzene, 3.98; stannic chloride, 2.87; carbon disulfide, 2.64; benzene, 2.28. As cited earlier for the polymerization at 35-40°C., the solvents demonstrated the following order of effectiveness in reducing molecular weight, *o*-C₆H₄Cl₂ > 1,2,4-C₆H₃Cl₃ > SnCl₄ ~ CS₂ > (C₆H₆). Thus, a good correlation exists between increasing dielectric constant and increasing effectiveness of the solvent in decreasing molecular weight.

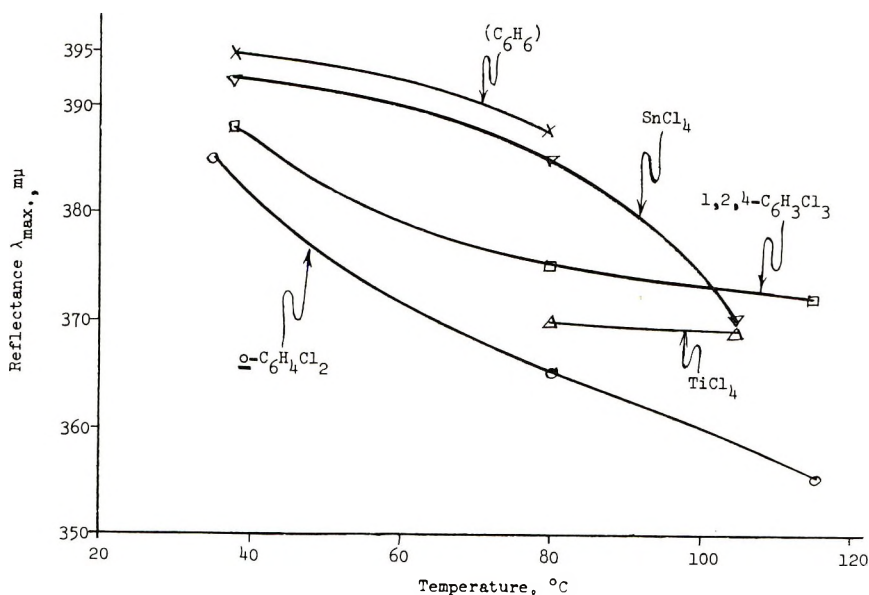


Fig. 4. Polymer reflectance vs. reaction temperature. Polymerization at solvent/C₆H₆ = 12 for 18 min.

Let us attempt a further rationalization of the effect of aromatic solvent on polymerization. π - and n -complexes³⁵ might so deactivate the growing end that the rate of propagation decreases and termination by proton loss assumes a more favored status.

The physical nature of the reaction medium in the benzene reactions should be borne in mind relative to theoretical considerations. A heterogeneous system is involved with metal halides and p -polyphenyl constituting the insoluble, solid phase.

Temperature Effect. Studies were usually carried out in the 35–115°C. range in order to determine the effect of temperature on relative molecular weights in the various solvent systems. Polymerizations were performed under the following conditions: solvent/benzene = 12 for 18 min. The results from the analyses are summarized in Figure 3 (solubility), Figure 4 (reflectance), and Figure 5 (infrared). In the case of o -dichlorobenzene, 1,2,4-trichlorobenzene, and stannic chloride, a decrease in molecular weight with increasing temperature is indicated by the reflectance technique which appears to be the most sensitive of the three methods. In addition, solubility and infrared data lead to a similar correlation with o -dichlorobenzene solvent. However, these two techniques were not of sufficient sensitivity to detect the changes in molecular weight effected with the other media. In general, at the different temperatures investigated, molecular weight decreased in the order, o -C₆H₄Cl₂ > 1,2,4-C₆H₃Cl₃ > SnCl₄. Since the polymer from titanium tetrachloride exhibits an erratic nature as mentioned earlier, no rationalizations were made in this case. With carbon

TABLE VI
 Polymerization of Benzene in Carbon Disulfide

CS ₂ / C ₆ H ₆ , molar ratio	Temp., °C.	Time, min.	Yield, %	Cl, %	C/(H + Cl), atomic ratio	Solubili- ty in CHCl ₃ , %	Infrared <i>para</i> band position, cm. ⁻¹	Reflect- ance λ _{max} , mμ
6	35-40	18	20	3.4	1.68	3.2	801.5	395
12	35-40	18	10	3.6	1.47	2.4	801.5	392
24	35-40	18	6	3.0	1.45	—	801.5	390
12	35-40	120	30	3.8	1.62	2.8	801.5	395
12	10-15	120	5	2.5	1.50	—	801.5	395

disulfide solvent, polymerization could be conveniently effected only over a narrow temperature range (10–40°C.). It is not surprising to find no detectable change in molecular weight with such a small change in temperature (Table VI).

Data for *p*-polyphenyl prepared from neat benzene (C₆H₆/AlCl₃/CuCl₂ = 13/1/0.5) are included in the figures for comparison. Whereas reflectance measurements showed that the highest molecular weights were attained in the undiluted system, the other two analytical methods could not differentiate between the products formed neat and those prepared in stannic chloride solvent.

In relation to the cationic polymerization of olefins, Pepper⁸ states that the most important single factor affecting the molecular weight is undoubtedly the reaction temperature.^{31b,4,c,36} The theoretical aspects of the temperature effect have received attention in the prior literature.^{8,36,37}

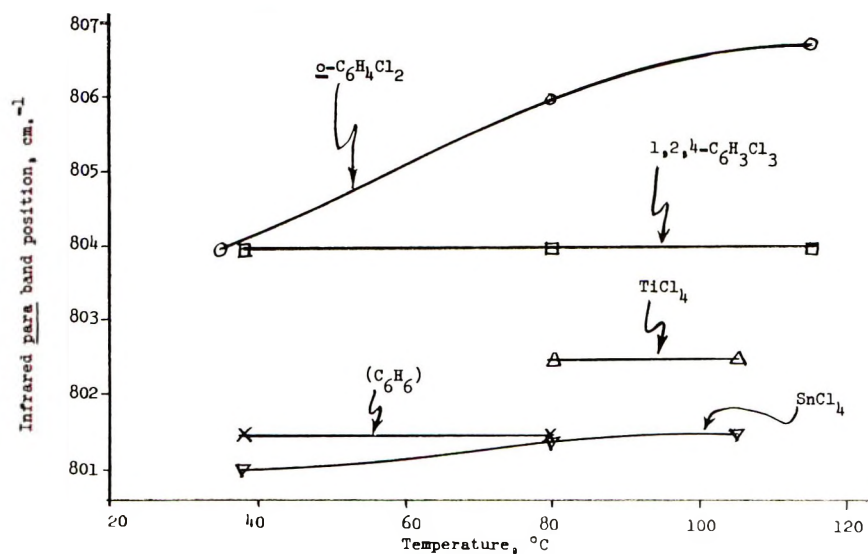


Fig. 5. Infrared *para* band position of the polymer vs. reaction temperature. Polymerization at solvent/C₆H₆ = 12 for 18 min.

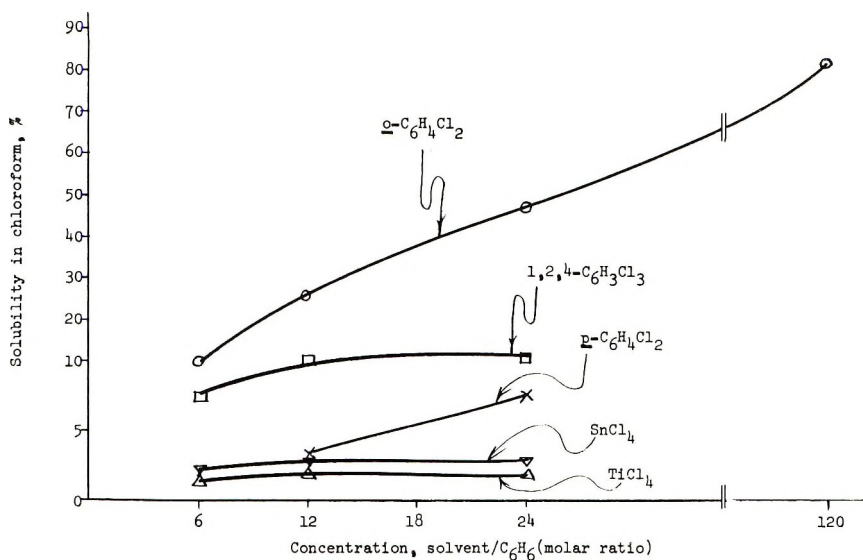


Fig. 6. Polymer solubility in chloroform vs. benzene concentration. Polymerization at 80°C. for 18 min.

Since our work concerns an aromatic monomer, it is reasonable to expect that the temperature-dependent reactions which compete with propagation may differ somewhat from those involved in the olefin systems. The decrease in molecular weight at higher temperatures in the benzene polymerization may be due to the increased importance of one or more of the following factors: (1) depropagation; (2) proton loss from the propagating carbonium ion; (3) termination by interaction of the growing end with a Lewis base, e.g., the solvent or chloride; (4) hydride abstraction involving the growing carbonium ion and an intermediate nonaromatic (e.g., cyclohexadiene) structure.

Concentration Effect. In the investigation of this variable, polymerizations were run at 80°C. for 18 min. at solvent/benzene ratios varying from 6 to 24 (occasionally 120). In general, with the various diluents there was a decrease in molecular weight with decreasing benzene concentration (Figs. 6–8). Usually the curves leveled out asymptotically. At the different concentration levels, the solvent effectiveness in decreasing the molecular weight was, *o*-C₆H₄Cl₂ > 1,2,4-C₆H₃Cl₃ > *p*-C₆H₄Cl₂ > SnCl₄. There was comparatively little change in molecular weight when the ratio was altered from 12 to 24 in the *p*-dichlorobenzene and 1,2,4-trichlorobenzene systems, in contrast with the other solvents. It is interesting that the polymers prepared in carbon disulfide displayed only a comparatively slight decrease in molecular weight over the dilution range studied at 35–40°C. (Table VI). The titanium tetrachloride data, although included, were not interpreted.

Since the polymer prepared at high dilution in *o*-dichlorobenzene (*o*-C₆H₄Cl₂/C₆H₆/AlCl₃/CuCl₂ = 120/1/1/0.5 at 80°C. for 18 min.) demon-

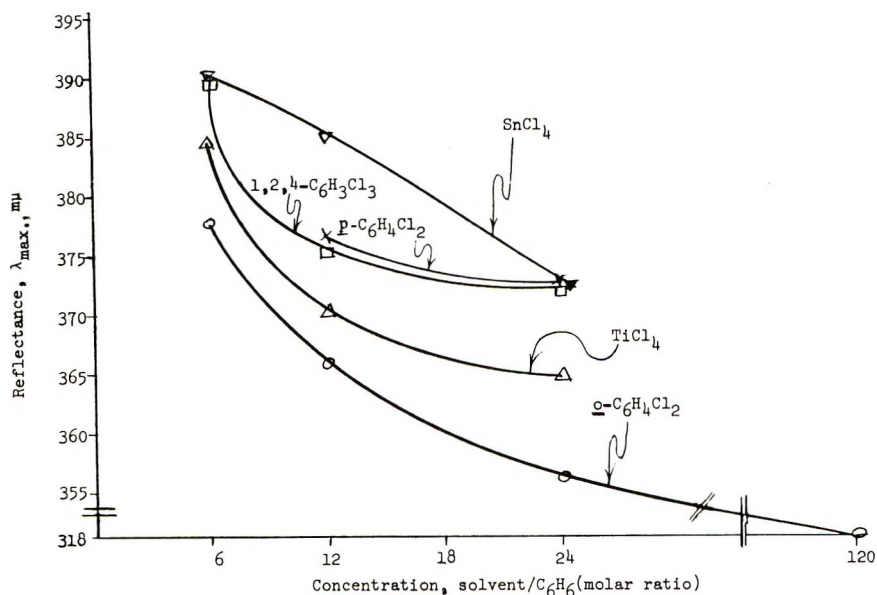


Fig. 7. Polymer reflectance vs. benzene concentration. Polymerization at 80°C. for 18 min.

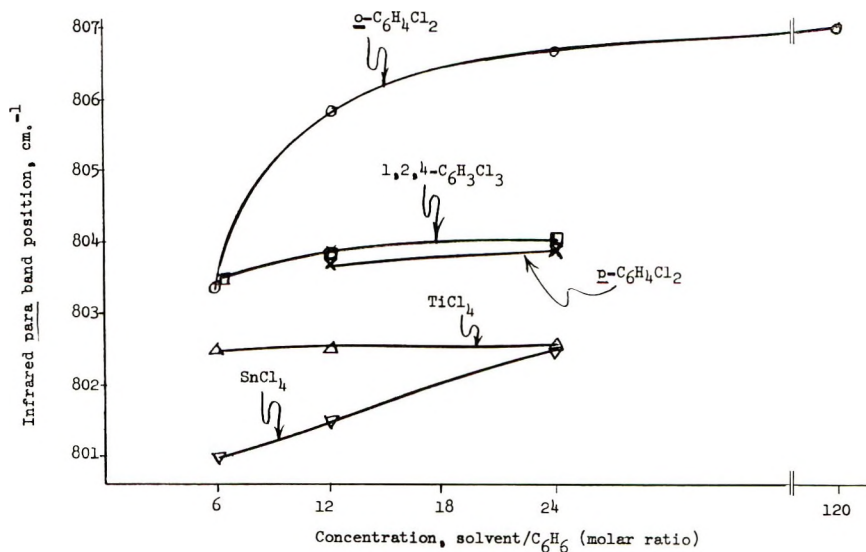


Fig. 8. Infrared *para* band position of the polymer vs. benzene concentration. Polymerization at 80°C. for 18 min.

strated high solubility (77% in chloroform at room temperature), molecular weight determinations were carried out by vapor pressure osmometry. An average value of about 460 was obtained, corresponding to the presence of 5-6 benzene units per chain.

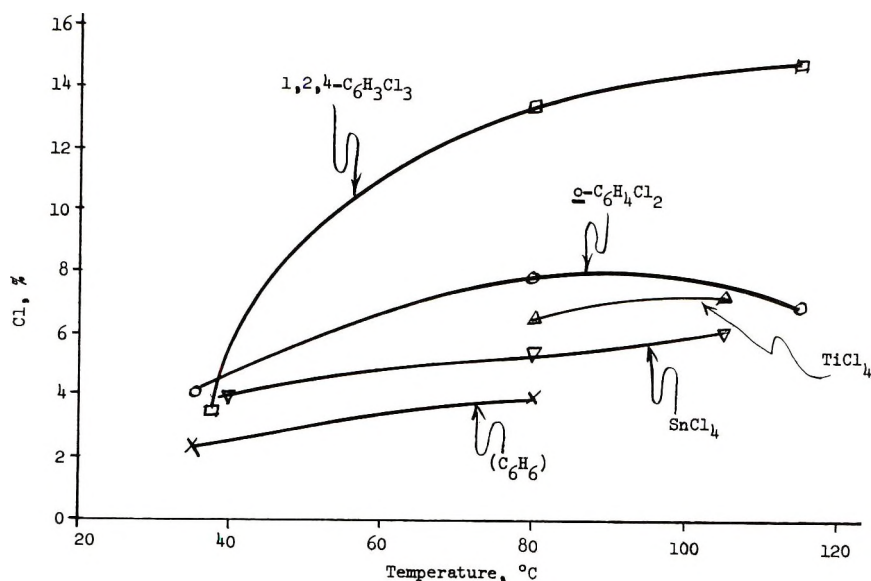


Fig. 9. Chlorine content of the polymer vs. reaction temperature. Polymerization at solvent/ C_6H_6 = 12 for 18 min.

Rather extensive studies on the subject of variation in degree of olefin polymerization with concentration indicate that the situation is complex.^{31b, 38}

Effect of Time. The effect of time on relative molecular weight was studied in the undiluted system at 80°C. (Table VII), and in carbon disulfide at 35–40°C. (Table VI). In both cases, a slight increase in molecular weight with increasing time was indicated by the reflectance technique, while essentially no change with time was observed by solubility and infrared measurements.

TABLE VII
Polymerization of Benzene Neat at 80°C.^a

Time, min.	Yield, %	Cl, %	C/(H + Cl), atomic ratio	Solubility CHCl ₃ , %	Infrared <i>para</i> band position, cm. ⁻¹	Reflectance λ _{max} , mμ
3.5	61	4.1	1.46	1.6	801	385
9	73	—	1.45	2	801	386
18	81	4.1	1.48	2	801.5	388
60	82	4.2	1.46	2	801	390

^a $C_6H_6/AlCl_3/CuCl_2 = 13/1/0.5$ (molar).

Chlorine Content

In general the chlorine content of the polymers increased with temperature (Fig. 9). The chlorination reaction, presumably effected by $CuCl_2$ –

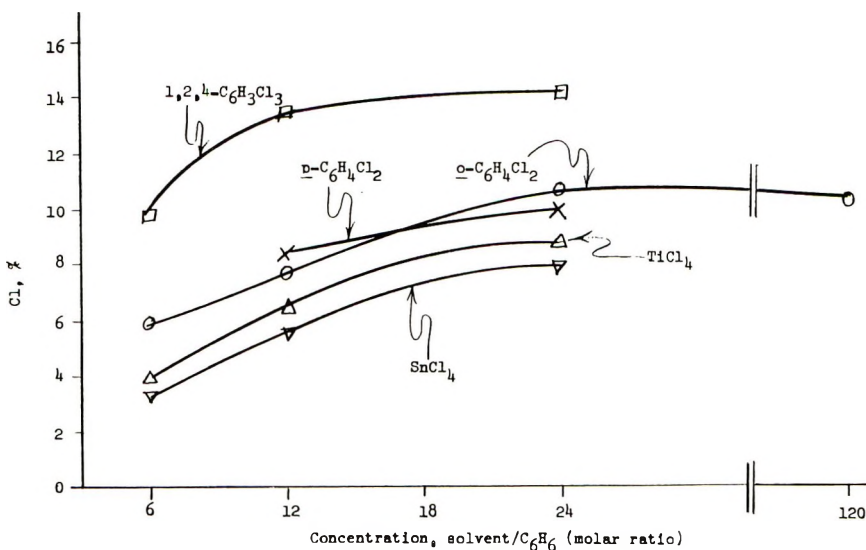


Fig. 10. Chlorine content of the polymer vs. benzene concentration. Polymerization at 80°C., for 18 min.

AlCl_3 , is relatively sluggish and strongly temperature-dependent. At about 40°C., the halogen content was uniformly low (2–4% in all cases). Extent of halogenation at higher temperatures was influenced by solvent in the following order: 1,2,4- $\text{C}_6\text{H}_3\text{Cl}_3 > o\text{-C}_6\text{H}_4\text{Cl}_2 > \text{TiCl}_4 > \text{SnCl}_4$.

The degree of chlorination also increased with decreasing concentration of benzene in the polymerization at 80°C. (Fig. 10). The effect of the medium decreased in the order: 1,2,4- $\text{C}_6\text{H}_3\text{Cl}_3 > o\text{-}$ and $p\text{-C}_6\text{H}_4\text{Cl}_2 > \text{TiCl}_4 > \text{SnCl}_4$. On the other hand, in carbon disulfide at 35–40°C., there was essentially no change with changing concentration (Table VI).

Since molecular weight decreases with decrease in benzene concentration and increase in temperature, apparently the shorter chains are more susceptible to chlorination. If halogen is incorporated during termination, then chlorine content would rise with decrease in molecular weight. The propagating carbonium ion could conceivably interact with chloride or the haloaromatic.

C/(H + Cl) Atomic Ratio

As mentioned previously, the limiting value of C/(H + Cl) for chlorine-containing p -polyphenyl is 1.5. It was observed that certain conditions led to the formation of polymers possessing ratios appreciably higher than 1.5. The nature of the solvent has an important bearing. C/(H + Cl) ratios increased according to the following order of the solvents, $\text{TiCl}_4 > \text{SnCl}_4 > \text{CS}_2 > 1,2,4\text{-C}_6\text{H}_3\text{Cl}_3 > o\text{-C}_6\text{H}_4\text{Cl}_2 > (\text{C}_6\text{H}_6)$ (Tables IV and V). It should be emphasized that the aromatic solvents are most effective in providing relatively low ratios, with neat benzene being the best.

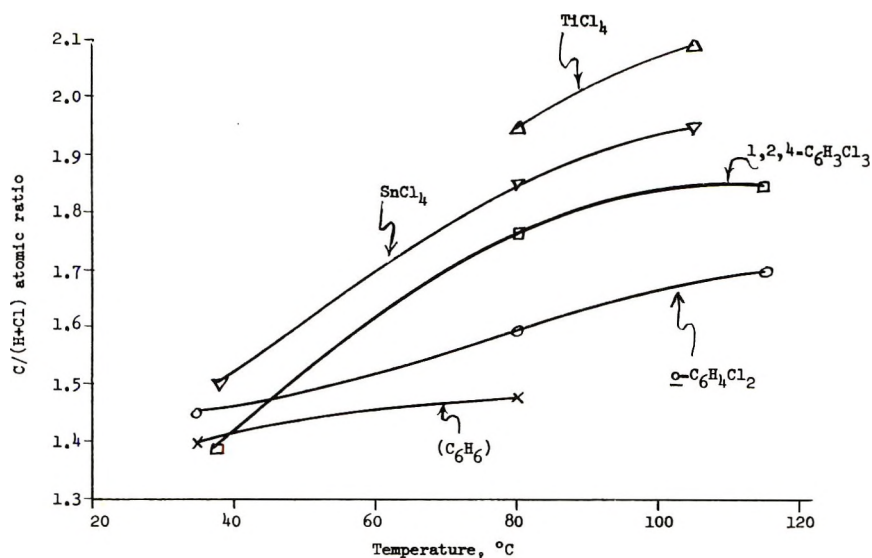


Fig. 11. C/(H + Cl) ratio of the polymer vs. reaction temperature. Polymerization at solvent/C₆H₆ = 12 for 18 min.

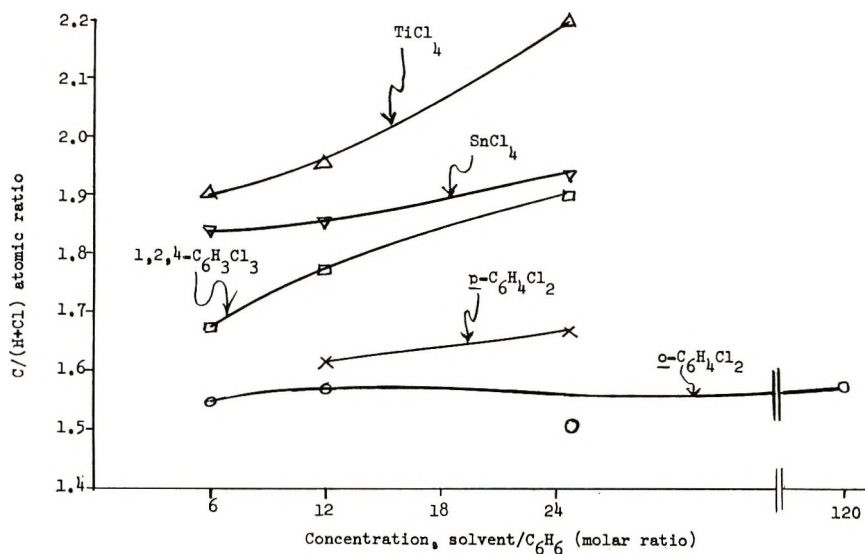


Fig. 12. C/(H + Cl) ratio of the polymer vs. benzene concentration. Polymerization at 80°C. for 18 min.

In addition, the C/(H + Cl) ratio increased with increasing temperature (Fig. 11). In all systems at low temperatures, values close to theory, 1.5, were obtained. For the polymerizations carried out at 80°C., in general there was an increase in the ratio with decreasing concentration (Fig. 12). Use of *o*-dichlorobenzene resulted in the smallest deviation from theory with

change in concentration. For some unknown reason, the effect of carbon disulfide (Table VI) was opposite to that of the other solvents.

In studies carried out in carbon disulfide, the $C/(H + Cl)$ ratio increased with increasing time (Table VI). However, there was essentially no change with time in the neat benzene system (Table VII).

Unexpectedly high $C/(H + Cl)$ ratios for benzene polymers have been observed previously. It is known that the nature of the metal halides used in the polymerization has an important influence.²⁻⁴ Although the exact cause of the high ratios is not known, it would appear that the increase results from the formation of polynuclear structures. Apparently *p*-polyphenyl is generated initially, and then polynuclear formation follows under the appropriate conditions.^{6,7} There is a limited amount of evidence indicating that the subsequent reaction involves benzene and *p*-polyphenyl.⁴

Color

The color of the polymers varied from brown to black. In general, polymers prepared at higher reaction temperatures were darker in color. A correlation exists between color darkening, increasing $C/(H + Cl)$, and chlorine content. It is noteworthy that polynuclear structures are stronger chromophores than polyphenyls. Apparently, the presence of chlorine contributes to the dark color.

Yield

The yield values, adjusted for the chlorine present, refer to the parent hydrocarbon polymers. Yields increased with increase in temperature

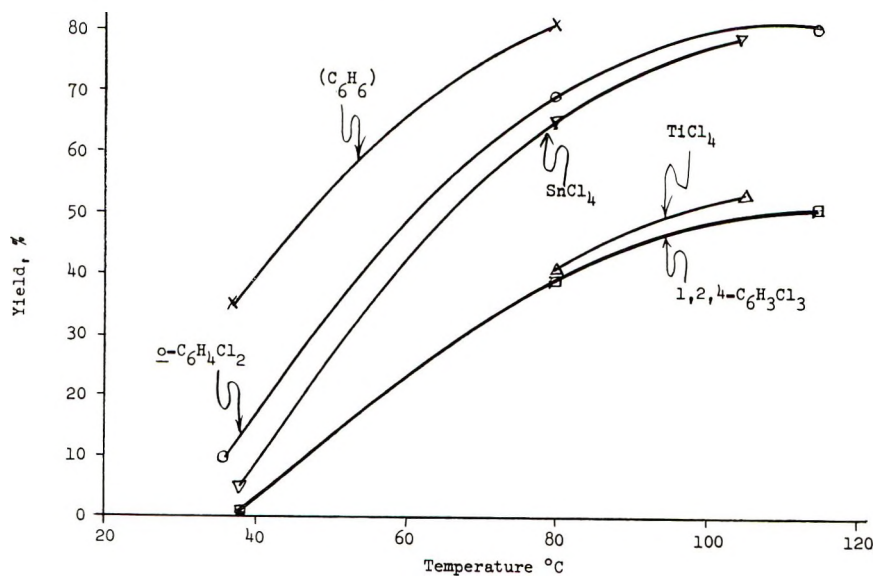


Fig. 13. Polymer yield vs. reaction temperature. Polymerization at solvent/ $C_6H_6 = 12$ for 18 min.

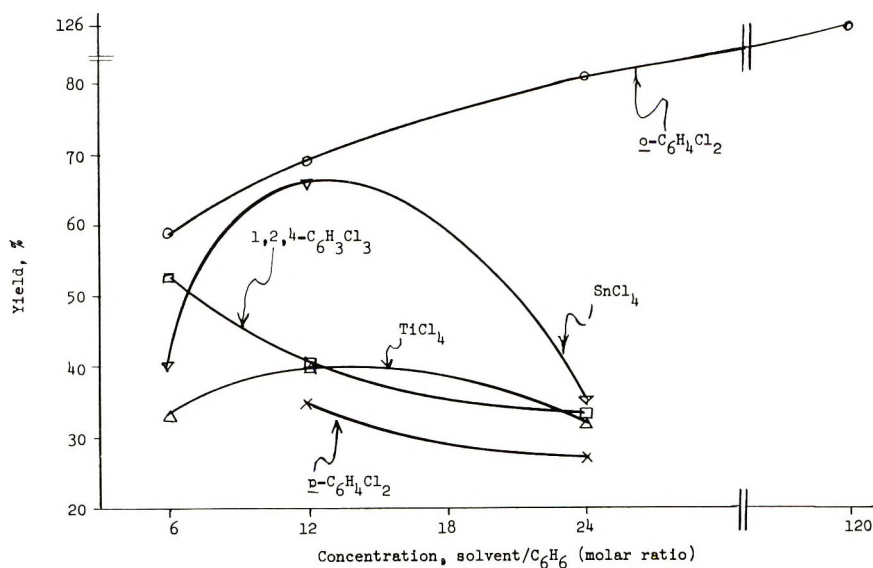


Fig. 14. Polymer yield vs. benzene concentration. Polymerization at 80°C. for 18 min.

(Fig. 13) and time (Tables VI and VII). The nature of the solvent correlated with yield as follows: (C₆H₆) > CS₂ > *o*-C₆H₄Cl₂ > SnCl₄ > TiCl₄ > 1,2,4-C₆H₃Cl₃. Interesting results were obtained from the investigation of concentration (Fig. 14, Table VI). In certain cases (*p*-C₆H₄Cl₂, 1,2,4-C₆H₃Cl₃, and CS₂), yield decreased with decreasing concentration which is characteristic of a reaction proceeding according to second- or higher-order kinetics.³⁹ On the other hand, yield increased with decreasing concentration in *o*-dichlorobenzene. The curves passed through a maximum in the case of stannic chloride and titanium tetrachloride.

The shapes of some of the curves, particularly for *o*-dichlorobenzene, may be artifacts due to the method of calculating yield. Data were obtained based on the following stoichiometry:



However, the stoichiometry changes with alteration in molecular weight. As is evident, the yield base is quite different in the case of a low molecular weight *p*-polyphenyl, such as, *p*-sexiphenyl.



EXPERIMENTAL

Materials

Reagent grade, thiophene-free benzene (Mallinckrodt) and mesitylene (Eastman) were dried over sodium and redistilled. *o*-Dichlorobenzene and

1,2,4-trichlorobenzene (Eastman) were distilled over calcium hydride before use. Anthracene (Aldrich) was purified by co-distillation from ethylene glycol. *p*-Quinquephenyl (K & K) was sublimed and then crystallized from pyridine. *p*-Sexiphenyl⁴⁰ was sublimed and crystallized from 1,2,4-trichlorobenzene, m.p. 464–467°C.

General Procedure for Polymerization of Benzene in Solvent by Aluminum Chloride–Cupric Chloride

The apparatus consisted of a three-necked flask fitted with paddle stirrer, condenser, thermometer, and gas-inlet tube. A solution of benzene (0.25 mole) and solvent (3 moles) was placed under an atmosphere of dry nitrogen. Anhydrous aluminum chloride (0.25 mole) was quickly weighed and added with stirring. The temperature was then raised to 80°C. and the flow of nitrogen adjusted to about 200 ml./min. After the anhydrous cupric chloride (0.125 mole) was introduced, time was followed with a stopwatch and the evolved hydrogen chloride titrated with standard base. After 18 min., the greenish-black mixture was quickly stirred with 500 ml. of ice-cooled 18% hydrochloric acid, and then steam-distilled. With titanium tetrachloride as solvent, the reaction mixture was boiled with concentrated hydrochloric acid (500 ml.) and filtered. The residue from either procedure was pulverized briefly with water in a blender and triturated with concentrated hydrochloric acid until the filtrate was colorless. In the case of stannic chloride, the residue was also heated at the boil with 10% caustic for 10–15 min. followed by treatment with 18% hydrochloric acid. In all cases final washings were made with boiling water until the test for chloride was negative.

The crude product, usually a brown to black powder, was dried overnight at 110–120°C. Yield is based on cupric chloride and calculated as pure polyphenyl (adjustment for chlorine content).

Analytical Procedures

Elemental Analyses. Carbon, hydrogen and chlorine analyses were performed in duplicate by Drs. Weiler and Strauss, Oxford, England or by Schwarzkopf Laboratory, Woodside, New York. Usually no residue was found upon combustion of the polymer.

Infrared Analyses. The potassium bromide technique was used. Usually only the region of interest (900–650 cm.^{-1}) was scanned with a Beckman IR-8 spectrophotometer.

Reflectance Measurements

The pellets were made by mixing (usually more than four times) 10 mg. of polymer with 1 g. of magnesium oxide in a Wig-L-Bug amalgamator followed by pressing the powder in a die of 1 in. diameter under 1500–2000 psi for several minutes. Both the particle size and homogeneity are important variables. The diffuse reflectance spectrum was obtained with a

Beckman DK-2 spectrophotometer. A deuterium lamp was used for the 220–360 $m\mu$ region and a tungsten lamp for the 360–450 $m\mu$ range.

Molecular Weight Determinations

The molecular weight of the chloroform soluble (at room temperature) fraction of the polymer was determined with a Mechrolab 301A vapor pressure osmometer in various solvents. The soluble portion of the polymer prepared in *o*-dichlorobenzene ($o\text{-C}_6\text{H}_4\text{Cl}_2/\text{C}_6\text{H}_6 = 120, 80^\circ\text{C.}, 18 \text{ min.}$) gave molecular weights of 450 in benzene and 475 in tetrahydrofuran, corresponding to an average of 5.3–5.6 benzene units per chain. Adjustment was made for the chlorine content in calculation of the average number of benzene units per chain.

Solubility in Chloroform

About 1 g. of the finely powdered polymer was weighed (three significant figures) into a predried, fritted, Pyrex thimble of known weight. After exposure to chloroform for 13 hr. in a Soxhlet extractor, the residue and thimble were dried first in air and then overnight at 110–120°C. The weight of the chloroform-insoluble portion was then calculated. After distillation of the chloroform from the extract, the residue was dried overnight at 110–120°C. and weighed as the chloroform-soluble fraction. The handling loss was usually 2–5%. In some cases the solubility was measured at room temperature.

Dechlorination with Sodium

In a three-necked, 125-ml. flask fitted with a 20,000 cpm Labline Stir-O-Vac stirrer, thermometer, and calcium chloride drying tube, a mixture of polymer (2 g.), sodium (2–6 g.) and mesitylene (50 ml.) was heated to gentle reflux (160°C.) while stirring was gradually increased to the rated speed. After 5 hr. the mixture was cooled, treated with an excess of isopropyl alcohol, neutralized with dilute hydrochloric acid and steam distilled. The residue, after treatment with boiling water, was dried overnight at 110–120°C.

Chlorination with Antimony Pentachloride

The apparatus consisted of a three-necked, 500-ml. flask equipped with paddle stirrer, thermometer, and condenser. A mixture of polymer (0.65 mole), antimony pentachloride (0.65 mole), and antimony trichloride (200 g.) was heated with stirring at 75°C. for 5 hr., then cooled and treated with concentrated hydrochloric acid. The residue was filtered, washed with water, and dried overnight at 110–120°C.; yield 96% (based on polymer). With 0.15 mole of antimony pentachloride the yield was 91%.

Oxidation with Chromic Anhydride

Polymer prepared in *o*-dichlorobenzene ($o\text{-C}_6\text{H}_4\text{Cl}_2/\text{C}_6\text{H}_6 = 12, 80^\circ\text{C.}, 18 \text{ min.}$) was oxidized. A solution of chromic anhydride (30 g.) in 40%

acetic acid (30 ml.) was added to the polymer (3 g.) suspended in glacial acetic acid (170 ml.). The mixture was stirred at reflux (107°C.) for 3 hr., cooled, and diluted with 40 ml. of 18% hydrochloric acid. The precipitated acids were filtered, washed with 5% hydrochloric acid (30 ml.), and suction-dried; yield, 0.32 g. After esterification with diazomethane, the solid residue (0.23 g.) of methyl esters was removed by filtration. An ethereal solution of the residue was analyzed with an Aerograph A-90-P2 gas chromatograph, with a 5 ft \times 1/4 in. copper column packed with 20% GE-SF-96 on 60/80 firebrick, with a helium flow rate of 100 ml./min. at 195°C. The indicated fractions were collected and identified by comparison of their retention times and infrared spectra with those of the authentic materials (component, retention time, relative peak areas): methyl *p*-chlorobenzoate, 2.2 min., 1; dimethyl terephthalate, 5.2 min., 24.4.

The combined filtrate and washings of the oxidation product were extracted with three, 100-ml. aliquots of ligroin (30–60°C.). After the extract was dried over anhydrous sodium sulfate, evaporation gave slightly yellow crystals, 0.07 g. Esterification and gas chromatographic analysis gave the following esters (component, retention time, relative peak areas): methyl benzoate, 1.2 min., 8; methyl *p*-chlorobenzoate, 2.2 min., 13.5; methyl 3,4-dichlorobenzoate, 4.4 min., 1.

Polymer prepared in 1,2,4-trichlorobenzene ($1,2,4\text{-C}_6\text{H}_3\text{Cl}_3/\text{C}_6\text{H}_6 = 12$, 80°C., 18 min.) was oxidized. A similar procedure yielded 0.9 g. of ligroin-insoluble and 0.4 g. of ligroin-soluble acids. Esterification and identification of the products were carried out as described in the preceding section. Methyl benzoate, methyl *p*-chlorobenzoate, and dimethyl terephthalate were identified. Four unknown esters with retention times at 3.2, 4.2, 6.2, and 7.4 min. were collected. The retention times and infrared spectra of the esters did not correspond to those of methyl 3,4-dichlorobenzoate.

We are grateful to the Petroleum Research Fund, administered by the American Chemical Society, for support of this work, and to Professor J. Reid Shelton for helpful suggestions and discussions.

This paper is abstracted from the Ph.D. thesis of Li-Chen Hsu, Case Institute of Technology, 1965.

References

1. Kovacic, P., and A. Kyriakis, *Tetrahedron Letters*, **1962**, 467.
2. Kovacic, P., and A. Kyriakis, *J. Am. Chem. Chem.*, **85**, 454 (1963).
3. Kovacic, P., and R. M. Lange, *J. Org. Chem.*, **28**, 968 (1963).
4. Kovacic, P., and F. W. Koch, *J. Org. Chem.*, **28**, 1864 (1963).
5. Kovacic, P., and J. Oziomek, *J. Org. Chem.*, **29**, 100 (1964).
6. Kovacic, P., F. W. Koch, and C. E. Stephan, *J. Polymer Sci.*, **A2**, 1193 (1964).
7. Kovacic, P., and C. Wu, *J. Polymer Sci.*, **47**, 45 (1960).
8. Pepper, D. C., *Friedel-Crafts and Related Reactions*, G. A. Olah, Ed., Interscience, New York, 1964, Vol. II, Chap. 30.
9. Overberger, C. G., and M. G. Newton, *J. Am. Chem. Soc.*, **82**, 3622 (1960).
10. Tokura, N., R. Asami, M. Matsuda, and H. Negishi, *Kogyo Kagaku Zasshi*, **64**, 717 (1961).

11. Tokura, N., M. Matsuda, and Y. Ogawa, *J. Polymer Sci.*, **A1**, 2965 (1963).
12. Overberger, C. G., P. J. Ehrig, and R. A. Marcus, *J. Am. Chem. Soc.*, **80**, 2456 (1958).
13. Higashimura, T., and S. Okamura, *Kobunshi Kagaku*, **13**, 342 (1956); *ibid.*, **17**, 57 (1960).
14. Zlamal, Z., A. Kazda, *J. Polymer Sci.*, **A1**, 3199 (1963).
15. Flett, M. St. C., and P. H. Plesch, *J. Chem. Soc.*, **1952**, 3355.
16. Throssell, J. J., S. P. Good, M. Szwarc, and V. Stannet, *J. Am. Chem. Soc.*, **78**, 1122 (1956).
17. Kennedy, J. P., I. Kirshenbaum, R. M. Thomas, and D. C. Murray, *J. Polymer Sci.*, **A1**, 331 (1963).
18. Flory, P. J., *Principles of Polymer Chemistry*, Cornell Univ. Press, Ithaca, N. Y., 1953, pp. 341-342.
19. Bauman, R. P., *Absorption Spectroscopy*, Wiley, New York, 1962, p. 184.
20. Jozefowicz, M., Ph.D. thesis, University of Paris, 1963.
21. Friedel, R. A., and M. Orchin, *Ultraviolet Spectra of Aromatic Compounds*, Wiley, New York, 1951.
22. Gillam, A. H., and D. H. Hey, *J. Chem. Soc.*, **1939**, 1170.
23. Dewar, M. J. S., *J. Chem. Soc.*, **1952**, 3544.
24. Davydov, A. S., *Zh. Ekspl. Teoret. Fiz.*, **18**, 515 (1948).
25. Jaffe, H. H., and M. Orchin, *Theory and Applications of Ultraviolet Spectroscopy*, Wiley, New York, 1962, p. 275.
26. Kovacic, P., and A. K. Sparks, *J. Org. Chem.*, **26**, 1310 (1961).
27. Kern, W., and O. H. Wirth, *Kunststoffe-Plastics*, **6**, 12 (1958).
28. Gillam, A. E., and E. S. Stern, *Electronic Absorption Spectroscopy*, Arnold, London, 1954, p. 44.
29. Ware, J. C., and E. E. Borchert, *J. Org. Chem.*, **26**, 2263, 2267 (1961).
30. *Beckman Instruction Manual 553-B*, Beckman Instruments, Inc., Fullerton, California, 1960, p. 18.
31. Plesch, P. H., ed., *The Chemistry of Cationic Polymerization*, MacMillan, New York, 1963, (a) Chap. 3; (b) Chap. 4; (c) Chap. 6; (d) Chap. 7; (e) Chap. 9.
32. National Research Council, *International Critical Tables*, McGraw-Hill, New York, 1926-1930, Vol. VI.
33. Musset, E., A. Nikuradse, and R. Ulbrich, *Z. Angew. Phys.*, **8**, 8 (1956).
34. *Handbook of Chemistry and Physics*, 43rd Ed., Chemical Rubber Publishing Co., Cleveland, Ohio, p. 2552.
35. Olah, G. A., and M. W. Meyer, in *Friedel-Crafts and Related Reactions*, G. A. Olah Ed., Interscience, New York, 1963, Vol. I, Chap. 8.
36. Kennedy, J. P., L. S. Minekler, and R. M. Thomas, *J. Polymer Sci.*, **A2**, 367 (1964).
37. Kennedy, J. P., and R. M. Thomas, *J. Polymer Sci.*, **55**, 311 (1961).
38. Plesch, P. H., *J. Chem. Soc.*, **1964**, 104.
39. Billmeyer, F. W., Jr., *Textbook of Polymer Science*, Interscience, New York, 1962, p. 278.
40. Kovacic, P., and R. M. Lange, *J. Org. Chem.*, **29**, 2416 (1964).

Résumé

Le poids moléculaire de *p*-polyphényle préparé à partir de benzène-chlorure d'aluminium-chlorure de cuivre, était influencé par le solvant, la concentration et la température. On a mesuré les poids moléculaires relatifs au moyen de la solubilité du polymère dans le chloroforme et par mesure infrarouge de la bande para et la réflectance λ_{mix} , dans la lumière ultraviolette. L'ordre d'efficacité des solvants du point de vue de la diminution du poids moléculaire est $o\text{-C}_6\text{H}_4\text{Cl}_2 > 1,2,4\text{-C}_6\text{H}_3\text{Cl}_3 > \text{SnCl}_4 \sim \text{CS}_2 > (\text{C}_6\text{H}_6)$. Une oxydation dégradante révèle que l'*o*-dichlorobenzène comme solvant était incorporé comme groupe terminal uniquement à un faible degré. En général, le poids moléculaire

laire du *p*-polyphényle, décroît avec une augmentation de température et une diminution de la concentration. On considère également les aspects théoriques.

Zusammenfassung

Das Molekulargewicht von *p*-Polyphenyl aus Benzol-Aluminiumchlorid-Kupferchlorid wurde durch Lösungsmittel, Konzentration und Temperatur beeinflusst. Relative Molekulargewichte wurden durch die Polymerlöslichkeit in Chloroform sowie durch die Lage der Infrarot-para-Bande und des λ_{\max} des Ultraviolettreflexionsvermögens bestimmt. Die Reihenfolge der Lösungsmittelwirksamkeit bei der Herabsetzung des Molekulargewichts war: *o*-C₆H₄Cl₂ > 1,2,4-C₆H₃Cl₃ > SnCl₄ ~ CS₂ > (C₆H₆). Der oxydative Abbau zeigte, dass *o*-Dichlorbenzol nur zu einem geringen Ausmass als Endgruppe eingebaut wurde. Im allgemeinen nahm das Molekulargewicht von *p*-Polyphenyl mit steigender Temperatur und fallender Konzentration ab. Die theoretischen Aspekte werden diskutiert.

Received March 18, 1965

Revised June 18, 1965

Prod. No. 4776A

Co^{60} γ -Radiation-Induced Copolymerization of Ethylene and Carbon Monoxide

P. COLOMBO, L. E. KUKACKA, J. FONTANA, R. N. CHAPMAN, and M. STEINBERG, *Brookhaven National Laboratory, Upton, L. I., New York*

Synopsis

The γ -radiation-induced free-radical copolymerization of ethylene and CO has been investigated over a wide range of pressure, initial gas composition, radiation intensity, and temperature. At 20°C., concentrations of CO up to 1% retard the polymerization of ethylene. Above this concentration the rate reaches a maximum between 27.5 and 39.2% CO and then decreases. The copolymer composition increases only from 40 to 50% CO when the gas mixture is varied from 5 to 90% CO. A relatively constant reactivity ratio is obtained at 20°C., indicating that CO adds 23.6 times as fast as an ethylene monomer to an ethylene free-radical chain end. For a 50% CO gas mixture, the above value of 23.6 and the copolymerization rate decrease with increasing temperature to 200°C. The kinetic data indicate a temperature-dependent depropagation reaction. Infrared examination of copolymers indicates a polyketone structure containing $-\text{CH}_2-\text{CH}_2-$ and $-\text{CO}-$ units. The crystalline melting point increases rapidly from 111 to 242°C., as the CO concentration in the copolymer increases from 27 to 50%. Molecular weight of copolymer formed at 20°C. increased with increasing CO, indicating \bar{M}_n values $>20,000$. Increasing reaction temperature results in decreasing molecular weight. Onset of decomposition for a 50% CO copolymer was measured at $\approx 250^\circ\text{C}$.

INTRODUCTION

An extensive study of Co^{60} γ -radiation-induced copolymerization reactions involving ethylene and other monomers¹ indicated that a more detailed study of the ethylene-CO system would be of interest. The peroxide-initiated copolymerization of ethylene and CO has been reported.^{2,3} The γ -radiation-induced copolymerization of ethylene and CO has been investigated over a limited range of conditions.⁴⁻⁷ In a previous paper⁸ a brief report was made of the monomer reactivity for this system at 20°C. The present paper presents an experimental investigation, an interpretation of the copolymerization rates over a wide range of pressure, temperature, and radiation intensity, and an evaluation of some of the properties of the copolymers formed.

EXPERIMENTAL

The polymerizations were carried out in 1-in. I.D., 100-cc. internal volume, high-pressure, stainless steel reaction vessels. The reaction

TABLE I
 Co^{60} γ -Radiation Copolymerization of Ethylene and CO. Summary of Experimental Conditions and Calculated Results

Expt. no.	Radiation			Temp. t , °C.	Radiation dose D $\times 10^3$, rads	Product composition, % CO	$\alpha = 1/\eta$	Yield Y , g./l.	Conversion, %	Overall rate R , g./l.-hr.	Overall G value, molecules/100 e.v.
	Initial concn., % CO	Intensity I $\times 10^3$, rads/hr.	Pressure P , atm.								
K-35 ^a	0.0	2.17	680	20	1.0	0.0	—	38.5	7.2	83.5	26,700
CO-A	50.0	2.17	680	20	6.51	47.52	9.61	3.4	0.7	1.1	376
CO-1	50.0	2.17	680	21	7.8	48.90	23.81	9.8	2.1	2.7	910
CO-1A	50.0	2.17	680	20	7.8	48.20	14.18	25.4	4.9	6.8	2,270
CO-2	50.0	2.17	680	20	15.2	47.05	8.00	70.9	14.0	10.1	3,180
CO-3	50.0	2.17	680	21	11.25	48.59	18.45	94.0	17.5	18.2	6,000
CO-4	50.0	2.17	680	20	30.0	46.94	7.57	369.0	52.2	26.7	8,860
CO-5	50.0	2.17	680	20	25.0	47.92	12.30	428.0	57.6	37.2	12,300
CO-6	50.0	2.17	340	20	11.25	47.51	8.53	53.2	12.9	10.3	4,550
CO-7	50.0	2.17	170	21	11.25	47.71	9.33	36.0	10.8	6.9	3,720
CO-9	50.0	0.76	340	21	11.25	48.99	24.39	79.5	17.9	5.4	6,680
CO-10	81.3	2.17	170	21	11.25	49.24	7.40	4.8	2.1	0.9	665
CO-11	81.3	2.17	340	32	11.25	49.41	9.58	13.2	4.1	2.5	1,320
CO-11A	81.3	2.17	340	22	11.25	48.97	5.48	12.1	3.5	2.3	1,117
CO-12	81.3	2.17	680	24	11.25	49.85	38.33	13.9	3.0	2.7	934
CO-12A	81.3	2.17	680	22	11.25	48.73	4.42	15.7	3.3	3.0	1,048
CO-13	94.8	2.17	680	20	30.38	51.87	—	6.0	1.3	0.4	146
CO-14	12.6	2.17	170	22	3.1	42.97	21.25	6.7	1.8	4.7	2,030
CO-15	12.6	2.17	340	22	2.17	42.94	21.12	9.7	2.2	9.7	3,540
CO-16	12.6	2.17	680	22	1.29	43.55	23.48	14.6	2.9	24.5	7,800
CO-17	4.8	2.17	170	20	3.97	42.32	53.99	2.8	0.7	1.5	628
CO-18	4.8	2.17	340	20	2.71	42.66	56.98	10.6	2.4	8.5	3,000
CO-19	4.8	2.17	680	20	1.63	42.19	52.97	13.3	2.6	17.7	5,500

CO-20	50.0	2.03	340	28	11.2	48.73	19.42	80.0	21.6	14.5	6,640
CO-21	50.0	2.03	550	157	11.2	43.18	3.20	29.0	7.8	5.3	2,400
CO-22	50.0	2.03	470	100	11.2	47.60	10.00	43.0	11.6	7.8	3,560
CO-23	50.0	2.03	539	135	11.2	43.88	3.62	54.0	14.6	9.8	4,460
CO-47	50.0	2.03	406	66	7.86	47.26	8.62	52.0	13.7	13.4	6,020
CO-48	50.0	2.03	423	84	9.13	46.88	7.52	38.9	10.3	8.7	3,870
CO-49	50.0	2.03	498	136	10.0	45.87	5.56	49.6	13.2	10.1	4,276
CO-29	50.0	2.03	476	200	11.2	35.25	1.21	10.0	2.6	1.8	813
CO-24	3.3	2.17	680	20	1.7	43.16	92.43	6.3	1.2	8.0	2,510
CO-24A	2.1	2.17	680	21	1.6	35.12	53.01	5.2	1.0	6.8	2,160
CO-25	98.8	2.17	680	22	140.0	60.02	—	1.3	0.3	0.02	7
CO-27	98.7	2.17	680	20	75.22	56.24	—	3.0	0.6	0.1	30
CO-28	100.0	8.47	680	20	60.0	—	—	1.7	0.4	0.02	2.1
CO-31	2.1	2.03	476	135	1.52	21.98	12.65	0.8	0.2	1.2	449
CO-32	10.8	2.03	470	135	2.54	34.85	9.55	3.6	0.8	2.9	1,115
CO-33	3.7	2.17	680	23	1.09	38.74	44.23	5.6	1.1	11.3	3,600
CO-34	3.7	2.17	680	24	1.30	39.76	50.48	4.8	1.0	8.0	2,550
CO-35	1.1	2.17	680	20	1.98	1.93	1.75	4.0	0.8	4.4	1,392
CO-36	39.2	3.85	340	20	11.25	48.76	30.39	148.8	30.0	50.9	13,100
CO-37	39.2	2.17	680	20	11.25	48.64	27.68	579.0	69.0	111.5	36,800
CO-38	39.2	2.17	340	21	11.25	47.92	17.82	231.5	42.2	44.6	18,100
CO-39	39.2	0.76	340	20	11.25	47.46	14.49	308.0	51.0	20.8	23,900
CO-40	27.5	2.17	680	20	2.0	48.97	62.62	2.6	0.5	2.8	900
CO-41	27.5	2.17	680	21	4.0	48.52	43.11	118.9	21.4	64.4	21,200
CO-42	27.5	2.17	680	20	6.0	45.39	129.6	249.5	39.1	90.4	35,700
CO-43	27.5	2.17	680	20	5.0	46.64	18.26	169.2	28.6	73.4	23,900
CO-44	19.4	2.17	680	20	1.5	—	—	0.0	0.0	0.0	0
CO-45	19.4	2.17	680	20	3.0	—	—	0.3	0.1	0.2	70
CO-46	19.4	2.17	680	22	4.15	46.64	28.82	10.2	2.1	5.3	1,730

(continued)

TABLE I (continued)

Expt. no.	Initial conc., % CO	Radiation		Temp., t_r , °C.	Radiation dose D , $\times 10^6$, rads	Product composition, % CO	$\alpha = 1/\eta$	Yield Y , g./l.	Conversion, %	Overall rate R_r , g./l.-hr.	Overall G value, molecules/100 e.v.
		$\times 10^6$, rads/hr.	Pressure P , atm.								
CO-53	13.6	2.03	490	65	6.26	36.2	8.33	17.5	4.1	5.7	2,240
CO-55	13.6	2.03	674	155	5.4	33.74	6.50	16.4	3.9	6.2	2,500
CO-32-7 ^b	7.7	1.56	650	20	7.8	40.65	25.93	73.0	13.5	14.6	6,000
CO-32-8	22.5	1.56	650	20	7.8	45.25	16.38	21.0	3.7	4.2	1,650
CO-32-10	15.9	1.53	650	20	7.8	43.86	18.89	87.0	15.9	17.4	7,000
CO-32-12	18.9	1.53	650	20	7.8	46.30	26.81	62.0	11.1	12.4	5,000
CO-32-15	25.0	1.56	650	20	7.8	46.30	18.75	17.0	3.1	3.4	1,400
CO-32-17	9.2	1.56	650	20	7.8	41.49	23.85	121.0	22.2	24.2	9,800
CO-32-11	4.8	1.56	650	20	7.8	27.47	12.19	25.0	4.6	5.0	2,000
CO-32-22	2.0	1.56	650	20	7.8	29.76	35.66	43.0	7.9	8.6	3,500
CO-32-23	1.1	1.56	650	20	7.8	31.05	72.38	21.0	3.9	4.2	1,700

^a High-purity ethylene.^b Series (CO-32-7 to CO-32-23) are falling pressure experiments.

temperature was measured by using a thermocouple located in a well that extended into the center of the vessel. Pressure measurements were made with a strain gauge. The monomers were premixed in gas cylinders. High purity ethylene, supplied by Phillips Petroleum Co., contained, by volume, 99.9% C₂H₄, 600 ppm C₁-C₄ saturated hydrocarbons, and <5 ppm O₂. The prepurified CO supplied by Air Products and Chemicals Inc., contained 60 ppm O₂, 225 ppm N₂, 70 ppm H₂, <1 ppm H₂O, and 425 ppm CO₂.

A gas chromatographic analysis of the initial mixture was made prior to each run to determine gas composition and oxygen concentration. For ambient temperature experiments, the reaction vessel was placed directly in water in a pool-type γ facility with the Co⁶⁰ sources in a retracted position. The vessel was evacuated through a tube connected to the vessel and then charged with a gas mixture to the desired pressure by means of a stainless steel diaphragm compressor. The reaction was initiated by moving Co⁶⁰ sources into predetermined positions surrounding the vessel. Most of the experiments were carried out under constant pressure conditions maintained by a compressor feeding makeup gas during the course of the reaction. The induction periods for some experiments were determined by isolating the vessel from the compressor. The start of polymerization was noted by the initial decrease in pressure as indicated by the pressure gauge. Experiments at elevated temperatures were performed by placing a thermocouple-controlled resistance furnace around the vessel and inserting the entire assembly into a duct leading into the Co⁶⁰ pool source. The vessels were heated to the desired temperature prior to initiating the reaction.

The radiation energy absorbed by the mass of gas inside the reaction vessel was measured by using a Fricke dosimeter and secondary standard solar cells. The polymer, in the form of a solid white mass, was recovered from the vessel at the end of the experiment and weighed for determination of yield. Copolymer composition was based on elemental analyses for C, H, and O, from which mass balances for ethylene and CO were calculated. No homopolymer was found to be present in this series of experiments, as determined by infrared and calorimetric techniques.

RESULTS AND DISCUSSION

The results are discussed in terms of the kinetics of copolymerization followed by an evaluation of the properties of the copolymers formed. A summary of the experimental conditions and the calculated results for yield, rate, and G value are given in Table I. Care was taken in correlating the data to select those experiments in which only small changes in the initial gas mixture occurred during the reaction. The experiments in Table I that indicate high conversions were performed by using gas mixtures containing ethylene and CO in proportions such that the ratio of the two gases, as previously determined,⁸ did not appreciably change during the reaction time. Experiments at the higher conversions were conducted,

where possible, to obtain sufficient amounts of material for property evaluation.

Effect of Gas Composition on Copolymer Yield and Rate

For a constant gas composition and at constant conditions of temperature, pressure, and radiation intensity, increasing the irradiation time in successive experiments gives typical yield curves, shown in Figure 1. The data indicate that for a given irradiation time an increase in the CO concentration from 19.4 to 39.2% results in an increase in yield. Above this concentration to 81.3% CO the yield decreases. It should be noted that the induction periods decreased with increasing CO concentration between 19.4 and 39.2% and increased thereafter. From experience with the radiation-induced homopolymerization of ethylene,⁹ the O₂ concentration was kept below 60 ppm to minimize the length of the induction period. For this reason ethylene gas containing <5 ppm O₂ and CO containing 60 ppm of O₂ were used. In a low-temperature free-radical polymerization reaction, O₂ is known to be influential in determining the induction period. Therefore, as the CO concentration is successively increased, as indicated in Figure 1, the induction period should increase pro-

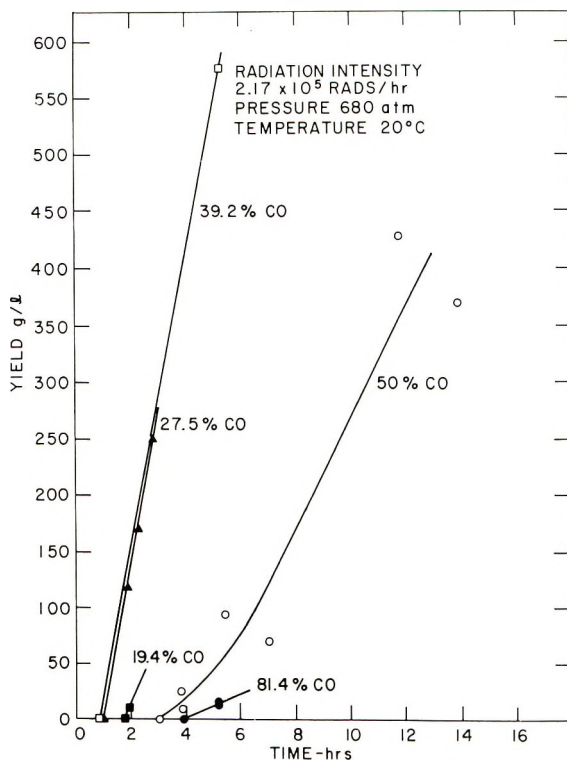


Fig. 1. Co⁶⁰ γ -copolymerization of ethylene and CO. Polymer yield vs. irradiation time.

portionally. The experimental results indicate that for variable O₂ concentrations, in the range of compositions used, the simple relationship between O₂ concentration and induction period does not hold. Induction periods decreased from 3.90×10^5 rads for the 19.4% CO to 1.75×10^5 rads for 39.2% CO and subsequently increased to 8.2×10^5 rads at 81.4% CO for the conditions shown in Figure 1.

The effect of gas composition, varying from 100% ethylene to 100% CO, on the differential copolymerization rate is shown in Figure 2. The differential rates in this figure were determined from the slopes of the typical yield curves shown in Figure 1.

At a pressure of 680 atm., temperature of 20°C., and radiation intensity of 2.17×10^5 rads/hr., the rate of polymerization of ethylene is ≈ 184 g./l.-hr. Addition of $\approx 1\%$ CO resulted in a marked decrease in polymerization rate to a value of 7.5 g./l.-hr. Further addition of CO up to a concentration of 39.2% increased the rate to a maximum of 133 g./l.-hr., corresponding to a G value of 42,000. Subsequent addition of CO resulted in a reduction in rate. A small, overall rate of 0.02 g./l.-hr and a G value of 2.1 were obtained for 100% CO gas. Similar effects based on fewer data were observed at 340 and 170 atm., as indicated in Figure 2. The dotted lines in the figure merely show trends in the data.

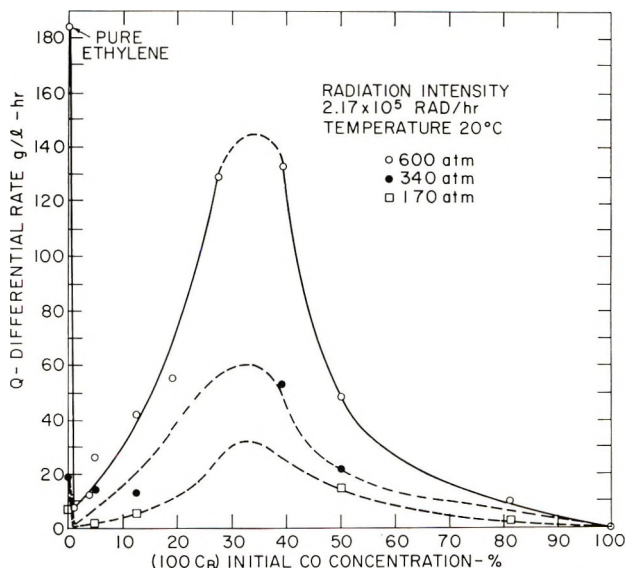


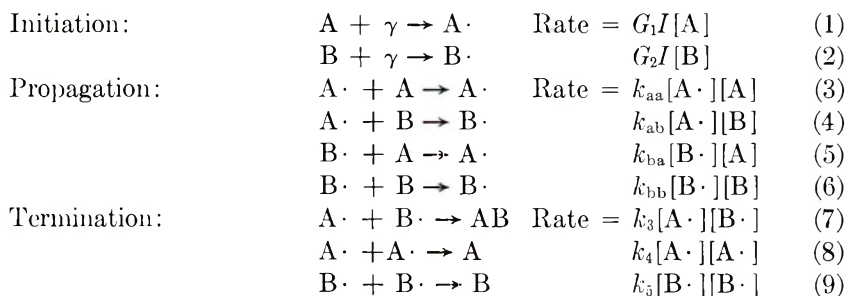
Fig. 2. Co⁶⁰ γ -copolymerization of ethylene and CO. Differential rate vs. CO concentration in initial gas mixture.

Copolymerization Kinetics

Previous studies^{2,3} on the copolymerization of ethylene and CO initiated by peroxide-type catalysts gave evidence that the reaction could proceed by a free-radical mechanism. It appeared that the radiation-induced

copolymerization of ethylene and CO could be interpreted in terms of a general mechanism developed for free-radical-initiated copolymerization reactions. However, the change in rate with gas composition noted under experimental conditions indicates more complicated kinetics than those suggested by classical free-radical copolymerization schemes. It is also important to note the complexities involved in the kinetics of static, heterogeneous-type, two-component gas-phase reactions. Adsorption of monomers by the polymer and trapping or occlusion of radicals in the precipitating polymer can strongly influence the mechanism. Because of the difficulties involved in the kinetic interpretation of heterogeneous systems, it was found convenient to assume, as a first approximation, a kinetic model based on homogeneous conditions. This model was used in an attempt to correlate the experimental data and to show where deviations from the model occur.

Denoting A as ethylene monomer, A· as an ethylene free radical, B as CO monomer, and B· as a CO free radical, the reactions (1)–(9) and corresponding rate equations can be considered.



In eqs. (1)–(9), the k 's are the reaction rate constants, and the concentrations (in brackets) are expressed in the usual molar concentration of reactant per unit volume. The rate constants for the radiation-initiated reactions are given in terms of the product of the G value for radical formation and the radiation intensity, I . In the initiation steps, the production of free radicals resulting from the interaction of gamma radiation with monomer proceeds with zero activation energy and is independent of the type of monomer. Therefore the rate constant for initiation, k_i , is temperature-independent and dependent only on the first power of intensity, i.e., $k_i = G_i I$, when G_i is the G value for radical formation. In considering a kinetic scheme of the type given, the following simplifying assumptions are usually made: (1) the chains are long, and therefore the monomer is consumed almost entirely in the propagation steps; (2) the rate constants are independent of radical size; (3) the concentration of each radical type remains constant during polymerization; (4) the rates of initiation and termination are equal.

With the above assumptions, the following kinetic equations have been derived for expressing the overall copolymerization rate^{10,11} and the in-

stantaneous copolymer composition, given as eqs. (10) and (11), respectively.

Copolymer rate equation:

$$\frac{-d([A] + [B])}{dt} = \frac{(r_1[A]^2 + 2[A][B] + r_2[B]^2)V_i^{1/2}}{(\delta_1^2 r_1^2 [A]^2 + 2\varphi\delta_1\delta_2 r_1 r_2 [A][B] + \delta_2^2 r_2^2 [B]^2)^{1/2}} \quad (10)$$

where

$$\begin{aligned} V_i &= \text{initial rate} = G_i I [A + B] \\ r_1 &= k_{aa}/k_{ab} \\ r_2 &= k_{bb}/k_{ba} \\ \delta_1^2 &= k_4/k_{aa}^2 \\ \delta_2^2 &= k_5/k_{bb}^2 \\ \varphi^2 &= k_3^2/k_4 k_5 \end{aligned}$$

Copolymer composition equation:

$$\frac{d[a]}{d[b]} = \left(\frac{[A]}{[B]} \right) \left(\frac{r_1[A] + [B]}{r_2[B] + [A]} \right) \quad (11)$$

where r_1 and r_2 are the reactivity ratios, $[a]/[b]$ is mole ratio of ethylene to CO in the copolymer, and $[A]/[B]$ is mole ratio of ethylene to CO in the initial monomer mixture.

From the experimental data it is noted that the homopolymerization of CO is negligibly small compared to that of ethylene. It thus can be assumed that $k_{bb} \approx 0$ and therefore r_2 approaches zero.

With the above assumption and substituting $\alpha = (1/r_1) = (k_{ab}/k_{aa})$ in eqs. (10) and (11), the following expressions are obtained

$$d[\text{cop}]/dt = G_i^{1/2} I^{1/2} k_{aa} ([A] + [B])^{1/2} ([A] + 2\alpha[B]) / (2k_4)^{1/2} \quad (12)$$

and

$$[a]/[b] = (1/\alpha)([A]/[B]) + 1 \quad (13)$$

It is convenient to express the gas concentrations in terms of the measured pressure. However, because of the nonideality of the gases at the experimental pressures and temperatures used, the compressibility of the gas mixture must be taken into account. If the assumption is made that the compressibility can be expressed as the sum of the product of concentration and compressibility of each gas, then

$$([A] + [B]) = P/ZRT \quad (14)$$

and

$$Z = C_A Z_A + C_B Z_B \quad (15)$$

where C is the concentration expressed in mole fraction, Z is the compressibility, R is the gas constant, and T is the absolute temperature. It should be noted that the molecular weights of ethylene and of CO are

equal, and therefore the mole fraction and weight fraction are equal. Collecting all independent constants into one constant, K , and inserting eqs. (14) and (15) into eq. (12), one obtains

$$d[\text{cop}]/dt = Kk_{aa}I^{0.5}(P/ZRT)^{1.5}(C_A + 2\alpha C_B) \quad (16)$$

The effect of temperature on the rate constants can be expressed in the form of the Arrhenius equation. Therefore,

$$k_{ab} = A_1 \exp \{-E_{ab}/RT\} \quad (17)$$

$$k_{aa} = A_2 \exp \{-E_{aa}/RT\} \quad (18)$$

where A_1 , A_2 are pre-exponential constants and E_{aa} and E_{ab} are activation energies.

α can then be expressed as a function of the activation energy of propagation.

$$\alpha = A_3 \exp \{(E_{aa} - E_{ab})/RT\} = A_3 \exp (\Delta E/RT) \quad (19)$$

On substituting the above expressions for k_{aa} and α into eq. (16), the following expression can be obtained.

$$d[\text{cop}]/dt = KA_2 \exp (-E_{aa}/RT)I^{0.5}(P/ZRT)^{1.5} \\ \times (C_A + 2C_B A_3 \exp \{(\Delta E/RT)\}) \quad (20)$$

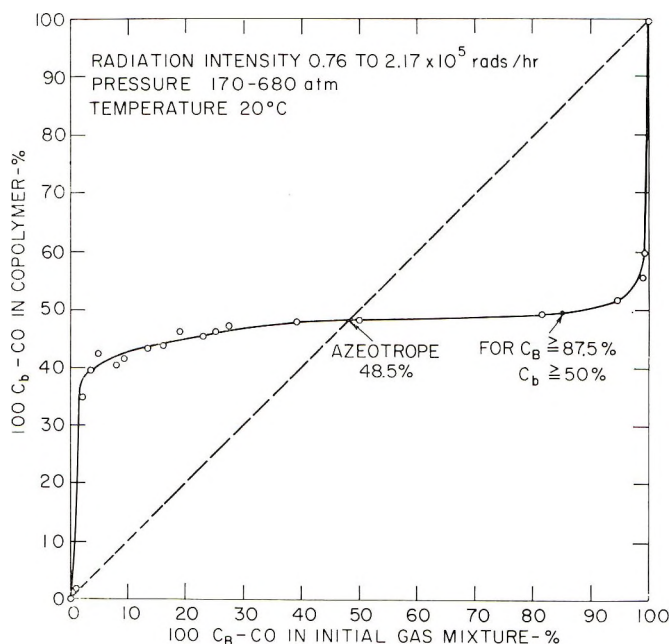


Fig. 3. Co^{60} γ -copolymerization of ethylene and CO. % CO in copolymer vs. % CO in initial gas mixture.

Effect of Initial Monomer Mixtures on the Copolymer Composition

Figure 3 is a plot of the concentration of CO in the copolymer as a function of the CO concentration in the initial monomer gas mixture over the entire range of gas compositions. These data were obtained for constant conditions of temperature, pressure, and radiation intensity. When more than one experiment was performed with the same gas composition the average point is shown. The curve indicates that as the CO concentration in the gas mixture is initially increased from 1 to 5%, the CO concentration in the copolymer increases very rapidly. Between 5 and 95% CO the copolymer CO concentration increases very slowly from 40 to 52%. The curve also indicates that at an initial gas composition of 87% CO, the CO concentration in the copolymer is 50% and $[a]/[b] = 1$. Above 87% CO, the copolymer contains more than 50% CO. The 45° line in the plot intersects the curve at the azeotropic composition of 48.5%. It is interesting to note that ethylene-CO copolymers containing more than 50% CO have not been reported previously. However, there has been some evidence reported for CO polymer formation in a radiation field.¹⁵

Experimental Determination of the α Value

Values for α were determined by use of eq. (13) for experiments listed in Table I in which the initial monomer concentrations and the corresponding copolymer compositions were measured. Figure 4 shows a plot

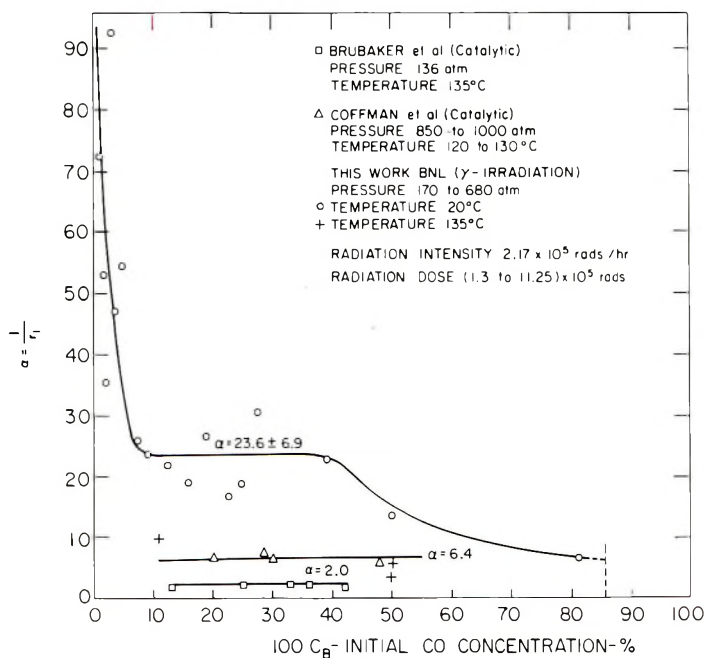


Fig. 4. Co⁶⁰ γ -copolymerization of ethylene and CO. α value vs. CO concentration in initial gas mixture.

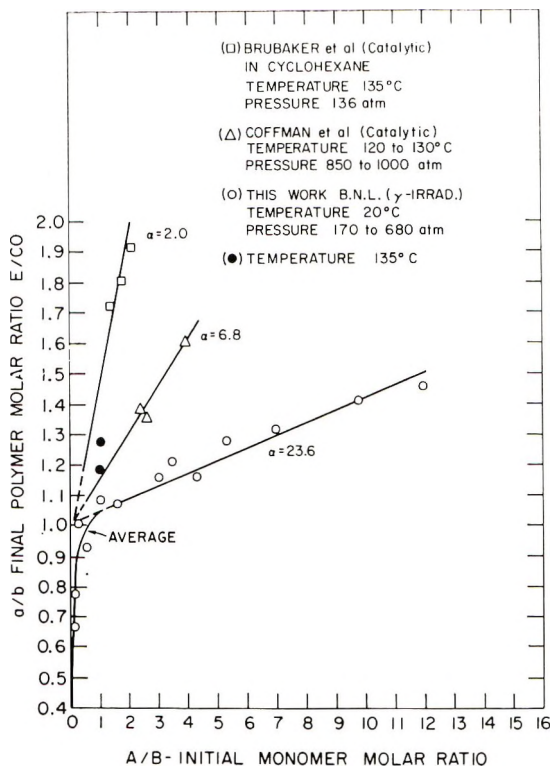


Fig. 5. Co^{60} γ -copolymerization of ethylene and CO. Final polymer molar ratio vs. initial monomer molar ratio.

of α as a function of the CO concentration. The α value decreases rapidly for small (1 to 8%) increases in CO concentration. Between 8 and 39% CO it remains essentially constant at an average value of 23.6 ± 6.9 . Average α values were plotted when more than one experiment with the same initial gas mixture was used.

The validity of eq. (13) for this system is shown in Figure 5, where $[a]/[b]$ is plotted as a function of $[A]/[B]$ from 1.5 to 12. The slope of the line is $1/\alpha$ and the extrapolated intercept has a value of 1 as predicted by eq. (13). A value for α calculated from the reciprocal of the slope is 23.6. The "copolymer composition equation" in the range indicated is expressed as follows.

$$[a]/[b] = 1/23.6 ([A]/[B]) + 1 \quad (21)$$

The α value of 23.6 was found to be independent of pressure and radiation intensity between 170 and 680 atm. and 0.76×10^5 to 3.85×10^5 rads/hr. All experiments for deriving this α value were performed at room temperature. The fact that α begins to change rapidly below an initial ethylene to CO molar ratio of 1.5 indicates that the kinetic model outlined above is no longer valid below this concentration. By definition, the value for α

means that CO adds 23.6 times as fast as an ethylene monomer to an ethylene free-radical chain end. Since the kinetic treatment is based on the assumption that CO does not readily add to a CO free-radical chain end and that r_2 , (k_{bb}/k_{ba}), approaches zero, the rate of addition of ethylene to a CO free-radical chain end cannot be determined. From the kinetic model, the α value should be independent of pressure and intensity and should remain constant at a constant temperature over a range of gas compositions.

Values for α were also calculated from experimental data presented by Brubaker et al.² and by Coffman et al.³ on the ethylene-CO system with the use of conventional peroxide catalysts. Straight-line correlations were obtained for these data, intercepting the $[a]/[b]$ axis at 1 as predicted by eq. (13). An α value of 2.0 was calculated from Brubaker's data for experiments carried out in cyclohexane at 136 atm. and 135°C. From Coffman's data for experiments at pressures in the range of 850–1000 atm. and temperatures of 120–130°C., in the absence of solvent, an α value of 6.8 was calculated. These data are shown in Figures 4 and 5.

A calculation for the copolymerization parameters Q and e for this system has been attempted by assuming a small finite value for r_2 . This value is based on the low rate of formation of CO polymer, shown in Table I, compared to the rate of ethylene-CO copolymer formation in the range where r_1 is essentially constant. Values of $Q_2 = +0.10$ and $e_2 = +3.76$ were obtained based on values of $Q_1 = +0.010$ and $e_1 = -0.21$ for ethylene.²¹

Effect of Temperature on the α Value

The effect on the α value of increasing temperature from 20 to 200°C. is shown on a $\log \alpha$ versus $1/T$ plot in Figure 6. These experiments were performed with a gas mixture containing 50% CO. Although the data exhibited considerable scatter, a straight line was fitted by using the method of least squares. The slope of this line represents the difference in activation energies for the two chain-propagating reactions (3) and (4), given by eq. (19). The equation for the straight line in Figure 6 is

$$\alpha = 0.069 \exp \{ +3400/RT \} \quad (22)$$

The copolymers formed over the temperature range 20–157°C. were in the solid-state form. The measured melting points for the copolymers obtained under these conditions were considerably higher than the reaction temperatures at which they were formed. A change in slope is indicated by an experiment conducted at 200°C. in which the copolymer was formed above the melting point. This break in the curve occurring between 157 and 200°C. may be due to a change in reaction mechanism between the two phases. Further investigation, however, is needed to substantiate this effect. The data indicate that the α value decreases from 23.6 to 3.2 with increasing temperature from 23 to 157°C. The data also indicate that the α values obtained at 135°C. in this work closely approximate

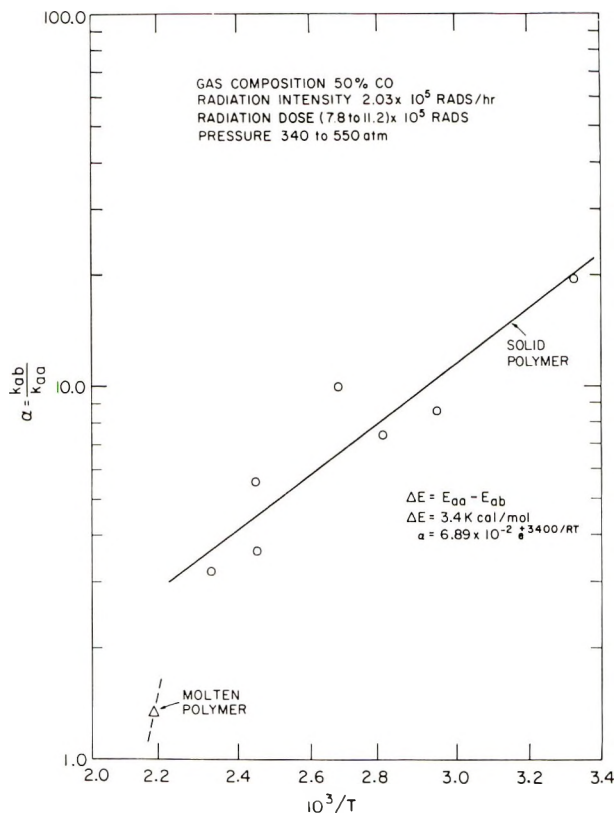


Fig. 6. Co^{60} γ -copolymerization of ethylene and CO. α vs. temperature.

those obtained by Coffman in the same temperature range. The trends appear similar for both the peroxide- and the radiation-induced synthesis. A significant conclusion, however, is that unless the reaction is initiated at low temperatures it may be difficult to obtain a copolymer approaching 50% CO. It is of interest to note that Coffman determined a $\Delta E = 8600$ cal./mole over a temperature range of 200 to 260°C. with a gas mixture containing 20% CO, i.e., $[A]/[B] = 4$. An azeotrope for this mixture was predicted at 240°C.

Effect of Temperature on Rate

The effect of temperature between 20 and 200°C. on the differential polymerization rate for a gas mixture containing 50% CO is shown in Figure 7. All experiments were performed at a constant mass concentration by initially charging the reaction vessel to 340 atm. at 20°C. and then heating to the desired temperature before initiating the reaction. As a result experiments were carried out at pressures varying from 340 to 550 atm. To express the data in terms of constant pressure, the experi-

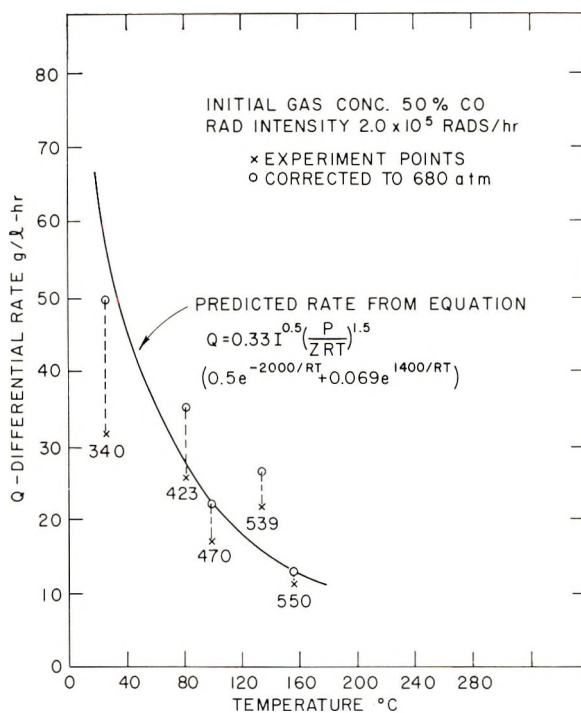


Fig. 7. Co⁶⁰ γ -copolymerization of ethylene and CO. Differential rate vs. temperature.

mental points were corrected to 680 atm. based on the concentration effect predicted by eq. (16).

$$Q = Q_1(680/Z)^{1.5}/(P_1/Z_1)^{1.5} \quad (23)$$

where Q = the differential rate in g./l.-hr.

Values for the compressibility Z were obtained from Figure 8 which gives Z as a function of pressure, P , for the pure gases over a range of constant temperature conditions.¹⁶

The data in Figure 7 shows a decrease in rate with increasing temperature for experiments conducted at constant concentration and for the corrected values. The linear extrapolation of the experimental data appears to indicate that the rate approaches zero at $\approx 240^\circ\text{C}$.

Effect of Pressure on Rate

The effect of pressure on rate was determined by a series of experiments at 20°C . in which the pressure was varied between 170 and 680 atm., as shown in Figure 9. Because of the relatively few data obtained, it was possible to give only a semiquantitative indication of the pressure dependence. Pressure dependencies of 1.33, 0.83, and 0.68 were obtained for gas mixtures containing 39.2, 50.0, and 81.4% CO, respectively. The predicted pressure dependence may be calculated for each gas mixture from

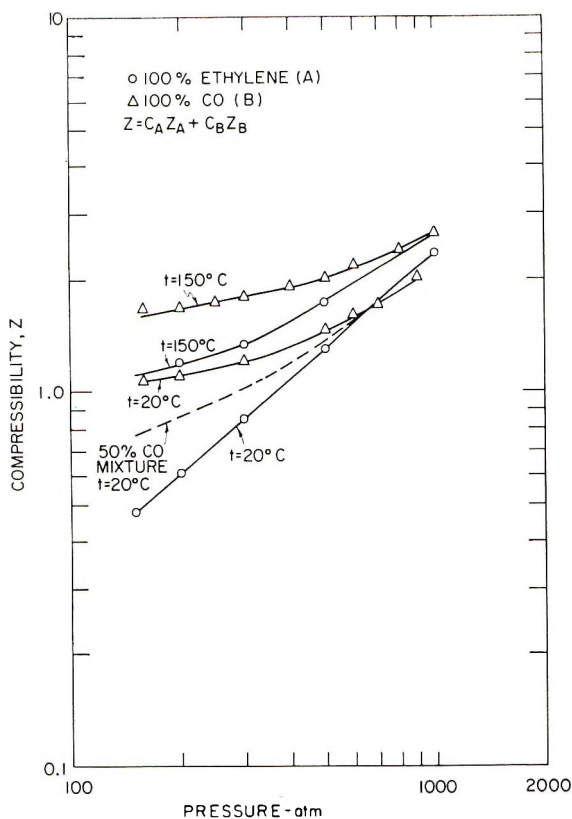


Fig. 8. Co^{60} γ -copolymerization of ethylene and CO. Compressibility vs. pressure.

the compressibility curves shown in Figure 8 and the term $(P/ZRT)^{1.5}$ from eq. (16). For a 50% CO composition, Z varies with the 0.56 power of the pressure, and therefore the theoretical rate equation predicts a pressure dependence of $P^{0.66}$. In a like manner $P^{0.45}$ and $P^{0.9}$ are predicted for compositions of 39.2 and 81.4% CO, respectively. The discrepancy is probably due to the nonideality of the gas mixture and the inaccuracy arising from using functions of pressure, compressibility, and mole fraction to represent a concentration term for each monomer in the kinetic equation.

Effect of Intensity on Rate

The effect of radiation intensity on the differential rate of copolymerization between dose rates of 0.76×10^5 to 3.85×10^5 rads/hr. is shown in Figure 10. For these experiments, gas mixtures containing 39.2, 50.0, and 81.4% CO were used at constant pressure and temperature, as indicated in Figure 10. The relatively few data indicate an average 0.60 power dependence of rate on intensity. The fact that this power is <1.0 and closer to 0.5 indicates a free-radical mechanism in which the growing chains are terminated predominately by a biradical chain process in accordance with the copolymerization rate equation [eq. (10)].

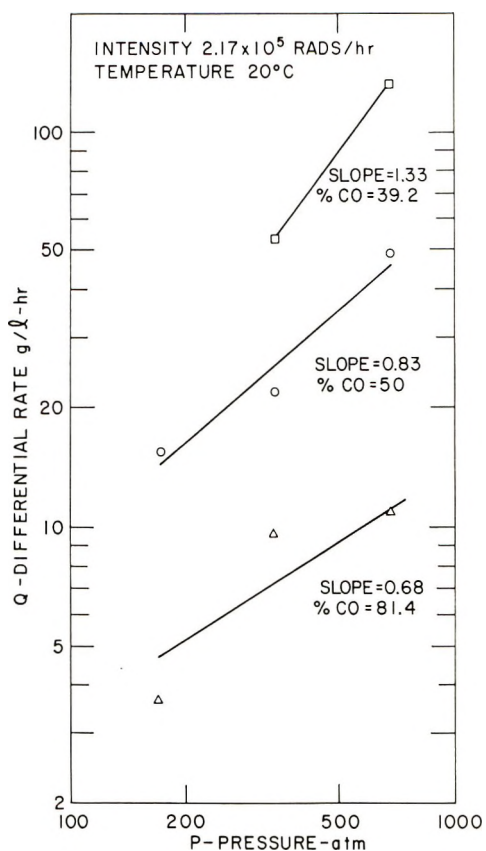


Fig. 9. Co⁶⁰ γ -copolymerization of ethylene and CO. Differential rate vs. pressure.

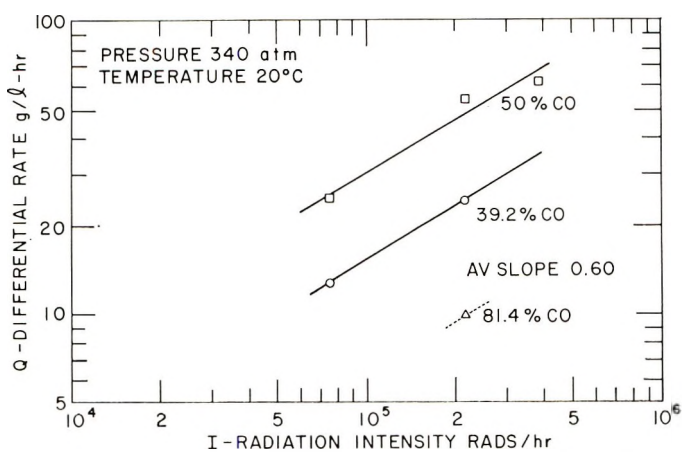


Fig. 10. Co⁶⁰ γ -copolymerization of ethylene and CO. Differential rate vs. radiation intensity.

Experimental Copolymerization Rate Equation

The experimental data were fitted to eq. (16) to test the kinetic model and obtain expressions of the rates over ranges of concentration, temperature, pressure, and intensity. The value of the product of the constant term Kk_{aa} in eq. (16) was found to be 0.75 ± 0.19 under the following conditions: constant temperature $t = 20^\circ\text{C}$.; α value = 23.6; radiation intensity $I = 0.76 \times 10^5$ – 3.85×10^6 rads/hr.; concentrations (mole fraction): ethylene; $C_A = 0.60$ – 0.92 , CO, $C_B = 0.08$ – 0.40 ; pressure $P = 170$ – 680 atm.

The differential rate dQ in grams/liter-hour can therefore be represented within 95% confidence limits of $\pm 25\%$ by the following equation:

$$dQ = 0.75I^{0.5}(P/582Z)^{1.5}(0.032C_A + 1.52C_B) \quad (24)$$

Substituting $C_A = (1 - C_B)$, and collecting terms, another form of the equation is

$$dQ = 5.32 \times 10^{-5}I^{0.5}[P/Z]^{1.5}(0.032 + 1.49C_B) \quad (24a)$$

The fact that the equation predicts an increase in rate in the region from 8 to 40% CO, as shown in Figure 2, and the relatively small deviation of the constant term lends some credence to the kinetic model chosen.

The data on the effect of temperature on rate were also fitted to eq. (16). Since k_{aa} is a variable, it is necessary to insert a value for E_{aa} , the activation energy for the addition of ethylene monomer to an ethylene free-radical chain end into eq. (16). A review by Chapiro¹⁷ of the rate of γ -induced polymerization of ethylene as a function of temperature has indicated that $E_{aa} = 2000$ cal./mole for reaction temperatures below the melting point of polyethylene. Polymerizations above the melting point gave $E_{aa} = 13,000$ cal./mole. The value of 2000 cal./mole was adopted because ΔE , determined from data in Figure 6, was obtained for conditions below the melting point of the copolymers. Since

$$\Delta E = E_{aa} - E_{ab},$$

then

$$E_{ab} = +2000 - 3400 = -1400 \text{ cal./mole}$$

This value for E_{ab} should be the activation energy of the addition of CO to an ethylene free-radical chain end. The value is negative and therefore cannot represent the activation energy of a reacting species. Since the exponent in the first concentration term in eq. (20) is negative, a positive exponent is needed in the second concentration term to allow the equation to predict the decrease in rate with increasing temperature as experimentally observed. This requirement is satisfied, since E_{ab} is negative.

It is evident from the above considerations that the adopted model does not describe the data correctly. However, the rate equation derived with the use of the activation energy predicts the rate with $\pm 30\%$ at a 95%

confidence limit for the following experimental conditions: gas composition = 50% ethylene, 50% CO; pressure $P = 170$ – 680 atm.; temperature $t, = 20$ – 155°C .; radiation intensity $I = 0.76 \times 10^5$ – 3.85×10^5 rads/hr.

$$dQ = 0.33 I^{0.5} (P/ZRT)^{1.5} (0.5 \exp\{-2000/RT\} + 0.069 \exp\{+1400/RT\}) \quad (25)$$

Figure 7 shows the rate as a function of temperature predicted by eq. (25). The rate equation does not extrapolate to a finite temperature for a zero rate but decreases asymptotically as the temperature increases.

Several interpretations can be made regarding the decrease in rate and in reactivity ratio (α) with increasing temperature. One consideration stems from the difference in the activation energies of the propagation rate constants k_{aa} and k_{ab} as described above. The implication here is that these rate constants are temperature dependent but that k_{aa} increases more rapidly than k_{ab} with increasing temperature. In this case α tends to approach unity, and the propagation rate constants must be defined at all temperatures.

Another consideration arises from the negative activation energy calculated for k_{ab} . Since this does not represent a propagating species, the negative value may be the sum of one or more depropagation reactions occurring simultaneously. The effect of depropagation on the reactivity ratio can be explained in terms of the stability of the bond between a $-\text{CO}-$ and an ethylene $-\text{C}-\text{C}-$ unit. From theoretical considerations the weakest bond in a polyketone structure of this type is the bond adjacent to the $-\text{CO}-$ unit. Depropagation would therefore occur at this point rather than at the ethylene carbon-carbon bond. Since the copolymer formed at these temperatures is not equimolar, complete depropagation cannot occur, and therefore no ceiling temperature can be reached. In considering the mechanics involved in a simple depropagation reaction, an ethylene-radical chain end with a CO penultimate unit can be assumed. Depropagation of the ethylene radical will result in a terminal CO unit which is prone to depropagate to the adjacent unit. In this case it must be an ethylene unit, since CO does not add to CO. This stepwise reaction can occur until two or more adjacent ethylene units are reached or until an ethylene radical reacts with another ethylene molecule. Kinetic expressions for this reaction must therefore contain rate constants for the propagation and depropagation steps over the entire range of temperatures.

It is also possible to consider the reacting species to be ethylene and a complex composed of an ethylene and a CO molecule, as proposed by Barb.¹⁸ As the reaction temperature is increased the equilibrium concentration of the ethylene-CO complex may favor ethylene and CO formation. This would result in a decrease in concentration of the propagating complex species and a subsequent increase in ethylene concentration which could account for the decrease in the α value with increasing temperature.

POLYMER CHARACTERIZATION

Crystallinity

X-ray diffraction patterns for ethylene-CO copolymers containing 43.5 and 56.2% CO are shown in Figure 11. Previous studies^{2,19} have shown that ethylene-CO copolymers containing up to 50% CO are crystalline. The data in Figure 11 indicate that copolymer containing more than 50% CO is also crystalline. Although no attempt was made to determine

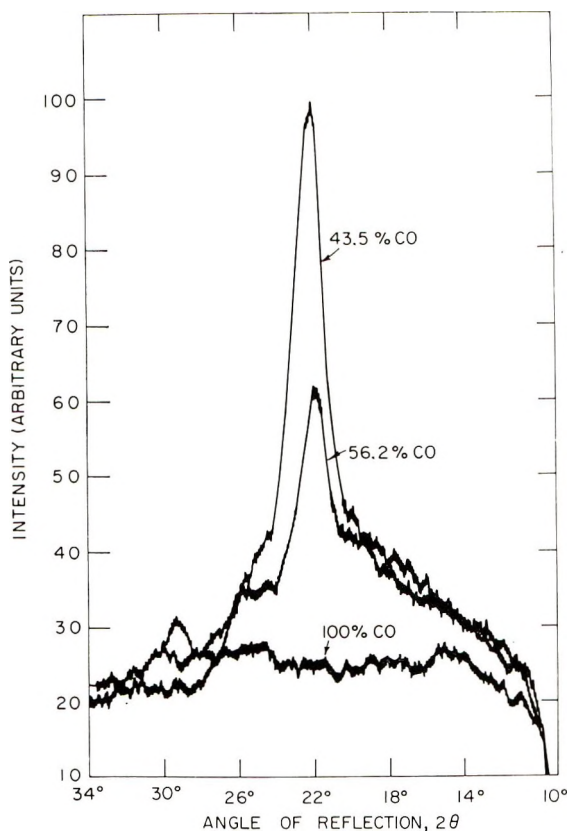


Fig. 11. Co^{60} γ -copolymerization of ethylene and CO. Typical x-ray diffraction patterns of copolymers.

the per cent crystallinity, a comparison of the relative peak heights for copolymers containing 43.5 and 56.2% CO indicates that the degree of crystallinity decreases with increasing CO composition. Crystallinity could not be detected for material resulting from the irradiation of pure CO gas.

Sample specimens were prepared by carefully pressing powdered polymer into $\frac{1}{4}$ -in. diameter 2S Al holders which were then mounted and measured on a Phillips x-ray diffractometer.

Infrared Analysis

An infrared scan made on a Perkin-Elmer 221 spectrophotometer of an ethylene-CO copolymer containing 38.8% CO is shown in Figure 12. The only absorption bands in the copolymer similar to those of polyethylene were the carbon-hydrogen stretch band at 3.4 μ and the carbon-hydrogen bending vibration at 6.8 μ . A strong carbonyl band at 5.8 μ with a harmonic at 2.95 μ indicates a polyketone structure. The absorption bands at 7.1 and 7.3 μ have been assigned as methylene structures adjacent to a carbonyl since they are characteristic of α -hydrogen structures. It was generally noted that as the CO concentration in the polymer was increased, the carbon-hydrogen bending vibration band at 6.8 μ decreased with an

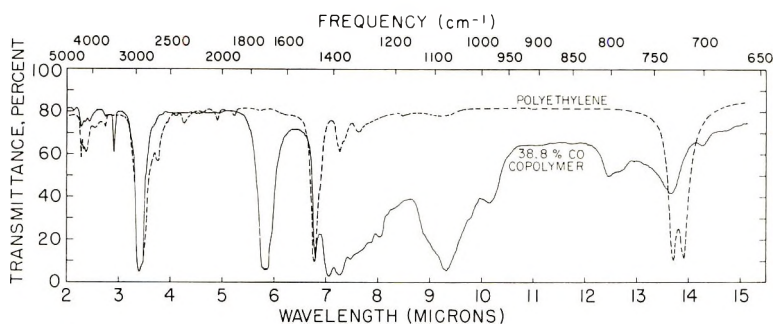


Fig. 12. Co⁶⁰ γ -copolymerization of ethylene and CO. Infrared spectrum of an ethylene-CO polymer containing 38.8% CO.

increase in absorption at 7.1 and 7.3 μ . The doublet at 13.7 and 13.9 μ , indicating four or more carbons in a chain, was found to decrease in intensity with increasing CO concentration. As the ratio of polyethylene to carbon monoxide approaches 1, the doublet is reduced to a singlet at 13.7 μ . For this study, a 0.5-mil film was prepared on a Carver press at a pressure of 1360 atm. and a temperature of 177°C. Exposure of the film to the atmosphere at temperatures above the melting point of the copolymer resulted in a yellowish discoloration. To minimize this effect, the specimens were cooled to room temperature prior to removal from the mold.

Density

The effect of composition on density for copolymers containing 31.05 to 49.85% CO is shown in Figure 13. As the CO concentration is increased, in the range given, the density increases linearly from 1.076 to 1.254 g./cc. The density in g./cc. is expressed as a linear function of the CO concentration in mole fraction, C_b , by the relationship

$$d = 0.958 C_b + 0.776 \quad (26)$$

The equation is applicable to CO concentrations in the copolymer from 30 to 50%.

TABLE II
 Co⁶⁰ γ -Radiation Copolymerization of Ethylene and CO. Physical Properties of Copolymers

Sample	Temp., °C.	Pressure, atm.	Initial composition, % CO	Final composition, % CO	Intensity 10^{-5} , rads/hr.	Total dose 10^{-5} , rads	Crystalline melting point, °C.	Density g./cc.
CO-32-7	20	650	7.7	40.65	1.56	7.8	147	1.161
CO-32-8	20	650	22.5	45.25	1.56	7.8	—	1.220
CO-32-10	20	650	15.9	43.85	1.56	7.8	—	1.201
CO-32-11	32	650	4.8	27.47	1.56	7.8	111	—
CO-32-12	24	650	18.9	46.29	1.56	7.8	203	—
CO-32-17	20	650	9.2	41.49	1.56	7.8	161	1.168
CO-32-22	20	650	2.0	29.76	1.56	7.8	114	—
CO-32-23	20	650	1.1	31.05	1.56	7.8	—	1.076
CO-K-1	21	680	50.0	49.0	2.17	7.8	235	—
CO-K-5	20	680	50.0	47.92	2.17	25.0	—	1.232
CO-K-6	20	340	50.0	47.51	2.17	11.25	—	1.233
CO-K-7	21	170	50.0	47.71	2.17	11.25	—	1.227
CO-K-9	21	340	50.0	48.99	0.76	11.25	—	1.245
CO-K-12	24	680	81.3	49.85	2.17	11.25	242	1.254
CO-K-16	22	680	12.6	43.47	2.17	1.29	176	—
CO-K-23	135	539	50.0	43.88	2.03	11.20	181	—
CO-K-24A	21	680	2.1	35.12	2.17	1.6	122	1.118
CO-K-32	135	470	10.8	34.85	2.03	25.4	112	—
CO-K-33	23	680	3.7	38.74	2.17	1.09	126	1.141
CO-K-47	66	406	50.0	47.26	2.03	7.86	213	—
CO-K-52	135	626	13.6	36.38	2.03	6.86	117	—

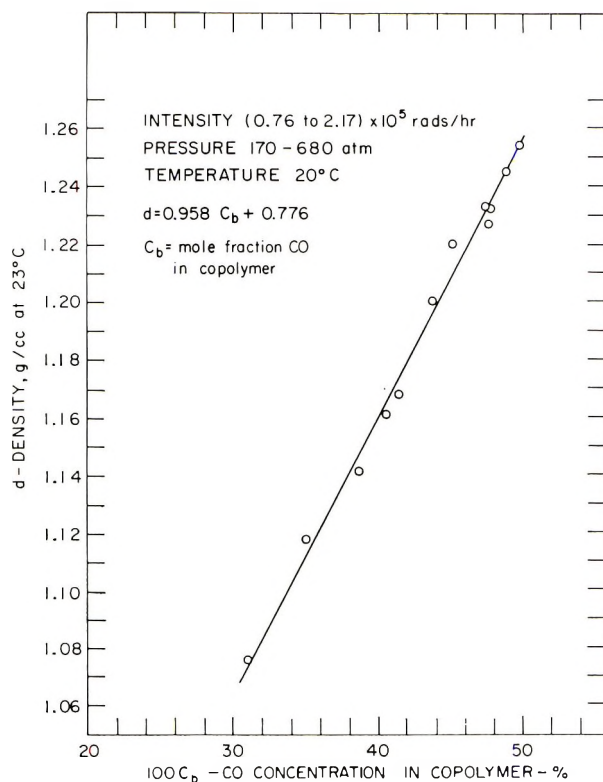


Fig. 13. Co⁶⁰ γ -copolymerization of ethylene and CO. Density vs. CO concentration in copolymer.

The copolymers were formed under a variety of experimental conditions (see Table II). Initial pressures ranged from 170 to 680 atm. at intensities of 0.76×10^5 – 2.17×10^5 rads/hr. and doses of 1.09×10^5 – 2.5×10^6 rads. All polymerizations were performed at room temperature (20°C.). The wide variation in pressure, intensity, and total dose shows the density to be dependent entirely on composition over the range of conditions used. Copolymer density was measured by the density gradient method described by Wiley.²⁰ A precision of ± 0.001 g./cc. was obtained with solutions of carbon tetrachloride and toluene at 23°C.

Melting Points

First-order transition temperatures were determined with a Perkin-Elmer differential scanning calorimeter (DSC), calibrated for a scan speed of 20°C./min. Figure 14 shows typical melting and crystallization thermograms for copolymers containing 38.8 and 50.0% CO. These copolymers were formed at 20°C. and were not subjected to thermal treatment prior to measurement. The temperature at the onset of melting was measured at the point of deflection from the base line, and the crystalline melting-point temperature was taken at the point at which the curve returns to the

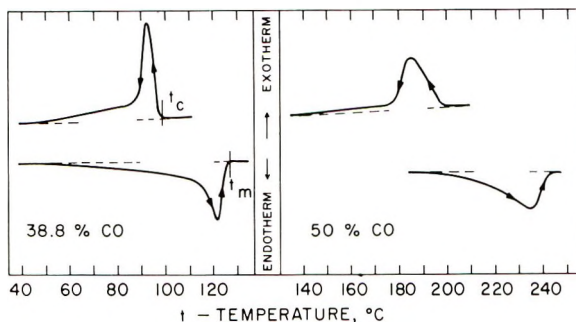


Fig. 14. Co^{60} γ -copolymerization of ethylene and CO. Typical (DSC) melting and crystallization thermograms for ethylene-CO copolymers.

base line. Peak maximum indicates the temperature and time at which the transition is proceeding at the maximum rate.

A plot of melting point versus per cent CO in the copolymer is shown in Figure 15. Copolymers used in determining melting points were formed at pressures of 400–680 atm. and temperatures of 20–135°C. (Table II). Irradiation doses ranged from 1.1×10^5 to 2.54×10^6 rads at intensities from 1.56×10^5 to 2.17×10^5 rads/hr. A large linear depression in the melting point of the copolymer results from a small decrease in CO concentration in the composition range from 49.85 to 38.74% CO. In this range, the melting point appears to be independent of the reaction temperature used to form the copolymer. It should be noted that these copolymers were formed at temperatures below their respective melting points, as indicated in Figure 15. At 38.74% CO a sharp break in the curve occurs, followed by a smaller melting-point depression to 27.41% CO. Copolymers obtained at the lower range of CO concentration and at 135°C. indicate slightly lower melting points than those obtained for copolymer formed at 20°C. The copolymers in this range of composition, however, were formed above their melting points. Extrapolation of the melting-point curve at the higher temperature gives an intercept at the same concentration point as that for the polymer formed at 20°C.

The crystalline melting points for polyethylene formed at room temperature and under the same experimental conditions²² shown in Figure 15 are in the same range as the melting points for copolymers containing 35 to 40% CO. An interesting effect is the increase in melting point of the copolymer with increasing amounts of the noncrystallizable —CO— unit. It is also interesting to note that Chatani¹⁹ found the unit cell dimension for the repeating structural unit, $(-\text{CH}_2-\text{CH}_2-\text{CO}-)_n$, in a 50% CO copolymer to be different from that of pure polyethylene. A significant change in unit cell dimension, however, was found to occur rather abruptly at 47% CO. Below this concentration the unit cell dimensions were the same as those for polyethylene. The effect noted by Chatani was not reflected in the melting-point data in Figure 15. The break in the curve occurring at $\approx 40\%$ CO corresponds to an ethylene:CO molar ratio of

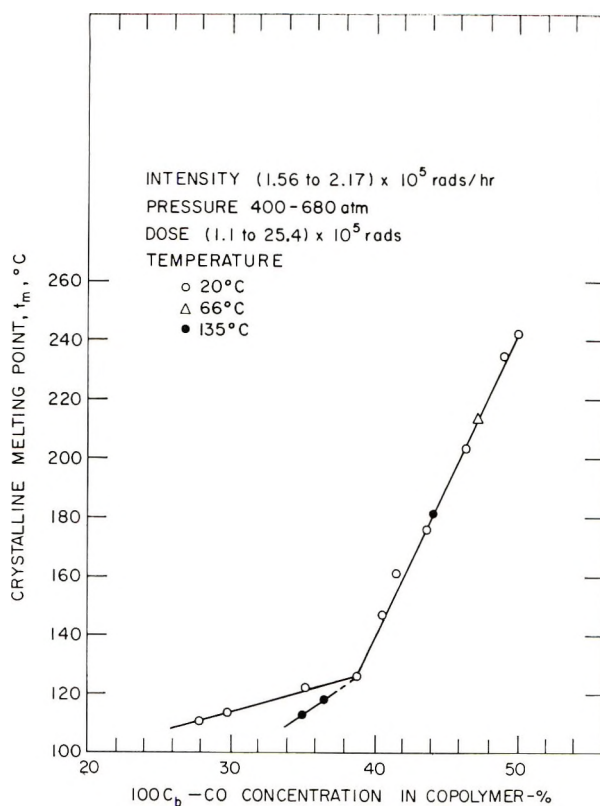


Fig. 15. Co⁶⁰ γ -copolymerization of ethylene and CO. Crystalline melting points vs. CO concentration in copolymer.

1.5:1. Below $\approx 40\%$ CO the linear crystalline melting-point behavior is probably influenced by the varying ethylene sequences in the chain lengths. Above $\approx 40\%$ CO the rapid increase in crystalline melting point is probably due to a new repeat sequence.

Solubility

The copolymers in the range of concentrations shown in Table III were found to be insoluble in hot benzene, xylene, Decalin, carbon tetrachloride, and dimethylformamide. Two solvents found to be effective were α -chloronaphthalene and *o*-dichlorobenzene at 130°C. Copolymers containing up to 43% CO were found to be readily soluble in these solvents. From 43 to 48% CO, they were only partially soluble. Above 48% CO they were completely insoluble, even at the boiling point temperatures of the solvents, with no indication of gel formation. The inference can be made that the incomplete solubility of copolymer above 43% CO may be due to the chain units becoming involved in intermolecular crosslinkages. However, such a conclusion is not entirely justifiable on the basis of solubility alone. Consideration must also be given to the efficiency of the solvent

TABLE III
Effect of Composition and Temperature on the Molecular Weight of Ethylene-CO Copolymers

CO concentration in polymer, %	Reaction temperature, °C.	Initial pressure, atm.	[η] (<i>o</i> -dichlorobenzene, 130°C.)	\bar{M}_n
35.12	20	680	0.368	5,100
38.75	20	680	0.505	—
39.76	20	680	0.485	9,950
40.65	20	680	0.546	14,550
43.16	20	680	—	>20,000
36.21	65	340	0.227	3,750
33.74	155	340	0.150	2,900
35.25	200	340	0.078	1,800

at the higher CO concentrations. Some evidence for this is given in Table III, which shows an increase in molecular weight with increasing CO in the copolymer. The soluble fraction obtained for copolymers containing >43% CO is probably the lower molecular weight fraction of the sample. It may also be mentioned that if crosslinking occurred above 43% CO, it would probably alter the linearity of the melting-point curve in Figure 15.

Molecular Weights

The dilute solution viscosity for copolymers containing from 35.12 to 40.65% CO, formed at reaction temperatures ranging from 20 to 200°C., was measured in a modified Ubbelohde viscometer at 130°C. with *o*-dichlorobenzene used as the solvent. Number-average molecular weights, \bar{M}_n , were also determined for the same samples on a Mechrolab Model 302 vapor pressure osmometer at 130°C. in *o*-dichlorobenzene. The values given in Table III for copolymers formed at 20°C. and 680 atm. indicate that the intrinsic viscosity [η] and the number-average molecular weight increase with increasing CO concentration in the copolymer. Samples formed at 20°C., containing > \approx 41% CO, indicate \bar{M}_n values >20,000. However, they could not be accurately measured because of the limitation of the instrument.

The effect of temperature on the molecular weight of copolymer formed at an initial pressure of 340 atm. and temperatures between 65 and 200°C. is also shown in Table III. Increasing the reaction temperature results in a decrease in molecular weight. These measurements were made for copolymers containing 33.74 to 36.21% CO.

The decrease in molecular weight with increasing temperature was found to be in agreement with the results of Brubaker et al.² and Coffman et al.³ The molecular weights for radiation-produced ethylene-CO copolymer over the range of conditions used in this study were found to be considerably higher than those reported by the above authors.

Preliminary measurements of the weight-average molecular weight M_w indicate values ranging from 455,000 to 1,330,000 for samples containing 27-43% CO.

Thermal Decomposition

Measurements of rates of decomposition were made by the loss-of-weight method with the differential scanning calorimeter. Copolymers containing 40 and 50% CO were studied in the temperature range of 257-327°C. The lower temperature represents a point slightly above the onset of decomposition ($\approx 250^\circ\text{C}$.) of a copolymer containing 50% CO. Weighed samples were heated in an inert atmosphere at the rate of 80°C./min. to a predetermined temperature which was maintained for 30 min. The temperature was then decreased at the rate of 80°C./min., and the samples were reweighed at room temperature. Data on rates of thermal decomposition of the copolymer are given in Table IV.

Figure 16 shows an Arrhenius-type plot of the copolymer decomposition data from which activation energies for thermal decomposition were calculated. Energies of 5.4 and 8.9 kcal./mole were obtained for polymers containing 40 and 50% CO, respectively. The data indicate that the rate of decomposition increases with increasing CO concentration in the copolymer. This behavior is not surprising, since the weakest link in a polyketone structure containing both $-\text{CH}_2-\text{CH}_2-$ and $-\text{CO}-$ units is the bond adjacent to the CO.

The products of thermal decomposition were qualitatively analyzed for a copolymer containing 50% CO with a pyrolysis unit attached to a gas chromatograph. The sample was pyrolyzed at 350°C. and the liberated gases were swept into the chromatograph using a molecular sieve column and helium as the carrier gas. The volatile products were identified as CO, C₂H₄, CH₄, and H₂, with the first two products predominating. This

TABLE IV
Thermal Decomposition of Ethylene-CO Copolymers

Sample no.	Initial sample wt., mg.	CO concentration, %	Decomposition temperature, °C.	Weight loss, mg. ^a	Per cent weight loss
CO-K-12	29.61	50	267	2.32	7.84
"	25.59	50	277	2.37	9.26
"	22.28	50	297	2.91	13.11
"	21.05	50	307	2.69	12.78
"	21.18	50	317	3.33	15.72
"	26.26	50	327	4.36	17.97
CO-K-34	13.60	40	257	0.93	6.84
"	12.71	40	277	1.05	8.26
"	12.69	40	297	1.26	9.93
"	12.15	40	317	1.41	11.60

^a In 30 min. at temperature given.

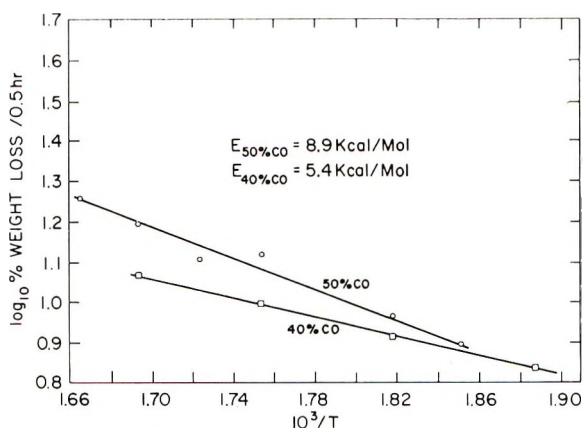


Fig. 16. Co^{60} γ -copolymerization of ethylene and CO. Arrhenius plot for the thermal decomposition of ethylene-CO copolymer.

indicates that a 50% CO copolymer decomposes to give essentially the initial monomeric units.

This work was performed under the auspices of the Division of Isotope Development, U. S. Atomic Energy Commission.

References

1. Steinberg, M., and P. Colombo, in *Industrial Uses of Large Radiation Sources* (Proc. IAEA Conf., Salzburg, Austria, May, 1963), Vol. 1, IAEA, Vienna, 1963, pp. 121-50.
2. Brubaker, M. M., D. D. Coffman, and H. H. Hoehn, *J. Am. Chem. Soc.*, **74**, 1509 (1952).
3. Coffman, D. D., P. S. Pinkney, F. T. Wall, W. H. Wood, and H. S. Young, *J. Am. Chem. Soc.*, **75**, 3391 (1952).
4. Tanimoto, T., Y. Nishimura, T. Takizawa, and S. Murahashi, *Ann. Rept. Textile Inst., Osaka Univ.*, **13**, 117 (1960).
5. Buckley, G. D., and L. Seed (assigned to Imperial Chemical Industries, Ltd.), Brit. Pat. 714,843 (1954).
6. Roberts, R., and S. J. Skinner (assigned to Monsanto Chemicals, Ltd.), Brit. Pat. 778,225 (1957).
7. Brando, E. E., and A. I. Dintses, *Neftekhimiya*, **4**, No. 1, 68 (1964).
8. Colombo, P., M. Steinberg, and J. Fontana, *J. Polymer Sci.*, **B1**, 447 (1963).
9. Steinberg, M., P. Colombo, L. E. Kukacka, R. N. Chapman, and G. Adler, *Proc. Intern. Symp. Radiation-Induced Polymerization and Graft Copolymerization, Battelle Memorial Inst., Columbus, Ohio, Nov. 1962*, 70-106, TID-7643, Nov., 1962.
10. Melville, H. W., B. Noble, and W. F. Watson, *J. Polymer Sci.*, **2**, 229 (1947).
11. Walling, C., *J. Am. Chem. Soc.*, **71**, 1930 (1949).
12. Alfrey, T., Jr., and G. Goldfinger, *J. Chem. Phys.*, **12**, 205 (1944).
13. Mayo, F. R., and F. M. Lewis, *J. Am. Chem. Soc.*, **66**, 1594 (1944).
14. Wall, F. T., *J. Am. Chem. Soc.*, **66**, 2050 (1944).
15. Smith, R. N., D. A. Young, E. N. Smith, and C. C. Carter, *Inorg. Chem.*, **2**, 829-38 (1963).
16. *Chemical Engineer's Handbook*, J. H. Perry, Ed., McGraw-Hill, New York, 1960, pp. 207-208.
17. Chapiro, A., *Radiation Chemistry of Polymeric Systems*, Interscience, New York, 1962, pp. 233-235.

18. Barb, W. G., *J. Am. Chem. Soc.*, **75**, 224 (1953).
19. Chatani, Y., T. Takizawa, S. Murahashi, Y. Sakata, and Y. Nishimura, *J. Polymer Sci.*, **55**, 811 (1961); Y. Chatani, T. Takizawa, S. Murahashi, *ibid.*, **62**, 527 (1962).
20. Wiley, R. E., *Plastics Technol.*, **8**, No. 3, 31 (1962).
21. Young, L. J., *J. Polymer Sci.*, **54**, 411 (1961).
22. Colombo, P., J. Fontana, L. E. Kukacka, and M. Steinberg, *Characterization Studies for Polyethylene Formed by Co⁶⁰ Gamma Radiation Under Constant Conditions in a Non-flow System*, Informal Report, BNL 9043, March, 1965.

Résumé

On a étudié la copolymérisation radicalaire induite par irradiation- γ de mélanges éthylène-oxyde de carbone sur une large gamme de pression, de composition initiale du mélange gazeux, d'intensité de radiation et de la température. A 20°C des concentrations de CO jusqu'à 1% retardent la polymérisation de l'éthylène. Au-dessus de cette concentration la vitesse atteint un maximum entre 27.5 et 39.2% de CO pour diminuer ensuite. La composition du copolymère augmente uniquement à partir de 40 à 50% de CO, lorsque le mélange des gaz varie de 5 à 90% de CO. On obtient un rapport de réactivité relativement constant à 20°C, qui indique que le CO s'additionne 23.6 fois plus rapidement que l'éthylène à un radical terminal éthylénique. Pour un mélange de gaz à 50% de CO, la valeur mentionnée ci-dessus de 23.6 et vitesse de copolymérisation diminue lorsque la température augmente à 200°C. Les résultats cinétiques indiquent une réaction de dépropagation qui dépend de la température. L'étude infrarouge des copolymères indique une structure de polycétone contenant des unités $-\text{CH}_2-\text{CH}_2-$ et $-\text{CO}-$. Le point de fusion cristalline croît rapidement de 111° à 242°C, lorsque la concentration de CO dans le copolymère monte de 27 à 50%. Le poids moléculaire du copolymère formé à 20°C. augmente lorsque la concentration en CO augmente, les valeurs \bar{M}_n étant supérieures à 20.000. Une augmentation de la température de réaction entraîne une diminution de poids moléculaire. Un début de décomposition a été mesuré dans le cas d'un copolymère à 50% CO à une température de 250°C environ.

Zusammenfassung

Die γ -strahlungsinduzierte radikalische Copolymerisation von Äthylen und CO wurde in einem weiten Druck-, Ausgangsgaszusammensetzungs-, Strahlungsintensitäts, und Temperaturbereiche untersucht. Bei 20°C verzögern CO-Konzentrationen bis zu 1% die Äthylenpolymerisation. Oberhalb dieser Konzentration erreicht die Geschwindigkeit zwischen 27,5 und 39,2% CO ein Maximum und nimmt dann ab. Die Copolymerzusammensetzung nimmt bei einer Variierung der Gasmischung von 5 auf 90% CO nur von 40 auf 50% CO zu. Bei 20°C wird ein verhältnismässig konstantes Reaktivitätsverhältnis erhalten, CO addiert sich hier 23,6 mal so rasch an ein radikalisches Äthylenkettenende als das Monomere Äthylen. Für eine Gasmischung mit 50% CO nehmen der obige Wert von 23,6 sowie die Copolymerisationsgeschwindigkeit mit zunehmender Temperatur bis zu 200°C ab. Die kinetischen Daten sprechen für eine temperaturabhängige Depropagierungsreaktion. Die Infrarotuntersuchung der Copolymeren lässt eine Polyketonstruktur mit $-\text{CH}_2-\text{CH}_2-$ und $-\text{CO}-$ Einheiten erkennen. Mit Zunahme der CO-Konzentration im Polymeren von 27 auf 50% steigt der kristalline Schmelzpunkt rasch von 111 auf 242°C an. Das Molekulargewicht des bei 20°C gebildeten Copolymeren nahm mit steigendem CO-Gehalt zu und entsprach \bar{M}_n -Werten >20.000 . Steigende Reaktionstemperatur führt zu einer Abnahme des Molekulargewichts. Für ein Copolymeres mit 50% CO wurde der Beginn der Zersetzung bei $\approx 250^\circ\text{C}$ beobachtet.

Received November 4, 1964

Revised June 5, 1965

Prod. No. 4780A

Polybenzoylenebenzimidazoles

J. G. COLSON,* R. H. MICHEL, and R. M. PAUFLER,
*Film Department, E. I. du Pont de Nemours & Company, Inc.,
Buffalo, New York*

Synopsis

A polyamide amino acid was prepared by the solution condensation of 3,3'-diaminobenzidine and pyromellitic dianhydride. This polymer was cast as a film and converted to a polybenzoylenebenzimidazole. The gross conversion path was elucidated by spectroscopy and was substantiated by model compound studies. A novel ladder polymer was prepared from 1,2,4,5-tetraaminobenzene and pyromellitic dianhydride.

INTRODUCTION

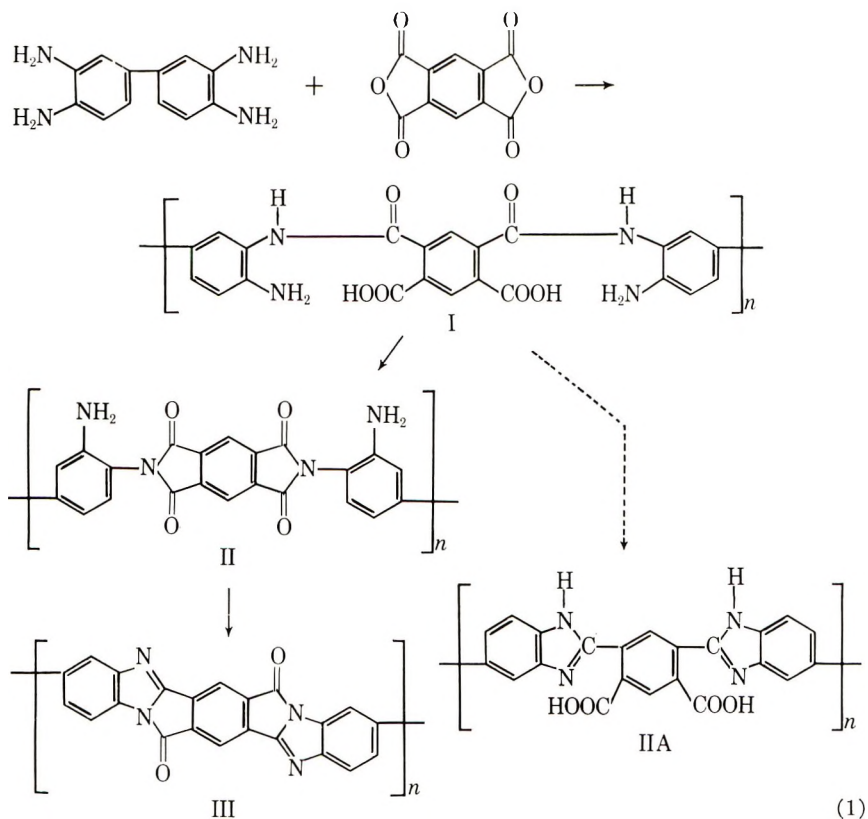
We have studied the formation of benzoylenebenzimidazole polymers [III, eqs. (1)] from aromatic tetraamines and pyromellitic dianhydride because of the high thermal stability of such related heterocyclic polymers as the polybenzimidazoles¹ and polyimides.² Furthermore, polybenzoylenebenzimidazoles presented the possibility of preparing ladder polymers which may give organic materials of exceptional thermal stability.^{3,4}

RESULTS AND DISCUSSION

Model Compounds

A soluble polymer thought to be a polyamide amino acid was prepared by condensing 3,3'-diaminobenzidine with pyromellitic dianhydride (PMDA) in an aprotic hydrogen bonding solvent at room temperature or below. Films cast from this solution were dried and converted to a polybenzoylenebenzimidazole on heating. Neither the structure of the soluble polymer nor the path of cyclization (through polyimide amine II or polybenzimidazolecarboxylic acid IIA) was known. Initial experiments showed that after the polymers, especially those exhibiting high inherent viscosities (1.0-1.5), reached 120-140°C., they became insoluble in common organic solvents. This precluded nuclear magnetic resonance (NMR) and ultraviolet studies on high molecular weight polymer. Infrared examination showed broad carbonyl absorptions. The situation was further complicated by the fact that three of the structures of interest absorbed over a small wavelength range (5.65-5.85 μ). In order to study

* Present address: Hooker Chemical Corp., Buffalo, N. Y.

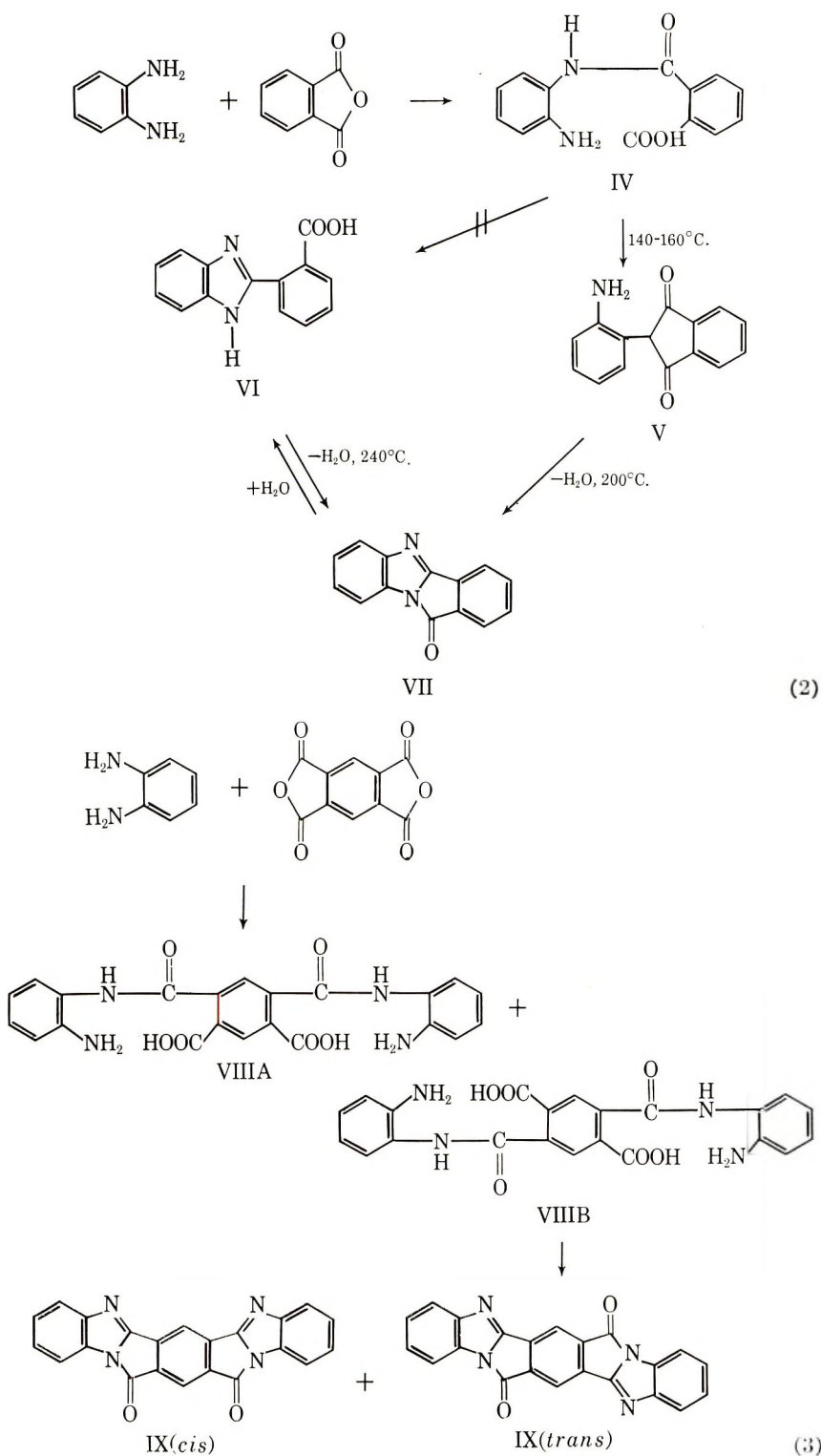


the chemistry of this system more closely, model compounds were prepared and investigated.

The initial condensation product of 1,2-diaminobenzene and phthalic anhydride in *N,N*-dimethylacetamide (DMAc) under polymerization conditions was proved by infrared and nuclear magnetic resonance to be *N*-(*o*-aminophenyl)phthalamic acid [IV, eqs. (2)].

The condensation of 1,2-diaminobenzene with pyromellitic dianhydride [eqs. (3)] gave the corresponding amino acid amide VIII, probably a mixture of two isomers, having spectral characteristics similar to the amino acid amide IV.

The amino acid amide IV was heated at 140–160°C. for 1/2 hr., either *N*-(*o*-aminophenyl)phthalimide (V). This structure was proved by NMR, infrared, and comparison to literature melting point. Mechanistically it is important that this product was the imide and not the benzimidazolecarboxylic acid VI. To further substantiate the predominance of an imide intermediate, a 25% DMAc solution of the amino acid amide IV was heated to 160°C. for 1/2 hr. The solvent was removed and the resulting product was crystallized. Three crops of crystals comprising 94% of the total weight were identified as the pure imide amine V.



The amide amino acid from 1,2-diaminobenzene and pyromellitic dianhydride was converted similarly to the symmetrical bisimide. Infrared and NMR data resembled those for imide V.

The imide V, as a solid, was converted to 1,2-benzoylenebenzimidazole (VII) in $\frac{1}{2}$ hr. at 200–210°C. Melting point and infrared and ultraviolet spectra corresponded to the expected structure. On the other hand, the benzoylenebenzimidazole could not be formed from 2-(*o*-carboxyphenyl)benzimidazole (VI) below 240–250°C. This is additional evidence against the benzimidazole path of ring closure.

The bisimide from 1,2-diaminobenzene and pyromellitic dianhydride, behaved similarly to V. However, it should be noted that in this case both *cis* and *trans* lactam structures (IX) could be formed.

In summary, the initial condensation product is an amino acid amide.

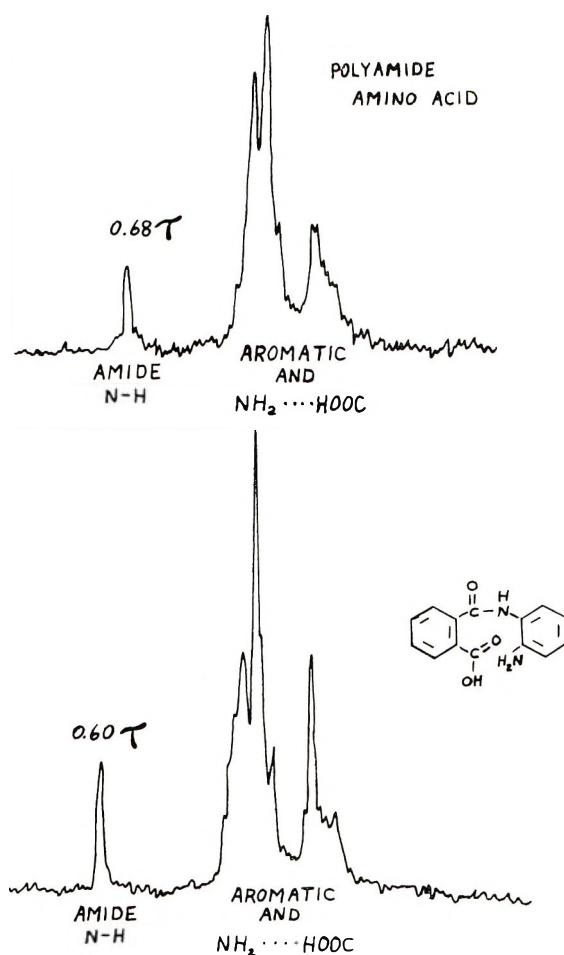


Fig. 1. Nuclear magnetic resonance spectra of polyamide amino acid and model compound.

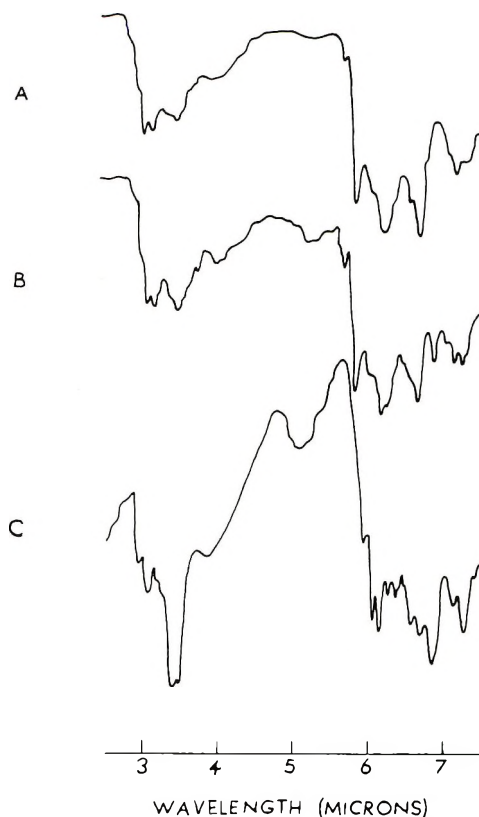


Fig. 2. Infrared spectra of polyamide amino acid and model compounds: (A) polyamide amino acid (film on BaF₂); (B) model compound VIII (smear of uncrystallized compound); (C) model compound IV (Nujol mull).

This converts to an imide amine. No benzimidazolecarboxylic acid is observed. The imide amine converts easily to the desired benzoylenebenzimidazole at 200°C., while the benzimidazolecarboxylic acid does not convert until 250°C.

Polymers

Polymer from 3,3'-Diaminobenzidine and Pyromellitic Dianhydride. The condensation of 3,3'-diaminobenzidine and pyromellitic dianhydride must be carried out under carefully controlled conditions to obtain a high inherent viscosity polymer. The anhydride is added in *N,N*-dimethylacetamide (DMAc) solution slowly in order to avoid gelation. The stoichiometry must be adhered to strictly. Experiments have shown that as little as 0.5% excess anhydride can cause gelation and as little as 0.5% excess amine can result in inherent viscosities below 1.0. Unless extreme care is taken with polymerization conditions, purity of reagents and solvents, high polymer is not obtained.

The above-mentioned condensation results in a polymer solution exhibiting inherent viscosities of 1.0–1.5. The solution is concentrated to 15% solids and cast on a glass plate. Solvent is removed further in a vacuum oven at 45°C. to give a yellow film which is easily removed from the plate. Physical measurements on this film vary, since it is plasticized with a time-temperature-dependent amount of solvent. A nuclear magnetic resonance spectrum of this film in DMAc is identical to that of the original solution polymer and is similar to that of model amino acid amide (Fig. 1).

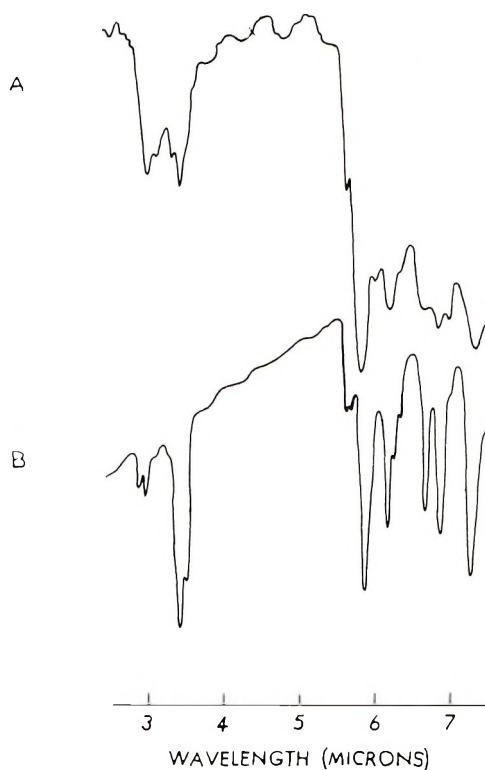


Fig. 3. Infrared spectra of polyimide amine and model compound: (A) polyimide amine film; (B) model compound V (Nujol mull).

The infrared spectra of the polyamide amino acid and of two model compounds are shown in Figure 2. The simple amino acid IV is not strictly comparable; the bis model VIII is. The change in appearance of the carbonyl region may be accounted for by variation in zwitterion character.

The film is converted to the polyimide amine II at 130–150°C. An infrared spectrum shows imide absorption at 5.85 μ . Characteristic carboxyl absorptions are absent. Again, model compound and polymer have similar infrared spectra (Fig. 3).

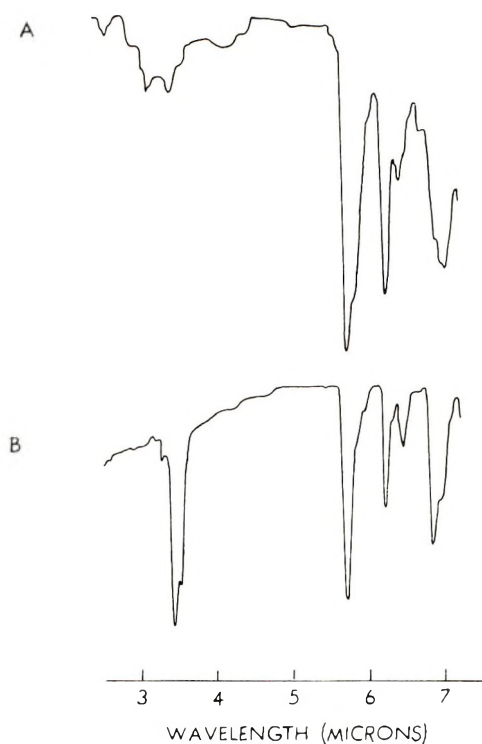


Fig. 4. Infrared spectra of polybenzoylenebenzimidazole and model compound: (A) polymer from 3,3'-diaminobenzidine and pyromellitic dianhydride (film); (B) model compound IX (Nujol mull).

Differential thermal analysis of the polyamide amino acid shows an endotherm at 135°C., and thermogravimetric analysis shows a weight loss at 132°C., substantiating the temperature at which the rate of imide formation becomes significant. This correlates well with the thermal behavior of the model compounds.

The polyimide film is converted to the desired polybenzoylenebenzimidazole film at 225–250°C. Most of the conversion can be accomplished at 200°C., but it is not complete until a higher temperature is used. This may either be as a result of an entropy effect (chain stiffening) in the final stages or due to the presence of the more difficult to convert benzimidazole-carboxylic acid (IIA). This latter structure could result from the back hydrolysis of the benzoylenebenzimidazole by water eliminated in the cyclization. The final film's infrared spectrum (Fig. 4A) does not have a sharp carbonyl absorption, probably due to *cis-trans* isomerism analogous to that postulated for the bislactam model in eq. (3). The infrared spectrum of the model (Fig. 4B) is basically similar but has a relatively small 5.8 μ shoulder on the carbonyl band at 5.7 μ . The model, as prepared and purified here, may be predominantly one of the two possible isomers. However, further work must be done to clarify this point.

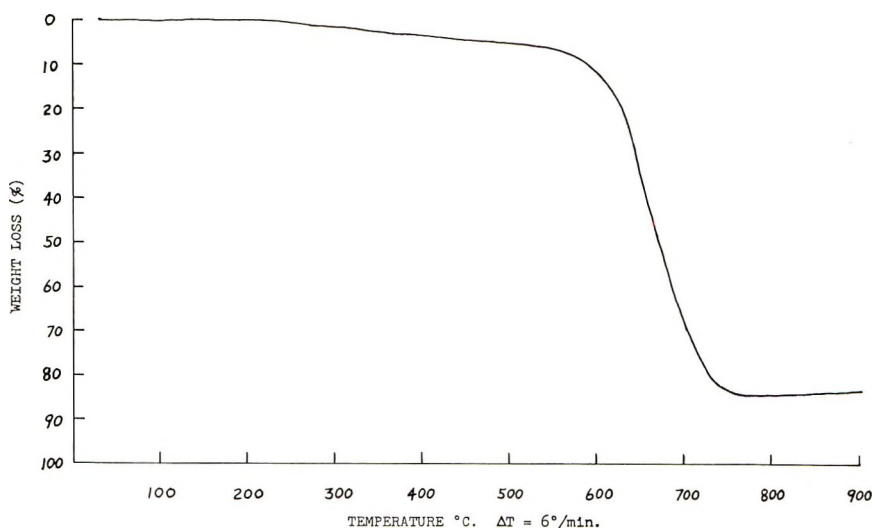


Fig. 5. Thermogravimetric analysis in dry air of polybenzoylenebenzimidazole from 3,3'-diaminobenzidine and pyromellitic anhydride.

Even after heating to 500°C. there are still X-H absorptions (centered at $3\ \mu$) in the polymer spectrum. These are believed to come from benzimidazole structures left by the decarboxylation of benzimidazolecarboxylic [2-(*o*-Carboxyphenyl)benzimidazole has been shown to decarboxylate rapidly at 280°C.⁵].

The deep red film is flexible and has the following tensile properties: modulus, 700,000 psi; tenacity, 11,000 psi; elongation, 2%. Differential thermal analysis shows no exotherm below 600°C., the limit of our instrument. Thermogravimetric analysis in dry air shows no significant weight loss until 550–600°C. (Fig. 5).

Polymer from 1,2,4,5-Tetraaminobenzene and Pyromellitic Dianhydride.

Basically, the condensation of 1,2,4,5-tetraaminobenzene and pyromellitic dianhydride is similar to the above. However, additional precautions were taken to prevent oxidation of the sensitive tetraamine. The dianhydride addition was even more carefully controlled to avoid gelation. Dimethyl sulfoxide was used as solvent because the amine has limited solubility in DMAc. Only low inherent viscosity polymer was obtained ($\eta = 0.2\text{--}0.3$), and cast film could not be removed from the glass plate until the film had been heated to 250°C. At this time the black film was flexible but not creasable. The attenuated total reflectance spectrum was essentially that of a polybenzoylenebenzimidazole. It showed a broad carbonyl at $5.6\ \mu$. Absorption was still apparent in the $3\ \mu$ region.

EXPERIMENTAL

Monomers and Solvents

3,3'-Diaminobenzidine. 3,3'-Diaminobenzidine was prepared by the method of Vogel and Marvel⁶ as an off-white powder, m. p. 179–179.5°C.

(reported 178–179°C.). Neither sublimation at 185°C./0.08 mm. nor recrystallization from methanol improved the quality of polymer prepared from it.

Pyromellitic Dianhydride. Pyromellitic dianhydride was supplied by E. I. du Pont de Nemours & Co., Inc., as a white powder, m.p. 284–286°C., and was sublimed twice at 0.1 mm. before use.

1,2-Diaminobenzene. 1,2-Diaminobenzene (Eastman) was crystallized from ether giving white crystals, m.p. 102–103°C.

***N,N*-Dimethylacetamide.** *N,N*-Dimethylacetamide (Du Pont) was distilled at 65°/0.1 mm. and passed through an alumina column (Merck acid-washed) in a dry box just before use. Karl Fischer titrimetry indicated 8–10 ppm water.

Dimethyl Sulfoxide. Dimethyl sulfoxide (Baker) was distilled at 75°C./0.5 mm. and passed through an alumina column in a dry box just before use. Karl Fischer titrimetry indicated 10–14 ppm water.

1,2,4,5-Tetraaminobenzene. 1,2,4,5-Tetraaminobenzene was prepared by nitration of 1,3-dichlorobenzene and subsequent ammonolysis.⁷ The resulting dinitrodiaminobenzene was catalytically reduced by using 10% palladium-on-charcoal in an ethanol–hydrochloric acid mixture. The resulting tetraaminobenzene tetrahydrochloride was purified by crystallization from water. The tetraamine was liberated by neutralization of the hydrochloride in boiling water with 40% aqueous sodium hydroxide. The precipitate was collected under nitrogen, washed with cold ethanol, and dried to constant weight at 75°C./1 mm.

Model Compounds

***N*-(*o*-Aminophenyl)phthalamic Acid (IV).** A solution of 14.8 g. phthalic anhydride in 200 ml. chloroform was added to a stirring solution of 10.8 g. 1,2-diaminobenzene in chloroform. After stirring overnight, the precipitate was collected and washed with refluxing chloroform. It melted at 151–152°C. and exhibited carbonyl absorptions at 5.9, 6.02, and 6.12 μ and X-H stretching at 3–4 μ (Fig. 2). A nuclear magnetic resonance spectrum (Fig. 1) in *N,N*-dimethylacetamide showed peaks at 0.60 τ (amide NH) and at 2.83 τ (aromatic) in a ratio of 1/11. Note that the exchange peak due to —COOH \cdots NH₂— appeared under the aromatic protons.

ANAL. Calculated for C₁₄H₁₂O₃N₂: C, 65.62%; H, 4.72%; N, 10.93%. Found: C, 65.17%; H, 4.46%; N, 10.16%.

Products prepared in DMAc were identical to the above.

***N*-(*o*-Aminophenyl)phthalimide (V).** A 10% DMAc solution of the above amino acid amide IV was heated at 140°C. for 1/2 hr. The solvent was removed on a rotary evaporator, leaving a yellow solid which on crystallization from chloroform melted at 194–195°C. (reported⁸ m.p. 193°C.). The infrared spectrum (Fig. 3) showed peaks at 5.80 μ (imide) and at 2.95 μ (amino). An NMR spectrum substantiated the structure.

This imide amine V was also prepared on heating the amino acid amide IV at 160°C. for 1½ hr. However, an insoluble residue (~10–15%) remained when this method was used.

1,2-Benzoylenebenzimidazole (VII). A nitrobenzene solution containing 2.6 g. of 1,2-diaminobenzene and 3.3 g. of phthalic anhydride was refluxed for 1½ hr. The yellow solid was collected and crystallized from acetic anhydride to give yellow crystals, m.p. 214–215°C. (reported⁹ m.p. 212°C.).

1,2-Benzoylenebenzimidazole was also prepared directly by heating amino acid amide IV at 210°C. for 2 hr.

2-(*o*-Carboxyphenyl)benzimidazole (VI). This compound was prepared according to Arient⁹ by the reaction of 1,2-diaminobenzene and phthalic anhydride in dilute hydrochloric acid at reflux.

Condensation Products of 1,2-Diaminobenzene and Pyromellitic Dianhydride (VIII and IX). To a stirring solution of 6.48 g. 1,2-diaminobenzene in 80 ml. DMAc was added 6.74 g. of solid pyromellitic anhydride over a period of 20 min. The solution was stirred 1 hr. under nitrogen. The solvent was then removed on the rotary evaporator at 0.5 mm. The gummy residue was crystallized to a yellow solid by washing with acetone. The solid was dried at room temperature under vacuum. The infrared spectrum showed a complex carbonyl region and X-H stretching at 3–4 μ indicative of amino acid amide (Fig. 2). The NMR spectrum in DMAc was similar to that of the simple amino acid amide IV. No further purification was attempted on this product which was probably a mixture of the isomeric amino acid amides VIII. Heating this material at 240°C. for 2 hr. and recrystallization from *N,N'*-dimethylformamide gave an orange-red compound whose infrared spectrum was identical to that of authentic bislactam IX prepared according to the literature¹⁰ (see Fig. 4 for spectrum). The recrystallized bis lactam prepared by us, like the authentic sample, had a fairly sharp carbonyl band at 5.7 μ with only a small 5.8 μ shoulder.

The amino acid amide VIII could be converted also to the imide amine by heating at lower temperatures (140–160°C.), but attempts to purify the product by recrystallization were unsuccessful.

Polymer

A four-necked round-bottomed flask was fitted with an overhead stirrer, condenser, dropping funnel, a serum cap, and connections for a continuous nitrogen flow. The entire apparatus was flamed and cooled under dried (sulfuric acid) nitrogen. The tip of the dropping funnel was so fashioned that drops were introduced directly into the solution. Solutions of PMDA were prepared by placing a weighed amount of material into a dried serum bottle. The requisite volume of solvent was added and the PMDA dissolved. The solution was injected into the dropping funnel. The amine was placed in the flask and dried DMAc added. The flask was externally cooled with ice water during the polymerization. A typical polymerization required about 4–5 hr.

Condensation of 3,3'-Diaminobenzidine and Pyromellitic Dianhydride.

In the apparatus described above a solution containing 2.181 g. of pyromellitic dianhydride in 25 ml. of DMAc was added slowly to a stirring solution of 2.143 g. of 3,3'-diaminobenzidine in 25 ml. of DMAc at a rate of 20–25 drops/min. After the addition was completed, an aliquot was removed and diluted to 0.5% with dry DMAc, and the inherent viscosity was determined at 30°C. These viscosities were usually between 1.0 and 1.6. Slight deviation from stoichiometry caused low viscosity (0.25–0.35), gross gelation, or gel particles.

Film Casting and Conversion. This solution was concentrated to 10–15% solids under vacuum (0.01 mm.) at room temperature and then the barely pourable mixture was cast on a glass plate in a nitrogen dry bag. The plate was heated to 45°C. in a vacuum oven at 1 mm. overnight.

The film could be removed easily (especially when cast from higher viscosity polymer). This was a tough yellow film, soluble in DMAc. An infrared spectrum showed a complex carbonyl centered at 6.1 μ and X-H stretching at 3–4 μ , not unlike the initial condensation product of a 1,2-diaminobenzene and pyromellitic dianhydride. A nuclear magnetic resonance spectrum in DMAc showed amide NH at 0.68 τ and aromatic hydrogen at 2.83 τ . The relative area ratios were 1/11.

The above film, on heating at 150°C. for 5–8 hr., converted to a yellow-brown film exhibiting a carbonyl vibration at 5.85 μ .

It was then heated at 225°C. overnight and then to 400°C. for 10 min. At this time the carbonyl frequency at 5.65 μ had sharpened considerably and there was little X-H stretching at 3 μ . The dark red film was creasable.

Condensation of 1,2,4,5-Tetraaminobenzene and Pyromellitic Dianhydride. This polymerization required essentially the same apparatus as the above system except that dimethyl sulfoxide (DMSO) was used as the solvent, due to limited solubility of the amine in DMAc. It was necessary to take some additional precautions. All solvent was sparged with dry nitrogen for 2 hr. and passed through a short alumina column just before use. If this was not done oxidation of the tetraamine occurred quickly. The initial 50% of pyromellitic dianhydride was added during a 20-min. period, but the remainder was slowly added over a 5-hr. period. The inherent viscosity reached a maximum 1 hr. after complete addition. The solution was concentrated quickly under vacuum to 10% solids and cast without delay to avoid gelation.

To a solution containing 1.382 g. (0.01 mole) of 1,2,4,5-tetraaminobenzene in 35 ml. of dimethyl sulfoxide was added 2.181 g. (0.01 mole) of pyromellitic dianhydride in 25 ml. of DMSO as indicated above. In this case external cooling was carefully monitored so that the solution would not freeze. The dark solution was concentrated on the rotary evaporator at 0.1 mm. to 10% solids. The inherent viscosity was 0.25.

The concentrate was then poured and cast on a glass plate. After removing gross solvent overnight at room temperature under 1 mm., the film on the glass plate was heated to 150°C. for 3 hr. at 5 mm., then at

250°C. for 8 hr. At this time, in contrast to the initial drying stage, the film could be lifted from the plate.

Instruments

Infrared spectra were recorded on the Perkin-Elmer Model 137 spectrometer, a 6-min. scan time being used.

Nuclear magnetic resonance spectra were obtained on the Varian DP 60 instrument and were calibrated by the side-band technique.

Differential thermal analyses were made with the Du Pont 900 differential thermal analyzer using a 20°C./min. temperature program.

Thermogravimetric analysis was obtained with the Aminco Thermo-Grav.

We wish to acknowledge numerous helpful discussions concerning the preparation of these polymers and their chemistry with Dr. A. H. Frazer, Textile Fibers Department, E. I. du Pont de Nemours & Co., Inc.

References

1. Vogel, H., and Marvel, C. S., *J. Polymer Sci.*, **50**, 511 (1961).
2. Sroog, C. E., A. L. Endrey, S. V. Abramo, C. E. Berr, M. W. Edwards, and K. L. Olivier, paper presented at 147th Meeting, American Chemical Society, Philadelphia, April 1964; *Polymer Preprints*, **5**, No. 1, 132 (1964).
3. Marvel, C. S., paper presented at 147th Meeting, American Chemical Society, Philadelphia, April 1964; *Polymer Preprints*, **5**, No. 1, 167 (1964).
4. Brown, J. F., Jr., *J. Polymer Sci.*, **C1**, 83 (1963).
5. Thiele, J., and Falk, K. G., *Ann.*, **347**, 129 (1906).
6. Vogel, H., and C. S. Marvel, *J. Polymer Sci.*, **A1**, 1531 (1963).
7. Nietzki, R., and A. Schedler, *Ber.*, **30**, 1666 (1897).
8. Oskaja, V., and G. Vanags, *Latvijas PSR Zinatnu Akad. Vestis*, **8**, 45 (1961).
9. Arient, J., and Carhan, J., *Collection Czechoslov. Chem. Commun.*, **26**, 98 (1961).
10. de Diesbach, H., and H. Riat, *Helv. Chim. Acta*, **24**, 1314 (1941).

Résumé

On a préparé un acide polyamide-aminé au moyen de la condensation en solution de 3,3' diaminobenzidine et du dianhydride pyromellitique. On a coulé ce polymère sous forme de film et transformé en un polybenzoylènebenzimidazole. On a élucidé en grande partie la transformation qui a lieu au moyen de spectroscopie et on l'a confirmée au moyen d'études sur des substances-modèles. Un nouveau polymère en échelle a été préparé à partir de 1,2,4,5-tétraaminobenzène et de dianhydride pyromellitique.

Zusammenfassung

Eine Polyamidaminosäure wurde durch Kondensation von 3,3'-Diaminobenzidin und Pyromellitsäuredianhydrid in Lösung dargestellt. Aus diesen Polymeren wurde ein Film gegossen und dieser in ein Polybenzoylenbenzimidazol umgewandelt. Der Umwandlungsweg wurde spektroskopisch aufgeklärt und durch Untersuchungen an Modellverbindungen bestätigt. Aus 1,2,4,5-Tetraaminobenzol und Pyromellitsäuredianhydrid wurde ein neues Leiterpolymeres dargestellt.

Received March 23, 1965

Prod. No. 4785A

Kinetics of Styrene Homogeneous Polymerization to Atactic Polypropylene

R. A. WALLACE and K. L. HADLEY,* *Department of Chemical Engineering, University of California, Berkeley, California*

Synopsis

The rate of polymerization of styrene initiated by hydroperoxidized atactic polypropylene in a homogeneous toluene solution has been measured at 60 and 70°C. The reaction is first-order with respect to styrene concentration and independent of the polymeric hydroperoxide concentration above $2 \times 10^{-5}N$ hydroperoxide. The individual rate constants, length and frequency of the grafted polystyrene chains along the polypropylene backbone have been calculated and their significance discussed. The initiation rate constant compares closely with values reported for the analogous *tert*-butyl hydroperoxide-initiated polymerization. The rate constant for the chain transfer termination elementary step at 70°C., however, is 18 times the value reported for the *tert*-butyl hydroperoxide-initiated polymerization of styrene. This high constant accounts for the relatively low rates of polymerization observed and high termination rates. Chain deactivation is presumably accelerated by increased collisions between growing styrene chains and inactive propylene hydroperoxide and polystyrene molecules. Distribution of polystyrene grafts on polypropylene is estimated from knowledge of effects of styrene concentration, polymeric hydroperoxide concentration, and temperature upon the rate of polymerization.

I. INTRODUCTION

The molecular structure of polypropylene provides a convenient backbone to create active polymeric radical sites. One half of the carbon atoms of the main propylene chain are attached to electron-releasing methyl groups. Oxidation occurs readily at the tertiary carbons of the main chain, with formation of polymeric hydroperoxides. These hydroperoxides may be decomposed into free radicals capable of initiating polymerization when heated in the presence of a vinyl monomer. Polypropylene can be hydroperoxidized by (1) direct oxidation with air or oxygen at elevated temperatures,¹ (2) pre-irradiation with γ -rays in the presence of oxygen,² and (3) oxidation of dissolved or swollen polymer in a solution of cumene³ or tetralin⁴ by air or oxygen.

Divergent kinetic results have been reported for graft polymerizations to hydroperoxidized poly- α -olefins. For instance, in the heterogeneous grafting of methyl methacrylate to peroxidized polypropylene, Geleji and Odor² report that the rate of grafting strongly increases

* Present address: Humble Oil Company, Baytown, Texas.

with increasing oxygen content of the backbone. On the other hand, Natta et al.³ note in the surface grafting of several poly- α -olefins that the rate of polymerization remains virtually constant even when the oxygen concentration in the backbone increases by three orders of magnitude. Knowledge of the velocity coefficients of the individual steps of initiation, propagation, and termination are needed to understand first the detailed kinetics of graft polymerization processes and then to estimate the distribution of grafted polystyrene chains along the polypropylene backbone.

Kinetic interpretation for heterogeneous polypropylene grafting is plagued, however, by polymerization rates which are often controlled by the rate of diffusion of monomer to active sites of the polymer backbone and by the Trommsdorff effect resulting from the increased viscosity within the swollen propylene matrix. Treatment of kinetic data, on the other hand, for the more uniform, homogeneous grafting to dissolved polymers is more rewarding and informative.

In this paper a kinetic analysis of homogeneous grafting of styrene to atactic, soluble polypropylene hydroperoxide is presented. Individual rate constants for this polymerization are given and interpreted. From these kinetic results the length and frequency of polystyrene chains grafted to polypropylene are estimated and related to several polymerization parameters.

Polymerization Kinetic Equations

The rate of purely thermal autodecomposition of hydroperoxide groups on oxidized polypropylene is low.⁵ Only in the presence of a vinyl monomer or other reactive species, such as growing chains, with which the initiator polymeric hydroperoxide may react, does the induced decomposition rate of hydroperoxides become appreciable. An explanation of this behavior is the "cage" effect proposed by Matheson.⁶

Assumption of a steady-state concentration of the caged radical pairs ($2R\cdot$) leads to

$$([2R\cdot]) = k_d[I]/(k_r + k_i[M]) \quad (1)$$

where k_d is the velocity coefficient for the decomposition of polymeric hydroperoxide I in the initiation elementary step, k_r is the velocity coefficient for the recombination of the two caged radicals, and k_i is the velocity coefficient for the reaction of monomer M with the caged radical pair. Substitution of eq. (1) into the expression for the rate of initiation yields:

$$(R_i)_I = 2f(k_i k_d [I][M]) / (k_r + k_i [M]) \quad (2)$$

The term $2f$ is the number of polymer chains initiated by each hydroperoxide disappearing in the initiation step; f may have a value between 0.5 and 1.0. When $k_i [M]$ is much larger than k_r , the equation simplifies to

$$(R_i)_I = 2fk_d[I] \quad (3)$$

The mode of decomposition of the hydroperoxide may involve the splitting of either $-O-O-$ or $-O-H$ bonds. In the former case

two growing chains—one graft attached to the polypropylene backbone, one unattached homopolymer—are initiated by each decomposing peroxide. In the latter case only the homopolymer chain is created; the peroxy radical, $-\text{O}-\text{O}\cdot$, remaining on the backbone would react with styrene slowly.

In 1954 Walling and Chang⁷ initiated the polymerization of styrene with cumene and *tert*-butyl hydroperoxides and concluded that the splitting of the $-\text{O}-\text{H}$ bond is more likely. Their conclusion, if extended to the initiation of polymerization with hydroperoxidized polymers, excludes the formation of grafts. In the light of the fact that true graft copolymers have been produced since the work of Walling and Chang, it appears that considerable initiation must occur by cleavage at the $-\text{O}-\text{O}-$ position. Other work buttresses this conclusion.⁸

Walling and Chang also conclude that a hydrogen atom is extracted in the chain transfer step to the hydroperoxide. If this is the case, the relatively inert peroxy radical, $-\text{O}-\text{O}\cdot$, is created, and the chain transfer step effectively kills the reactivity of the radical. The rate of termination by transfer may be expressed as a bimolecular reaction between the growing polymer chain ($\text{RM}\cdot$) and the hydroperoxide (I).

$$(R_t)_I = k_{tr}[\text{I}][\text{RM}\cdot] \quad (4)$$

where k_{tr} is the velocity coefficient of the chain transfer step.

At high polymeric hydroperoxide concentrations, the rates of initiation and termination by the hydroperoxide may be equated by invoking the steady-state assumption.

$$2fk_d[\text{I}] = k_{tr}[\text{I}][\text{RM}\cdot] \quad (5)$$

Solving for $[\text{RM}\cdot]$ and substituting into the rate of polymerization equation yields

$$R_p = 2fk_d k_p / k_{tr} \quad (6)$$

At low polymeric hydroperoxide concentrations, in addition to the rate of termination by chain transfer to the hydroperoxide, the rate of termination by bimolecular combination of the growing polymer chains must be considered. Similarly, two reactions contribute significantly to the initiation of growing polymer chains. At low polymeric hydroperoxide concentrations the rate of the hydroperoxide-induced initiation, $(R_i)_I$, is sufficiently low that "thermal" initiation rate, $(R_i)_0$, is also important. This latter reaction, whose rate is dependent upon the monomer concentration, is complex and not completely understood.

Invoking the steady-state assumption for the case of low polymeric hydroperoxide concentrations and equating the sum of the rates of hydroperoxide- and thermal-induced initiation with the sum of the rates of termination gives the following:

$$(R_i)_0 + (R_i)_I = k_t[\text{RM}\cdot]^2 + k_{tr}[\text{I}][\text{RM}\cdot] \quad (7)$$

The following relationships are developed for substituting into eq. (7): The radical concentration $[RM\cdot]$ may be replaced by

$$[RM\cdot] = R_p/(k_p[M]) \quad (8)$$

At zero polymeric hydroperoxide concentration, the steady-state assumption leads to

$$\begin{aligned} (R_i)_0 &= k_t[RM\cdot]_0^2 \\ &= k_t(R_p)_0^2/(k_p^2[M]^2) \end{aligned} \quad (9)$$

where the subscript zero indicates values for the purely thermally initiated polymerization. At high polymeric hydroperoxide concentrations, equating the rate of initiation to the rate of termination yields

$$2fk_p = k_{tr}(R_p)_I/(k_p[M]) \quad (10)$$

Substituting eqs. (8), (9), and (10) into eq. (7) modifies the latter equation to a more usable form.

$$k_t \frac{(R_p)_0^2}{k_p^2[M]^2} + k_{tr} \frac{(R_p)_I[I]}{k_p[M]} = k_{tr} \frac{(R_p)[I]}{k_p[M]} + k_t \frac{(R_p)^2}{k_p^2[M]^2} \quad (11)$$

Solving this equation for k_{tr} gives a result useful for calculating the chain transfer velocity coefficient from experimental polymerization data:

$$k_{tr} = \frac{k_t}{k_p[M][I]} \left\{ \frac{\frac{(R_p)_0^2}{k_p[M]} - \frac{(R_p)^2}{k_p[M]}}{(R_p) - (R_p)_I} \right\} \quad (12)$$

II. EXPERIMENTAL

Materials

Freshly distilled styrene (Dow Chemical Company) was prepared by washing with 10% sodium hydroxide solution and distilled water, followed by vacuum distillation. Analytical grade toluene was refluxed under a nitrogen blanket for at least 24 hr. to remove dissolved air.

Unstabilized powdered polypropylene (Avisun Company), having a density of 0.857 g./cm.³ and a viscosity-average molecular weight of about 140,000, was used as the backbone polymer. (The viscosity-average molecular weight may be converted to the number-average molecular weight (\bar{M}_n) of about 100,000 by applying the factor of 0.72 of Overberger et al.⁹) A completely atactic fraction soluble in styrene-toluene solutions was prepared by partially dissolving the polymer in heptane at room temperature, filtering the solution through glass wool, and recovering the soluble polymer from the filtrate by precipitation in methanol.

Analytical grade chemicals were used in the determination of the peroxide content of the hydroperoxidized atactic polypropylene. Hydriodic acid (Merck) was treated by adding 10% hypophosphorous acid to remove excess amounts of iodine. Hydriodic acid containing a small amount of

iodine was distilled in darkness with the fraction distilling at 126–127°C. collected.

Cumene and cumene hydroperoxide (Eastman Organic Chemicals) used in the hydroperoxidation step were of technical grade.

Apparatus

Hydroperoxidation of atactic polypropylene was carried out in 100-ml. test tubes with oxygen supplied through a sintered glass dispersion tube. Hydroperoxide content was analyzed in the apparatus as described by Sully.¹⁰ Dilatometers were constructed of 15–20 ml. test tubes with ground-glass tops fitted with capillary tubes of about 0.4 mm. bore. The volumes of the dilatometer and capillary were calibrated with mercury. All reactions were conducted in a Sargent viscometric bath controlled to $\pm 0.01^\circ\text{C}$. Capillary liquid levels were observed to 0.01 cm. with a Gaertner cathetometer.

Procedure

Hydroperoxidation of Atactic Polypropylene. The technique for hydroperoxidizing poly- α -olefins in cumene solution has been previously described by Natta et al.³ Polypropylene (2–3 g.) was dissolved in 50 ml. of cumene. Oxygen was dispersed through this mixture maintained at 60°C. for 24 hr. The resulting hydroperoxidized polymer was precipitated in an excess of methanol. The polypropylene was purified by redissolving in heptane and reprecipitating in methanol twice.

Polypropylene Hydroperoxide Content. The total peroxidic oxygen analysis described by Beati¹ was utilized. The polymer sample (0.1–0.2 g.) and several pieces of Dry Ice were placed in a 100-ml. round-bottomed flask connected to the condenser tube and heated to reflux temperature. A 1-ml. portion of freshly distilled hydriodic acid was introduced into the flask. After 30 min. the flask was cooled, and the liberated iodine was titrated with 0.005*N* sodium thiosulfate solution using a starch indicator.

The determination was done in duplicate together with two blanks containing no polypropylene. A value of 0.0431 wt.-% oxygen with an average deviation of 3% was measured. (This concentration of hydroperoxides is equivalent to one hydroperoxide group every 2000 propylene monomeric units.)

Attempts to measure reproducible hydroperoxide contents exclusive of other peroxides by the reaction with potassium iodide in chloroform-acetic acid¹¹ were unsuccessful. It was found that the determination was dependent upon the solvent ratio and the time of refluxing. The maximum results obtained in these determinations, however, approximated those obtained in the total peroxidic hydriodic acid method. Therefore it was assumed that virtually all of the oxygen in the polypropylene was in the hydro- rather than in the di-peroxide form.

Polymerization. Hydroperoxidized polypropylene was dissolved in degassed toluene under an inert atmosphere of nitrogen. Freshly distilled

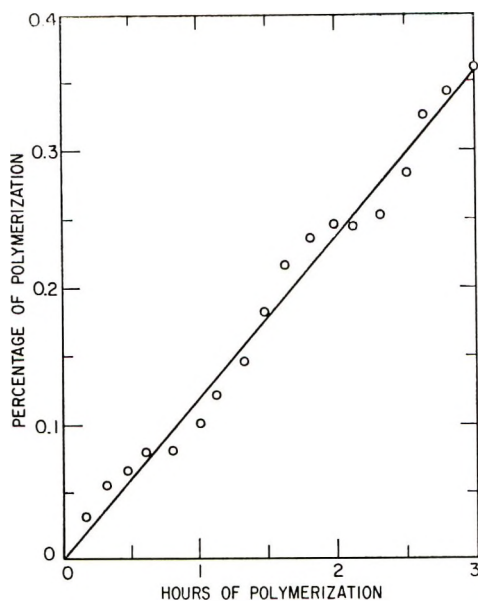


Fig. 1. Course of the polymerization of 2.26*M* styrene in toluene with polypropylene hydroperoxide initiator at 70°C.

styrene was added to the reaction mixture, and the solution was transferred rapidly to the dilatometer. The dilatometer was placed in a mineral oil bath at either 60–70°C. The lack of an induction period before the polymerization reaction indicated that negligible amounts of inhibiting oxygen were absorbed in the transfer step.

As polymerization takes place in the dilatometer, the liquid level in the capillary falls due to the difference in the specific volumes of styrene and polystyrene. The capillary liquid height was recorded every 2–5 min. for a total period of 350–500 min. The best straight line, whose slope is proportional to the rate of polymerization, was drawn through these data. A plot of a typical experiment with the capillary height change converted to percentage of polymerization is given in Figure 1. The sinusoidallike fluctuations are a reflection of the regular changes of temperature in the oil bath, since the dilatometer also acts as a highly sensitive thermometer.

A 1-g. polymerization sample of grafted poly(styrene-propylene hydroperoxide) dissolved in 50 ml. benzene at 40°C.; ungrafted hydroperoxidized atactic polypropylene remained insoluble in boiling benzene. This indicates that polystyrene is chemically bonded to atactic polypropylene in a sufficient amount to alter its solubility properties in benzene. Also, this buttresses the assumption made in the kinetic analysis that a considerable amount of initiation must occur by —O—O— cleavage, resulting in one graft chain for every homopolymer chain, rather than by the splitting of the —OH— grouping yielding only homopolymer.

Dilatometer Calibration. Relating the observed rate of change in the dilatometer capillary liquid height with the rate of polymerization requires

a knowledge of the difference in the density of styrene and the apparent density of polystyrene dissolved in styrene and toluene. The difference between the specific volumes of styrene and polystyrene dissolved in the reaction solution, $V_{\text{styrene}} - V_{\text{polystyrene}}$, is termed the dilatometric constant. Density values for styrene and polystyrene dissolved in pure styrene reported by Matheson¹² were used to calculate values of 0.205 and 0.231 cm.³/g. for the dilatometric constant at 60 and 70°C.

If the specific volume of polystyrene in toluene is the same as the value for polystyrene dissolved in styrene, the same dilatometric constants can be used for any styrene-toluene reaction solution. The density of toluene and the density of a solution of toluene containing 1.5 wt.-% polystyrene were determined by using a type of Westphal balance. A weighted hollow glass bulb of about 10 cm.³ was suspended from a Cahn electrobalance in solutions of toluene, styrene, and toluene-polystyrene. The apparent weight of the bulb in each of these solutions was noted. Based upon the density of styrene reported by Matheson,¹² the density of polystyrene in toluene was calculated. Values of 1.060 g./cm.³ at 60 g. and 0.949 g./cm.³ at 70°C. were obtained. These values agree closely with the values reported by Matheson for polystyrene dissolved in pure styrene.

Since the apparent density of polystyrene is approximately the same in solutions of styrene and toluene, and since the volumes of styrene and toluene are additive,* the same dilatometric constants were used for all styrene-toluene ratios.

III. RESULTS AND DISCUSSION

Effect of Monomer Concentration

As seen in Figure 2, the rate of polymerization is linear with respect to the monomer concentration. This same first-order dependence has been reported with cumene and *tert*-butyl hydroperoxide-initiated polymerizations by Johnson and Tobolsky¹³ and by Howard and Simpson.¹⁴

The experimental observation of the first-order effect justifies the assumption that $k_t[M] \gg k_r$, made in developing eq. (3). Thus, the reactivity of the monomer molecule with the caged radical pair is so large that few of the pairs recombine. Therefore, the rate of decomposition of the polymeric hydroperoxide into the two caged radicals is the rate-controlling step of the initiation reaction. Even though the reaction is much more complicated, the initiation step can be treated as the simpler case of autodecomposition of the hydroperoxide into radicals capable of initiating the growth of polymer chains.

Effect of Polypropylene Hydroperoxide Concentration

The concentration of polypropylene hydroperoxides in the polymerization solution was changed by varying the concentration of peroxidized poly-

* A plot of liquid solution specific volume of styrene-toluene mixtures versus the mole fraction styrene is linear.

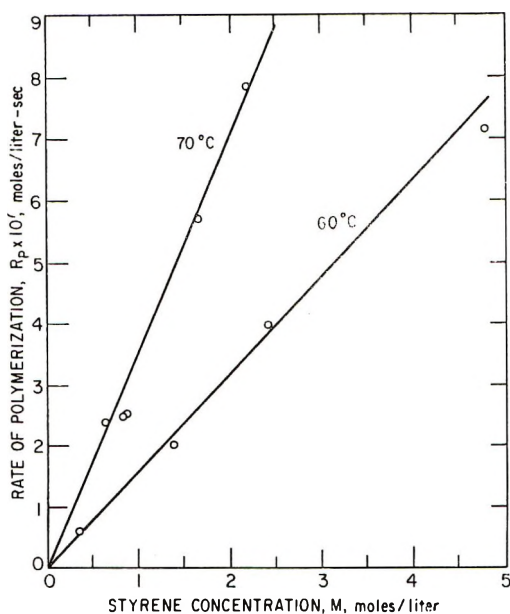


Fig. 2. Dependence of polymerization rate to hydroperoxidized polypropylene in toluene on the concentration of styrene.

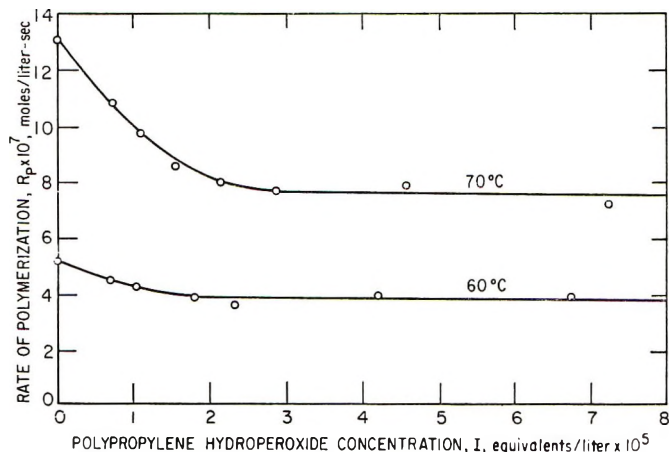


Fig. 3. Effect of polypropylene hydroperoxide concentration on the polymerization rate with monomer concentrations of 2.46M at 60°C. and 2.26M at 70°C.

propylene containing 0.0431 wt.-% oxygen (equivalent to one hydroperoxide group every 2000 propylene monomeric units). Curves of Figure 3 illustrate the polymerization rate to be independent of the hydroperoxide concentration above about 2 eq./l. At lower polymeric hydroperoxide concentrations, the rate increases with decreasing hydroperoxide content to a maximum at zero.

These results are in agreement with the equations developed in this paper. Differentiating eq. (11) gives

$$\frac{dR_p}{d[I]} = k_{tr} \left\{ \frac{(R_p)_I - (R_p)}{k_{tr}[I] + \frac{2k_t(R_p)}{k_p[M]}} \right\} \quad (13)$$

The term of the numerator of eq. (13) has a maximum absolute value for zero hydroperoxide concentration. As the polymeric hydroperoxide concentration increases, (R_p) approaches $(R_p)_I$, and their difference approaches zero. The slopes of the curves of Figure 3, the rate of polymerization versus the polymeric hydroperoxide concentration, agree with the behavior of the derivative $dR_p/d_p[I]$ as given by eq. (13).

The assumptions made in deriving the kinetic equations are borne out: (1) at high polymeric hydroperoxide concentrations, only the hydroperoxide-induced initiation and termination rates are significant; (2) at low hydroperoxide concentrations, thermal initiation and bimolecular radical termination by coupling must also be considered.

Effect of Temperature

The rate of polymerization in the region of high polymeric hydroperoxide concentrations increases by a factor of 2.11 ± 0.35 when the temperature increases from 60 to 70°C. On applying reaction rate theory to the grafting process, one can calculate an experimental activation energy of 18.6 ± 4.2 kcal./mole. The error of 4.2 is the negative deviation for the calculated activation energy with uncertainties in the reported values of $2fk_d k_p/k_{tr}$.

Polymerization Rate Constants

The ratio of individual rate constants $2fk_d k_p/k_{tr}$ is evaluated from the experiments conducted with a polymeric hydroperoxide concentration greater than 2×10^{-5} eq. l.¹ Rate constant results are summarized in Table I. The chain transfer velocity coefficient k_{tr} has been estimated from data with less than 2×10^{-5} eq. l. polymeric hydroperoxides. At greater than this hydroperoxide concentration, the rate is largely controlled by initiation and termination by the polymeric hydroperoxides. Below this concentration, however, thermal initiation and the bimolecular radical termination by combination of the growing polymer chains must also be considered. Values of k_{tr} have been computed by using eq. (12) and the values of k_p and k_t reported by Matheson.¹²

The chain transfer constant k_{tr}/k_p relates the number-average molecular

TABLE I
Evaluation of Individual Polymerization Rate Constants for Styrene Grafting to Atactic Polypropylene Hydroperoxide

Temp., °C.	$2fk_d k_p/k_{tr} \times 10^7$, sec. ⁻¹	k_{tr} , l./mole-sec.	C_I
60	1.60 ± 0.11	178 ± 27	1.01 ± 0.15
70	3.39 ± 0.24	275 ± 75	1.14 ± 0.30

weight of the grafted polystyrene chains with the polymerization parameters. Calculated values, again based upon the k_p of Matheson,¹² are also shown in Table I.

The closeness of the two values of C_I at 60°C. and 70°C. points out that (1) the activation energy of the propagation step (7.8 kcal./mole, according to Matheson¹²) is approximately equal to that of the chain transfer step; and (2) the chain length of the grafted polystyrene is relatively unaffected over this polymerization temperature range. Increasing the temperature of the polymerization from 60 to 70°C. decreases the length of the grafts by about 10%.

The chain transfer constant at 73°C. is 280 l./mole-sec., 18 times the chain transfer constant of 0.06 reported by (Walling and Chang⁹ for the *tert*-butyl hydroperoxide-initiated polymerization of styrene. This high constant accounts for the relatively low rates of polymerization observed. Walling and Chang also report that the rate of polymerization is proportional to the 0.21 power of the hydroperoxide concentration in the range between 0.01 and 0.1*M* hydroperoxide. For termination by bimolecular radical combination only, one would expect the rate of polymerization to be proportional to the 0.5 power of the hydroperoxide concentration; for termination by chain transfer only, the rate of polymerization would be proportional to the zero power of the hydroperoxide concentration. There it appears that under the reaction conditions of Walling and Chang, both forms of termination occur to a significant extent. However with the hydroperoxidized polypropylene system, termination by chain transfer, as shown by the zero-order effect of the polymeric hydroperoxide, is rate-controlling at polypropylene hydroperoxide concentrations as low as $2 \times 10^{-5}N$.

The initiation rate constant, $2fk_d$, is approximated for comparison with the *tert*-butyl hydroperoxide system. One calculates values of $2fk_d$ of $(1.61 \pm 0.35) \times 10^{-7}$ l./mole-sec. at 60°C. and $(3.87 \pm 1.35) \times 10^{-7}$ l./mole-sec. at 70°C. The value at 60°C. is just slightly lower than the mean of two values, 2.11 and 1.39×10^{-7} , estimated from the data of *tert*-butyl hydroperoxide-initiated polymerization of styrene at the same temperature. The activation energy of polypropylene hydroperoxide-induced initiation, estimated to be 22 ± 2 kcal./mole, is comparable with the reported value of 24 kcal./mole for the analogous *tert*-butyl hydroperoxide system.¹⁴ Apparently then, the decomposition of both hydroperoxide initiators are similar.

Length and Frequency of Grafted Polystyrene Chains

Inspection of calculated number-average molecular weight data indicates that the length of polystyrene graft chains is directly proportional to the styrene concentration, inversely proportional to the polypropylene hydroperoxide concentration, and slightly affected by polymerization temperature. As noted previously, the validity of this conclusion is dependent upon a negligible amount of —O—O— bond cleavage in the chain transfer step.

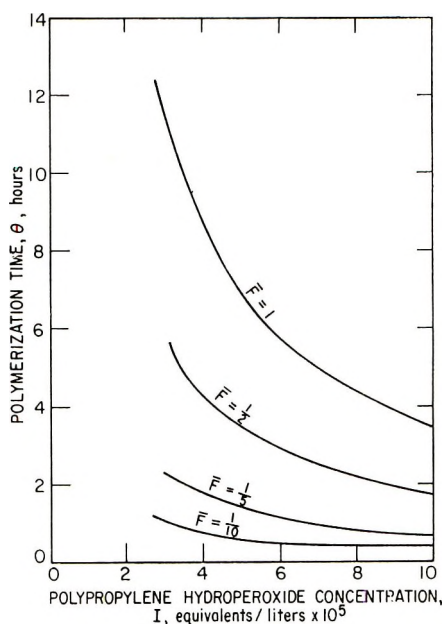


Fig. 4. Frequency of polystyrene grafts per 100,000 monomeric units of the polypropylene backbone as a function of the polypropylene hydroperoxide concentration and the polymerization time at 70°C. Polypropylene concentration: 1 g./l.

The average number of polystyrene graft chains per 100,000 backbone propylene monomeric units F is linearly proportional to both polymerization time and the weight percentage of oxygen in the hydroperoxidized polypropylene backbone. Figure 4 presents a semiempirical correlation relating the frequency of polystyrene chains on polypropylene to polypropylene hydroperoxide concentration and polymerization time at 70°C. Increasing the temperature of the polymerization from 60 to 70°C. increases the frequency of polystyrene grafts by a factor of 2.4. The length of graft chains is relatively unaffected by the temperature in this temperature range, so the increased rate of polymerization at the higher temperature goes into creating more rather than longer polystyrene chains.

The Office of Saline Water under grant 14-01-0001-439 and the Water Resources Center of the University of California at Berkeley jointly supported this work. The authors wish to express their thanks to Profs. H. P. Gregor and G. Oster, Polytechnic Institute of Brooklyn, for their technical advice.

References

1. Beati, E., F. Severini, and S. Toffano, *J. Polymer Sci.*, **51**, 455 (1961).
2. Geleji, F., and L. Odor, *J. Polymer Sci.*, **C4**, 1223 (1963).
3. Natta, G., E. Beati, and F. Severini, *J. Polymer Sci.*, **34**, 685 (1959).
4. Manson, J., and I. Cragg, *Can. J. Chem.*, **36**, 858 (1958).
5. Dudorov, V. V., A. L. Samvelyan, A. F. Lukovnikov, and P. O. Levin, *Izv. Akad. Nauk Arm. SSR, Khim. Nauki*, **15**, 311 (1962).
6. Matheson, M. S., *J. Chem. Phys.*, **13**, 584 (1945).

7. Walling, C., and Y. Chang, *J. Am. Chem. Soc.*, **76**, 4878 (1954).
8. Seubold, F. H., F. F. Rust, and W. E. Vaughan, *J. Am. Chem. Soc.*, **73**, 18 (1951).
9. Overberger, C. G., P. Fram, and T. Alfrey, *J. Polymer Sci.*, **6**, 539 (1951).
10. Sully, D., *Analyst*, **79**, 84 (1954).
11. Wheeler, D. H., *Oil Soap*, **9**, 89 (1932).
12. Matheson, M. S., E. E. Auer, E. B. Bevilacqua, and E. J. Hart, *J. Am. Chem. Soc.*, **73**, 1700 (1951).
13. Johnson, D. H., and A. V. Tobolsky, *J. Am. Chem. Soc.*, **74**, 938 (1952).
14. Haward, R. N., and S. Simpson, *Trans. Faraday Soc.*, **47**, 212 (1951).

Résumé

On a mesuré la vitesse de polymérisation à 60 et 70°C du styrène initiée par du polypropylène atactique hydroperoxyde en solution homogène dans le toluène. La réaction est de premier ordre par rapport à la concentration en styrène et indépendante de la concentration en hydroperoxyde polymérique aux teneurs en hydroperoxyde supérieurs à $2 \times 10^{-6} N$. On a calculé les constantes de vitesse individuelles, la longueur et la fréquence des chaînes greffées de polystyrène le long du squelette de polypropylène et on a discuté leur signification. La constante de vitesse d'initiation est très voisine des valeurs rapportées pour la polymérisation analogue initiée par l'hydroperoxyde de *t*-butyle. La constante de vitesse pour l'étape élémentaire de terminaison par transfert de chaînes à 70°C est cependant 18 fois supérieure à la valeur rapportée par la polymérisation du styrène initiée par l'hydroperoxyde de *tert*-butyle. Cette constante élevée est responsable des vitesses de polymérisation relativement faibles et des vitesses élevées de la terminaison; La dés-activation des chaînes est vraisemblablement accélérée par un accroissement du nombre de collisions entre les chaînes du polystyrène en croissance et les molécule inactives d'hydroperoxyde de propylène et de polystyrène. On estime la distribution des greffons de polystyrène sur le polypropylène au départ de la connaissance des effets de concentration du styrène, de la concentration en hydroperoxyde polymérique et de la température sur la vitesse de polymérisation.

Zusammenfassung

Die Geschwindigkeit der durch hydroperoxydiertes ataktisches Polypropylen in homogener Toluollösung gestarteten Styrolpolymerisation wurde bei 60 und 70°C gemessen. Die Reaktion ist bezüglich der Styrolkonzentration von erster Ordnung und oberhalb $2 \cdot 10^{-6} N$ Hydroperoxy von der Konzentration des polymeren Hydroperoxyds unabhängig. Die individuellen Geschwindigkeitskonstanten, Länge und Häufigkeit der auf die Polypropylenhauptkette aufgepfropften Polystyrolketten werden berechnet und ihre Bedeutung diskutiert. Die Startgeschwindigkeitskonstante ist mit k_{dd} für die analoge *tert*-Butylhydroperoxydestartete Polymerisation gut vergleichbar. Die Geschwindigkeitskonstante des Elementarschritts des Kettenübertragungsabbruchs bei 70°C besitzt jedoch den 18 fachen Werte der für die *tert*-butylhydroperoxygestarteten Polymerisation von Styrol bekannten Grösse. Dieser hohe Werte ist für die beobachtete verhältnismässig niedrige Polymerisationsgeschwindigkeit und die hohe Abbruchgeschwindigkeit verantwortlich. Die Kettendesaktivierung wird vermutlich durch eine erhöhte Zahl von Zusammenstößen zwischen wachsenden Styrolketten und inaktivem Propylenhydroperoxyd sowie Polystyrolmolekülen beschleunigt. Die Verteilung der Polystyrolaufpfropfungen auf Polypropylen wird aus der Kenntnis des Einflusses der Styrolkonzentration, der Konzentration des polymeren Hydroperoxyds und der Temperatur auf die Polymerisation abgeschätzt.

Received May 11, 1965

Revised June 28, 1965

Prod. No. 4789A

Effects of Concentration of Urethane Linkage, Crosslinking Density, and Swelling upon the Viscoelastic Properties of Polyurethanes

KYOICHI SHIBAYAMA and MINEKAZU KODAMA, *The Central Research Laboratories, Mitsubishi Electric Corporation, Amagasaki, Japan*

Synopsis

Viscoelastic properties of unswollen and swollen specimens of homologous series of polyurethanes were studied in the glass-to-rubber transition region. In the case of unswollen specimens, a large discrepancy was found to exist between the thermal expansion coefficient of specific volume and that of free volume derived by comparing the WLF equation with Doolittle's equation in which the parameter B was assumed to be unity. As a possible way to account for this discrepancy, B is assumed to be a decreasing function of temperature supposing that the thermal dissociation of secondary linkage between polar groups may have a decreasing effect on the size of elemental unit of molecular motion. In the case of swollen specimens, this discrepancy was found to disappear. Differences between specimens swollen in ethyl acetate and n -propanol were observed in the spread of the array of relaxation modulus versus temperature curves in a homologous series. As a cause of this phenomenon it is suggested that the mechanisms of imparting free volume to the system are different for ethyl acetate and n -propanol because of characteristic interactions between swelling agents and polymers.

INTRODUCTION

Polyurethanes are widely used for various purposes as foams, elastomers, paints, adhesives, and so on. Investigations on the relation between structure and properties of polyurethanes have been made by several workers. For elastomers, the dependences of glass temperature, tensile strength, and degree of swelling upon the polymer constitution have been studied.^{1,2} For rigid polyurethanes, the relation between dynamic mechanical properties and the type of diol used as a constituent has been studied.³ Dependences of glass temperature and logarithmic decrement upon the types of polyesters and polyisocyanates used as constituents have been studied for films of polyurethane paints.⁴

At the present, it seems to be necessary to separate and clarify the effect of each polar group and crosslinking density upon the properties so as to get a full understanding. Further, the internal structure of a polar polymer may be affected by interactions with solvents. Thus, the study of mechanical properties of swollen polymer will be useful for understanding not only the nature of interaction of polymer with solvent but also the relation between structure and properties of polymer itself.

In this investigation, rigid polyurethanes have been prepared from glycol, triol, tolylene diisocyanate, and water so as to get homologous series of polymers with respect to the concentration of urethane linkage and crosslinking density, and viscoelastic properties of unswollen and swollen specimens have been studied in the glass-to-rubber transition region.

EXPERIMENTAL

Composition of Sample

Homologous series of polymers with respect to concentrations of polar groups and crosslinking density were prepared by adjusting the composition of ingredients: tolylene diisocyanate, dipropylene glycol, polypropylene glycol, triol, and water. These ingredients will be abbreviated as TDI, DPG, PPG, Tr, and H₂O, respectively. Polymers prepared by mixing these five ingredients can contain urethane, urea, biuret, and allophanate linkages in the chain. Biuret and allophanate linkages are trifunctional groups and can act as crosslinking units. According to the chemistry of polyurethane formation, concentrations of functional groups in polymers can be calculated by eqs. (1) and (2), assuming that the conversion of each reactant is complete and the rate of formation of biuret linkage is greater than that of allophanate linkage.⁵

When $(\text{H}_2\text{O}) > \{(\text{NCO}) - (\text{OH}) - 2(\text{H}_2\text{O})\}$:

$$\left. \begin{aligned} [\text{U}] &= \frac{(\text{OH})}{W} \\ [\text{Ur}] &= \frac{3(\text{H}_2\text{O}) + (\text{OH}) - (\text{NCO})}{W} \\ [\text{B}] &= \frac{(\text{NCO}) - (\text{OH}) - 2(\text{H}_2\text{O})}{W} \\ [\text{A}] &= 0 \\ [\rho] &= [\text{Tr}] + [\text{B}] \end{aligned} \right\} \quad (1)$$

When $(\text{H}_2\text{O}) < \{(\text{NCO}) - (\text{OH}) - 2(\text{H}_2\text{O})\}$:

$$\left. \begin{aligned} [\text{U}] &= \frac{(\text{OH})}{W} \\ [\text{Ur}] &= 0 \\ [\text{B}] &= \frac{(\text{H}_2\text{O})}{W} \\ [\text{A}] &= \frac{(\text{NCO}) - (\text{OH}) - 3(\text{H}_2\text{O})}{W} \\ [\rho] &= [\text{Tr}] + [\text{B}] + [\text{A}] \end{aligned} \right\} \quad (2)$$

TABLE I
Preparation and Calculated Values of Functional Group Concentration for Series I

No.	Charge, mole			Calculated values of functional groups, mole/g.					
	(TDI)	(Tr)	(DPG)	(PPG)	(H ₂ O)	[B] _c × 10 ⁶	[A] _c × 10 ⁵	[ρ] _c × 10 ⁴	[U] _c × 10 ³
11	0.1505	0.0172	0.1267	0.0040	0.00039	1.58	5.77	3.05	5.97
12	0.1380	"	0.0999	0.0185	0.00043	1.74	4.47	2.93	5.48
13	0.1251	"	0.0731	0.0330	0.00046	1.85	1.70	2.67	4.98
14	0.1150	"	0.0492	0.0465	0.00050	2.00	2.40	2.75	4.50
15	0.1000	"	0.0194	0.0615	0.00053	2.10	1.25	2.65	3.96

TABLE II
Preparation and Calculated Values of Functional Group Concentration for Series II

No.	Charge, mole			Calculated values of functional groups, mole/g.					
	(TDI)	(Tr)	(DPG)	(PPG)	(H ₂ O)	[U] _c × 10 ³	[B] _c × 10 ⁶	[A] _c × 10 ⁵	[ρ] _c × 10 ⁴
21	0.1250	0.0755	0.0424	0.0055	0.00018	4.98	7.65	4.15	10.60
22	"	0.0368	0.0627	0.0240	0.00019	4.98	"	3.75	5.40
23	"	0.0218	0.0702	0.0315	0.00020	4.98	"	3.75	3.38
24	"	0.0143	0.0746	0.0350	0.00020	4.99	"	2.14	2.22

TABLE III
Preparation and Calculated Values of Functional Group Concentration for Series III

No.	Charge, mole			Calculated values of functional groups, mole/g.					
	(TDI)	(Tr)	(DPG)	(PPG)	(H ₂ O)	[U] _c × 10 ³	[B] _c × 10 ⁶	[ρ] _c × 10 ⁴	[A] _c × 10 ⁵
31	0.1375	0.0374	0.0717	0.0157	0.00029	4.99	1.16	9.85	47.30
32	0.1275	0.0674	0.0502	0.0072	0.00031	4.99	1.23	9.83	7.09
33	0.1253	0.0743	0.0452	0.0054	0.00032	4.99	0 ^a	9.83	0

^a [Ur]_c = 8.0 × 10⁻⁶.

where NCO, OH, U, Ur, B, A, ρ , and \bar{W} represent isocyanate group, hydroxyl group, urethane linkage, urea linkage, biuret linkage, allophanate linkage, crosslinking density, and total weight, respectively. Brackets and parentheses represent mole in one gram sample and gram equivalent, respectively.

Compositions of samples and calculated values of functional group concentrations are given in Tables I–III where series I, II, and III are homologous series of polymers with respect to concentration of urethane linkage, crosslinking density, and concentration of allophanate linkage, respectively.

Materials and Sample Preparation

TDI(2,4-80%, 2,6-20%) was distilled at 105–108°C. under the pressure of 5 mm. Hg. PPG (molecular weight 400), DPG, and Tr (addition product of propylene oxide to glycerine, molecular weight 400) were dried for 3 hr. at 75°C. under the pressure of 2–3 mm. Hg. The water content of the polyol mixture was determined by the method of Karl Fischer immediately before mixing polyols and TDI. Curing of the mixture of polyols and TDI was conducted between two glass plates covered by Teflon film first at 40°C. for 3 hr., then at 60°C. for 48 hr., and finally at 100°C. for 3 hr.

X-Ray Diffraction

Intensity curves of x-ray diffraction were determined at room temperature for selected samples by use of an x-ray diffractometer (FeK α radiation 35 k.v., 10 ma., Mn filter).

Determination of Specific Volume of Unswollen and Swollen Specimens

Specific volume versus temperature curves of unswollen samples were derived by measuring weight changes of a specimen immersed in a silicone oil (10 cstokes, KF 96, supplied by Shinetsu Chem. Co.) at various temperature. For swollen samples, the specific volume was derived by measuring weight of a specimen immersed in swelling agent at 30°C. Rodlike specimens of 2 to 3 g. were used in both cases.

Viscoelastic Properties and Thermal Expansion Coefficient

Relaxation moduli of specimens from 1 to 10 sec. were calculated from the slopes of stress-strain curves derived from constant rate extension experiments by means of an Instron-type apparatus at various temperature. Maximum extensions were less than 1%, in which the linearity of viscoelastic behavior held satisfactorily. In the case of swollen specimens, extension experiments were carried out in an immersion set-up. Equilibrium swelling of the specimens had been attained in an auxiliary vessel prior to their being placed in the immersion equipment.

It had been reported in earlier papers^{6,7} that the temperature dependence of λ , which is the time derivative of the relaxation modulus, can be ex-

pressed as eq. (3) when the relaxation modulus versus time curve is fitted by an empirical eq. (4) which has been proposed by Tobolsky⁸ and is readily transcribed into a form of temperature dependence by using the WLF equation:

$$\lambda(T) = \frac{\sqrt{\pi}}{2} h \log \frac{E_1}{E_2} \exp \left\{ - \left[\frac{hC_1(T - T_m)}{C_2 + T - T_m} \right]^2 \right\} \quad (3)$$

$$\log E(t) = 1/2 \{ \log E_1 E_2 + \log (E_1/E_2 \operatorname{erf} [h \log (t/k)]) \} \quad (4)$$

where E_1 and E_2 are upper and lower equilibrium values of the relaxation modulus, h is a parameter representing steepness of transition, C_1 and C_2 are constants appeared in the WLF equation, T_m is the temperature at which λ exhibits its maximum value, and k is time when $\log E(t)$ equals $1/2 \log E_1 E_2$.

It is possible to evaluate C_1 , C_2 , and h from the measurement of relaxation moduli for a short time, at various temperatures, which is necessary to evaluate λ . Equations (5) and (6), derived from eq. (3), can be used conveniently for this purpose,

$$h = 2\lambda(T_m)/\sqrt{\pi} \log (E_1/E_2) \quad (5)$$

$$hC_1(T - T_m)/(C_2 + T - T_m) = [\ln \lambda(T_m)/\lambda(T)]^{1/2} \quad (6)$$

Advantages of this method of analyzing results of viscoelastic measurements, over the standard method of the so-called time-temperature superposition, are its simplicity and greater accuracy in estimating values of the WLF constants because errors of superposing the relaxation curves can be avoided.

Master relaxation curves were constructed by the time-temperature superposition technique to examine the applicability of eq. (4) to the present system. Validity of eq. (3) was then examined directly by plotting $(T - T_m)/[\ln \lambda(T_m)/\lambda(T)]^{1/2}$ against $T - T_m$ and, further, by comparing values of the WLF constants thus obtained with those derived from the temperature dependence of the shift factor.

For some swollen specimens, the thermal expansion coefficient was determined by measuring the linear expansion.

Swelling Agents and Adjustment of Degree of Swelling

Ethyl acetate and *n*-propanol were selected as swelling agents because the degree of swelling can be varied widely by both of them and furthermore they are believed to differ in nature of swelling action.

Adjustment of degree of swelling was made by mixing the swelling agent with an appropriate amount of silicone oil (10 cstokes, KF 96). It was verified that silicone oil was not absorbed in the specimen from the facts that the weight of deswollen specimen, obtained by evaporating the swelling agent near its boiling temperature, was the same as that of the unswollen specimen and the amount of extractable materials in a swollen specimen was less than 0.5%.

The degree of swelling was expressed as weight fraction of polymer, W_2 , which was determined gravimetrically from the difference of weight between unswollen and swollen specimen.

RESULTS

X-Ray Diffraction

In Figure 1, intensity curves of x-ray diffraction are shown for specimens 13, 24, and 33 at room temperature. These results indicate that the polymers obtained here have no crystalline region at all.

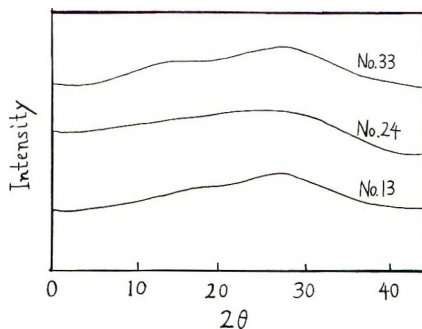


Fig. 1. X-ray intensity curves.

Specific Volume

Specific volume versus temperature curves of unswollen specimens for series I, II, and III are shown in Figure 2. In series I and II, curves shift toward higher temperatures when the concentration of urethane linkage or crosslinking density increases. In series III, curves above glass temperature overlap each other and those below glass temperature change

TABLE IV
Values of Characteristic Parameters Representing Temperature Dependence of Specific Volume for Unswollen Specimens

Series	No.	T_g , °C.	v_g , cc./g.	$\alpha_a \times 10^4$	$\alpha_b \times 10^4$
I	11	54	0.815	5.90	1.97
	12	45	0.824	6.11	1.58
	13	35	0.831	6.76	1.57
	14	24	0.841	7.43	1.57
	15	17	0.852	7.48	1.58
II	21	47	0.826	5.81	1.21
	22	37	0.827	5.93	1.21
	23	33	0.831	6.52	1.08
	24	24	0.832	6.61	0.96
III	31	42	0.820	7.05	0.84
	32	44	0.824	6.44	0.85
	33	46	0.825	6.32	0.73

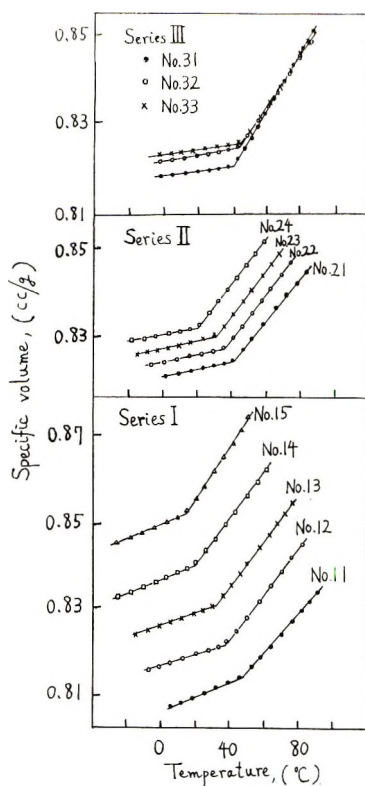


Fig. 2. Specific volume vs. temperature curves for unswollen specimens.

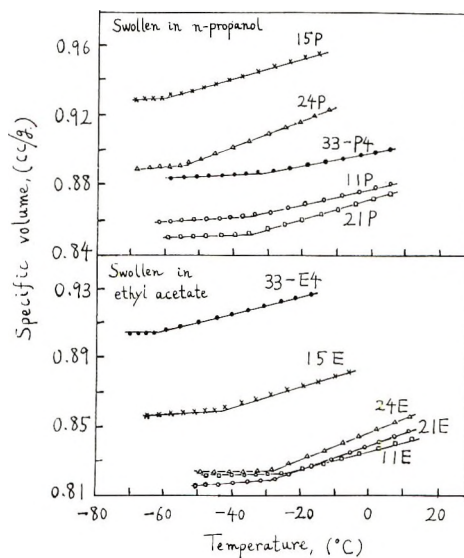


Fig. 3. Specific volume vs. temperature curves for swollen specimens. Degree of swelling is tabulated in Table VI.

TABLE V
Values of Characteristic Parameters Representing Temperature Dependence of Specific Volume for Selected Swollen Specimens

Symbol ^a	T_{ms} , °C.	T_{gs} , °C.	$\alpha_{as} \times 10^4$	$\alpha_{bs} \times 10^4$
33-E4	-44	-63	5.48	1.22
11E	-4	-24	6.02	1.28
15E	-25	-43	7.27	1.23
21E	-10	-29	7.91	1.59
24E	-9	-28	9.72	1.50
33-P4	-14	-33	4.56	1.32
11P	-13	-34	5.00	1.50
15P	-45	-60	6.00	1.50
21P	-17	-35	6.53	1.50
24P	-34	-54	8.10	1.72

^a The meaning of symbols is shown in Table VI.

TABLE VI
Specific Volume of Swollen Specimen in Ethyl Acetate and *n*-Propanol at 30°C.

Symbol	Sample no.	Swelling agent	W_2	v_1 , cc./g.	v_2 , cc./g.
11E	11	Ethyl acetate	0.826	0.851	0.875
12E	12		0.832	0.861	0.881
13E	13		0.818	0.877	0.893
14E	14		0.820	0.891	0.904
15E	15		0.822	0.905	0.915
21E	21	Ethyl acetate	0.822	0.866	0.888
22E	22		0.825	0.868	0.889
23E	23		0.825	0.870	0.891
24E	24		0.820	0.872	0.897
11P	11	<i>n</i> -Propanol	0.749	0.890	0.948
12P	12		0.757	0.904	0.959
13P	13		0.751	0.931	0.968
14P	14		0.748	0.961	0.977
15P	15		0.742	0.983	0.990
21P	21	<i>n</i> -Propanol	0.767	0.889	0.956
22P	22		0.756	0.918	0.963
23P	23		0.742	0.938	0.969
23P	24		0.749	0.956	0.896
33-E1	33	Ethyl acetate	0.810	0.871	0.893
33-E2	"		0.752	0.902	0.909
33-E3	"		0.701	0.920	0.923
33-E4	"		0.662	0.940	0.948
33-P1	33	<i>n</i> -Propanol	0.878	0.880	0.916
33-P2	"		0.855	0.887	0.929
33P-3	"		0.820	0.890	0.944
33-P4	"		0.792	0.902	0.953

their positions regularly. Characteristic parameters representing glass transition are listed in Table IV, where v_g is the specific volume at T_g and α_a and α_b are thermal expansion coefficients above and below T_g , respectively.

Figure 3 shows specific volume versus temperature curves for selected cases of swollen specimens calculated from the results of linear expansion measurements assuming isotropic expansions. Glass temperature T_{gs} and thermal expansion coefficients α_{as} and α_{bs} obtained from the results of Figure 3 are listed in Table V.

Specific volumes of swollen specimens in ethyl acetate and *n*-propanol

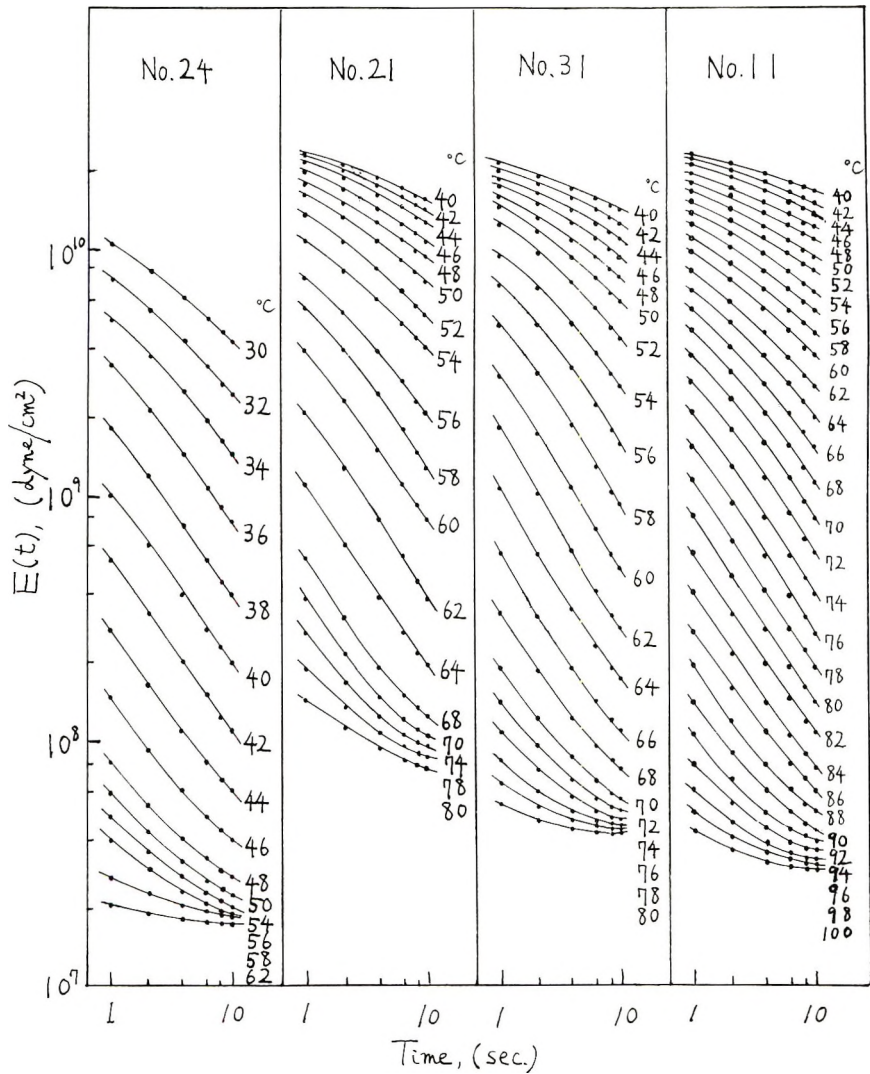


Fig. 4. Relaxation modulus vs. time curves at various temperatures. Curve (1) No. 24; (2) No. 21; (3) No. 31; (4) No. 11.

at 30°C. are listed in Table V, where v is the observed value and v_c is the value calculated assuming additivity between the volumes of polymer and swelling agent. It is apparent from the comparison of v with v_c that the additivity between the volumes of polymer and swelling agent does not hold in these systems.

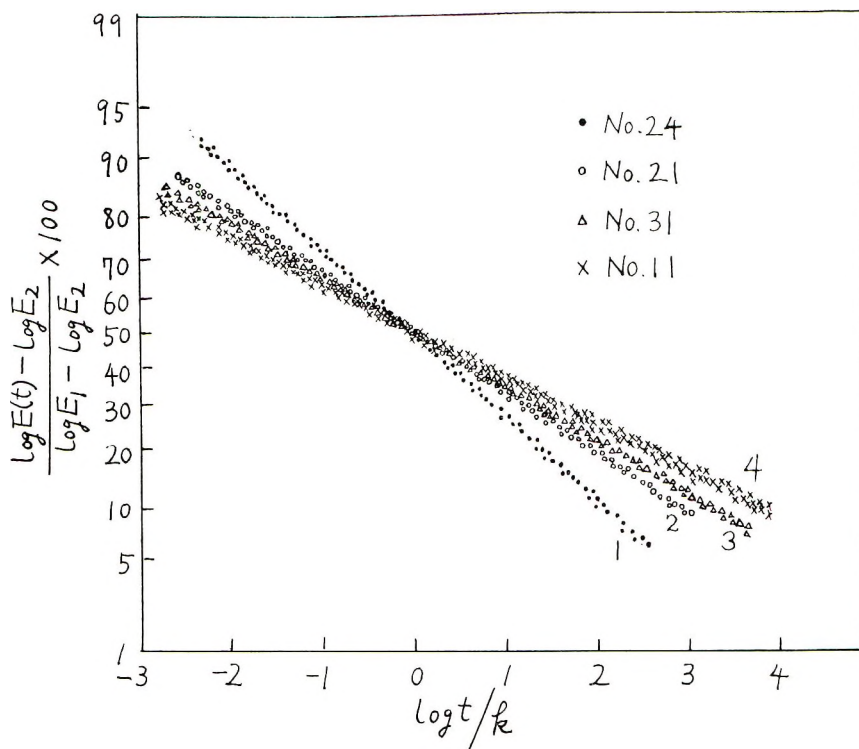


Fig. 5. Probability paper plots of master relaxation curves constructed from the results of Fig. 4 for a reference temperature of 50°C.

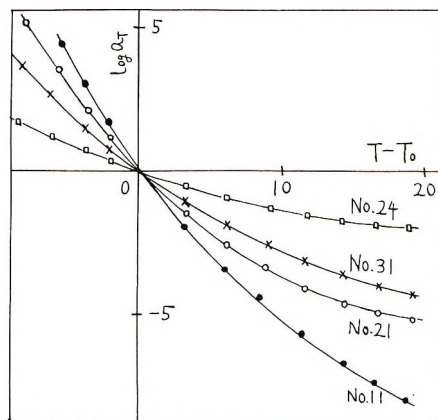


Fig. 6. Shift factor vs. temperature curves.

Viscoelastic Properties

Figure 4 shows typical examples of relaxation modulus curves measured at various temperatures. Master relaxation curves, which are derived by the time-temperature superposition technique and plotted on the probability paper, yield straight lines as shown in Figure 5 for selected specimens. Applicability of eq. (4) is thus verified. Shift factor versus temperature curves are shown in Figure 6, from which values of C_1^g and C_2^g , the WLF constants referred to glass temperature, are obtained as listed in Table VII.

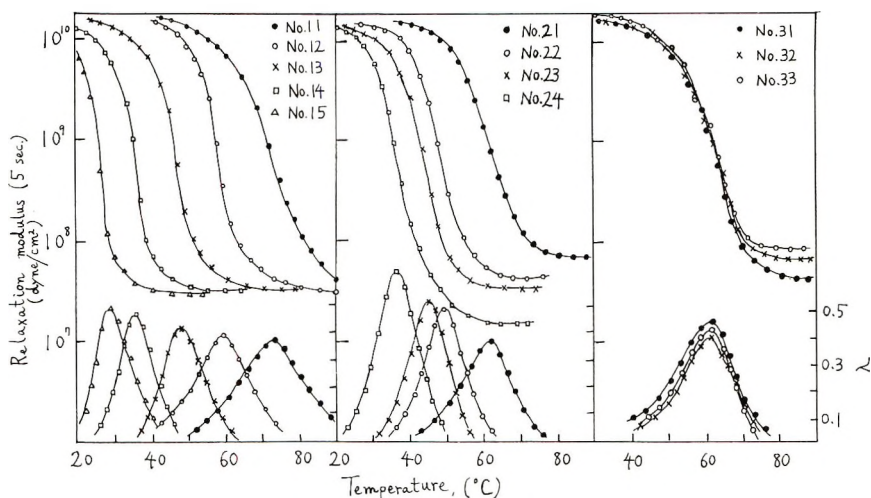


Fig. 7. Relaxation modulus and λ vs. temperature curves for unswollen specimens.

Relaxation modulus and λ versus temperature curves of unswollen specimens are shown in Figure 7. In series I, the transition region is shifted toward higher temperature, the λ versus temperature curve is broadened, and the peak height of λ is lowered with increasing $[U]_c$. The rubbery modulus shows nearly constant values for all specimens in series I. In series II, the transition region is shifted toward higher temperatures, the λ versus temperature curves are broadened, and the peak height of λ is lowered with increasing $[\rho]_c$. In series III, relaxation modulus versus temperature curves in the transition region overlap, while rubbery modulus increases with decreasing $[A]_c$.

TABLE VII
Parameters in the WLF Equation Calculated from Shift Factors

No.	C_1^g	C_2^g
11	17.7	37.4
21	15.2	29.0
24	12.0	26.1
31	15.0	42.0

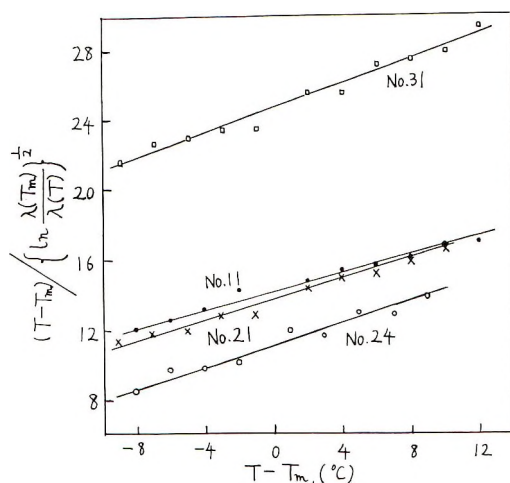


Fig. 8. Plots of temperature dependence of λ according to eq. (6).

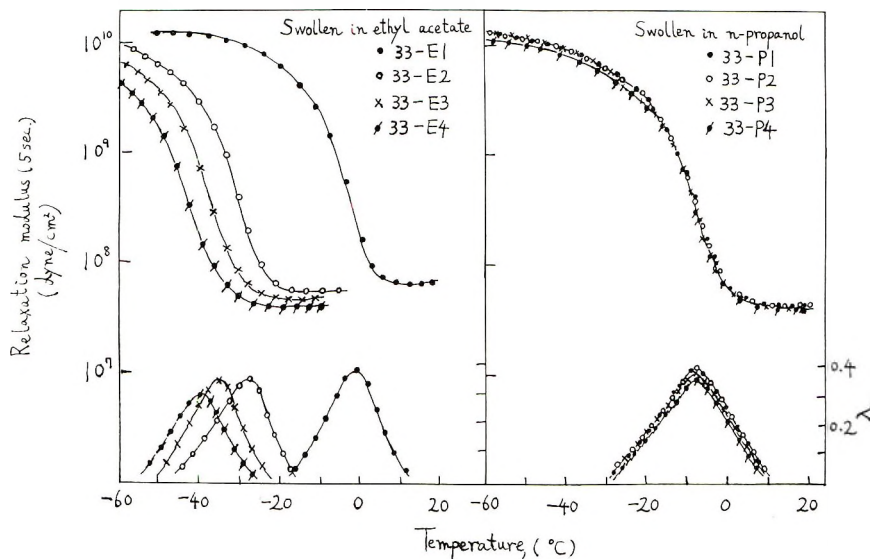


Fig. 9. Relaxation modulus and λ vs. temperature curves for specimens of sample 33 at varying degree of swelling. Degree of swelling is tabulated in Table VI.

Plots of $(T - T_m) / \ln[\lambda(T_m) / \lambda(T)]^{1/2}$ against $T - T_m$, according to eq. (6), yield straight lines, as shown in Figure 8 which includes a few examples. Characteristic parameters representing viscoelastic properties are listed in Table VIII, where α_f and f_g , which are calculated from C_1^g and C_2^g assuming that the parameter B in Doolittle's equation is unity, are thermal expansion coefficients of free volume and fractional free volume at T_g . The crosslinking density $[\rho]_e$ is calculated from the rubbery modulus E_2 by the familiar relation $E_2 = 3d[\rho]_eRT$, where d is the density of the polymer. From the comparison of Table VII with Table VIII it is apparent that the agreement between both methods for derivation of C_1^g and C_2^g is fairly good.

TABLE VIII

Values of Characteristic Parameters Representing Viscoelastic Properties for Unswollen Specimens

Series	No.	T_m °C.	$[\rho]_e$ $\times 10^4$, mole/g.	h	C_1^{σ}	C_2^{σ}	α_f $\times 10^4$	f_{θ}
I	11	72	2.88	0.257	22.2	36.5	5.35	0.0196
	12	58	2.80	0.263	21.4	30.6	6.63	0.0203
	13	47	2.90	0.282	19.9	29.9	7.31	0.0218
	14	36	2.88	0.315	18.8	29.8	7.75	0.0231
	15	29	2.88	0.338	18.0	29.4	8.21	0.0242
II	21	62	7.85	0.308	16.0	31.5	8.60	0.0272
	22	49	4.49	0.361	15.8	25.9	11.30	0.0274
	23	45	3.48	0.371	13.8	25.2	12.50	0.0314
	24	36	1.72	0.401	12.2	24.8	14.40	0.0354
III	31	62	4.48	0.294	13.5	42.8	7.53	0.0321
	32	62	7.80	0.297	13.1	45.8	7.21	0.0311
	33	63	8.26	0.313	13.0	48.1	6.95	0.0333

Relaxation modulus and λ versus temperature curves are shown for specimens of sample 33 at varying degrees of swelling in ethyl acetate and *n*-propanol in Figure 9. For specimens swollen in ethyl acetate, the relaxation modulus and λ versus temperature curves are shifted toward lower temperatures, their shapes are flattened, and rubbery moduli are lowered with increasing degree of swelling. For specimens swollen in *n*-propanol, although the degree of swelling is somewhat smaller than in the case of swelling in ethyl acetate, relaxation modulus, and λ versus temperature curves hardly change their positions on the temperature axis with increasing degree of swelling.

Characteristic parameters representing viscoelastic properties derived from the results of Figure 9 are listed in Table IX. The crosslinking density $[\rho]_s$ per unit weight of polymer in swollen system is calculated by the relation $E_2 = 3dv_2^{1/3}[\rho]_sRT$, where v_2 is volume fraction of polymer.

TABLE IX

Values of Characteristic Parameters Representing Viscoelastic Properties for Swollen Specimens at Varying Degree of Swelling

Symbol	$[\rho]_s$ $\times 10^4$, mole/g.	T_{ms} °C.	$T_{\theta s}$ °C.	h	C_1^{σ}	C_2^{σ}	α_{fs} $\times 10^{-4}$	$f_{\theta s}$
33-E1	7.29	-6	-25	0.281	22.0	35.0	5.64	0.0197
33-E2	7.23	-33	-52	0.257	22.8	38.0	5.05	0.0191
33-E3	6.80	-40	-59	0.245	23.0	42.3	4.48	0.0189
33-E4	6.46	-44	-63	0.215	23.6	40.8	4.55	0.0184
33-P1	5.11	-12	-31	0.280	33.0	29.7	4.45	0.0132
33-P2	5.19	-12	-31	0.273	33.3	33.8	3.87	0.0131
33-P3	5.29	-13	-32	0.280	36.0	44.7	2.70	0.0121
33-P4	5.27	-14	-33	0.265	39.0	44.8	2.67	0.0120

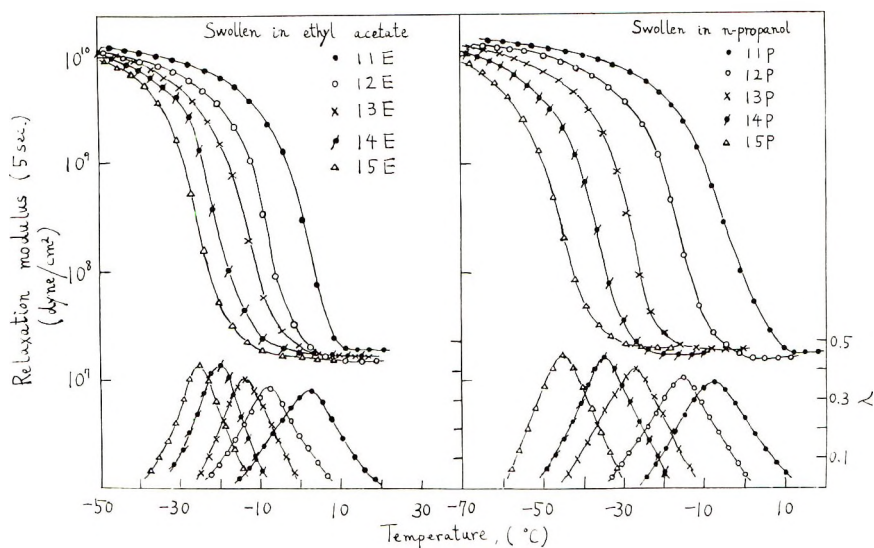


Fig. 10. Relaxation modulus and λ vs. temperature curves for swollen specimens of series I. Degree of swelling is tabulated in Table VI.

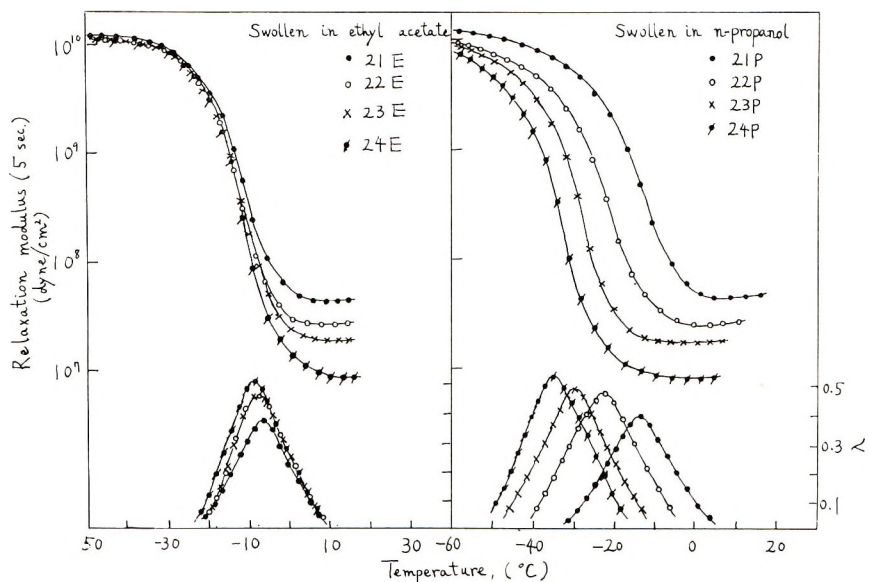


Fig. 11. Relaxation modulus and λ vs. temperature curves for swollen specimens of series II. Degree of swelling is tabulated in Table VI.

Relaxation modulus and λ versus temperature curves for series I and II swollen in ethyl acetate and *n*-propanol at nearly constant degree of swelling are shown in Figures 10 and 11. Relaxation modulus and λ versus temperature curves for a homologous series form a regular array of lines in the transition region as is seen from Figures 7, 10, and 11, from which one can

see that the spread of the array is reduced by swelling. This effect is more marked in series II than in series I and is more in the case of swelling in ethyl acetate than in *n*-propanol.

Characteristic parameters representing viscoelastic properties of swollen specimens for series I and II are listed in Table X. The glass temperature of swollen polymers, T_{gs} , for specimens other than those cited in Table V are calculated according to the relation $T_{gs} = T_{ms} - a$, which holds for selected specimens, as is seen from Table V. The constant a is assumed here to have the same value as in the case of the selected specimens, that is, 19.

TABLE X
Values of Characteristic Parameters Representing Viscoelastic Properties for Swollen Specimens at Constant Degree of Swelling

Symbol	$[\rho]_s$ $\times 10^4$ mole/g.	T_{ms} , °C.	T_{gs} , °C.	h	C_1^g	C_2^g	α_{fs} $\times 10^4$	f_{gs}
11E	2.21	-4	-24	0.226	27.4	36.5	4.35	0.0159
12E	1.94	-9	-28	0.228	30.6	27.7	5.10	0.0142
13E	2.40	-12	-31	0.249	30.4	25.8	5.53	0.0143
14E	2.44	-19	-38	0.270	32.2	24.7	5.47	0.0136
15E	2.60	-25	-43	0.276	28.4	26.1	5.85	0.0153
11P	2.16	-13	-34	0.233	35.2	40.5	3.06	0.0124
12P	2.09	-17	-36	0.237	37.0	32.7	3.61	0.0118
13P	2.53	-27	-46	0.259	36.8	32.9	3.60	0.0118
14P	2.43	-34	-53	0.283	35.4	31.8	3.87	0.0123
15P	2.70	-45	-60	0.291	34.5	31.5	3.99	0.0126
21E	6.09	-10	-29	0.277	27.6	25.4	6.21	0.0157
22E	3.68	-8	-27	0.303	32.8	17.9	7.00	0.0132
23E	2.50	-8	-27	0.288	33.1	17.4	7.58	0.0132
24E	1.60	-9	-28	0.295	32.3	16.9	7.93	0.0135
21P	6.66	-17	-35	0.285	35.9	26.4	4.61	0.0121
22P	3.22	-23	-42	0.321	38.1	22.4	5.08	0.0114
23P	2.09	-30	-49	0.300	36.4	22.2	5.37	0.0119
24P	1.08	-34	-54	0.301	34.7	22.3	5.65	0.0125

DISCUSSION

Crosslinking Density

The rate of formation of allophanate linkage is reported to be appreciably smaller than that of other polar linkages; relative rates of formation of allophanate, biuret, urea, and urethane linkage are 1, 100, 400, and 400, respectively.⁹ It is, therefore, possible that the concentrations of allophanate linkages are overestimated in Tables I-III when polyurethanes are synthesized by the one-step method as practiced here.

Comparison of calculated values of crosslinking density with observed rubbery modulus may serve as a guide to the extent of allophanate linkage formation because the formation of allophanate linkage contributes to an

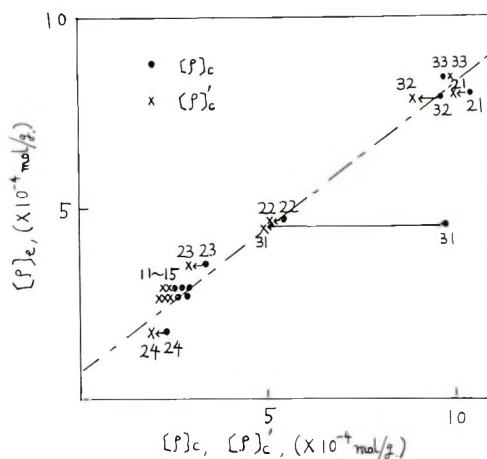


Fig. 12. Correlation among crosslinking densities $[\rho]_e$, $[\rho]_c$, and $[\rho]_c'$.

increase in the crosslinking density and then rubbery modulus. Figure 12 shows correlation among $[\rho]_e$, $[\rho]_c$, and $[\rho]_c'$. The last is defined by the relation, $[\rho]_c' = [\rho]_c - [A]_c$, excluding the possibility of allophanate linkage formation. Although $[\rho]_c$ and $[\rho]_c'$ are generally larger than $[\rho]_e$, $[\rho]_e$ is closer in magnitude to $[\rho]_c'$ than to $[\rho]_c$. This trend is especially marked for polymers which have large $[A]_c$ value.

The allophanate linkage is reported to dissociate gradually at elevated temperatures (110–130°C.).¹⁰ Since the polymers prepared here show rubberlike elasticity below 100°C., it is considered that thermal dissociation of allophanate linkage hardly occurs in the temperature range investigated here. It is, therefore, concluded that even though the formation of allophanate linkage can not be ignored completely, the concentration of allophanate linkage present in the polymer is negligibly small as compared with the concentration of other linkages.

In subsequent descriptions, the value of crosslinking density is expressed by $[\rho]_e$ and the concentration of polar groups is expressed by the value listed in Tables I–III, except for $[A]_c$, which is equated to zero.

Viscoelastic Properties of Unswollen Polymers

Series I can be regarded as a homologous series with respect to the concentration of urethane linkage $[U]_c$ since $[B]_c$ is small and nearly constant compared with $[U]_c$ as is seen from Tables I–III. Parameters which characterize properties in the transition region for series I are plotted against $[U]_c$ in Figure 13. When $[U]_c$ is increased, T_g increases regularly, and the glass-to-rubbery transition becomes less steep, as is seen from the value of h . The effect of $[U]_c$ on T_g can be attributed to both the rigidity of the phenyl ring in TDI and the cohesive energy density of the urethane linkage.⁴ The high packing density of molecular chains is considered to be realized by increasing $[U]_c$ as exemplified by the fact that the occupied

volume v_o , which was estimated by $v_o = v_o (1 - f_o)$, decreases with increasing $[U]_c$. Series I can be termed an iso-free volume series since f_o is nearly constant in the series. The thermal expansion coefficient of specific volume and free volume, α_a and α_f , respectively decrease with increasing $[U]_c$. Values of α_f and $\alpha_a - \alpha_b$ should be similar in magnitude from the usual point of view that the thermal expansion above T_g is composed of an increase in free volume and a lattice expansion. This requirement is not satisfied, α_f being always larger than $\alpha_a - \alpha_b$. Discussion of this discrepancy will be presented in the next section, since the same trend is found in other series.

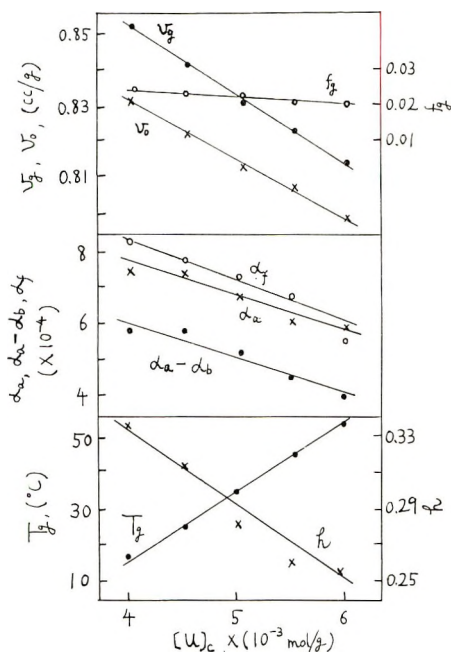


Fig. 13. Values of characteristic parameters representing viscoelastic properties vs. urethane group concentration for unswollen specimens of series I.

Parameters which characterize properties in the transition region for series II are plotted against crosslinking density in Figure 14. T_g increases linearly with the logarithm of $[\rho]_c$. This can be explained by a concept reported in an earlier paper.¹¹ The value of f_o decreases with increasing $[\rho]_c$, while the occupied volume v_o remains at a nearly constant value. Thus, series II can be considered an iso-occupied volume series in the same way as with other crosslinked systems.¹² The dependences of h , α_f , and α_a on $[\rho]_c$ are qualitatively similar to those on $[U]_c$ as described for series I. However, the discrepancy between α_f and $\alpha_a - \alpha_b$ is much larger than that in series I.

Series III is considered to be a series with varying crosslinking density and the concentration of some unknown polar groups formed by reactions

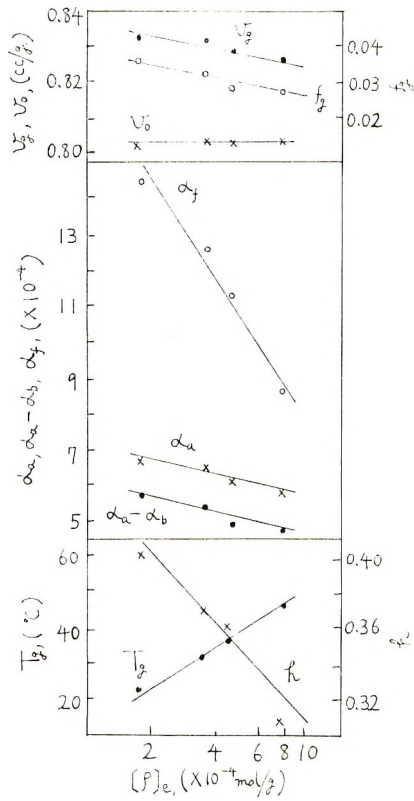


Fig. 14. Values of characteristic parameters representing viscoelastic properties vs. crosslinking density for unswollen specimens of series II.

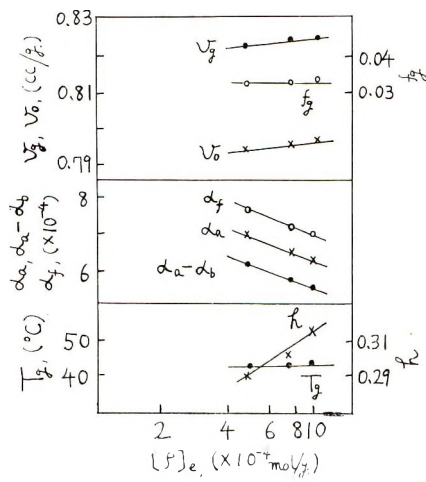


Fig. 15. Values of characteristic parameters representing viscoelastic properties vs. crosslinking density for unswollen specimens of series III.

of the isocyanate group with moisture or else, as the formation of allophanate linkage is considered to be negligibly small.

Characteristic parameters representing viscoelastic properties are plotted against $[\rho]_c$ in Figure 15, from which we can see that α_a and α_f decrease with increasing $[\rho]_c$, T_g , and f_g have nearly constant values irrespective of varying crosslinking density, and v_g and h increase with $[\rho]_c$. These tendencies are considered to arise from the combined effects of concentrations of unknown polar groups and crosslinking density and cannot be discussed in detail at the present.

Dependence of Free Volume on Temperature

It is natural to consider the secondary linkages between polar groups dissociate gradually with increasing temperature for a polymer, such as polyurethane, which has polar groups capable of causing interactions of various levels between molecular chains. It may be possible to explain the discrepancy between α_f and $\alpha_a - \alpha_b$ by considering that the dissociation of secondary linkage is accompanied by the creation of free volume which was a part of the occupied volume prior to the dissociation.

However, it seems difficult to explain the cause of such a large discrepancy between α_f and $\alpha_a - \alpha_b$ as encountered in series II in this way. As an alternative, it will be better to examine the value of parameter B appearing in Doolittle's equation, which was assumed to be unity. Williams¹³ and Saito¹⁴ have made α_f agree with α_a or $\alpha_a - \alpha_b$ by assuming appropriate values for the parameter B . According to Hirai¹⁵ and Cohen and Turnbull,¹⁶ the parameter B is considered to be related to the size of hole necessary for the motion of a chain segment. It can be assumed further that the parameter B is not a constant but a decreasing function of temperature when the size of the elemental unit of molecular motion is to be reduced by the thermal dissociation of intermolecular linkages. On representing the functional form of B simply as eq. (7), the WLF equation may be transcribed into the form of eq. (8).

$$B = 1/(1 + A\Delta T) \quad (7)$$

where $\Delta T = T - T_g$ and A is a factor.

$$-2.303 \log a_T = \frac{(1/f_g')\{\Delta T + [A\alpha_f'/(Af_g' + \alpha_f')]\Delta T^2\}}{[f_g'/(Af_g' + \alpha_f')] + \Delta T + [A\alpha_f'/(Af_g' + \alpha_f')]\Delta T^2} \quad (8)$$

Values of f_g' and A calculated by eq. (8) and by using the value of $\alpha_a - \alpha_b$ for α_f' are listed in Table XI. Though eq. (8) differs in its form from the WLF equation, the numerical relation between a_T and ΔT , derived by eq. (8) for the values of A and f_g' listed in Table XI, can be fitted closely by the WLF equation, as is seen from apparent linearities of usual WLF plots shown in Figure 16. Careful inquiry is, therefore, necessary to avoid erroneous conclusions drawn from the meaning of the WLF constants.

TABLE XI
Parameters in Modified WLF Equation [eq. (8)].

Series	No.	A	f'_0
I	11	0.013	0.0222
	12	0.013	0.0223
	13	0.014	0.0246
	14	0.013	0.0255
	15	0.013	0.0270
II	21	0.020	0.0310
	22	0.025	0.0310
	23	0.027	0.0352
	24	0.029	0.0396
III	31	0.010	0.0372
	32	0.010	0.0385
	33	0.010	0.0392

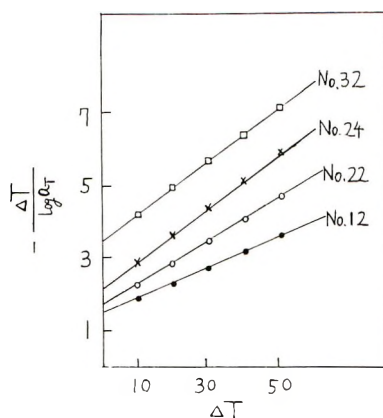


Fig. 16. WLF plots of modified eq. (8).

Assumption of the temperature dependence in B thus provides a possible way to explain the discrepancy between α_f and $\alpha_a - \alpha_b$. Values of f'_0 in Table XI have the same trend with those listed in Table VIII. Further investigations seem to be needed to discuss the values of A which differ considerably among the three series, as is seen from Table XI.

Effects of Swelling upon the Viscoelastic Properties

Characteristic parameters representing viscoelastic properties listed in Table X are plotted against concentration of functional groups in Figures 17 and 18. Decreases in h , f'_0 , and crosslinking density and agreement of α_f with $\alpha_a - \alpha_b$ are commonly observed in cases of swelling in both ethyl acetate and *n*-propanol. The decrease in crosslinking density by swelling is largely attributed to dissociations of secondary linkages which have been evaluated as crosslinkages in unswollen specimens, since values of crosslinking density of deswollen specimens coincide with those of corresponding

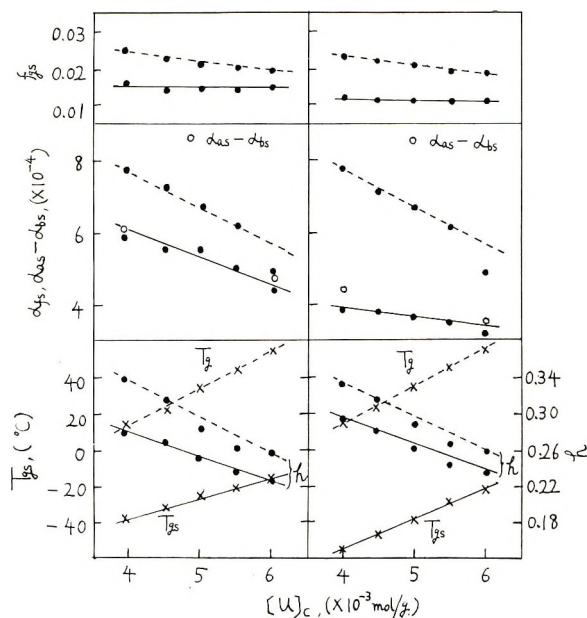


Fig. 17. Characteristic parameters representing viscoelastic properties vs. concentration of urethane group for (---) unswollen specimens and (—) swollen specimens: (left) swollen in ethyl acetate; (right) swollen in *n*-propanol.

unswollen specimens. The decrease in h , namely broadening of viscoelastic transition, has been often observed for polymer-diluent systems. As an explanation for this phenomenon, we can consider that an inhomogeneity of segmental mobility is caused by solvation of swelling agent molecule, according to a concept reported earlier.¹⁷ The most marked effect of swelling is the disappearance of the discrepancy between α_f and $\alpha_a - \alpha_b$. This is considered to be caused by dissociation of secondary linkages by the action of swelling agent and can be regarded to substantiate the assumption, made in the preceding section, that thermal dissociation of a secondary linkage would be responsible for the apparent discrepancy between α_f and $\alpha_a - \alpha_b$. A decrease in f_0 on swelling has been reported for the poly(vinyl chloride)-dioctyl phthalate system from the measurement of dielectric relaxation.¹⁴ According to Gibbs and Dimarzio,¹⁸ who define glass temperature as the temperature at which configurational entropy becomes zero, the decrease in f_0 means that the configurational entropy has a nonvanishing value until the free volume of the system is reduced to a smaller value when diluent molecules coexist. This statement seems to be reasonable. Dependences of f_0 on concentration of urethane linkage and crosslinking density are found to be suppressed by swelling.

Differences between the effects of ethyl acetate and *n*-propanol are observed in the spread of the array of relaxation modulus versus temperature curves for a series of specimens homologous with respect to concentration of urethane linkage, crosslinking density, or degree of swelling, as illus-

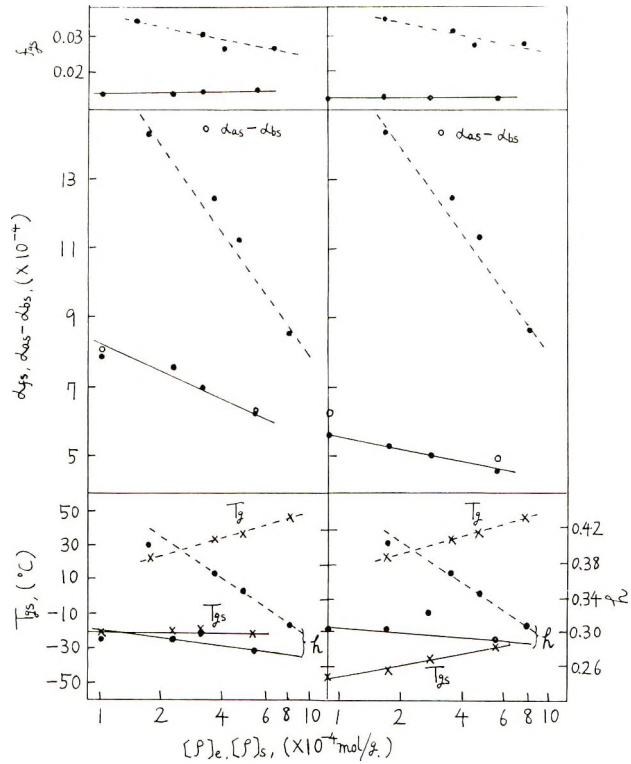


Fig. 18. Characteristic parameters representing viscoelastic properties vs. cross-linking density for (---) unswollen specimens and (—) swollen specimens: (left) swollen in ethyl acetate; (right) swollen in *n*-propanol.

trated in Figures 9–11. These differences are thought to arise from detailed mechanisms of free volume-imparting actions of the swelling agents. It seems to be a reasonable course to explore the volume change accompanied by swelling in order to elucidate the effects of swelling agents mentioned above. For this purpose, the calculated occupied volume $v_{o,c}$ and calculated free volume $v_{f,c}$, which are obtained from occupied and free volumes of swelling agent and polymer v_{o1} , v_{o2} , v_{f1} , and v_{f2} , respectively, assuming additivity, are compared with observed occupied volume v_o and observed free volume v_f , which are obtained from specific volume of swollen specimen v tabulated in Table VI. These volumes are calculated according to eqs. (9)–(16). The subscripts 1 and 2 represent swelling agent and polymer, respectively.

$$v_{o1} = v_1 \{ 1 - f_{g1} - \alpha_{a1}(T - T_{g1}) \} \quad (9)$$

$$v_{o2} = v_2 \{ 1 - f_g - (\alpha_a - \alpha_b)(T - T_{g1}) \} \quad (10)$$

$$v_{o,c} = v_{o1}(1 - W_2) + v_{o1}W_2 \quad (11)$$

$$v_{f1} = v_1 \{ f_{g1} + \alpha_{a1}(T - T_{g1}) \} \quad (12)$$

$$v_{f2} = v_2 \{ f_{\theta} + (\alpha_a - \alpha_b)(T - T_{\theta 1}) \} \quad (13)$$

$$v_{f,c} = v_{f1}(1 - W_2) + v_{f1}W_2 \quad (14)$$

$$v_o = v \{ 1 - f_{\theta s} - \alpha_{fs}(T - T_{\theta s}) \} \quad (15)$$

$$v_f = v \{ f_{\theta s} + \alpha_{fs}(T - T_{\theta s}) \} \quad (16)$$

In eqs. (9) to (16), $f_{\theta 1}$ is assumed to be 0.025 for the both swelling agents, and α_{a1} for ethyl acetate and *n*-propanol are assumed to be 1.1×10^{-3} and 0.8×10^{-3} , respectively.¹⁹ $T_{\theta 1}$ for ethyl acetate and *n*-propanol are calculated as 160 and 120°K., respectively, according to Bueche's theory.²⁰ Values of f_{θ} and $\alpha_a - \alpha_b$ are taken from Tables IV and VIII, and those of α_{fs} , $f_{\theta s}$, and $T_{\theta s}$ are taken from Tables IX and X. Occupied and free volumes thus derived are tabulated in Table XII.

The additivity between specific volume of swelling agent and that of polymer does not hold for the system investigated here, as pointed out already. It has been reported^{21,22} for several cases that the volume of polymer diluent systems is smaller than that calculated assuming the

TABLE XII
Calculated and Observed Values of Occupied and Free Volumes for Swollen Specimens at 30°C.

Symbol	$v_{o,c}$	v_o	$v_{f,c}$	$v_{f,c}$	$v_{o,c}$ v_o	$v_{f,c}$ v_f
11E	0.818	0.817	0.048	0.034	1.000	1.412
12E	0.824	0.821	0.048	0.040	1.004	1.200
13E	0.830	0.832	0.052	0.045	0.998	1.156
14E	0.839	0.843	0.052	0.048	0.996	1.083
15E	0.847	0.849	0.053	0.056	0.997	0.946
21E	0.822	0.818	0.053	0.048	1.005	1.100
22E	0.821	0.817	0.054	0.051	1.005	1.059
23E	0.821	0.816	0.056	0.054	1.006	1.037
24E	0.822	0.818	0.060	0.060	1.005	1.000
11P	0.857	0.865	0.066	0.030	0.991	2.200
12P	0.862	0.870	0.065	0.034	0.991	1.912
13P	0.885	0.890	0.067	0.039	0.994	1.718
14P	0.909	0.916	0.069	0.045	0.992	1.533
15P	0.925	0.933	0.071	0.050	0.992	1.420
21P	0.850	0.850	0.066	0.039	1.000	1.692
22P	0.859	0.871	0.069	0.047	0.986	1.468
23P	0.870	0.884	0.074	0.054	0.984	1.370
24P	0.896	0.895	0.076	0.061	1.001	1.246
33-E1	0.818	0.826	0.060	0.045	0.990	1.333
33-E2	0.824	0.846	0.071	0.052	0.974	1.378
33-E3	0.835	0.865	0.079	0.055	0.966	1.436
33-E4	0.844	0.882	0.086	0.061	0.957	1.420
33-P1	0.826	0.844	0.050	0.036	0.979	1.389
33-P2	0.832	0.854	0.054	0.033	0.974	1.636
33-P3	0.839	0.864	0.060	0.026	0.971	2.308
33-P4	0.846	0.872	0.065	0.025	0.970	2.600

simple additivity. As a cause of this phenomenon, a more compressed state of diluent molecules in the polymer network is suggested than in the state of bulk diluent.

Additivity is considered to hold for the occupied volume, as the ratio $v_{o,c}/v_o$ is nearly unity in all cases, as seen from Table XII. This result is compatible with the meaning of occupied volume and provides a basis for discussing the mechanism of swelling agent action in terms of free volume. From Table XII, we can see the ratio $v_{f,c}/v_f$ is always larger than unity, and the decrease in volume on swelling is due to collapse of free volume. This phenomenon will be referred as "overlap of free volume, since it cannot be distinguished in principle whether the collapsed free volume has so far belonged to polymer or swelling agent. The degree of overlap of free volume is measured by the ratio $v_{f,c}/v_f$, for which following trends are seen from Table XII.

(a) Generally, $v_{f,c}/v_f$ for specimens swollen in *n*-propanol is larger than in ethyl acetate.

(b) The concentration of urethane linkage has the effect of increasing the overlap of free volume, irrespective of the kind of swelling agent. The magnitude of this effect is larger for *n*-propanol than for ethyl acetate.

(c) For the series of polymers homologous with respect to crosslinking density, $v_{f,c}/v_f$ remains at a nearly constant value in the case of ethyl acetate, while it increases with increasing crosslinking density in the case of *n*-propanol.

(d) For specimens of varying degree of swelling, $v_{f,c}/v_f$ remains at a nearly constant value in the case of ethyl acetate, but increases with increasing degree of swelling in the case of *n*-propanol.

Relation between the above statements and behaviors of modulus curves shown in Figures 9–11 is apparent, considering that the shift of modulus curves along the temperature axis by swelling is caused by an increase in the amount of free volume of the system and this increment is governed by the degree of overlap of free volume. The overlap of free volume must be caused by a specific attraction between molecules of polymers and swelling agents. This attraction may be a kind of solvation. The solvated molecule of swelling agent is thought to be less effective in increasing the free volume of the system. As a possible explanation for the differences between actions of ethyl acetate and *n*-propanol, it can be inferred that (1) the solvation of the ethyl acetate molecule occurs at some selected parts of the polymer chain, i.e., urethane linkage, while (2) the solvation of the *n*-propanol molecule occurs over a wider range, e.g., both urethane and ether linkages, and, further, (3) a stronger or multimolecular solvation of the *n*-propanol molecule occurs at some selected parts of the polymer chain, i.e., urethane linkage.

From inferences (1) and (3), the overlap of free volume is expected to increase with increasing concentration of urethane linkage with both ethyl acetate and *n*-propanol. This can be met with the statement (b) mentioned above. The statement (d) is similarly explained by combining the

inferences (1) and (2). For the case of ethyl acetate in the statement (c), the inference (1) provides an explanation. For the case of *n*-propanol in the statement (c), a possible explanation is that overlap of free volume is enhanced by the presence of crosslinkages when solvation occurs over the entire contour of polymer chain because of the inference (2). The statement (a) is apparent from the inferences (1) and (2).

References

1. Smith, T. L., and A. B. Magnusson, *J. Polymer Sci.*, **42**, 391 (1960).
2. Yokoyama, T., *Kogyo Kagaku Zasshi*, **63**, 2050 (1960).
3. Jacobs, H., and E. Jenckel, *Makromol. Chem.*, **43**, 132 (1961).
4. Tazawa, T., and Y. Inoeue, *Shikizai*, **35**, 433 (1962).
5. Saunders, J. H., *Rubber Chem. Technol.*, **33**, 1259 (1960).
6. Shibayama, K., *Shikizai*, **35**, 1 (1962).
7. Shibayama, K., *Kobunshi Kagaku*, **19**, 543 (1962).
8. Bischoff, J., E. Catsiff, and A. V. Tobolsky, *J. Am. Chem. Soc.*, **74**, 3378 (1952).
9. Saunders, J. H., *Rubber Chem. Technol.*, **32**, 337 (1959).
10. Kogan, I. C., *J. Org. Chem.*, **23**, 1594 (1958).
11. Shibayama, K., *Kobunshi Kagaku*, **19**, 219 (1962).
12. Shibayama, K., and Y. Suzuki, *J. Polymer Sci.*, **3A**, 2637 (1965).
13. Williams, M. L., *J. Appl. Phys.*, **29**, 1395 (1958).
14. Saito, S., *Kolloid-Z.*, **189**, 116 (1963).
15. Hirai, N., *Kobunshi Kagaku*, **19**, 191 (1962).
16. Cohen, M. H., and D. Turnbull, *J. Chem. Phys.*, **31**, 1164 (1959).
17. Shibayama, K., and T. Tanaka, *Kobunshi Kagaku*, **21**, 690 (1964).
18. Gibbs, J. H., and E. A. Dimarzio, *J. Chem. Phys.*, **28**, 373 (1958).
19. Heibron, I., and H. M. Bunbury, *Dictionary of Organic Compounds*, Eyre & Spottiswoode, London, 1953, Vol. 2, p. 486; *ibid.*, Vol. 4, p. 242.
20. Kelley, F. N., and F. Bueche, *J. Polymer Sci.*, **50**, 547 (1961).
21. Ham, J. S., M. C. Bolen, and J. K. Hughes, *J. Polymer Sci.*, **57**, 25 (1962).
22. Horth, A., D. Patterson, and M. Rinfret, *J. Polymer Sci.*, **39**, 189 (1959).

Résumé

On a étudié les propriétés viscoélastiques de spécimens gonflés et non gonflés de séries homologues de polyuréthanes dans la région de transition verre/Caoutchouc. On a trouvé que dans le cas de spécimens non gonflés, une grande différence existe entre le coefficient d'expansion thermique du volume spécifique et celui du volume libre obtenu en comparant l'équation WLF avec l'équation de Doolittle dans laquelle on suppose que le paramètre *B* est l'unité. Il est possible d'expliquer cette différence en décrivant *B* comme une fonction décroissante de la température. On suppose alors que la dissociation thermique du lien secondaire entre groupes polaires peut avoir un effet décroissant sur la grandeur de l'unité élémentaire du mouvement moléculaire. On a trouvé que dans le cas d'échantillons gonflés, cette différence disparaissait. On a observé des différences entre les échantillons gonflés dans l'acétate d'éthyle et le *n*-propanol en ce qui concerne la largeur de l'étalement des courbes du module de relaxation en fonction de la température pour une série homologue. Pour cause de ce phénomène, on suggère que les mécanismes de répartition du volume libre au système sont différents pour l'acétate d'éthyle et pour le *n*-propanol à cause des interactions caractéristiques entre les agents gonflants et les polymères.

Zusammenfassung

Die viskoelastischen Eigenschaften ungequollener und gequollener Proben aus homologen Polyurethanreihen wurden im Glas-Kautschikumwandlungsbereich untersucht.

Im Falle ungequollener Proben wurde eine grosse Diskrepanz zwischen dem thermischen Ausdehnungskoeffizienten des spezifischen Volumens und demjenigen des freien Volumens, welcher aus einem Vergleich der WLF-Gleichung mit der Gleichung von Doolittle unter Annahme des Wertes eins für den Parameter B abgeleitet worden war, aufgedeckt. Als mögliche Erklärung für diese Diskrepanz wird angenommen, dass B eine abnehmende Funktion der Temperatur ist, was auf die thermische Dissoziation der sekundären Bindungen zwischen polymeren Gruppen und deren herabsetzenden Einfluss auf die Grösse der Elementareinheit der Molekülbewegung zurückgeführt wird. Im Falle gequollener Proben verschwindet diese Diskrepanz. In der Streubreite der Abhängigkeit des Relaxationsmoduls von der Temperatur bei einer homologen Reihe wurden Unterschiede zwischen in äthylacetat und n -Propanol gequollenen Proben beobachtet. Als Ursache dieser Erscheinung wird angenommen, dass der Mechanismus der Bildung des freien Volumens im System für äthylacetat und n -Propanol wegen der charakteristischen Wechselwirkung zwischen Quellungsmittel und Polymeren verschieden ist.

Received April 12, 1965

Revised June 22, 1965

Prod. No. 4797A

Epoxy Compounds. VIII. Stereoregular and Stereorandom Polymerization of Phenyl Glycidyl Ether with Tertiary Amines, and Infrared Spectra of Poly(phenyl Glycidyl Ether)*

YOSHIO TANAKA and HIROSHI KAKIUCHI, *Department of Applied Chemistry, Faculty of Engineering, Yokohama National University, Yokohama, Japan*

Synopsis

Crystalline and amorphous polymers have been obtained from the polymerization of phenyl glycidyl ether in the presence of tertiary amines. The crystalline fraction is high melting and insoluble at room temperature. The amorphous fractions are soluble at room temperature and their molecular weights are found to be ~ 950 in benzene at 30°C . The yields of the crystalline fraction and the amorphous paste fraction decreased considerably with increasing the catalyst concentration and reaction temperature above 50°C . The yield of the liquid fraction, however, increased with increasing concentration of the catalyst and the reaction temperature. The x-ray diffraction analysis of the crystalline fraction shows that the fraction has 47–50% crystallinity and that its diffraction pattern is similar to that of poly(phenyl glycidyl ether) obtained by Noshay and Price. The infrared spectra of these fractions have been obtained in the region of 650–4000 cm^{-1} . These data are compared with those of polystyrene and poly(styrene oxide) and are used to make an assignment of the normal modes of the poly(phenyl glycidyl ether) molecule. On the basis of analyses of polystyrene and poly(styrene oxide), and a study of the combination bands, it has been possible to make a fairly satisfactory assignment of all of the benzene ring fundamentals of the CH_2 , CH , and skeletal modes.

INTRODUCTION

Several workers have investigated the polymerization of phenyl glycidyl ether. Earlier work,² with the use of sodium or potassium hydroxide as catalysts, has been reported to produce brown, transparent resins of low molecular weight. Trialkylaluminum,³ such as AlEt_3 or $\text{Al}(i\text{-PrO})_3/\text{ZnCl}_2$, lead to amorphous polymers or low yield of crystalline polymers of low molecular weight. The catalyst systems, $\text{ZnEt}_2/\text{H}_2\text{O}$ or $\text{AlEt}_3/\text{H}_2\text{O}$,^{4,5} induce the polymerization of phenyl glycidyl ether to polymers of high molecular weight. In recent publications, Takahashi and Kambara^{6,7} reported a number of systems from AlEt_3 and transition-metal chelate compounds to catalyze polymerization of phenyl glycidyl ether to crystalline polymers of high molecular weight. On the other hand, Staudinger⁸

* For Part VII see Kakiuchi and Tanaka.¹

reported that ethylene oxide was polymerized to low molecular weight polymer with number-average degree of polymerization of 50 by using 5% trimethylamine at 20°C. for 1-2 weeks.

Although the use of various organometallic compounds for the stereospecific polymerization of epoxides has received an increasing amount of attention in the recent literature, relatively little attention has been paid to epoxides other than ethylene oxide and propylene oxide. In addition, very little work has appeared concerning the use of various amines for the polymerization of phenyl glycidyl ether.

In the present paper, the polymerization of phenyl glycidyl ether by various tertiary amines and infrared spectra of the resulting polymers were investigated.

EXPERIMENTAL

Reagents

Reagent grade phenyl glycidyl ether (PGE) was dried over calcium hydride for several days and distilled under reduced pressure. The distillate at 109-110°C./5 mm. Hg was used for the polymerization. The thus purified monomer was found to be more than 99.8% pure by gas chromatography on a 1-m. column packed with polydiethylene glycol adipate at 180°C.

Reagent grade tertiary amines were used after distillation under reduced pressure.

Polymerization Procedure

A sample of PGE, together with the catalyst, was degassed *in vacuo*, sealed (sealed system) or not sealed (open system) in a test tube after the test tube had been flushed with dry nitrogen, and placed in a constant temperature bath. At the end of the reaction time the tube was cooled and opened. The reaction mixture was dissolved into a small amount of tetrahydrofuran (THF) and poured into a methanol-HCl solution to remove the catalyst. The methanol-insoluble polymer was dissolved again in THF and the solution was added to acetone. The insoluble material was collected and washed successively with cooled acetone and methanol. A white powder (fraction I) was reprecipitated from THF solution by adding acetone.

Acetone-THF solution separated from the fraction I was added dropwise with stirring to a large volume of methanol. A pasty mass separated out of solution in all cases. The precipitate was further fractionated by washing with methanol in which it was partly soluble. The insoluble fraction (fraction II) was reprecipitated from acetone solution with methanol.

The acetone-methanol solution separated from fraction II and methanol washing of fraction II, were combined, concentrated to a small volume, and poured into a large excess of water, then centrifuged to give the third fraction, fraction III, which was a viscous transparent resin.

Infrared Absorption Spectra

The infrared absorption spectra in the region of 650–4000 cm^{-1} were measured for the polymers obtained with tertiary amines and BF_3 etherate by a Hitachi Model EPI-2 infrared spectrophotometer equipped with a NaCl prism.

X-Ray Diffraction

The x-ray diffraction pattern of the powdered polymer was taken by a Rigakudenki x-ray diffractometer, using Ni-filtered $\text{CuK}\alpha$ radiation.

RESULTS AND DISCUSSION

Polymerization in Sealed Tube

The results of the polymerization of phenyl glycidyl ether (PGE) (6.38×10^{-2} mole) with various tertiary amines (6.7×10^{-3} mole) at 70°C. for 58 hr. (Table I) show that yields of the fractions of I and II are related to the basicities of the tertiary amines. Tertiary amines with small acidic dissociation constants $\text{p}K_a$, such as *N,N*-dimethyl aniline and pyridine, produced no crystalline polymer (fraction I) but yielded viscous transparent resins under these conditions.

In order to determine the effect of reaction temperatures on conversion, the polymerization of PGE by dimethylhexadecylamine (10 mole-% to monomer) was carried out at various temperatures. The results are illustrated in Table II. It shows that the total conversion reached an equilibrium; however, the yield of the fraction I or II had a maximum value at 50°C. These results seem to show that a chain transfer reaction occurs more markedly at 70°C. or more. There are no differences in infrared spectra and in carbon and hydrogen contents of fractions I obtained at various temperatures.

In succeeding experiments the effect of reaction time was investigated. The polymerization of PGE (6.38×10^{-2} mole) was carried out at 70°C. by using dimethylhexadecylamine (6.7×10^{-3} mole). The effects of reaction temperature and time are shown in Figures 1 and 2, respectively. The total yield reached about 99.5–99.7% in all cases but was 70% at 2 days, as shown in Table III. The fractions of I and II increase with increasing reaction time and reach an equilibrium after 20 days, but the fraction III reaches a maximum value at about 10 days and reaches equilibrium after 20 days, as shown in Figure 2. In Figure 2, the points (triangles) on the right ordinate are the results for the open system polymerization of PGE under the same conditions. There are significant differences in the yields of the three fractions between the open and closed system polymerizations of PGE. The total yield or conversion of PGE does not change about after 10 days, and the increase of the fractions of I and II corresponds to the decrease of the fraction III.

TABLE I
 Polymerization of PGE (6.38×10^{-2} mole) with Various Amines (6.7×10^{-3} mole) at 70°C. for 58 hr.

Amines	pK_a^a	Total yield, % ^b	Fraction I ^c			Fraction II			Fraction III	
			Yield, % ^d	C, %	H, %	Yield, % ^d	C, %	H, %	Yield, % ^d	
Dimethyloctadecylamine	ca. 10.5	52	7.0	71.60	7.58	15.0	71.25	7.65	78.0	
Dimethylhexadecylamine	"	55	3.8	71.83	7.39	17.2	71.92	7.52	79.0	
Dimethyl-dodecylamine	"	52	4.7	71.14	7.63	24.4	71.82	7.21	70.9	
Dimethylbenzylamine	"	53	7.9	71.32	8.01	30.6	71.95	7.83	61.5	
<i>N,N</i> -Dimethylamine	5.06	38	0.0	—	—	0.0	—	—	100	
Pyridine	5.17	78	0.0	—	—	3.6	—	—	96.4	

^a Values in literature.¹⁶

^b Ratio to monomer.

^c Melting point of 115–130°C. in all cases and $[\eta]$ of 0.04–0.06 in cyclohexanone at 25°C.

^d Ratio in polymerization product.

TABLE II
Effect of Temperature on Polymerization of PGE (6.38×10^{-2} mole) with Dimethylhexadecylamine (6.7×10^{-3} mole)

Temp., °C.	Time days + hr.	Fraction I			Fraction II	Fraction III	Total Yield, % ^b
		Yield, % ^a	C, %	H, %	Yield, % ^a	Yield, % ^a	
25	11	7.1	71.63	7.70	54.2	38.7	97
50	9 + 7	7.6	70.17	7.84	57.5	35.0	95
70	11	3.8	72.09	7.83	14.1	82.1	97
90	10 + 10	0.8	—	—	9.8	89.4	99
110	11 + 10	0.0	—	—	2.8	97.2	96

^a Ratio in polymerization product.

^b Ratio to monomer.

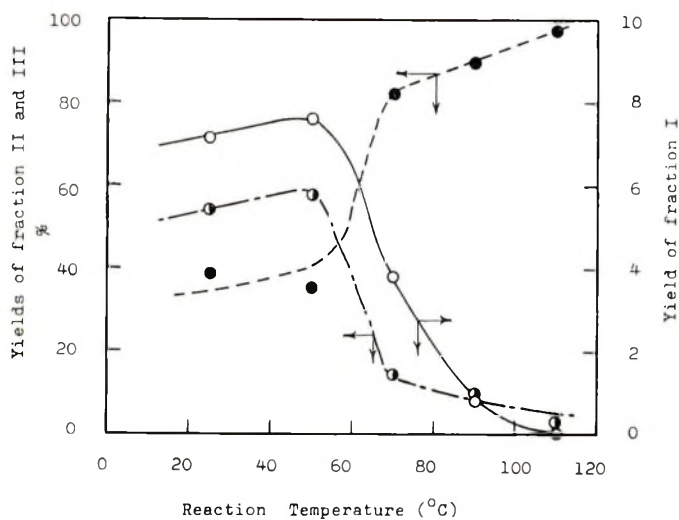


Fig. 1. Effect of temperature on polymerization of PGE (6.38×10^{-2} mole) with dimethylhexadecylamine (6.7×10^{-3} mole): (○) fraction I; (●) fraction II; (●) fraction III.

TABLE III
Effect of Time on Polymerization of PGE (6.38×10^{-2} mole) with Dimethylhexadecylamine (6.7×10^{-3} moles) at 70°C.

Time, days	Total yield, % ^a	Fraction I			Fraction II			Fraction III
		Yield, % ^a	C, %	H, % ^a	Yield, % ^a	C, %	H, %	Yield % ^a
2	70%	0.6	71.63	7.70	18	71.06	7.43	51.4
9	98.9	2.6	72.02	7.81	22	72.19	7.62	74.3
11	99.6	3.6	71.78	7.68	24	72.34	7.53	72.0
20	99.8	9.6	71.72	7.83	31	71.86	7.39	59.2
30	—	10.0	71.80	7.73	36	71.67	7.75	53.6

^a Ratio to monomer.

The effect of catalyst concentrations on conversion is illustrated in Table IV and in Figures 3 and 4. Varying amounts of dimethylhexadecylamine and tributylamine from 1.3×10^{-3} to 9.75×10^{-3} moles were used with 6.38×10^{-2} mole PGE at 25°C . for 11 days. As might be expected, the increasing catalyst concentration resulted in increasing conversion and the maximum yields of the fractions of I and II are reached

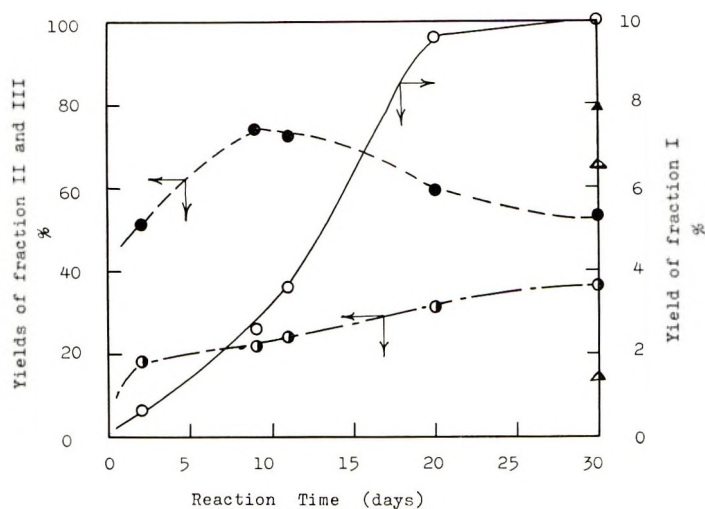


Fig. 2. Effect of time on polymerization of PGE (6.38×10^{-2} mole): (O) fraction I; (●) fraction II; (○) fraction III; (Δ) fraction I, open system; (▲) fraction II, open system; (▲) fraction III, open system.

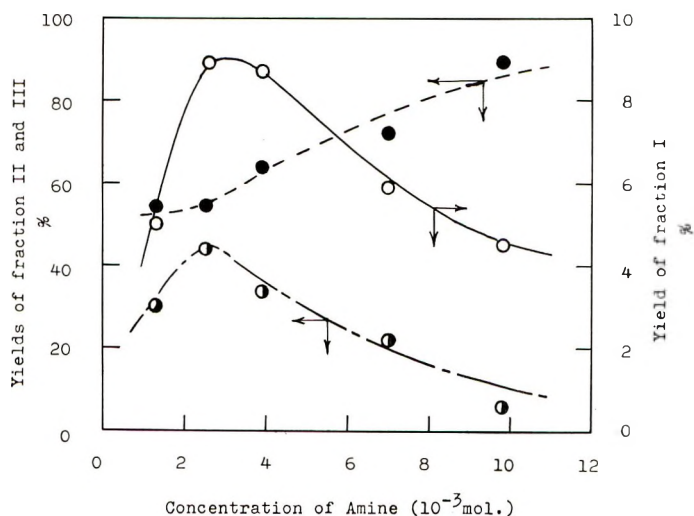


Fig. 3. Effect of concentration of dimethylhexadecylamine on polymerization of PGE (6.37×10^{-2} mole) at 25°C . for 11 days: (O) fraction I; (●) fraction II; (●) fraction III.

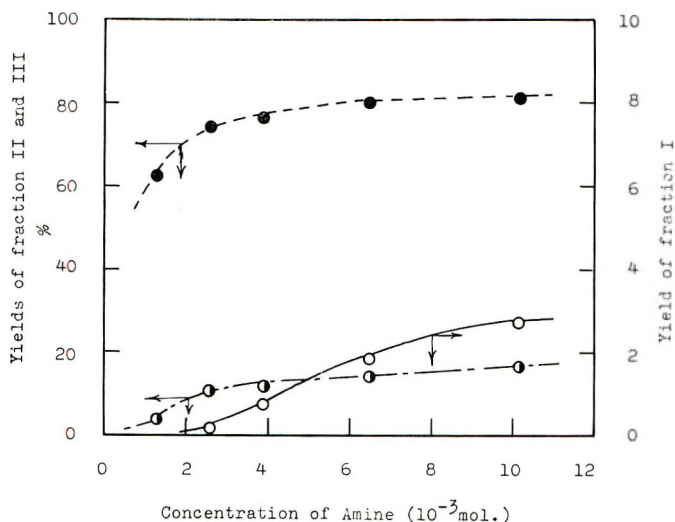


Fig. 4. Effect of concentration of tributylamine ($pK_a = 10.89$) on polymerization of PGE (6.37×10^{-2} mole) at 25°C . for 11 days: (O) fraction I; (●) fraction II; (●) fraction III.

at about a concentration of 3×10^{-3} mole in the case of dimethylhexadecylamine. The melting point and the intrinsic viscosity in cyclohexanone at 25°C . of fraction I are, respectively, $124\text{--}130^\circ\text{C}$. and $0.05\text{--}0.06$ dl./g. for the closed system and $109\text{--}111^\circ\text{C}$. and $0.02\text{--}0.04$ dl./g. for the open system in all cases. The suitable concentration of the catalyst seems to be dependent on the reaction temperature and the characteristics of the tertiary amine. The difference in catalytic effects between dimethylhexadecylamine and tributylamine cannot be explained reasonably by the basicity only, shown by pK_a , but is also a function of steric effects of the tertiary amine. There is observed a large difference between the open and closed systems in yields of the fractions of I and II.

Lidarik et al.¹⁰ studied the polymerization of PGE with tributylamine and found that the polymerization rate and molecular weight of polymer increased with addition of water. Our results, shown in Tables I–V are

TABLE IV
Effect of Concentration of Dimethylhexadecylamine on Polymerization of PGE (6.37×10^{-2} mole) at 25°C . for 11 Days

Concentration of of amine, mole $\times 10^3$	Yield, g.		
	Fraction I	Fraction II	Fraction III
1.3	0.559	3.32	6.00
2.6	0.977	4.38	6.01
3.9	0.954	3.70	7.02
6.5	0.697	2.65	8.50
9.8	0.494	0.65	10.0

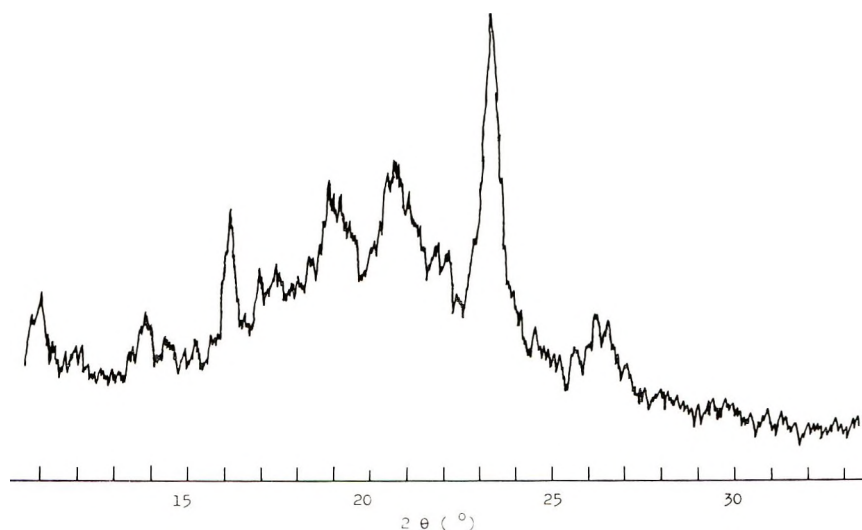


Fig. 5. X-ray diffraction of the crystalline poly(phenyl glycidyl ether).

somewhat different from Lidarik's results,¹⁰ and more detailed kinetic studies are now in progress and will be reported elsewhere.

TABLE V
Sealed and Open System Polymerizations of PGE (6.38×10^{-2} mole)
with Tertiary Amines

Amine	Concentration, mole $\times 10^3$	System	Temp., °C.	Time, days	Yield, % ^a		
					Frac- tion I	Frac- tion II	Frac- tion II
Dimethylhexadecyl- amine	6.7	Sealed	70	30	9.9	36	54
"	6.7	Open	70	30	6.5	14	79
Tributylamine	2.6	Sealed	25	11	0.5	11	74
"	2.6	Open	25	11	1.6	27	54

^a Ratio of product to monomer.

TABLE VI
X-Ray Diffraction of Powdered Crystalline Poly(PGE)

<i>d</i> spacing, Å.	Relative intensity
8.00	m
6.32	vw
5.47	s
4.95	vw
4.67	s
4.29	s
4.09	vw
3.81	vs
3.57	vw
3.35	m

The molecular weights of fractions II and III in benzene, and fraction I in THF at 30°C. were 850–950, 700–800, and 1300–1600, respectively, as determined with a Mechrolab vapor-pressure, Model 301 A osmometer.

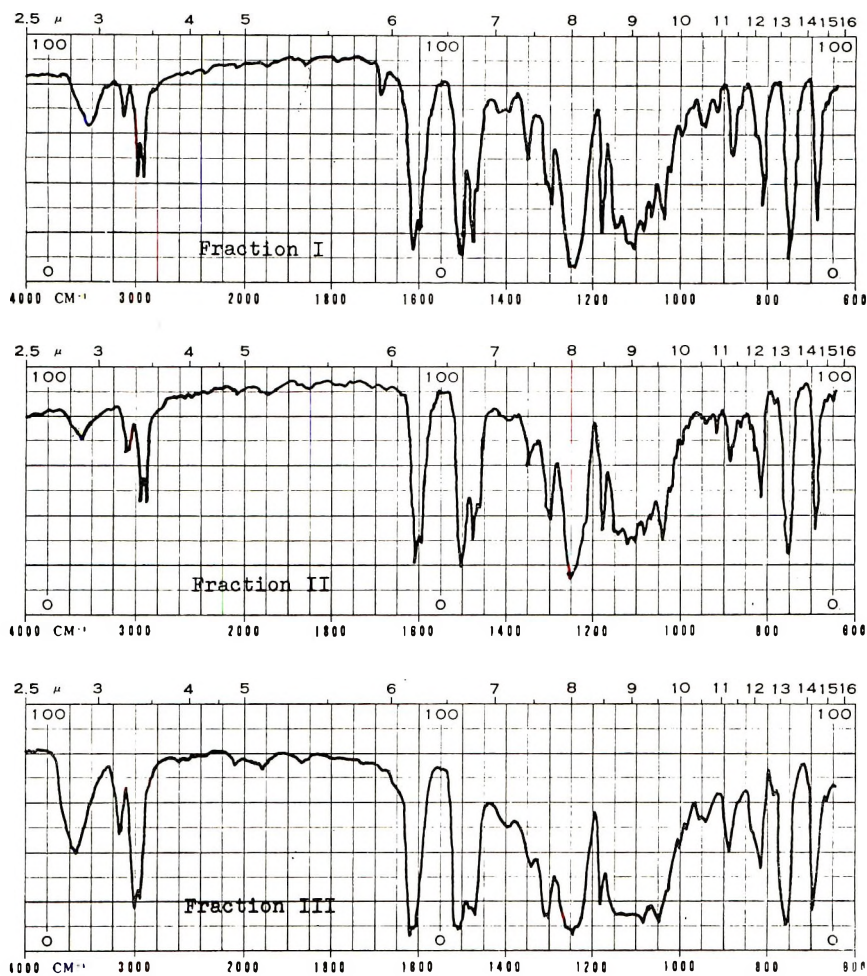


Fig. 6. Infrared spectra of the fractions of PPGE-A.

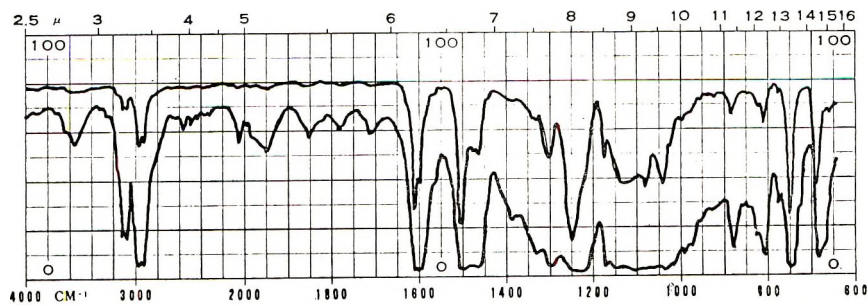


Fig. 7. Infrared spectra of PPGE-B.

TABLE VII
 Infrared Spectra of Poly(phenyl Glycidyl Ether) and Vibrational Assignments

PSt, cm. ^{-1a}	PSTO, cm. ^{-1a}	PPGE-A, cm. ⁻¹	Assignment ^b	Note
698	697	689 (693) ^c	$\nu_{11}(B_2)$, or $\nu_4(B_2)$ ^d	f
758	755	750	$\nu_{10B}(B_2)$, or $\nu_{11}(B_2)$ ^d	
—	782	780	—	e
839	843	815, 830 (815) ^e	$\nu_{10A}(A_2)$	f
—	—	860 (862) ^c	—	f
903	872, 912	880, 916 (915) ^e	$\nu_{17B}(B_2)$ or $\nu_{10B}(B_2)$ ^d	e, f
939	940, 948	940 (939) ^c	$\nu_4(B_2) + \nu_{16A}(A_2)$	f
961	972	977	$\nu_{17A}(A_2)$	
978	981	995	$\nu_5(B_2)$	
1024	1023	1020 (1018) ^c	$\nu_{18A}(A_1)$	f
1067	—	1080	$\nu_{18B}(B_1)$, $\nu(\text{CC})$	
1105	—	1105, 1125	$\nu_{11}(B_2) + \nu_{16A}(A_2)$	
—	1030-1140	1040-1140	$\nu(\text{COC})$	f
1150	1150	1143, 1153	$\nu_{15}(B_1)$	f
1177	1172, 1176	1175 (1172) ^c	$\nu_5(B_2) + \nu_{16B}(B_2)$	f
1190	1195	1210	$\nu_{18A}(A_1)$	e (1185 cm. ⁻¹)
1240	1247	1250	$\nu_{10A}(A_2) + \nu_{16A}(A_2)$	
1287	1285	1298 (1290) ^c		e (1297 cm. ⁻¹), f
1307	1307	1306	$\nu_3(B_1)$	e (1314 cm. ⁻¹)
1323	1324	1339-1333 ^e	$\nu_{14}(B_1)$	
1376	1344, 1385	1340-1356, 1390-1410	$\delta(\text{OH})$, $\delta(\text{CH})$, $\nu_5(B_2) +$ $\nu_{16A}(A_2)$	e (1364 cm. ⁻¹)
1447	1445	1455	$\nu_{19B}(B_1)$ or $\nu_4(B_2) +$ $\nu_{17B}(B_2)$	
—	1468	1473	$\delta(\text{CH}_2)$, $\nu_{11}(B_2) + \nu_{10B}(B_2)$	f

(continued)

The x-ray diffraction pattern of a powdered polymer, fraction I, was observed, and the results are shown in Figure 5 and Table VI. Fraction I was found to have a crystallinity of about 47-50% by the method of Hermans and Weidinger.¹⁷ The x-ray pattern of fraction I shown in Table VI is similar to that of the polymer I obtained with aluminum isopropoxide-zinc chloride catalyst by Noshay and Price.³

Infrared Spectra of Poly(phenyl Glycidyl Ether)

The infrared spectra of the poly (PGE) obtained with a tertiary amine and with BF_3 etherate (denoted as PPGE-A and PPGE-B, respectively) are shown in Figures 6 and 7. The samples used in the present study were in the form of a KBr disk for fraction I of PPGE-A, and in the form of thin liquid films for fractions II and III of PPGE-A and PPGE-B. The fre-

TABLE VII (continued)

PSt, cm. ^{-1a}	PSTO, cm. ^{-1a}	PPGE-A, cm. ⁻¹	Assignment ^b	Note
1489	1490	1500	$\nu_{19A}(A_1), \nu_4(B_2) + \nu_{17A}(A_2)$	
1531	1532	1570	$\nu_{11}(B_2) + \nu_{10A}(A_2)$	
1579	1579	1590	$\nu_{9A}(A_1)$	
1595	1596	1610	$\nu_{9B}(B_1)$	
1660	1640, 1670	1645, 1685	$\nu_{10B}(B_2) + \nu_{17B}(B_2)$	
1731	1715, 1745	1713	$\nu_{17B}(B_2) + \nu_{10A}(A_2)$	
1795	1800	1785	$\nu_{10A}(A_2) + \nu_{17A}(A_2)$	
—	1810	1825	$\nu_5(B_2) + \nu_{10A}(A_2)$	
—	1855	1855	$\nu_{17B}(B_2) + \nu_6(B_2), \text{ or } \nu_{17B}(B_2) + \nu_{17A}(A_2)^d$	
1870	1877	—	$\nu_{17B}(B_2) + \nu_{17A}(A_2)$	
—	1885	1945	$\nu_{17B}(B_2) + \nu_5(B_2)$	
1935	1945	1945, 1985	$\nu_5(B_2) + \nu_{17A}(A_2)$	
—	1958	2060	$2 \times \nu_5(B_2)$	
2845	2850	2870–2920 ^b	$\nu_s(\text{CH}_2)$	f
2921	2890	2920–2970 ^b	$\nu_a(\text{CH}_2)$	f
3019	3019	3040–3080 ^b	$\nu_{30A}(A_1)$	f
3052	3045	3080–3110 ^b	$\nu'_2(A_1)$	f
3072	3070	3140	$\nu_{20B}(B_1)$	
—	3450	3450–3540 ^b	$\nu(\text{OH})$	f

^a Data of Kawasaki et al.¹¹

^b According to Liang and Krimm.¹²

^c Data of Takahashi and Kambara.⁷

^d According to Whiffen¹³ and Kakiuchi.¹⁴

^e Data connected with the bands found in the spectra of a crystalline isotactic polystyrene.

^f Data concerned with the crystallinity of poly(phenyl glycidyl ether).

^g Data of Noshay and Price.³

^h The bands at the higher wave number are found in fractions II and III of PPGE-A and in PPGE-B.

quency of each band is listed in Table VII. The assignments given in Table VII will be discussed in detail in the succeeding sections.

The spectrum of Fraction I of PPGE-A shown in Figure 6 is in essential agreement with spectra of the crystalline polymers obtained by Takahashi and Kambara⁷ (PPGE-C), and by Noshay and Price³ (PPGE-D). The only significant difference is that PPGE-C has no absorption band due to an intermolecular hydrogen bond, $\nu(\text{OH})$, of the OH group of a polymer, while PPGE-A, PPGE-B, and PPGE-D show the corresponding absorption band about at 3500 cm.⁻¹. The absorption bands of fraction I of PPGE-A at 1140–1050 cm.⁻¹ are different from those of the other fractions of PPGE-A, PPGE-B, and poly(styrene oxide), PStO, obtained by Kawasaki et al.¹¹

Takahashi and Kambara,⁷ who studied the temperature dependence of infrared spectra of PPGE-C, showed that absorption bands at 1471, 1290, 1172, 1036, 1018, 939, 883, 862, 815, and 693 cm.⁻¹ decrease when the

measuring temperature is high and decrease substantially or disappear near the melting point of the specimen, and they have considered that absorption at 1290, 1036, 883, and 815 cm^{-1} are the most crystalline-sensitive bands.

In PPGE-A, the corresponding absorption bands are 1470, 1290, 1175, 1040, 1020, 940, 917, 885, 860, 814, and 688 cm^{-1} . The absorption bands which fraction I of PPGE-A shows but which the other fractions of PPGE-A and PPGE-B lack are those at 1470, 1345, 1306, 1155, 1125, 1105, 1065, 916, and 860 cm^{-1} .

The absorption bands of PPGE appearing in the region of infrared seem to arise almost from the vibrations of the benzene ring in the polymer as those of polystyrene (PSt)¹²⁻¹⁴ and poly(styrene oxide).¹¹ In fraction I of PPGE-A, the orientation of the $\text{C}_6\text{H}_5\text{OCH}_2$ group seems to be regular, since the x-ray diffraction study indicates that the polymer is crystalline. The chain of crystalline PPGE is probably stiffened somewhat as a result of the interference between neighboring $\text{C}_6\text{H}_5\text{OCH}_2$ groups, and there is some indication⁷ that a regularity exists along the polymer backbone. In the other fractions of PPGE-A and PPGE-B, however, the polymers are completely amorphous. This implies that, for spectroscopic purposes, no specific interactions exist between monomeric units in the chain. It should, therefore, be a good first approximation to consider separately the normal vibrations of the phenyl, CH_2 , and CH groups, and to interpret the spectrum as essentially a linear superposition of the contributions of these parts.

Absorption Bands Arising from Vibrations of the Benzene Ring

Assignment of A_2 and B_2 Fundamentals. As Liang and Krimm¹ have noted, the three A_2 vibrations derived from E_{1g} and E_{2u} modes of benzene are not expected to be active in the infrared absorption, but as a result of our not having such strictly C_{2v} symmetry these modes might be expected to be weakly active. The absorption band of PPGE-A and PPGE-B at 689 cm^{-1} corresponds to the band of PPGE-C at 693 cm^{-1} , of PPGE-D at 14.45–14.50 μ (692–689 cm^{-1}), of PStO at 697 cm^{-1} , and of PSt at 698 cm^{-1} . In the case of PSt, Liang and Krimm¹² assigned it to the out-of-plane hydrogen-deformation mode, $\nu_{11}(B_2)$, and Whiffen,¹³ to the out-of-plane skeletal-deformation mode, $\nu_4(B_2)$, of benzene. The band at 750 cm^{-1} agrees with the band at 13.35–13.43 μ (749–745 cm^{-1}) of PPGE-D and corresponds to the bands of PSt and PStO at 758 and 755 cm^{-1} , respectively. In the case of PSt, Liang and Krimm¹² assigned this band to the out-of-plane hydrogen-deformation mode, $\nu_{10B}(B_2)$, and Whiffen¹³ and Kakiuchi¹⁴ assigned it to the $\nu_{11}(B_2)$ mode. In the case of PStO, Kawasaki et al.¹¹ considered that, since the absorption bands at 755 and 697 cm^{-1} are active for polarized infrared radiation, both assignments of these vibration bands by Krimm and Liang,¹² and Whiffen¹³ or Kakiuchi¹⁴ lead us to the conclusion that a plane of benzene in the polymer is parallel to a stretching direction. Takahashi and Kambara⁷ showed that the corresponding absorption bands of PPGE-C are crystallinity-sensitive.

These results seem to suggest that a plane of benzene in poly(PGE) is ordered similarly as in PStO.

The band with a weak shoulder at 780 cm^{-1} is not observed in PPGE-D but is found in PPGE-C. The corresponding band is found at 782 cm^{-1} and has not been assigned for PStO. The corresponding absorption band is not observed in infrared spectra of noncrystalline isotactic PSt, but is seen in that of crystalline isotactic PSt. This shoulder has been observed in infrared spectra of all fractions of PPGE-A and in PPGE-B.

Comparison of infrared spectra of fraction I of PPGE-A with those of the other fractions of PPGE-A and of PPGE-B, shown in Figures 6 and 7, shows that the band at 860 cm^{-1} is related to the crystallinity of the polymer. This agrees with the fact, shown by Takahashi and Kambara,⁷ that this band in PPGE-C is crystallinity-sensitive. The fraction I of PPGE-D has the corresponding band at 11.63 (859.8 cm^{-1}).

The bands at 830 and 814 cm^{-1} are considered from its frequency and strength to correspond to a band in PSt at 839 cm^{-1} , in PStO at 843 cm^{-1} and to be here to the out-of-plane hydrogen-deformation mode, $\nu_{10A}(A_2)$, as are those of PSt and PStO. This band is shifted to a smaller wave number than that of PStO. The same shoulder as that of PPGE-A is found at 815 and 830 cm^{-1} in PPGE-C. A band at $12.35\ \mu$ (809.7 cm^{-1}) is found in the infrared spectra of fractions I and II of PPGE-D, and no corresponding band at 830 cm^{-1} is found in those of all fractions of PPGE-D.

The band which appears at 903 cm^{-1} in the spectra of an amorphous PSt splits into two bands at 920 (σ) and 898 (π) cm^{-1} in those of a crystalline isotactic PSt. The dichroism is not clear for the bands at 912 and 872 cm^{-1} in the spectra of PStO. Kawasaki et al.¹¹ suggested that the bands of PStO at 912 and 872 cm^{-1} correspond to the bands of PSt at 920 and 898 cm^{-1} . Fraction I of PPGE-A is found to have the corresponding bands at 877 – 885 and 916 cm^{-1} , fraction II of PPGE-A has the band at 880 cm^{-1} and a broad shoulder at 915 – 918 cm^{-1} , and fraction III has the bands at 880 and 935 cm^{-1} . The corresponding bands are found at 880 and 935 cm^{-1} in the spectra of PPGE-B. Therefore, the band at 880 cm^{-1} in the spectra of noncrystalline PPGE splits into two bands at 877 – 885 and 915 cm^{-1} in those of crystalline PPGE. There are observed the corresponding bands at 883 and 915 cm^{-1} for PPGE-C, at 11.35 – $11.37\ \mu$ (881.1 – 879.5 cm^{-1}) for fraction III (in CCl_4) of PPGE-D, and at $11.35\ \mu$ (881.1 cm^{-1}) and $10.80\ \mu$ (925.9 cm^{-1}) for fractions I and II of PPGE-D. The band at 880 cm^{-1} in the spectra of PPGE-A might be assigned to the skeletal deformation mode, δ (COC), as that of PStO at 872 cm^{-1} .

Liang and Krimm¹² assigned the band of PSt at 903 cm^{-1} to the out-of-plane hydrogen-deformation mode, $\nu_{17B}(B_2)$, and Whiffen¹³ and Kakiuchi¹⁴ assigned it to $\nu_{10B}(B_2)$.

The band at 977 cm^{-1} found in the spectra of PPGE-A, PPGE-B, PPGE-C, and of fraction III of PPGE-D, corresponds to the band of

PSt at 961 cm^{-1} and of PStO at 972 cm^{-1} , and is assigned to the out-of-plane hydrogen deformation mode, $\nu_{17A}(A_2)$.

The band of PPGE-A and PPGE-B at 995 cm^{-1} is also observed for fraction III of PPGE-D, but is not found for the other fractions of PPGE-D and for PPGE-C. This corresponds to the band of PSt at 978 cm^{-1} and of PStO at 981 cm^{-1} , and is assigned to the out-of-plane hydrogen-deformation mode, $\nu_3(B_2)$.

These results show that the absorption bands which are found in the infrared spectra of PPGE and can be assigned to the bands arising from the vibrations of the out-of-plane hydrogen-deformation modes of the benzene ring in polymer shift to the higher wave number regions, compared with the corresponding absorption bands of PSt and PStO as shown in Table VII.

Assignment of A_1 and B_1 Fundamentals. The bands, which are found in the spectra of fractions of I, II, and III of PPGE-A and of PPGE-B, at 1020–1015 cm^{-1} , correspond to the bands of PSt at 1024 cm^{-1} and of PStO at 1023 cm^{-1} , and can be assigned to the in-plane hydrogen-deformation mode, $\nu_{18A}(A_1)$. The corresponding bands are found at 1018 cm^{-1} for PPGE-C, at 9.70–9.80 μ (1031–1020 cm^{-1}) for fraction I of PPGE-D, and at 9.77 μ (1024 cm^{-1}) for fraction III of PPGE-D.

The band corresponding to the band of PSt at 1067 cm^{-1} and assigned to the in-plane hydrogen-deformation mode, $\nu_{18B}(B_1)$, is found at 1068 cm^{-1} in the spectra of fraction I of PPGE-A. No such band, however, can be observed in the spectra of the other fractions of PPGE-A and of PPGE-B, because of the broad bands of $\nu(\text{COC})$. This is the case of the spectra of PStO or PPGE-D.

The band which corresponds to the band of PSt at 1150 cm^{-1} and can be assigned to the in-plane hydrogen-deformation mode, $\nu_{15B}(B_1)$, is found at 1150 cm^{-1} shoulder for fractions II and III of PPGE-A and for PPGE-B, and splits into two bands at 1143 and 1153 cm^{-1} in the spectra of fraction I of PPGE-A. PPGE-D has no such corresponding band in this region, but PPGE-C has the band at 1150 cm^{-1} .

The band at 1180 cm^{-1} found in the spectra of both PPGE-A and PPGE-B corresponds to the bands of PSt at 1190 cm^{-1} and of PStO at 1195 cm^{-1} and can be assigned to the in-plane hydrogen-deformation mode, $\nu_{18A}(A_1)$. The corresponding band is found at 8.53–8.55 μ (1172–1170 cm^{-1}) for PPGE-D and at 1172 cm^{-1} of PPGE-C whose band is related to the crystallinity of the polymer. As Tadokoro et al.¹⁵ have noted in the case of the infrared spectra of isotactic PSt, this absorption band may include the bands arising from the vibrations of CH_2 , CH , and CC of polymer chain.

The band which corresponds to the bands of PSt at 1297 cm^{-1} and of PStO at 1285 cm^{-1} is found at 1298 cm^{-1} for PPGE-A and PPGE-B, at 7.75 μ (1290 cm^{-1}) for fraction III of PPGE-D and at 1290 cm^{-1} for PPGE-C. This band of PPGE-C is crystallinity sensitive,⁷ and the band of fraction I of PPGE-A is deeper than that of the other fractions of PPGE-A.

These results suggest that this band seems to include the absorption band arising from the vibrations which are sensitive to the conformation of the main chain in PPGE as Tadokoro et al.¹⁵ pointed out in the case of the spectra of isotactic PSt.

The band found at 1306 cm.⁻¹ in the spectra of PPGE-A is considered to correspond to the band of PSt or PStO at 1307 cm.⁻¹, and can be assigned to the in-plane hydrogen-deformation mode, $\nu'_3(B_1)$. The corresponding band is observed at 7.70–7.76 μ (1299–1289 cm.⁻¹) for PPGE-D, but no such band is found in the spectra of PPGE-C. The ratio of the absorption strength of the band at 1298 cm.⁻¹ to that at 1306 cm.⁻¹ is found to be different from the ratio of the absorption strength of the band at 1285 cm.⁻¹ to that at 1307 cm.⁻¹ in the spectra of PStO.

PPGE-A, -B, and -C have no band corresponding to that of PSt at 1323 cm.⁻¹ and to that of PStO at 1324 cm.⁻¹, but PPGE-D has a shoulder at 7.50–7.47 μ (1333–1339 cm.⁻¹) in the spectra of all fractions. This band may be assigned to the skeletal stretching vibration, $\nu_{14}(B_1)$.

The band found at 1455 cm.⁻¹ in the spectra of PPGE-A seems to correspond to the band of PSt at 1447 cm.⁻¹ and of PStO at 1445 cm.⁻¹. The corresponding band is found at 6.84 or at 6.85 μ (1462 or 1460 cm.⁻¹) for the fractions of PPGE-D. PPGE-C has a shoulder at 1470 cm.⁻¹. In the case of the spectra of PSt, Liang and Krimm¹² have assigned this band to the $\delta(\text{CH}_2)$ vibration and the skeletal stretching mode, $\nu_{19B}(B_1)$, or the combinations of $\nu_{11}(B_2) + \nu_{10B}(B_2)$ and $\nu_4(B_2) + \nu_{17B}(B_2)$.

$$\nu_{11}(B_2) (689 \text{ cm.}^{-1}) + \nu_{10B}(B_2) (750 \text{ cm.}^{-1}) = 1439 \text{ cm.}^{-1}$$

The band at 1475–1471 cm.⁻¹ for fraction I of PPGE-A and at 6.78–6.80 μ (1475–1471 cm.⁻¹) for PPGE-C and PPGE-D corresponds to the weak band at 1468 cm.⁻¹ in the spectra of PStO. No such band is observed in the spectra of PSt. This band is stronger than that of PStO, and can be assigned to the $\delta(\text{CH}_2)$ vibration or the combination of $\nu_{11}(B_2) + \nu_{10B}(B_2)$.

The band which is found at 1500 cm.⁻¹ for PPGE-A and at 6.68 μ (1497 cm.⁻¹) for PPGE-C and PPGE-D corresponds to the bands at 1468 cm.⁻¹ for PSt and at 1490 cm.⁻¹ for PStO, and can be assigned to the skeletal stretching vibration, $\nu_{19A}(A_1)$, and the combination of $\nu_4(B_2) + \nu_{17A}(A_2)$.

$$\nu_4(B_2) (689 \text{ cm.}^{-1}) + \nu_{17A}(A_2) (977 \text{ cm.}^{-1}) = 1666 \text{ cm.}^{-1}$$

The bands found at 1410, and 1390 cm.⁻¹ in the spectra of fraction I of PPGE-A may be assigned to the combination of $\nu_{11}(B_2) + \nu_{10B}(B_2)$. This band becomes a broad one about at 1390 cm.⁻¹ in the spectra of the other fractions of PPGE-A and of PPGE-B. The fraction I of PPGE-D has the corresponding bands at 7.13–7.15 μ (1403–1399 cm.⁻¹), and fraction III of PPGE-D has a weak band at 7.20 μ (1389 cm.⁻¹).

The band which corresponds to the bands at 1579 cm.⁻¹ for PSt and at 1579 cm.⁻¹ PStO and is assigned to the skeletal stretching vibration, $\nu_{9A}(A_1)$ is found at 1590 cm.⁻¹ in the spectra of PPGE-A and PPGE-B,

and at 6.27 and 6.28 μ (1595–1592 cm^{-1}) for PPGE-D. No such bands are observed for PPGE-C.

The band found at 1610 cm^{-1} for PPGE-A and at 6.24–6.23 μ (1603–1608 cm^{-1}) for PPGE-D and PPGE-C corresponds to the band at 1595 cm^{-1} for PSt and at 1596 cm^{-1} for PStO and can be assigned to the skeletal stretching vibration, $\nu_{9B}(B_1)$.

The bands at 3080, 3110, and 3140–3160 cm^{-1} in the spectra of PPGE-A correspond to the bands at 3019, 3045, and 3073 cm^{-1} for PSt, and at 3019, 3045, and 3070 cm^{-1} for PStO, and can be assigned to the hydrogen stretching vibrations, $\nu_{20B}(B_1)$, $\nu_2'(A_1)$, and $\nu_{20A}'(A_1)$.

The bands found in the infrared spectra of PPGE and assigned to the bands arising from the vibrations of the A_1 and B_1 modes of the benzene ring in polymer shift to the higher wave number regions compared with those of PSt and of PStO.

Assignment of Overtone and Combination Bands. Liang and Krimm¹² have assigned the band at 939 cm^{-1} for PSt to the combination of the two out-of-plane skeletal-deformation modes, $\nu_4(B_2) + \nu_{16A}(A_2)$. The corresponding bands are found at 940 or 948 cm^{-1} as a very weak shoulder in the spectra of PStO, at 940 or 918 cm^{-1} for fraction I of PPGE-A, and at 940 cm^{-1} for PPGE-B and the other fractions of PPGE-A. These bands are also observed at 915 and 939 cm^{-1} for PPGE-C and at 10.80 μ (925.9 cm^{-1}) for fraction III of PPGE-D.

The band which corresponds to the band at 1105 cm^{-1} in the spectra of PSt and is assigned to the combination, $\nu_{11}(B_2) + \nu_{16A}(A_2)$, is found at 1105 and 1125 cm^{-1} for fraction I of PPGE-A. No such bands can be observed in the spectra of the other fractions of PPGE-A and of PPGE-B because of a strong broad band arising from $\nu(\text{COC})$ vibration. The corresponding band is found at 8.95 μ (1117 cm^{-1}) for the fraction I of PPGE-D and at 1105 and 1125 cm^{-1} for PPGE-C.

No corresponding band, which is observed at 1177 cm^{-1} in the spectra of PSt and at 1172 and 1176 cm^{-1} in those of PStO, is found for PPGE-A, -B, -C, and -D. This band of PSt is assigned to the combination of the out-of-plane skeletal-deformation modes, $\nu_5(B_2) + \nu_{16B}(B_2)$.

The band which corresponds to the band at 1240 cm^{-1} for PSt and at 1247 cm^{-1} for PStO can be assigned to the combination of the out-of-plane skeletal-deformation modes $\nu_{10A}(A_2) + \nu_{16A}(A_2)$. This band is stronger than that of PSt or PStO, and is found at 8.05 μ (1242 cm^{-1}) for PPGE-D and at 8 μ (1250 cm^{-1}) for PPGE-C.

The band found at 1350 cm^{-1} for fraction I of PPGE-A or at 1340 cm^{-1} for PPGE-B and the other fractions of PPGE-A corresponds to the band at 1365 cm^{-1} for PSt, at 1344 cm^{-1} for PStO, and at 7.50–7.47 μ (1333–1339 cm^{-1}) for PPGE-D. In the case of PSt, Liang and Krimm¹² assigned this band to the $\delta(\text{CH})$ vibration and the combination of the $\nu_5(B_2)$ and $\nu_{16A}(A_2)$, and Tadokoro et al.¹⁵ showed that this band is related to the conformation of the main chain of PSt. The broad band which is found at 1390 cm^{-1} in the spectra of PPGE-B and fraction II and III of PPGE-A

splits into two bands at 1415 and 1392 cm^{-1} for fraction I of PPGE-A and corresponds to the bands at 7.13–7.20 μ (1403–1389 cm^{-1}) for PPGE-D. This band can be assigned to the combination of the $\nu_5(B_2)$ and $\nu_{16A}(A_2)$ vibrations.

The shoulder at 1570–1560 cm^{-1} in the spectra of PPGE-A and PPGE-B corresponds to the band at 1532 cm^{-1} for PStO and at 1531 cm^{-1} and can be assigned to the combination¹² of the $\nu_{11}(B_2)$ and $\nu_{10A}(A_2)$ vibrations or to the combination¹³ of the $\nu_4(B_2)$ and $\nu_{10A}(A_2)$ vibrations.

$$\nu_4(B_2) (689 \text{ cm}^{-1}) + \nu_{10A}(A_2) (814 \text{ cm}^{-1}) = 1504 \text{ cm}^{-1}$$

or

$$\nu_4(B_2) (689 \text{ cm}^{-1}) + \nu_{10A}(A_2) (830 \text{ cm}^{-1}) = 1519 \text{ cm}^{-1}$$

The bands found at 1645 and 1680 cm^{-1} for PPGE-A correspond to the band at 1660 cm^{-1} for PSt and at 1645 and 1680 cm^{-1} for PStO and are assigned to the combination¹² of the $\nu_{10B}(B_2)$ and $\nu_{17B}(B_2)$ vibrations or the combination¹³ of the $\nu_{11}(B_2)$ and $\nu_{10B}(B_2)$ vibrations. No such bands are found in the spectra of PPGE-C and PPGE-D. The fact that the two absorption bands are observed in this region of the spectra of PPGE-A can be explained by the fact that the band which corresponds to the band at 903 cm^{-1} and is assigned to the $\nu_{17B}(B_2)$ or $\nu_{10B}(B_2)$ vibration splits into two bands at 880 and 916 cm^{-1} for PPGE-A as two bands at 912 and 872 cm^{-1} for PStO. No such bands are observed in the spectra of PPGE-B and fraction I of PPGE-A, but a stronger band is found at 1640 cm^{-1} in the spectra of the other fractions of PPGE-A.

Fractions II and III of PPGE-A have been found to have much carbon-carbon double-bond unsaturation in the polymer chain, and the band at 1640 cm^{-1} in the spectra of these fractions disappears after hydrogenation of the polymer. This result seems to show that the band at 1640 cm^{-1} in the spectra of PStO and PPGE does not arise from the combination of $\nu_{10B}(B_2)$ and $\nu_{17B}(B_2)$ vibrations or the combination of the $\nu_{11}(B_2)$ and $\nu_{10B}(B_2)$ vibrations.

$$\nu_{10B}(B_2) (750 \text{ cm}^{-1}) + \nu_{17B}(B_2) (880 \text{ cm}^{-1}) = 1630 \text{ cm}^{-1}$$

or

$$\nu_{10B}(B_2) (750 \text{ cm}^{-1}) + \nu_{17B}(B_2) (916 \text{ cm}^{-1}) = 1666 \text{ cm}^{-1}$$

The above calculation seems to show that the band at 916 cm^{-1} is more suitable than that at 880 cm^{-1} to be assigned to the $\nu_{17B}(B_2)$ vibration. Let us consider the combination of the $\nu_{17B}(B_2)$ and $\nu_{10A}(A_2)$ vibrations. The combination is calculated as:

$$\nu_{17B}(B_2) (880 \text{ cm}^{-1}) + \nu_{10A}(A_2) (830 \text{ cm}^{-1}) = 1710 \text{ cm}^{-1}$$

$$\nu_{17B}(B_2) (916 \text{ cm}^{-1}) + \nu_{10A}(A_2) (830 \text{ cm}^{-1}) = 1746 \text{ cm}^{-1}$$

$$\nu_{17B}(B_2) (880 \text{ cm}^{-1}) + \nu_{10A}(A_2) (815 \text{ cm}^{-1}) = 1695 \text{ cm}^{-1}$$

$$\nu_{17B}(B_2) (916 \text{ cm}^{-1}) + \nu_{10A}(A_2) (815 \text{ cm}^{-1}) = 1731 \text{ cm}^{-1}$$

The corresponding observed bands are at 1713 and 1685 cm^{-1} . Therefore, the bands at 916 and 880 cm^{-1} seem to correspond to the bands at 903 cm^{-1} for PSt and at 912 and 872 cm^{-1} for PStO. The bands which correspond to the bands at 1715 and 1745 cm^{-1} for PStO are found for PPGE-C, but no such bands are observed in the spectra of PPGE-D. No band is found at 1685 cm^{-1} for PPGE-B.

The band which corresponds to the bands at 1795 cm^{-1} for PSt and at 1800 cm^{-1} for PStO and is assigned to the combination of the $\nu_{10A}(A_2)$ and $\nu_{17A}(A_2)$ vibrations is found at 7185 cm^{-1} in the spectra of PPGE-A, PPGE-B, and PPGE-C.

$$\nu_{10A}(A_2) (815 \text{ cm}^{-1}) + \nu_{17A}(A_2) (977 \text{ cm}^{-1}) = 1792 \text{ cm}^{-1}$$

or

$$\nu_{10A}(A_2) (830 \text{ cm}^{-1}) + \nu_{17A}(A_2) (977 \text{ cm}^{-1}) = 1807 \text{ cm}^{-1}$$

The band found at 1945 cm^{-1} for PPGE-A and PPGE-B corresponds to the bands at 1870 cm^{-1} for PSt and at 1877 cm^{-1} for PStO and is assigned to the combination of the $\nu_{17B}(B_2)$ and $\nu_5(B_2)$ vibrations¹² or to the combination of the $\nu_{17B}(B_2)$ and $\nu_{17A}(A_2)$ vibrations.^{13,14} According to Liang's assignment,¹² the combination can be calculated as:

$$\nu_{17B}(B_2) (880 \text{ cm}^{-1}) + \nu_5(B_2) (995 \text{ cm}^{-1}) = 1875 \text{ cm}^{-1}$$

or

$$\nu_{17B}(B_2) (916 \text{ cm}^{-1}) + \nu_5(B_2) (995 \text{ cm}^{-1}) = 1911 \text{ cm}^{-1}$$

The combination, however, is calculated, according to Whiffen's,¹³ or Kakiuchi's assignment,¹⁴

$$\nu_{17B}(B_2) (880 \text{ cm}^{-1}) + \nu_{17A}(A_2) (977 \text{ cm}^{-1}) = 1857 \text{ cm}^{-1}$$

or

$$\nu_{17B}(B_2) (916 \text{ cm}^{-1}) + \nu_{17A}(A_2) (977 \text{ cm}^{-1}) = 1893 \text{ cm}^{-1}$$

The observed bands in this region are at 1945, 1855 cm^{-1} and at 1825 cm^{-1} (shoulder).

Kakiuchi¹⁴ has assigned the shoulder which is found at 1885 cm^{-1} in the spectra of PSt to the combination of the $\nu_{17B}(B_2)$ and $\nu_5(B_2)$ vibrations. According to this assignment, the bands found at 1945 and 1855 cm^{-1} , therefore, can be assigned to the combination of the $\nu_{17B}(B_2)$ and $\nu_5(B_2)$ vibrations, and the band found at 1855 cm^{-1} and the shoulder at 1825 cm^{-1} may be assigned to the combination of the $\nu_{17B}(B_2)$ and $\nu_{17A}(A_2)$ vibrations. This assignment can explain the strength of the absorption bands in this region of the spectra of PPGE.

The band which corresponds to the bands at 1935 cm^{-1} for PSt and at 1945 cm^{-1} for PStO and is assigned to the combination of the $\nu_5(B_2)$ and $\nu_{17A}(A_2)$ vibrations, is found at 1985 cm^{-1} in the spectra of PPGE.

$$\nu_5(B_2) (995 \text{ cm}^{-1}) + \nu_{17A}(A_2) (977 \text{ cm}^{-1}) = 1972 \text{ cm}^{-1}$$

The band found at 1825 cm^{-1} corresponds to the band at 1810 cm^{-1} in the spectra of PStO and may be assigned to the combination of the $\nu_5(B_2)$ and $\nu_{10A}(A_2)$.

$$\nu_5(B_2) (995 \text{ cm}^{-1}) + \nu_{10A}(A_2) (815 \text{ cm}^{-1}) = 1810 \text{ cm}^{-1}$$

$$\nu_5(B_2) (995 \text{ cm}^{-1}) + \nu_{10A}(A_2) (830 \text{ cm}^{-1}) = 1825 \text{ cm}^{-1}$$

The band found at 2060 cm^{-1} corresponds to the band at 1958 cm^{-1} in the spectra of PStO, and can be assigned to the overtone of the $\nu_5(B_2)$, according to Kakiuchi's assignment.¹⁴

$$2 \times \nu_5(B_2) (995 \text{ cm}^{-1}) = 1990 \text{ cm}^{-1}$$

Assignment of the Other Vibration Modes

The CH_2 modes of the poly(phenyl glycidyl ether) chain can be readily identified on the basis of studies on polystyrene¹²⁻¹⁴ and poly(styrene oxide).¹¹ The stretching modes $\nu_s(\text{CH}_2)$ and $\nu_a(\text{CH}_2)$, which are found in PSt at 2845 and 2921 cm^{-1} and in PStO at 2850 and 2890 cm^{-1} , respectively, are unambiguously identified with the bands at 2870 and 2920 cm^{-1} in the spectra of fraction I of PPGE-A. These bands are found in fractions II and III of PPGE-A at 2890 and 2930 cm^{-1} and at 2920 and 2970 cm^{-1} , respectively, and in PPGE-B at 2910 and 2960 cm^{-1} . The corresponding absorption bands are found in PPGE-C and at 3.40-3.45 μ (2941-2899 cm^{-1}) in the spectra of PPGE-D.

The bending mode, $\delta(\text{CH}_2)$, which is found in PSt at 1450 cm^{-1} and in PStO at 1447 cm^{-1} , is undoubtedly the main component of the PPGE band at 1455-1460 cm^{-1} . The fact that its intensity is greater than that expected seems to be reason to believe that it represents a superposition of bands, one of which is a ring frequency, $\nu_{19B}(B_1)$.

The CH_2 wagging mode is not observed in PSt because of extreme weakness of its intensity. It is unlikely that it appears in the spectrum of PPGE as in that of PStO.

The CH_2 rocking mode seems to occur at higher frequencies, and is generally much weaker than the comparable band in polyethylene. It has been identified in the spectra of PSt and of PStO and we therefore only nominally assign to it part of the weak band at 977-980 cm^{-1} .

The stretching mode of the lone CH group is generally too weak to be clearly identified,¹⁸ and is not observed in PSt and PStO.¹¹

The band arising from the CH bending mode, $\delta(\text{CH})$, is not observed in PSt¹² and in PStO. Liang and Krimm¹² only tentatively suggested that this mode might be contributing to the band at 1376 cm^{-1} in PSt. The corresponding band is found at 1390 cm^{-1} in PPGE and at 1385 cm^{-1} in PStO. Such modes might also mix with some of the ring vibrations and result in frequency shifts and intensity changes.

The band which corresponds to the band at 3450 cm^{-1} in PStO and is assigned to the $\nu(\text{OH})$ vibration is found at 3450-3460 cm^{-1} in fraction

I of PPGE-A and at 3500–3540 cm^{-1} in the other fractions of PPGE-A. The corresponding weak band is found in the spectra of PPGE-C and at 2.89–2.90 μ (3460–3448 cm^{-1}) in PPGE-D.

The skeletal modes of a planar zigzag C—O—C chain have not been considered in detail in present paper. We only assign part of the medium intensity band at 1080 cm^{-1} to a skeletal chain stretching mode and the bands at 1040–1140 cm^{-1} roughly to the $\nu(\text{COC})$. These assignments are, of course, speculative, and must always be considered in the light of possible mixing with benzene ring vibrations. These results are collected in Table VII.

The authors are grateful to Dr. Minoru Hirota for his discussion on the assignments of the infrared spectra of poly(phenyl glycidyl ether). We also wish to acknowledge the assistance of Mr. K. Kosuge in carrying out many of the experiments.

References

1. Kakiuchi, H., and Y. Tanaka, in preparation.
2. Furukawa, K., and R. Oda, *Kogyo Kagaku Zasshi*, **55**, 673 (1952).
3. Noshay, A., and C. C. Price, *J. Polymer Sci.*, **34**, 165 (1959).
4. Vandenberg, E. J., *J. Polymer Sci.*, **47**, 486, 489 (1960).
5. Garty, K. T., T. B. Gibb, Jr., and R. A. Clendinning, *J. Polymer Sci.*, **A1**, 85 (1963).
6. Kambara, S., and A. Takahashi, *Makromol. Chem.*, **63**, 89 (1963).
7. Takahashi, A., and S. Kambara, *Makromol. Chem.*, **72**, 92 (1964).
8. Staudinger, H., and H. Lehmann, *Ann.*, **505**, 41 (1933).
9. Lidarik, M., S. Stary, and I. Mleziva, *Vysokomol. Soedin.*, **5**, 1748 (1963).
10. Lidarik, M., S. Stary, N. Soukalova, and S. Pokorny, *Kunststoff-Rundschau*, **10**, 498 (1963).
11. Kawasaki, A., J. Furukawa, T. Tsuruta, T. Saegusa, and Q. Kakogawa, *Kogyo Kagaku Zasshi*, **63**, 871 (1960).
12. Liang, C. Y., and S. Krimm, *J. Polymer Sci.*, **27**, 241 (1958).
13. Whiffen, D. H., *J. Chem. Soc.*, **1956**, 1350.
14. Kakiuchi, U., *Nippon Kagaku Zasshi*, **77**, 134, 1572, 1591, 1839 (1956).
15. Tadokoro, H., N. Nishiyama, S. Nozakura, and M. Murahashi, *J. Polymer Sci.*, **36**, 553 (1959).
16. Kotake, M., *Constants of Organic Compounds*, Asakura Publishing Co., Tokyo, 1963.
17. Hermans, P. H., and A. Weidinger, *J. Appl. Phys.*, **19**, 491 (1948); *J. Polymer Sci.*, **4**, 709 (1949).
18. Krimm, S., and C. Y. Liang, *J. Polymer Sci.*, **22**, 95 (1956); S. Krimm, C. Y. Liang, and G. B. B. M. Sutherland, *J. Polymer Sci.*, **22**, 227 (1956).

Résumé

On a obtenu des polymères cristallins et amorphes en polymérisant l'éther de phényl-glycidyle en présence d'amines tertiaires. La partie cristalline a un haut point de fusion et est insoluble à température de chambre. Les fractions amorphes sont solubles à température de chambre et leur poids moléculaire est voisin de 950 dans le benzène à 30°C. Si on augmente la concentration et la température de réaction au-dessus de 50°C, on diminue considérablement la fraction cristalline et la fraction amorphe pâteuse; par contre, dans ces mêmes conditions, la fraction liquide augmente. La diffraction des rayons-X montre que le taux de cristallinité est voisin de 47–50% (pour la fraction cristalline). Son spectre est similaire au spectre de l'éther de poly(phényl-glycidyle)

obtenu par Noshay et Price. On a déterminé le spectre infra-rouge de ces fractions dans la région de 650 cm^{-1} à 4000 cm^{-1} . On compare ces spectres à ceux du polystyrène et du poly(styrène-oxyde) pour attribuer les bandes de la molécule d'éther poly(phénylglycidyle). En se basant sur l'analyse des spectres du polystyrène et du poly(styrène-oxyde) et sur l'étude de la combinaison des bandes, on a pu identifier de manière très satisfaisante les vibrations fondamentales du noyau benzénique des groupements CH_2 , CH et du squelette.

Zusammenfassung

Kristalline und amorphe Polymere wurden durch Polymerisation von Phenylglycidyläther in Gegenwart tertiärer Amine erhalten. Die kristalline Fraktion besitzt einen hohen Schmelzpunkt und ist bei Raumtemperatur unlöslich. Die amorphen Fraktionen sind bei Raumtemperatur löslich und ihr Molekulargewicht wurde in Benzol zu ~ 950 bei 30°C . bestimmt. Die Ausbeute an kristalliner Fraktion nahm mit steigender Katalysatorkonzentration und Reaktionstemperatur oberhalb 50°C . stark ab. Die Ausbeute an flüssiger Fraktion nahm jedoch mit steigender Katalysatorkonzentration und Reaktionstemperatur zu. Die Röntgenbeugungsanalyse der kristallinen Fraktion zeigt, dass sie 47–50% Kristallinität besitzt und dass ihr Röntgendiagramm demjenigen des von Noshay und Price erhaltenen Polyphenylglycidyläthers ähnlich ist. Die Infrarotspektren wurden an diesen Fraktionen im Bereich von 650 bis 4000 cm^{-1} aufgenommen. Die Ergebnisse werden mit denjenigen für Polystyrol und Polystyroloxyd verglichen und zur Identifizierung der Normalschwingungen des Polyphenylglycidyläthermoleküls benützt. Auf der Grundlage der Polystyrol- und Polystyroloxydanalyse und einer Untersuchung der Kombinationsbanden war eine recht befriedigende Identifizierung aller Grundschwingungen des Benzolrings und der CH_2 -, CH -, und Skelettschwingungen möglich.

Received April 6, 1965

Revised May 14, 1965

Prod. No. 4803A

Polymers and Telomers of Perfluoro-1,4-pentadiene

JAMES E. FEARN, DANIEL W. BROWN, and LEO A. WALL, *National Bureau of Standards, Washington, D. C.*

Synopsis

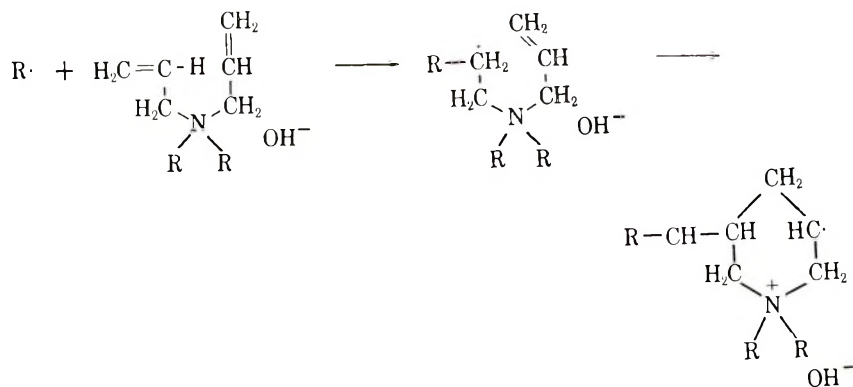
Perfluoro-1,4-pentadiene was prepared by pyrolysis of sodium 3,5,6-trichloroperfluorohexanoate and subsequent dehalogenation. The monomer was polymerized under a number of conditions of temperature and pressure using various periods and various dose rates of γ -ray initiation. The compound was found to undergo double-bond migration producing perfluoro-1,3-pentadiene. The polymer samples, some of them rubbery, others grainy, are assumed to be copolymers of the 1,4-pentadiene and the 1,3-pentadiene, the 1,4-diene polymerizing according to a cyclic mechanism and the 1,3-diene undergoing the 1,4-addition that is characteristic of butadienes under certain conditions. Infrared and nuclear magnetic resonance studies tend to support these assumptions. Under polymerization conditions the monomer also produced four distinct dimers and traces of two monomeric substances.

INTRODUCTION

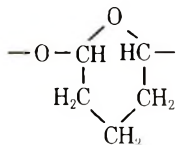
What is sometimes termed inter-intramolecular polymerization was apparently first observed during an investigation¹ of the polymerization of allyl ammonium salts. When quaternary salts containing two allyl groups are polymerized, soluble polymers result, whereas the presence of more than two allyl groups leads to the formation of insoluble polymers. A considerable number of studies have demonstrated that this type of polymerization often occurs¹⁻¹⁷ with unconjugated hydrocarbon dienes.

These polymerizations, in which soluble polymers are produced from dienes, have been explained^{6,7} by a mechanism involving an intermolecular radical attack on one of the olefinic groups in a molecule, followed by intramolecular attack by the resulting radical on the other olefinic linkage in the molecule, thus effecting cyclization. The reaction continues by the attack of the cyclic radical on another molecule of monomer.

Repetition results in the production of a polymer chain. Phosphorus may be substituted for the nitrogen atom of the quaternary salt and, again, soluble polymers are obtained.^{8,9} It has been demonstrated that the pimelates^{10,11} and methacrylic anhydrides¹² polymerize in the same fashion. On dehydrogenation, the polymers contain, in some cases, phenylene groups,¹² thus supporting the cyclic mechanism. Studies¹³ of the polymerization of allyltrimethylsilane and diallyldimethylsilane showed large differences between the activation energies for polymerization of the two monomers. It is difficult to ascribe the much greater activation energy (50 kcal./mole) of the diallyl compound (against 35 kcal./mole of the monoallyl



compound) to differences in the propagation reaction. With Ziegler catalysts, the diallyl monomer also gives soluble polymers.^{14,15} In the solid state, the polymerization of *N,N*-diallylmelamine¹⁶ also appears to occur by an inter-intramolecular mechanism. That the cyclic mechanism in polymerization is not restricted to dienes is demonstrated by the report¹⁷ of the preparation of linear polyglutaraldehyde. This polymer is believed to have an internal-external ether structure as in the repeating unit:



An earlier investigation in this laboratory¹⁸ demonstrated that 4-chloroperfluoro-1,6-heptadiene also polymerizes readily by a cyclic mechanism, since soluble polymers were obtained whose infrared patterns showed no absorption between 5 and 6 μ . 4-Chloroperfluoro-1,6-heptadiene was prepared, in three steps, from 3,5,7,8-tetrachloroperfluorooctanoic acid. The monomer, a clear liquid boiling at 112°C./759 mm. and with n_D^{27} 1.3311, was telomerized with bromine, chlorine, and dibromodifluoromethane, yielding telomers in each case. The absorption bands in the spectrum of the monomer between 5 and 6 μ , due to double bonds, were absent in the spectra of the products, indicating that, in all likelihood, cyclic telomers had been formed. Elemental analysis supported this conclusion. This diene also reacts to form a brittle polymer at low pressures and radiation doses, and a slightly rubbery material at very high pressures and lower doses of radiation. Infrared studies of films of these polymer samples indicated an absence of carbon-carbon double bonds in the polymer, just as in the telomers.

The work reported here involves the preparation of, and polymerization studies on, perfluoro-1,4-pentadiene. This material was prepared, in three steps, from 3,5,6-trichlorooctafluorohexanoic acid (Kel-F acid 683) obtained from Minnesota Mining and Manufacturing Company. Perfluoro-1,4-

pentadiene is a clear, colorless liquid with a pleasant odor when freshly distilled, but it becomes acid and sometimes cloudy on long standing. It boils at 36°C. and has n_D^{25} 1.2950 (interpolated). It was polymerized and telomerized in the manner described below. Certain by-products were also identified and studied.

EXPERIMENTAL

Preparation of Sodium 3,5,6-Trichlorooctafluorohexanoate

In a 4-liter beaker, 320 g. (8 mol.) of sodium hydroxide was dissolved in 2 liters of water. The solution was vigorously stirred and 2915 g. (8 mol.) of 3,5,6-trichlorooctafluorohexanoic acid was added. The solution became very viscous, but there was no precipitate. Chilling produced no precipitate, so the solution was poured into a clean vacuum desiccator and evaporated to near dryness by using an infrared lamp and an aspirator. The salt became syrupy, buttery, and then waxy, but did not crystallize. The salt was then dried at 10^{-2} mm. (Dry Ice-acetone trap) for three days. Water (500 ml.) was removed, and the wax became a white, crystalline material. Drying was continued for two more days, with removal of water (200 ml.), and the crystals became a fine, apparently amorphous, rather hygroscopic powder.

Pyrolysis of Sodium 3,5,6-Trichlorooctafluorohexanoate

3,5,6-Trichlorooctafluorohexanoate (2.2 kg.) was pyrolyzed under reduced pressure in a stainless-steel tube connected, through adapters, to a series of cooled traps (Dry Ice-acetone and heated to approximately 350°C. in a furnace controlled by two 10-amp., variable transformers. Pyrolysis took place smoothly, yielding 1520 g. of products (theoretical yield, 1600 g.). This was 95% based on the salt. The product was carefully distilled through a 10-in. glass column packed with glass helices. A fraction boiling at 91°C. was collected as the desired product. It amounted to 1360 g. (85%, based on the acid salt).

ANAL. Calcd. for $C_8Cl_3F_8$: C, 21.2%; Cl, 25.1%; F, 53.7%. Found: C, 21.0%; Cl, 24.8%.

In the same distillation, a second fraction was obtained, boiling at 120°C. This amounted to 145 g. (9%, based on the acid salt). The remaining material would not distill at atmospheric pressure, and was assumed to be a coupling product. No further effort was made to characterize it. The 120°C. fraction showed three peaks on a gas-liquid chromatogram, and a deep, split band between 5 and 6 μ in its infrared spectrum. This appeared to be a mixture of the isomers of trichloroheptafluoropentene. This was supported by the elemental analysis and by conversion into a mixture of a three monochloroheptafluoropentadienes.

ANAL. Calcd. for $C_5Cl_3F_7$: C, 20.3%; Cl, 35.2%. Found: C, 20.1%; Cl, 34.9%.

Dechlorination of 4,5-Dichlorooctafluoro-1-pentene

Dechlorination was effected by a slight variation of the method of Park and Lacher.¹⁹ In a beaker, 130 g. (2.0 moles) of powdered zinc was suspended in acetone, and 100 ml. of concentrated hydrochloric acid was added slowly with stirring. Stirring was continued for 30 min. The zinc was filtered off with suction, washed thoroughly with acetone, dried briefly in air, and then overnight in a vacuum oven at 70°C. This activated zinc was placed in a 500-ml., three-necked flask (equipped with an efficient stirrer, a dropping funnel, and a 6-in. glass column packed with glass helices and topped by a still-head) and 200 ml. of bis[2-(2-methoxyethoxy)ethyl] ether was added. Stirring was commenced, and the flask was heated (Thermowell heater) to 70°C. 4,5-Dichlorooctafluoro-1-pentene (284 g., 1 mole) was added in small portions until the reaction started, and then dropwise until addition was complete. Perfluoropentadiene distilled out of the column at about the same rate as the pentene was added. The rate of addition of the pentene and the heat applied to the flask were so controlled that the temperature of the distillate never exceeded 40°C. The yield of crude pentadiene was 194 g. (91%); this was distilled through a 10-in. glass column, packed with glass helices, yielding a pure product, boiling at 36°C., that showed one major peak (and two minor peaks with 1% and 0.3% of the area of the major peak) on an analytical gas-liquid chromatogram. The yield of pure compound was 160 g. (89%). Recovered starting material (34 g.) was recycled. Its infrared spectrum showed a single band at 5.6 μ , the band being somewhat broader and deeper than that of the parent compound. Elemental analysis confirmed the composition of the diene.

ANAL. Calcd. for C_5F_8 : C, 28.3%; F, 71.7%. Found: C, 28.1%; F, 70.9%.

Dechlorination of Trichloroheptafluoropentene Fraction

The dechlorination procedure described for the preparation of perfluoro-1,4-pentadiene was repeated. A 60-g. (0.2 mole) portion of the trichloroheptafluoropentene fraction was added to the flask containing the high-boiling ether and activated zinc. During the dechlorination, the distillate came over below 70°C. The crude yield was 42 g. or 92%. Upon careful distillation at 65°C., 39 g. of a mixture of monochloroheptafluoropentadienes was obtained, which was 85% based on the pentene; 5 g. of starting material was recovered and recycled.

ANAL. Calcd. for C_5ClF_7 : C, 26.3%; Cl, 15.5%; F, 58.2%. Found: C, 26.6%; Cl, 15.2%; F, 58.1%.

Polymerization of Perfluoro-1,4-pentadiene

Perfluoro-1,4-pentadiene (11 g., 0.05 mole) was placed in a glass tube attached to a vacuum line, thoroughly degassed, and the tube sealed. It was maintained at a temperature of 157°C. and subjected to a radiation dose of 0.3 Mrad/hr. from a Co^{60} source for 233.5 hr. The tube was then

opened and the contents, a viscous oil, was poured into xylene. The oil separated from the xylene, becoming more viscous in the process. This oil was vacuum dried to remove as much xylene as possible, dissolved in hexafluorobenzene, and freeze-dried. The yield was 4.5 g. (21% conversion) of a brown, extremely viscous oil that would not distil at 0.1 mm. Some starting material was recovered by carefully distilling the xylene solution.

A series of polymerizations of perfluoro-1,4-pentadiene at 11,300 atm. was carried out by means of a procedure previously described.²⁰ The conditions of these experiments and the data obtained are given in Table I.

TABLE I
Polymerization of Perfluoro-1,4-pentadiene at 110°C. and 11,300 Atm.

Dose rate		Content after reaction, % of original ^a			Type of polymer	Polymer, %
$\times 10^{-3}$, rad/hr.	Dose $\times 10^{-3}$, rad	1,4-Diene	1,3-Diene	Dimer		
0.00	0.00	98	1.1	0.00	Powder	0.12
7.20	14.30	98	1.6	~0.00	Powder	0.01 ^b
0.99	0.99	98	1.5	<0.20	Powder	0.22
2.05	4.10	96	3.2	0.46	Powder	0.34
7.16	14.30	75	6.7	17.00	Rubber	2.17
205.00	490.00	68	6.8	15.00	Rubber	10.30

^a The monomer originally contained 1.1% of 1,3-diene and no dimer.

^b This experiment was performed at autogenous pressure, i.e., about 3 atm.

Reaction of Perfluoro-1,4-pentadiene with Bromine

Perfluoro-1,4-pentadiene (22 g., 0.1 mole) and bromine (32 g., 0.2 mole) were placed in a thick-walled glass tube and thoroughly degassed. Upon warming to the melting point of bromine ($-7.3^{\circ}\text{C}.$), reaction began, with considerable evolution of heat, and was moderated in an ice bath. After 2 hr., the contents of the tube was clear and colorless. The tube was opened, and the liquid removed and shaken with dilute, aqueous sodium bisulfite. Distillation under reduced pressure produced 50 g. of a clear, colorless, oily liquid which boiled at $120^{\circ}\text{C}/30$ mm. (92% based, on the pentadiene).

ANAL. Calcd. for $\text{C}_5\text{Br}_4\text{F}_8$: C, 11.3%; Br, 60.1%; F, 28.3%. Found: C, 11.5%; Br, 59.9%; F, 28.3%.

DISCUSSION

The pyrolysis of the sodium salt of 3,5,6-trichlorooctafluorohexanoic acid produced the expected 4,5-dichlorooctafluoro-1-pentene in 84% yield and, in addition, a by-product collected as a fraction boiling at $120^{\circ}\text{C}.$ Elemental analysis of this material was that of a trichloroheptafluoropentene. On careful chromatography, the substance showed three peaks and is apparently a mixture of isomers. Lovelace²¹ asserts that "in the pyrolysis of

the sodium salts of carboxylic acids which contain fluorine and chlorine in the β position, sodium chloride is preferentially eliminated." It is conceivable, however, that, to some small extent, sodium fluoride is eliminated, and this result may be detected if the reaction is run on a sufficiently large scale, but, in that case only, a single trichloropentene would be produced. The trichloropentene fraction was dehalogenated to a mixture of chloroheptafluoropentadienes, also confirmed by elemental analyses and infrared studies. The isomers were not isolated or further characterized. An explanation for the presence of more than one trichloroheptafluoropentene could involve migration of the double bond due to the presence of fluoride ion or could be due to the presence of impurities in the acid used as starting material. The former explanation is unlikely, because the dichloropentene formed as the major product was about 99% pure. The acid is prepared by telomerizing $\text{CClF}_2\text{CClFI}$ and $\text{CF}_2=\text{CClF}$. Some $\text{CF}_2\text{ICCl}_2\text{F}$ or an occasional head-to-head addition (instead of the usual head-to-tail addition) would yield acid salts which, on pyrolysis and dechlorination, could yield chloropentadienes of various configurations.

The dechlorination of 4,5-dichlorooctafluoro-1-pentene to perfluoro-1,4-pentadiene went smoothly, producing a monomer containing about 1.3% of impurities. The 1% of impurity was identified as the 1,3-diene by boiling point (28°C .) and infrared absorption ($5.8, 5.6 \mu$).²² The 1,3-diene could arise if traces of 4,5-dichlorooctafluoro-2-pentene are formed by a shift of the double bond of the 1-pentene. From the work of Miller et al.,^{22,23} this phenomenon is known to occur in the presence of fluoride ion. Apparently, it is also caused by chloride ion.²⁴ The impurity present to the extent of 0.3% is probably perfluoro-2,3-pentadiene. Gas-liquid chromatography indicated the presence of a compound with a lower retention time and, accordingly, a lower boiling point than the other two compounds present. This is consistent with the findings of Miller et al.²² that migration of the double bond continues toward the center of the molecule. The impurity present would indicate that at least some migration takes place in the dechlorination step.

TABLE II
Unsaturation in Polyperfluoro-1,4-pentadiene Samples

Polymerization conditions			Portion of sample used	Molar ratio	
Temperature, $^\circ\text{C}$.	Pressure $\times 10^{-3}$, atm.	Character of polymer		C_5F_8	C_5F_8
				$\text{CF}_2=\text{CF}-$	$-\text{CF}=\text{CF}$
125	11.5	Rubber	Whole polymer	50	3
125	11	Rubber	1st fraction 31%	210	3
125	11	Rubber	2nd fraction 44%	250	4
125	11	Rubber	3rd fraction 10%	170	5
202	8-10	Liquid	Dimer	35	5
53	11.5	Powder	Whole polymer	10	20
125	11.5	Rubber	Made in C_7F_{16}	20	6

Attempts to prepare a telomer comprising one molecule of bromine and one monomer unit of perfluoro-1,4-pentadiene resulted in 1,2,4,5-tetrabromooctafluoropentane; thus, cyclization did not occur. However, the oily polymer formed under autogenous pressure showed small peaks at 5.6 and 5.8 μ in its infrared spectrum. Calculations made from the magnitude of their absorption coefficients indicated the presence of less than one double bond per monomer unit. The presence of two peaks in this region indicates unsaturation other than that due to vinyl groups, and accordingly, indicates double-bond migration.

At 8000–11,500 atm. and at 53–202°C., various polymer samples were produced. These are shown in Table II. Some were rubbery, but others were powdery or brittle. All showed the same two absorption peaks in the infrared at 5–6 μ . Absorption at 5.6 μ is characteristic of perfluorovinyl groups in the materials under discussion; that at 5.8 μ is characteristic of $-\text{CF}=\text{CF}-$ groups in fluorohydrocarbon molecules.

Calculations of the numbers of both types of double bond were made by using the absorption coefficients of perfluoro-1-heptene and perfluoro-2-butene. The results are given in Table II. The rubbery polymers contain 3–5 monomer units per internal double bond and 20 or more monomer units per perfluorovinyl group. Fractions of the rubbery polymer contained as many as 250 molecules per perfluorovinyl group. A sample of powder contained about 20 monomer units per internal double bond and 10 monomer units per perfluorovinyl group. The monomer recovered from the polymerizations in which rubbery polymer formed contained considerably more perfluoro-1,3-pentadiene than the starting pentadiene. Thus, it is inferred that the internal double bonds in the polymers come from incorporation of 1,3-pentadiene units in the polymer. If such units are present in large enough proportion (20–30% of the monomer units), the copolymer appears rubbery. When only 5% of the polymer consists of 1,3-pentadiene units, the material is glassy at room temperature.

The high ratio of monomer units to perfluorovinyl groups shows that the 1,4-units entering the polymer cyclize between additions of either monomer; otherwise, the ratio would be about 1.2–1.3, if allowance is made for the presence of the 1,3-units. All samples are soluble in hexafluorobenzene, showing that crosslinking has not increased the ratio markedly. The relatively low value of this ratio for the powder probably is due to its lower molecular weight. Powdery samples dissolve much more quickly than the rubbery ones, indicating that different molecular weights are formed.

The quantitative infrared determinations were made on the Perkin-Elmer 221 instrument. Other infrared studies were made on the Perkin-Elmer 137 instrument, sodium chloride optics being used in all cases.

Fluorine nuclear magnetic resonance spectra were obtained in an effort to check the structures postulated. Photographs of the superimposed spectra are shown in Figure 1. From the area under the absorption peaks in the appropriate regions, it is concluded that the rubber contains about three times as many CF_3 groups and one-third as many CF_2 groups as the glass.

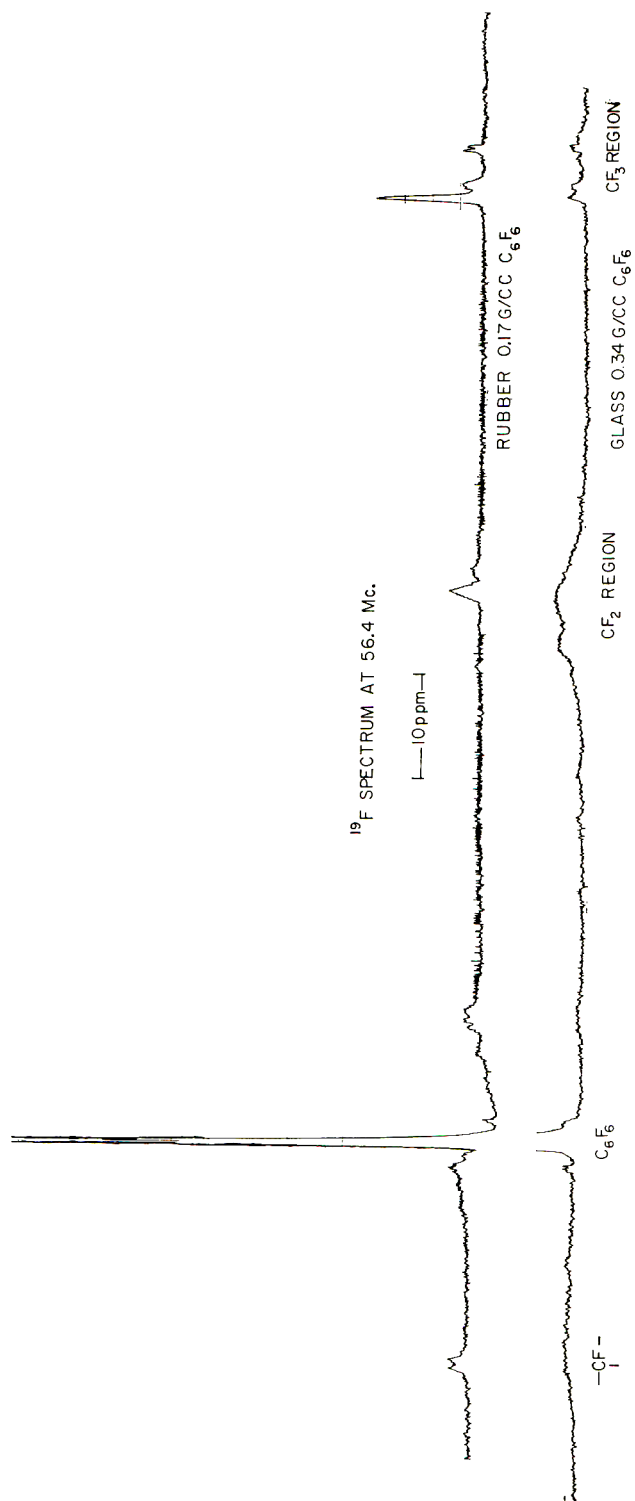
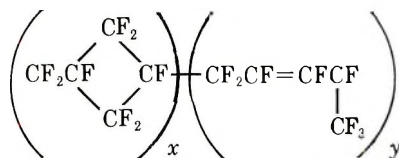


Figure 1.

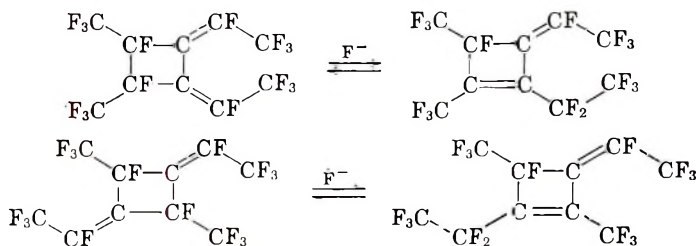
From the infrared absorptions, which are due to internal double bonds, the corresponding ratios were calculated to be 6 and 0.6, respectively. It is felt this constitutes reasonable agreement since a homopolymer of the 1,4-diene would have no CF_3 groups. The presence of multiple peaks due to CF_3 in each spectrum shows that another structure containing this group is present. These may be due to the next monomer unit being one or the other of the dienes or to some 1,2-addition of the 1,3-diene.

Thus, it is believed that the average structure of the polymers can be shown as:



In the powders, $[(x + y)/y]$ is approximately 20; in the rubbers, it is 3–5. The 1,3-units are thought to enter by 1,4-addition, because a sample of polyperfluorobutadiene made at high pressure contains many more internal double bonds than terminal double bonds.

The dimers obtained in these investigations were clear, colorless liquids. They were separated from dissolved or suspended polymer by distillation at $40^\circ\text{C}/5$ mm. Vapor-phase chromatography indicated the presence of at least three, and sometimes four, substances. Elemental analysis of the mixture confirmed the supposed empirical formula, and the boiling points and infrared pattern leave little doubt as to the composition of the material. These data suggest that the dimers obtained have the same structure as those advanced by Miller and co-workers^{22,23} in their work with perfluoro-1,4-pentadiene and cesium fluoride.



The authors acknowledge with gratitude the elemental analyses by Robert J. Hall and are singularly grateful to Dr. Ronald F. Dehl for the nuclear magnetic resonance spectra and for his assistance in their interpretation.

This paper is based on research supported by the Bureau of Naval Weapons, Department of the Navy.

References

1. Butler, G. B., and R. L. Bunch, *J. Am. Chem. Soc.*, **71**, 3120 (1949).
2. Butler, G. B., and F. L. Ingley, *J. Am. Chem. Soc.*, **73**, 895 (1951).
3. Butler, G. B., and R. L. Goette, *J. Am. Chem. Soc.*, **74**, 1939 (1952).
4. Butler, G. B., R. L. Bunch, and F. L. Ingley, *J. Am. Chem. Soc.*, **74**, 2543 (1952).
5. Butler, G. B., and R. J. Angelo, *J. Am. Chem. Soc.*, **78**, 4797 (1956).
6. Butler, G. B., and R. J. Angelo, *J. Am. Chem. Soc.*, **79**, 3128 (1957).

7. Butler, G. B., *J. Polymer Sci.*, **48**, 279 (1960).
8. Berlin, K. D., and G. B. Butler, *J. Am. Chem. Soc.*, **82**, 2712 (1960).
9. Butler, G. B., and K. D. Berlin, *J. Org. Chem.*, **25**, 2006 (1960).
10. Marvel, C. S., and R. D. Vest, *J. Am. Chem. Soc.*, **79**, 5771 (1957).
11. Marvel, C. S., *J. Polymer Sci.*, **48**, 101 (1960).
12. W. E. Gibbs and J. T. Murray, Abstracts of papers presented at the IUPAC Meeting, Montreal, 1960, Number C 31; ASD Technical Report 61-409 (1960).
13. Mikulasova, D., and A. Hrivik, *Chem. Zvesti*, **11**, 641 (1957).
14. Marvel, C. S., and R. G. Woolford, *J. Org. Chem.*, **25**, 1641 (1960).
15. Butler, G. B., and R. W. Stackman, *J. Org. Chem.*, **25**, 1643 (1960).
16. Gibbs, W. E., and R. L. Van Deusen, *J. Polymer Sci.*, **54**, S1 (1961); *Abstracts Papers Am. Chem. Soc. Meeting*, p. 23U (1961).
17. Moyer, W. W., Jr., and D. A. Grev, *J. Polymer Sci.*, **B1**, 29 (1963).
18. Fearn, J. E., and L. A. Wall, *SPE Trans.*, **3**, 231 (1963).
19. Park, J. D., and J. R. Lacher, W.A.D.C. Tech. Rept. 56-590, Part 1, pp. 21-22 (1957).
20. Wall, L. A., D. W. Brown, and R. E. Florin, paper presented to Division of Polymer Chemistry, 140th Meeting, American Chemical Society, Chicago, Illinois, September 1961; *Preprints*, **2**, 366 (1961).
21. Lovelace, A. M., D. A. Rausch, and W. Postelnek, *Aliphatic Fluorine Compounds*, Reinhold, New York, 1958, p. 107.
22. Miller, W. T., W. Frass, and P. R. Resnick, *J. Am. Chem. Soc.*, **83**, 1767 (1961).
23. Miller, W. T., and W. Frass, private communication.
24. Brehm, W. J., K. G. Bremer, H. S. Eleuterio, and R. W. Meschke, U.S. Pat. 2,918,501 (1959).

Résumé

On a préparé le perfluoropentadiène 1-4, par pyrolyse du 3,5,6-trichloroperfluorocaproate de sodium suivie d'une déshalogénéation. La polymérisation du monomère a été opérée dans des conditions variées de température et de pression, l'initiation étant provoquée par des doses variées de rayons γ . Il s'est avéré que ce composé subissait une migration de la double liaison engendrant du perfluoropentadiène 1-3. On admet que les échantillons polymériques, les uns caoutchouteux, les autres granuleux, sont des copolymères des pentadiènes 1-3 et 1-4, le diène 1-4 polymérisant suivant un mécanisme cyclique et le diène 1-3 subissant l'addition 1-4, ce qui est caractéristique des butadiènes dans certaines conditions. Des études infrarouges et de résonance magnétique nucléaire semblent soutenir ces hypothèses. Dans les conditions de polymérisation, le monomère produit aussi quatre dimères distincts et deux substances monomériques à l'état de traces.

Zusammenfassung

Perfluor-1,4-pentadien wurde durch Pyrolyse von Natrium-3,5,6-trichlorperfluorocaproat und darauffolgende Dehalogenierung dargestellt. Das Monomere wurde unter verschiedenen Temperatur- und Druckbedingungen mit γ -Strahlen bei variierter Bestrahlungsdauer und Dosisleistung polymerisiert. Es trat eine Wanderung der Doppelbindung unter Bildung von Perfluor-1,3-pentadien auf. Es wird angenommen, dass die Polymeren, die zum Teil kautschukartig, zum Teil körnig sind, Copolymere aus dem 1,4-Pentadien und dem 1,3-Pentadien sind, wobei das 1,4-Dien nach einem zyklischen Mechanismus polymerisiert, und das 1,3-Dien die für Butadien unter gewissen Bedingungen charakteristische 1,4-Addition eingeht. Infrarot- und kernmagnetische Resonanzuntersuchungen bilden eine Stütze für diese Annahme. Unter Polymerisationsbedingungen entstehen aus den Monomeren auch vier verschiedene Dimere sowie Spuren zweier monomerer Substanzen.

Received May 27, 1965

Revised July 10, 1965

Prod. No. 4807A

Effect of Metal Salts on Polymerization. Part I. Polymerization of Vinylpyridine Initiated with Cupric Acetate

SHIGEO TAZUKE and SEIZO OKAMURA, *Department of Polymer Chemistry, Kyoto University, Kyoto, Japan*

Synopsis

The polymerization of vinylpyridine initiated by cupric acetate has been studied. The rate of polymerization was greatly affected by the nature of the solvent. In general polar solvents increased the rate of polymerization. Polymerization was particularly rapid in water, acetone, and methanol. The initial rate of polymerization of 4-vinylpyridine (4-VP) in a methanol-pyridine mixture at 50°C. is $R_p = 6.95 \times 10^{-6}[\text{Cu}^{11}]^{1/2}[\text{4-VP}]^2$ l./mole-sec. The activation energy of initiation by cupric acetate is 5.4 ± 1.6 kcal./mole. Polymerization of 2-vinylpyridine and 2-methyl-5-vinylpyridine with the same initiator was much slower than that of 4-VP. Dependence of R_p on monomer structure and solvent is discussed. Kinetic and spectroscopic studies led to the conclusion that the polymerization of 4-VP is initiated by one electron transfer from the monomer to cupric acetate in a complex having the structure, $(\text{4-VP})_2\text{Cu}(\text{CH}_3\text{COO})_2$.

INTRODUCTION

The effect of inorganic salts on polymerization may be divided into the following three categories. The first category is retardation or inhibition of radical polymerization by metal salts. This is the most intensively studied field among the effects of metal salts. Retardation of polymerization has been attributed to oxidation or reduction of the growing polymer radical by metal salts. The redox reaction may proceed either by electron transfer¹ or by ligand transfer,² depending upon the redox pair. The second category is acceleration of radical polymerization. This occurs when metal salts interact with the growing active endgroup, without redox reaction taking place. The effect of lithium chloride on radical polymerization of acrylonitrile³ is an example of this category. Another explanation for the accelerating effect of metal salts on polymerization is complex formation of monomer with metal salts affecting the reactivity of monomer. Examples are effect of zinc chloride on the polymerization of acrylonitrile⁴ and methyl methacrylate.⁵ However, the most essential point, why monomer complexes polymerize faster than free monomer, has not yet been elucidated. The formation of a coordination bond between monomer and metal salts will certainly affect the electronic configuration of the whole

molecule, which could bring about spontaneous initiation of polymerization.

The third category involves two possible mechanisms for the initiation of polymerization by metal salts. One is direct activation of ethylenic double bonds by π -type complex formation. The rhodium chloride-initiated polymerization of butadiene⁶ is an example. The other mechanism involves a redox reaction between metal salt and monomer. This mechanism is similar to the well-known redox initiator system, i.e., peroxide-ferrous salt, with the difference that the monomer is an integral part of the initiator. Examples have not been presented until recently.⁷

The present authors have reported that cupric acetate could initiate radical polymerization when the salt is complex with 4-vinylpyridine (4-VP).⁸ The present publication represents a detailed study on the nature of polymerization of vinylpyridine initiated by cupric salts.

EXPERIMENTAL

Materials

4-Vinylpyridine (4-VP) and 2-vinylpyridine (2-VP) (Yuki Gosei Kogyo Co., Ltd.) and 2-methyl-5-vinylpyridine (MVP) (Tokyo Kasei Kogyo Co., Ltd.) were refluxed over potassium hydroxide pellets and distilled in a stream of nitrogen under reduced pressure at 6 mm. Hg.

Cupric acetate monohydrate (G.R. grade) was used without further purification.

All solvents used for polymerization were purified by accepted procedures.

Shrinkage Factors

Shrinkage factors used for rate measurements were determined from the density difference between the monomer and the polymer in the temperature range of 50–70°C. The densities of monomer and monomer solution containing a known amount of polyvinylpyridine were measured by a pycnometer at different temperatures. Shrinkage factors thus calculated were averaged graphically by plotting the shrinkage factors against temperature. The values are shown in Table I.

Shrinkage factors at temperatures other than those given in Table I were estimated by interpolation or extrapolation.

TABLE I
Shrinkage Factors of Vinylpyridines

Monomer	Volume contraction at 100% conversion to polymer, %		
	50.0°C.	60.0°C.	70.0°C.
4-Vinylpyridine (4-VP)	18.9	19.4	19.9
2-Methyl-5-vinylpyridine (MVP)	18.8	19.2	19.6
2-Vinylpyridine (2-VP)	18.5	19.1	20.0

Polymerization

A solution containing the metal salt and the monomer was degassed by repeated freezing and thawing at reduced pressure of 10^{-3} mm. Hg. The degassed solution was then transferred into a dilatometer (capacity: 5 ml.) equipped with a capillary of 0.5 or 1.0 mm. diameter. Polymerization was followed dilatometrically. The polymerization mixture was precipitated by pouring it into a large excess of petroleum ether. The polymer was dissolved in 5% sulfuric acid and reprecipitated by pouring it into a large amount of dilute ammonia solution containing ammonium chloride. Metal salts incorporated in the polymer were thoroughly removed by this procedure.

Kinetic measurements were always carried out at less than 5% conversion.

Electronic Absorption Spectra

Electronic absorption spectra were measured by Hitachi automatic recording spectrophotometer using a cell having an optical length of 1 cm.

Molecular Weight of Poly 4-vinylpyridine

Molecular weights of poly 4-vinylpyridine were determined by viscosity measurements at 25°C. in pyridine solution by using the equation:⁹

$$[\eta] = 3.055 \times 10^{-5} M^{1.26}$$

RESULTS

Effect of Solvent on the Rate of Polymerization of 4-VP Initiated by Cupric Acetate

The dependence of rate of polymerization on solvent is shown in Table II.

TABLE II
Solution Polymerization of 4-VP Initiated by Cupric Acetate Monohydrate at 50°C.^a

Solvent	$R_p \times 10^5$, mole/l.-sec.	Dielectric constant of solvent at 25°C.
Bulk polymerization	3.29	~12
Pyridine	0.715	12.3
Acetone	15.9	20.7
Methanol	15.5	32.6
Ethanol	2.76	24.3
<i>n</i> -Butanol	0.503	17.1
Dimethylformamide	1.06	
Benzene	0.0	2.3
Ethylene chloride	~0	10.4

^a $[\text{Cu}^{II}] = 1.0 \times 10^{-2}$ mole/l.; 4-VP/solvent = 1/1 by volume.

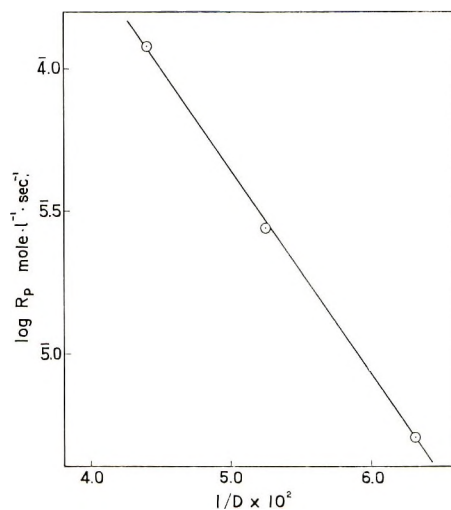


Fig. 1. Plot of $\log R_p$ vs. reciprocal of dielectric constant D . R_p measured for the system, 4-VP/alcohol = 1/1 by volume at 50°C.; D = arithmetic average of the dielectric constants for the alcohols and pyridine ($D_{\text{pyridine}} \approx D_{4\text{VP}}$ is assumed).

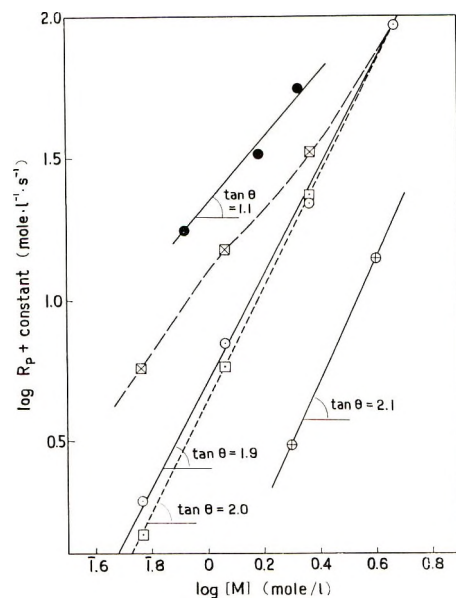


Fig. 2. Dependence of the rate of polymerization on monomer concentration in various media with cupric acetate as an initiator: (●) in 30% aqueous methanol at 30°C., $[\text{Cu}^{\text{II}}] = 9.09 \times 10^{-2}$ mole/l.; (○) in methanol, (4-VP + pyridine)/methanol, $[\text{Cu}^{\text{II}}] = 1.0 \times 10^{-2}$ mole/l. at 50°C.; (⊕) in pyridine, $[\text{Cu}^{\text{II}}] = 1.0 \times 10^{-2}$ mole/l. at 50°C.; (⊕) $[\text{Cu}^{\text{II}}(4\text{VP})_2]$ assumed as initiator; (⊗) $[\text{Cu}^{\text{II}}(4\text{VP})_2]$ and $[\text{Cu}^{\text{II}}(4\text{VP})(\text{Py})]$ are assumed as initiators.

The rate of polymerization R_p could not be determined in water because the reaction is too fast and the system is heterogeneous. Although polar solvents seem to increase the rate of polymerization, the dielectric constant D alone is not rate-determining since, for example, the polymerization is faster in acetone ($D = 20.7$) than in methanol ($D = 32.6$) or in ethanol ($D = 24.3$). However, for any series of alcohols, the rate of polymerization increases with the dielectric constant of the solvent. Figure 1 shows the plot of $\log R_p$ vs. reciprocal dielectric constant of the system. A straight line was obtained, indicating the importance of polar effect.

Dependence of R_p on Monomer Concentration

Dependence of R_p on monomer concentration in various solvent systems is shown in Figure 2. The slopes in Figure 2 are 1.2 for the 4-VP-30% aqueous methanol system, 1.9 for the 4-VP-pyridine system, and 2.1 for the methanol-pyridine-4-VP system [(4VP + pyridine)/methanol = 1/1 by volume].

Dependence of R_p on Cupric Acetate Concentration

Dependence of R_p on cupric acetate concentration is shown in Figure 3. The rates of polymerizations in methanol and in 30% aqueous methanol are nearly proportional to the square root of the cupric salt concentration. This finding suggests that the cupric salt behaves just like an ordinary radical initiator and that termination of growing polymer radicals is by bimolecular recombination.

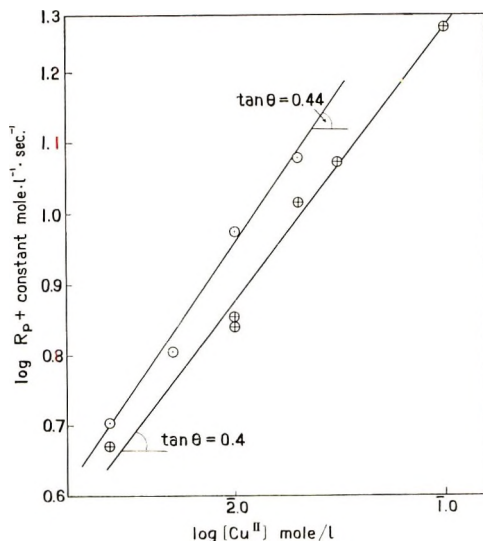


Fig. 3. Dependence of R_p on cupric acetate concentration: (O) [4-VP] = 4.67 mole/l. in methanol at 50°C.; (⊕) [4-VP] = 0.87 mole/l. in 30% aqueous methanol at 30°C.

Dependence of Molecular Weight of Poly-4-VP on Monomer and Cupric Acetate Concentration

Figure 4 shows plots of viscosity-average molecular weights versus monomer and initiator concentrations. Molecular weights are proportional to monomer concentration and almost independent of initiator concentration. This could be explained by assuming that the chain length of the polymer is determined by solvent chain transfer and the cupric salt does not take part in the termination step.

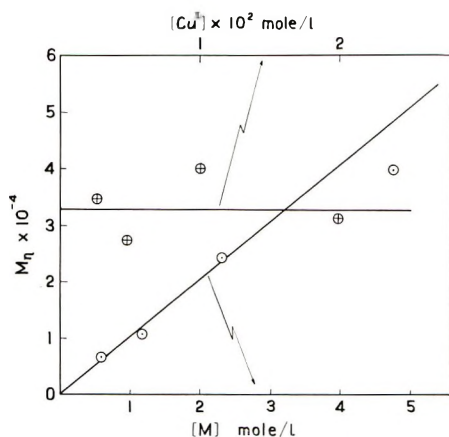


Fig. 4. Dependence of molecular weight of polymer on monomer and cupric acetate concentrations in polymerization at 50°C.: (○) M_n vs. [4VP], $[Cu^{II}] = 1.0 \times 10^{-2}$ mole/l.; (⊕) M_n vs. $[Cu^{II}]$, [4VP] = 4.67 mole/l.

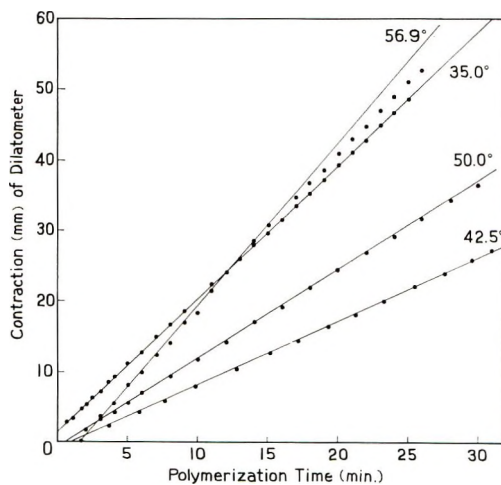


Fig. 5. Dilatometric measurements of time-conversion curves for the polymerization of 4-vinylpyridine initiated by cupric acetate at different temperatures. [4VP] = 4.67 mole/l., $[Cu^{II}] = 1.0 \times 10^{-2}$ mole/l. in methanol. (Sizes of dilatometers are not the same.)

Dependence of R_p on Temperature

Since the dead-end nature of the 4-VP polymerization has been observed, R_p was measured at relatively low temperatures. Typical time-conversion curves are shown in Figure 5. Deviation from linearity is observed for the run at 56.9°C. This deviation cannot be due to a decrease in monomer concentration during rate measurement, since the conversion is less than 5% when the deviation occurs.

Figure 6 shows Arrhenius plots of initial rates obtained with cupric acetate and azobisisobutyronitrile catalysts. The overall activation energies for cupric acetate- and AIBN-initiated polymerization of 4-VP are 14.3 ± 0.3 and 26.9 ± 0.5 kcal./mole, respectively.

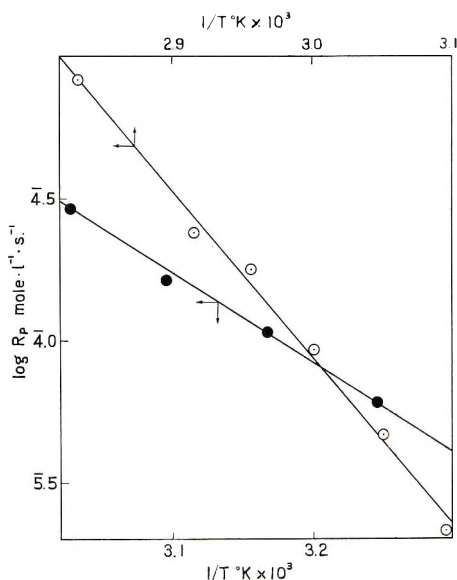


Fig. 6. Arrhenius plots of polymerization of 4-vinylpyridine: (●) initiated by cupric acetate; (○) initiated by azobisisobutyronitrile. Solvent: methanol; [4-VP] = 4.67 mole/l.; [Cu^{II}] = 1.0×10^{-2} mole/l.; [AIBN] = 4.9×10^{-3} mole/l.

Comparison of Cupric Acetate-Initiated Polymerization of 4-VP, 2-VP, and MVP

2-VP and MVP can also be polymerized by cupric acetate. Values of R_p measured at different temperatures are shown in Table III.

The remarkable difference in R_p in the polymerization of 4-VP, MVP, and 2-VP could be attributed to different rates of initiation, since the rates of polymerizations of these three vinylpyridines are about equal with azobisisobutyronitrile initiator.

Accurate measurement of R_p for 2-VP is difficult. As will be mentioned in the following section, the fast reduction of cupric to cuprous species by 2-VP hinders rate measurement. Initiator efficiency of cupric acetate-

TABLE III
Rate of Polymerization of 4-VP, MVP, and 2-VP Initiated by Cupric Acetate^a

Polymerization temperature, °C.	R_p , mole/l.-sec.		
	4-VP	MVP	2-VP
35.0	0.603×10^{-4}		
42.5	1.07×10^{-4}		
50.0	1.55×10^{-4}	0.334×10^{-4}	} $< 10^{-5}$
55.0		0.556×10^{-4}	
56.9	2.92×10^{-4}		
60.0		0.760×10^{-4}	
65.0		1.11×10^{-4}	
70.0		1.21×10^{-4}	
80.0			

^a Monomer/methanol = 1/1 by volume; $[Cu^{II}] = 1.0 \times 10^{-2}$ mole/l.

initiated polymerization of 2-VP seems to be much smaller than that of MVP or 4-VP. Although R_p of 2-VP is quite small, initiation by cupric acetate is obvious, since the rate of thermal polymerization of 2-VP under the same conditions is less than 5×10^{-7} mole/l.-sec. at 80°C.

Electronic Spectra of the Vinylpyridine-Cupric Acetate System

Complex formation between the pyridine ring and metal salts has often been studied.^{10,11a} However, vinylpyridine complexes have not yet been

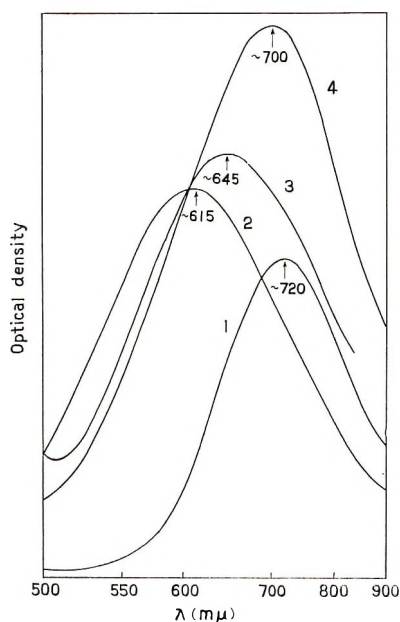


Fig. 7. Electronic absorption spectra of cupric acetate in mixture of vinylpyridine and methanol (1/1 by volume), arbitrary concentration: (1) blank (cupric acetate in methanol); (2) MVP/methanol; (3) 4-VP/methanol; (4) 2-VP/methanol.

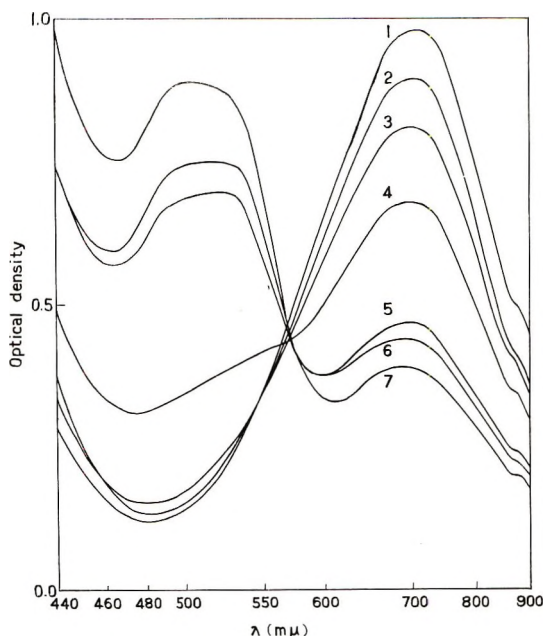


Fig. 8. Visible absorption spectra of 2-vinylpyridine-methanol-cupric acetate system: (1) before reaction; (2) after reaction *in vacuo* at 50°C. for 160 min.; (3) after reaction *in vacuo* at 55°C. for 160 min.; (4) after reaction *in vacuo* at 65°C. for 160 min.; (5) after reaction *in vacuo* at 80°C. for 93 min.; (6) after reaction *in vacuo* at 70°C. for 160 min.; (7) after reaction *in vacuo* at 80°C. for 160 min. 2-VP/methanol = 1/1 by volume; $[Cu^{II}] = 1.0 \times 10^{-2}$ mole/l.

studied. Figure 7 shows complex formation between vinylpyridines and cupric acetate in methanol.

The absorptions due to vinylpyridine-cupric acetate complexes decrease with polymerization time. Among the three vinylpyridine complexes, the MVP complex is the most stable, and the spectrum shows only a slight decrease at its maximum after 150 min. of polymerization at 65°C. In contrast, the bright green-blue color of 4-VP and 2-VP complexes changes to dark brown through brownish green, and the spectra also change. Figure 8 shows the absorption spectra of the 2-VP-cupric acetate system before and after polymerization. An absorption at 700 $m\mu$ decreases with reaction time, and the rate is faster at elevated temperatures. A new broad peak at 490–530 $m\mu$, probably due to oxidation of 2-VP by cupric acetate, increases in intensity with reaction time and with reaction temperature. The fact that the optical density-wavelength curves cross at a point near 570 $m\mu$ may indicate that a stoichiometric relationship exists between the concentration of species having an absorption at 490–530 $m\mu$ and the decreased concentration of 2-VP-cupric acetate complex.

It has been found that the 2-VP-cupric acetate system after polymerization is readily oxidized by air when the reaction mixture is exposed to the atmosphere. Figure 9 shows the change in the spectrum due to oxidation

by air. Reproduction of cupric species is evident on comparing curve 2 with curve 3, and curve 4 with curves 5 and 6. On the other hand, the intensity of the broad peak at 490–530 $m\mu$ does not decrease. If cuprous species were responsible for the broad absorption, increased intensity at

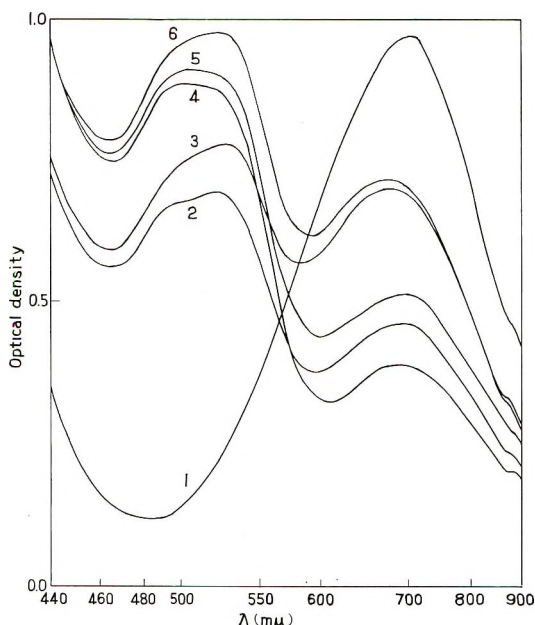


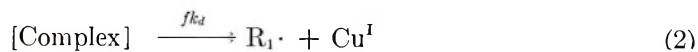
Fig. 9. Change in visible absorption spectra of 2-vinylpyridine-methanol-cupric acetate system when the reaction mixture is exposed to air: (1) before reaction; (2) after reaction *in vacuo* at 80°C. for 93 min.; (3) 2 exposed to air at room temperature for 25 min.; (4) after reaction *in vacuo* at 80°C. for 160 min.; (5) 4 exposed to air at room temperature for 10 min.; (6) 4 exposed to air at room temperature for 30 min. 2VP/methanol = 1/1 by volume; $[Cu^{II}]_0 = 1.0 \times 10^{-2}$ mole/l.

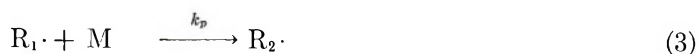
700 $m\mu$ would result in a decreased intensity of the broad peak. Optical density-wavelength curves in Figure 9 do not cross each other, indicating that the species responsible for the two absorptions are not convertible.

DISCUSSION

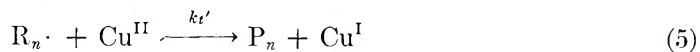
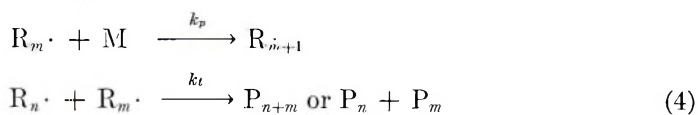
Kinetics

The reactions considered are shown in eq. (1)–(6).





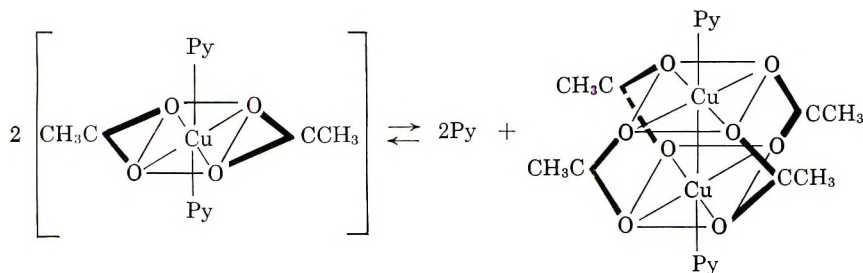
⋮
⋮
⋮



Possibility of competition between reactions (4) and (5) is unlikely, since R_p is proportional to $[\text{Cu}^{\text{II}}]^{1/2}$. Considering therefore eq. (4) as representing the termination process, the kinetic equation, eq. (7) is derived from stationary kinetic treatment.

$$R_p = f^{1/2} k_d^{1/2} k_p k_t^{-1/2} [\text{complex}]^{1/2} [\text{M}] \quad (7)$$

The fact that R_p is proportional to $[\text{Cu}^{\text{II}}]^{1/2}$ indicates that the complex should be mononuclear. Two forms of complexes between cupric acetate and pyridine have been discussed.¹²⁻¹⁴ One is a distorted octahedral mononuclear complex $\text{Cu}(\text{CH}_3\text{COO})_2\text{Py}_2$ (I) and the other is a binuclear one (II).



Complex I is favored in polar solvent. Formation of the mononuclear complex in water and of the binuclear complex in ethanol and dioxane has been suggested on the basis of electronic spectra of pyridine-cupric carboxylate complex.¹⁴ Though no published data are available for vinylpyridine complexes, a crystalline complex of 4-VP with cupric acetate was isolated from a saturated methanol solution of the salt added with 4-VP, of which analytical data agree with the mononuclear complex [Calculated value of Cu content for $\text{Cu}(\text{CH}_3\text{-COO})_2(4\text{VP})_2$: 16.2%; found: 16.2%]. Together with the kinetic data, this indicates that cupric acetate exists as a mononuclear complex in the 4-VP-methanol mixture.

The solvent affects the dependence of R_p on monomer concentration. When the polymerization proceeds in pyridine or in pyridine-methanol

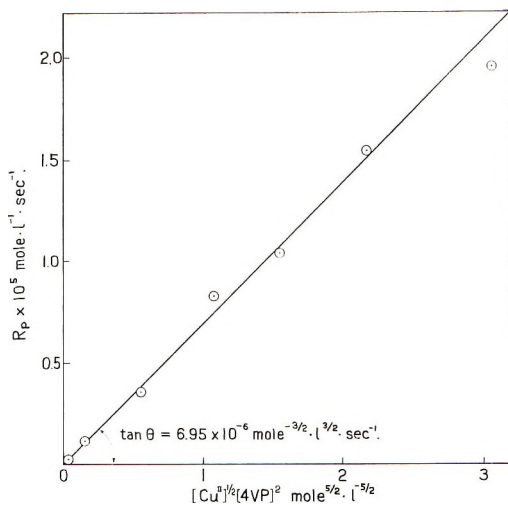


Fig. 10. Linear relationship between R_p and $[\text{Cu}^{\text{II}}]^{1/2}[4\text{-VP}]^2$ for the polymerization of 4-vinylpyridine initiated by cupric acetate at 50°C . (4-VP + pyridine)/methanol = 1/1 by volume.

mixture [(4-VP + Py)/methanol = constant] R_p is nearly proportional to $[4\text{-VP}]^2$. Since the stability constant of pyridine-cupric ion complex is large ($\log \beta_2 = 4.33$ in water at 25°C .¹¹ where β_2 is the overall stability constant of $\text{Cu}^{\text{II}}\text{Py}_2$) and the stability constant is rather insensitive to substituents introduced to the pyridine ring,^{11b} cupric acetate may be assumed to be completely in the complex form. Consequently, the stability constant of the 4-VP-cupric acetate complex could be assumed to be reasonably close to the value given for the pyridine complex.

In a mixture of 4VP and pyridine, cupric species will exist as $[\text{Cu}^{\text{II}}(4\text{-VP})_2]$, $[\text{Cu}^{\text{II}}(\text{Py})(4\text{-VP})]$, and $[\text{Cu}^{\text{II}}(\text{Py})_2]$. Assuming the same stability for these three species, the fraction of $[\text{Cu}^{\text{II}}(4\text{-VP})_2]$ is given by eq. (8).

$$\frac{\beta_2[\text{Cu}^{\text{II}}][4\text{-VP}]^2}{\beta_2[\text{Cu}^{\text{II}}][4\text{-VP}]^2 + 2\beta_2[\text{Cu}^{\text{II}}][4\text{-VP}][\text{Py}] + \beta_2[\text{Cu}^{\text{II}}][\text{Py}]^2} = \frac{[4\text{-VP}]^2}{([4\text{-VP}] + [\text{Py}])^2} \quad (8)$$

If $\text{Cu}(\text{CH}_3\text{COO})_2(4\text{-VP})_2$ alone is involved in initiation, R_p can be expressed by eq. (9), which is in agreement with the experimental results.

$$R_p = K[\text{Cu}^{\text{II}}]^{1/2}[\text{M}]^2 \quad (9)$$

Figure 2 shows the dependence of R_p on monomer concentration calculated by assuming that $\text{Cu}(\text{CH}_3\text{COO})_2(4\text{-VP})(\text{Py})$ is also an initiating species. This does not agree with the results.

Validity of the rate expression, eq. (9), is shown in Figure 10.

The monomer concentration dependence of R_p is nearly unity in 30% aqueous methanol. In this case, the concentration of the complex is almost equal to total cupric acetate, since β_2 is very much larger than unity and 4-VP is added in large excess of cupric acetate. Consequently, the initiator concentration is independent of 4-VP and the rate is expressed by eq. (10).

$$R_p = K'[\text{Cu}(\text{CH}_3\text{COO})_2]^{1/2}[\text{M}] \quad [10]$$

An unusual monomer exponent as in eq. (9) has been observed also in the polymerization of methyl methacrylate initiated by ethylsilver.¹⁵ The rate of polymerization is proportional to $[\text{M}]^{1/2}[\text{Ag}]^{1/2}$, and complex formation between the monomer and the initiator has been suggested.

On the other hand, silver nitrate-initiated polymerization of acrylonitrile¹⁶ follows $R_p = [\text{AgNO}_3]^{1/2}[\text{M}]$. No evidence of complex formation between the monomer and silver nitrate has been obtained either by electronic or infrared spectroscopy. Both examples are thought to be radical polymerizations, but the mechanism of initiation would depend largely on the combination between metal compound and monomer.

Effect of Solvent

In general, the solvents listed in Table II are unlikely to affect strongly the rate of radical polymerization. The polymerization is faster in alcohols having large chain transfer constants than in bulk, and it does not proceed in benzene at all which is a good solvent for radical polymerization. These solvent effects are therefore due to changes in the initiation process.

Among other things the solvent may effect coordination and polarity. Coordination depends on the individual system and cannot be treated quantitatively, polarity may be estimated by the dielectric constant. The solvent effect in Table II represents the combination of these two influences, and a unified explanation cannot be given at the present time. The solvent effect of a series of monofunctional alcohols could be studied by the polar effect as shown in Figure 1. This relation has been derived by Laidler and Landskroener¹⁷ and is applicable to reactions when electrostatic interaction is more important than nonelectrostatic interaction, i.e., ion-ion, ion-dipole, or dipole-dipole reactions. Since propagation and termination processes will be independent of polar effect, the origin of the solvent effect is probably due to monomer-metal salt interactions.

Spectroscopic evidence for the reduction of cupric species indicates that the oxidation of 4-VP by cupric acetate through coordination is important during initiation. For example, Laidler's equation can be applied to the redox reaction between an organic compound and a metal ion such as the reaction of 2,2'-diphenyl-1-picrylhydrazyl (DPPH) with reducing metal ions in aqueous methanol.¹⁸

Mechanism of Initiation

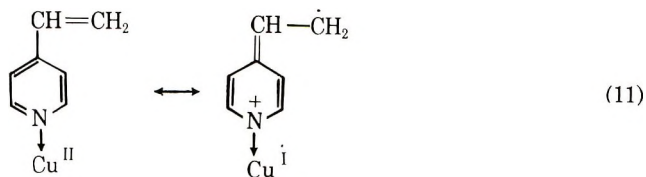
The above results and considerations might indicate that polymerization initiation occurs by the spontaneous (unimolecular) decomposition of 4-

VP-cupric acetate complex involving the reduction of cupric to cuprous species. There is no doubt that the polymerization proceeds by radical mechanism. Therefore the problem is the manner of radical formation by oxidative decomposition of the complex.

Two mechanisms have been proposed to elucidate the redox reaction, particularly in connection with isotope exchange reactions. One mechanism involves electron transfer mechanism and the other material transfer. Characteristics of the former mechanism¹⁹ are small activation energies and a small frequency factor. True electron transfer is thought to proceed with little interaction between reactants, and the requirement for configurational rearrangement for the formation of activated complexes is small. Since the distances are large, the probability for electron transfer will be small. However, some electron transfer reactions require the close approach of reactants and the formation of compact activated complexes; then the energy requirement for electron transfer may be as large as for material transfer. Consequently a small activation energy is good evidence for an electron transfer mechanism, but the converse is not true.

The activation energy of initiation by cupric acetate ($E_i^{\text{Cu}^{II}}$) can be calculated from the Arrhenius plot in Figure 6. From the kinetics of this polymerization the total activation energy of 14.3 ± 0.3 kcal./mole for 4VP is known to correspond to $1/2 E_i^{\text{Cu}^{II}} + E_p - 1/2 E_t$. When azobisisobutyronitrile is used as initiator, the total activation energy, $1/2 E_i^{\text{AIBN}} + E_p - 1/2 E_t$, is 26.9 ± 0.5 kcal./mole. Since the activation energy for thermal decomposition of AIBN is 31.3 kcal./mole,²⁰ $E_i^{\text{Cu}^{II}}$ becomes 5.4 ± 1.6 kcal./mole. This is a very small activation energy for initiation and may be an indication for electron transfer mechanism.

Another factor in favor of electron transfer mechanism is the close correlation between polymerizability and conjugation from nitrogen to vinyl group of the monomer. 4-VP will assume resonance structures during electron transfer such as those shown in eq. (11). A similar structure is not expected for MVP. Conductivity of ligand is certainly larger for 4-VP than for MVP, and this is reflected in the polymerizabilities of 4-VP



and MVP. The slow rate of a polymerization initiation of MVP may be attributed to the absence of suitable conjugation through which an electron can migrate from the vinyl group to the cupric salt.

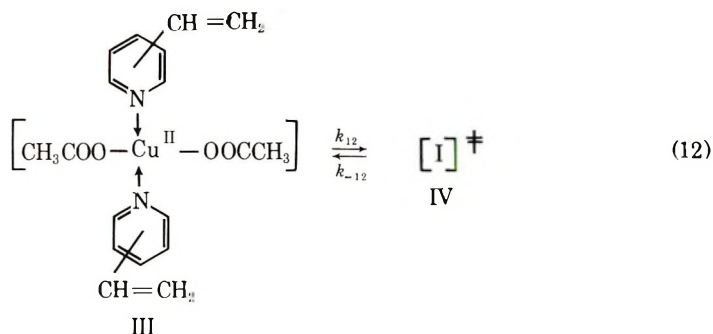
The behavior of 2-VP derivatives are complicated by steric effects. Ease of electron transfer from the vinyl group of 2-VP to cupric acetate through nitrogen is comparable to that with 4-VP. In fact, reduction of

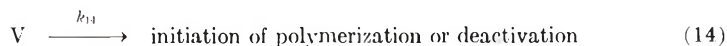
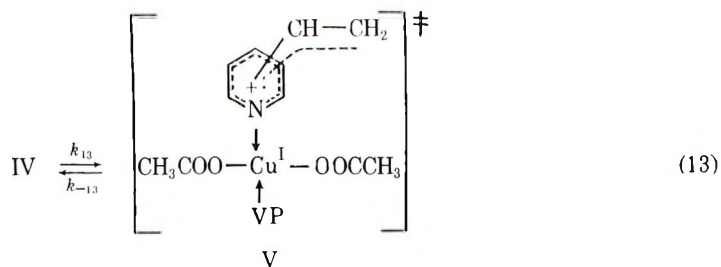
cupric to cuprous species by 2-VP is faster than by MVP. However, polymerization initiation seems to be a different matter. The slow initiation, even slower than with MVP, could be explained by steric interference of cupric acetate coordinated to the nitrogen atom adjacent to the vinyl group. The vinyl group of 2-VP will therefore be out of the plane of the conjugated pyridine ring, and the active intermediate may be unstable so that it will be unable to initiate polymerization. The problem of initiator efficiency will be discussed elsewhere, together with the dead-end nature of the polymerization.

These effects of monomer structure of R_p could not be reconciled with a material transfer mechanism.

Several reports support the above explanation. The double-bond character of coordination bonds between nitrogen and metal ion has been mentioned for metal-pyridine complexes.²¹ A good example of electron transfer through the pyridine ring was investigated by Taube and Gould.²² These authors demonstrated the reduction of pyridine carboxylate pentaamminecobalt (III) with Cr(II) to proceed via acidic and basic mechanisms. While the former mechanism involves $\text{Co}^{\text{III}}\text{-LH}$, where LH indicates the acid form of pyridinecarboxylate, in the second mechanism the conjugate base, $\text{Co}^{\text{III}}\text{-L}^-$, is the reacting species. Cr(II) coordinates to the nitrogen of the pyridine ring in the basic path and the rate of electron transfer is determined by the conductivity between carboxylate and the nitrogen. Therefore this basic path prevails in pyridine-2-carboxylate and pyridine-4-carboxylate complexes, but not in the 3-isomer. These results are good evidence for electron transfer through conjugated ligands. The importance of conjugated ligands during electron transfer was also discussed in connection with the oxidation of polyacrylamide radical by Fe^{III} complexed with bidentate nitrogen containing heterocyclic compounds.¹ The reaction was explained by assuming that an electron released from the radical is transferred through conjugated heterocyclic ligands. The rate of electron transfer was found to increase with increasing conjugation of the ligand.

According to Marcus's view²⁵ on the theory of electron transfer reaction, the present redox initiation system may be visualized as shown in eq. (12).





IV and V are in an energy-matched state which allows an electron to be transferred without conformational change in both IV and V. Building-up of IV from III requires energy. Since IV should have conformation intermediate between III and the inactivated form of V in which the $\text{Cu}^{\text{I}}-\text{N}$ bond is thought to be very much weakened, the $\text{Cu}^{\text{II}}-\text{N}$ bond in IV would be partially dissociated or stretched. The dielectric constant of the system would therefore affect reaction (12). The stabilization of pyridine complexes in less polar solvents has been reported^{11a} and this is certainly disadvantageous for the formation of IV also.

CONCLUSION

Cupric acetate acts as an oxidant of the one-electron transfer type in combination with vinylpyridine. This mechanism requires the formation of radical-cations as intermediates of polymerization initiation. It is theoretically possible to initiate both radical and cationic polymerizations by a radical-cation. However, the inertness of vinylpyridine toward cationic initiation might be the reason that a radical mechanism is preferred to a cationic mechanism. Evidence indicating cationic mechanism has been obtained for the polymerization of N-vinylcarbazole with cupric salts.²⁴

It is possible to envision that simple redox systems could function as cationic and/or free-radical initiators depending on the nature of the monomer and perhaps reaction conditions. These initiator systems are amphoteric initiators.

References

1. Collinson, E., F. S. Dainton, B. Mile, S. Tazuke, and D. R. Smith, *Nature*, **198**, 26 (1963).
2. Bamford, C. H., A. Jenkins, and R. Johnston, *Proc. Roy. Soc. (London)*, **A239**, 214 (1957).
3. Bamford, C. H., A. D. Jenkins, and R. Johnston, *Proc. Roy. Soc. (London)*, **A241**, 364 (1957).
4. Imoto, M., T. Otsu, and M. Nakabayashi, *Makromol. Chem.*, **65**, 194 (1963).

5. Imoto, M., T. Otsu, and Y. Harada, *Makromol. Chem.*, **65**, 180 (1964).
6. Rinehart, R. E., H. P. Smith, H. S. Witt, and H. Romeyn, Jr., *J. Am. Chem. Soc.*, **83**, 4864 (1961); *ibid.*, **84**, 4145 (1962).
7. Wang, Chi-Hua, *Chem. Ind. (London)*, **1964**, 751.
8. Tazuke, S., and S. Okamura, *J. Polymer Sci.*, **B3**, 135 (1965).
9. Onyon, P. I., *Trans. Faraday Soc.*, **51**, 400 (1955).
10. *Stability Constants*, Special Publication, Chemical Society, London, No. 6, part I, 1957, p. 28.
11. *Stability Constants*, Special Publication, Chemical Society, London, No. 17, 1964, (a) p. 440; (b) pp. 475-476.
12. Hanic, F., D. Stempelova, and K. Hanicova, *Chem. Zvesti.*, **15**, 102 (1961).
13. Kato, M., H. B. Jonassen, and J. C. Fanning, *Chem. Revs.*, **64**, 99 (1964).
14. Tonnet, M. L., S. Yamada, and I. G. Ross, *Trans. Faraday Soc.*, **60**, 840 (1964).
15. Bawn, C. E. H., W. H. James, and A. M. North, *J. Polymer Sci.*, **58**, 335 (1962).
16. Schnecko, H. W., *Makromol. Chem.*, **66**, 19 (1963).
17. Laidler, K. T., and P. A. Landskroener, *Trans. Faraday Soc.*, **52**, 200 (1956).
18. Bawn, C. E. H., and D. Verdin, *Trans. Faraday Soc.*, **56**, 519 (1960).
19. Marcus, R. J., B. J. Zwolinski, and H. Eyring, *J. Phys. Chem.*, **58**, 432 (1959).
20. Walling, C., *Free Radicals in Solution*, Wiley, New York, 1957, p. 513.
21. Sacconi, L., G. Lombardo, and P. Paoletti, *J. Chem. Soc.*, **1958**, 848.
22. Gould, E. S., and H. Taube, *J. Am. Chem. Soc.*, **86**, 1318 (1964).
23. Marcus, R. A., *J. Chem. Phys.*, **24**, 996 (1956); *ibid.*, **26**, 867 (1956).
24. Tazuke, S., K. Nakagawa, and S. Okamura, *J. Polymer Sci.*, **B3**, 923 (1965).

Résumé

On a étudié l'initiation de la polymérisation de la vinylpyridine par l'acétate cuivrique comme catalyseur. La vitesse de polymérisation dépend fortement de la nature du solvant. Les solvants polaires accroissent en général, la vitesse de polymérisation, la polymérisation étant particulièrement rapide dans l'eau, l'acétone et le méthanol. La vitesse initiale de polymérisation de la 4-vinylpyridine (4-VP) dans un mélange méthanol-pyridine à 50°C est donnée par: $R_p = 6.95 \times 10^{-6} [\text{Cu}^{11}]^{1/2} [4\text{-VP}]^2 / \text{mole}/\text{sec}$. L'énergie d'activation de l'initiation par l'acétate cuivrique est de $5,4 \pm 1,6$ Kcal/mole. La polymérisation de la 2-vinylpyridine et de la 2-méthyl-5-vinylpyridine avec le même initiateur étaient plus lentes que celle de la 4-VP. On discute de la relation qui existe entre la structure du monomère et la nature du solvant d'une part et la vitesse de polymérisation d'autre part. La cinétique et des études spectroscopiques permettent de conclure que la polymérisation de la 4-VP est initiée par un transfert monoélectronique du monomère à l'acétate de cuivre formant un complexe de structure $(4\text{-VP})_2\text{Cu}(\text{CH}_3\text{COO})_2$.

Zusammenfassung

Die Polymerisationsanregung von Vinylpyridin mit Kupferacetat als Katalysator wurde untersucht. Die Polymerisationsgeschwindigkeit wurde stark durch die Natur des Lösungsmittels beeinflusst. Im allgemeinen steigerten polare Lösungsmittel die Polymerisationsgeschwindigkeit. Die Polymerisation war besonders rasch in Wasser, Aceton und Methanol. Die Anfangsgeschwindigkeit der Polymerisation von 4-Vinylpyridin (4-VP) in einer Methanol-Pyridinmischung bei 50°C ist $R_p = 6,95 \cdot 10^{-6} [\text{Cu}^{11}]^{1/2} [4\text{VP}]^2$ l/Mol.-sec. Die Aktivierungsenergie der Anregung durch Kupferacetat beträgt $5,4 \pm 1,6$ kcal/Mol. Die Polymerisation von 2-Vinylpyridin und 2-Methyl-5-vinylpyridin mit dem gleichen Starter war viel langsamer als diejenige von 4-VP. Die Abhängigkeit von R_p von der Monomerstruktur und vom Lösungsmittel wird diskutiert. Kinetische und spektroskopische Untersuchungen führen zu dem Schluss, dass die Polymerisation von 4-VP durch einen Enelektronenübergang vom Monomeren zum Kupferacetat in einem Komplex mit der Struktur $(4\text{VP})_2\text{Cu}(\text{CH}_3\text{COO})_2$ angeregt wird.

Received June 15, 1965

Prod. No. 4810A

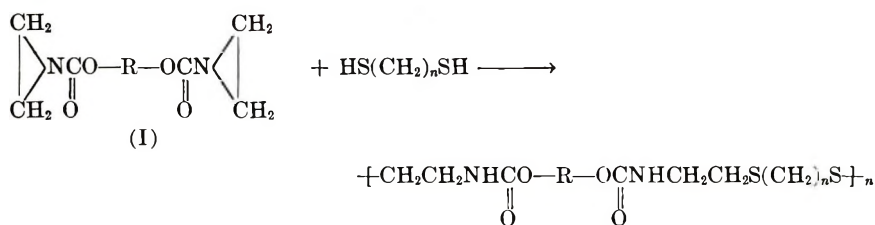
Polyaddition Reactions of Bisethyleneureas and 1,1,3,3-Diethyleneurea with Polymethylene Dimercaptans in LiCl-Dimethylformamide

YOSHIO IWAKURA, MUNENORI SAKAMOTO,* and MICHIO
YONEYAMA, *The Department of Synthetic Chemistry, Faculty of
Engineering, The University of Tokyo, Bunkyo-ku, Tokyo, Japan*

Synopsis

Polyaddition reactions of 1,1'-tetramethylenebis(3,3-ethyleneurea) (IIa), 1,1'-octamethylenebis(3,3-ethyleneurea) (IIb), 1,1'-*p*-phenylenebis(3,3-ethyleneurea) (IIc), 1,1'-(4,4'-diphenylmethane)bis(3,3-ethyleneurea) (II'd) and 1,1,3,3-diethyleneurea (III) with polymethylene dimercaptans were investigated. 1,1'-Polymethylenebis(3,3-ethyleneureas) and polymethylene dimercaptans successfully reacted at 80–95°C. in the presence of triethylamine to give poly(urea sulfides) with intrinsic viscosities up to 1.1 in about 90% yield when dimethylformamide, dimethylacetamide, or *N*-methyl-2-pyrrolidone containing lithium chloride as a solvent were used. The other ethyleneureas, however, failed to give high molecular weight polymers.

In preceding papers of this series on polyaddition reaction¹ it has been reported that high molecular weight, linear poly(urethane sulfides) were obtained by the reactions of bis-*N,N*-ethyleneurethanes (I) with polymethylene dimercaptans.^{2,3}

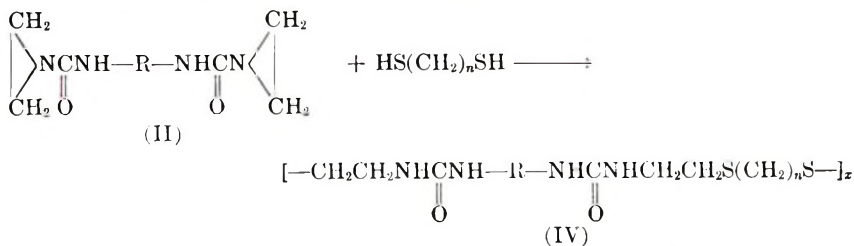


The present work is concerned with the polyaddition reactions of bis-3,3-ethyleneureas (II) and 1,1,3,3-diethyleneurea (III) with polymethylene dimercaptans and the properties of the poly(urea sulfides) obtained by these reactions.

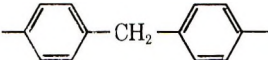
Basic catalysts such as tertiary amines induce self-polymerization of *O*-butyl-*N,N*-ethyleneurethane,⁴ and are very effective in promoting the polyaddition reactions of I with polymethylene dimercaptans to give poly-

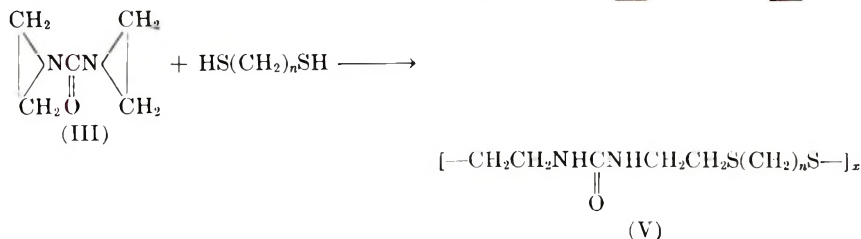
* Present address: The Department of Textile Engineering, Tokyo Institute of Technology, Meguro-ku, Tokyo, Japan.

(urethane sulfides).² It has been considered that this is because tertiary amines increase the nucleophilic reactivity of mercaptan so much that the polyaddition reaction proceeds exclusively, suppressing the competitive self-polymerization of I. Basic catalysts are expected to be also effective in the polyaddition reactions of II and III with polymethylene dimercaptans due to the similarity of the molecular structures of the reactants.



where IIa:R = $\text{—}(\text{CH}_2)_4\text{—}$, IIb:R = $\text{—}(\text{CH}_2)_8\text{—}$, IIc:R = 

and IId:R = 



EXPERIMENTAL

Materials

1,1'-Tetramethylenebis(3,3-ethyleneurea) (IIa), 1,1'-octamethylenebis(3,3-ethyleneurea) (IIb), 1,1'-*p*-phenylenebis(3,3-ethyleneurea) (IIc), and 1,1'-(4,4'-diphenylmethane)bis(3,3-ethyleneurea) (IId) were prepared from corresponding diisocyanates and ethylenimine by the method of Bestian.⁵ IIa, IIb, and IId were purified by recrystallization from acetone: IIa, m.p. 114–116°C. (lit.⁵ 122°C.), IIb, m.p. 103–105°C. (lit.⁵ 104°C.), and IId, m.p. 166–169°C. (sinter) (lit.⁵ 168–169°C. sinter). As IIc could not be purified by recrystallization, it was always freshly prepared just before use, m.p. ca. 325°C. (decomp.) (lit.⁵ 322–234°C. decomp.).

1,1,3,3-Diethyleneurea (III) was prepared according to the method reported⁵, m.p. 37–39°C. (lit.⁵ 39–41°C.).

Reaction of 1-Phenyl-3,3-ethyleneurea with Butyl Mercaptan

A solution of 1.6 g. of 1-phenyl-3,3-ethyleneurea and 1.0 g. of butyl mercaptan in 1 ml. of dioxane was treated with one drop of triethylamine at

room temperatures. 1-Phenyl-3- β -butylthioethylurea was obtained in 87% yield. It melted at 86.0–86.5°C. after repeated recrystallization from ethanol.

ANAL. Calcd. for $C_{13}H_{20}O_2N_2S$: N, 11.1%. Found: N, 11.4%.

Polyaddition Reaction

In a typical run, a solution of 2.12 g. (7.5 mmole) of 1,1'-octamethylenebis(3,3-ethyleneurea), 1.02 g. (7.5 mmole) of pentamethylene dimercaptan and 0.15 g. (1.5 mmole) of triethylamine in 15.0 ml. of dimethylformamide containing 5% of lithium chloride was placed in a 20-ml. glass tube, and the tube was sealed under an atmosphere of nitrogen. The solution was kept at 95°C. No precipitates were observed. After 24 hr. the tube was opened, and the resulting hot viscous solution was poured into 500 ml. of pure water with stirring. The precipitated white polymer was collected by filtration and dried *in vacuo* at 60°C. for about 20 hr.

Measurements of Physical Properties

Intrinsic or inherent viscosities were calculated from the viscosities measured in *m*-cresol or in dimethylformamide containing 5% lithium chloride at 30.0°C.

Melting points were measured on a metal block. Temperatures at which the polymers became transparent or decomposed were recorded.

Infrared absorption spectra were recorded with a Hitachi infrared spectrometer, Model EPI-S2.

RESULTS AND DISCUSSION

Catalyst and Solvent

It has been reported that bis-*N,N*-ethyleneurethanes react with butyl mercaptan in the absence of catalyst to give addition products, bis-*N*- β -butylthioethylurethanes.⁷ On the other hand, when 1-phenyl-3,3-ethyleneurea was treated with butyl mercaptan in boiling ethyl acetate, only a polymeric substance was obtained.⁸ With the aid of a basic catalyst this reaction was observed to produce an addition product, 1-phenyl-3- β -butylthioethylurea (see Experimental). Thus, base catalysis would be essential to the preparation of the poly(urea sulfides) by the polyaddition reactions of bis-3,3-ethyleneureas with dimercaptans.

According to this consideration, polyaddition reaction of 1,1'-tetramethylenebis(3,3-ethyleneurea) (IIa) with tetramethylene dimercaptan was carried out under such conditions as employed in the polyaddition reactions of bis-*N,N*-ethyleneurethanes (I) with dimercaptans.^{2,3} Reaction product, however, precipitated during the reaction, and no high molecular weight poly(urea sulfide) was obtained. This was likely to be due to the poorer solubility of the poly(urea sulfide). Dimethylformamide, dimethylacetamide, *N*-methyl-2-pyrrolidone, or dimethyl sulfoxide contain-

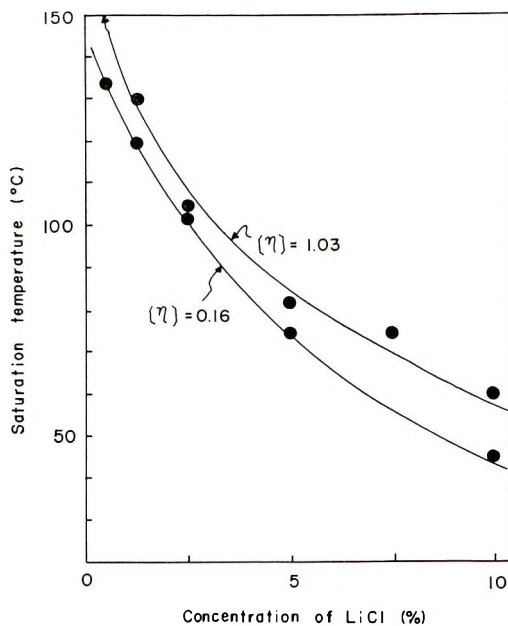


Fig. 1. Effect of concentration of lithium chloride on the solubility of dimethylformamide. In a test tube were placed 50 mg. of the poly(urea sulfide) prepared from IIa and tetramethylene dimercaptan, and 1.0 ml. of dimethylformamide containing lithium chloride. The temperature where the mixture became homogeneous on heating was recorded, which was plotted versus the concentration of lithium chloride.

ing an inorganic salt such as lithium chloride has been found to be a good solvent for polyamide, polyurethane, or polyurea.⁹ Dimethylformamide containing lithium chloride was also found to be a good solvent for the

TABLE I
Polyaddition Reaction of 1,1'-Tetramethylenebis(3,3-ethyleneurea) (IIa) with Tetramethylene Dimercaptan

Reaction conditions							Results	
Solvent ^a	LiCl, g./dl.	IIa, mole/l.	Catalyst ^b	Molar ratio of catalyst to IIa	Temperature, °C.	Time, hr.	Yield, %	$[\eta]^c$
A	0	0.50	E	0.40	23	24	75	0.16
B	0	1.0	F	0.09	60	17	67	0.21
B	4	0.50	F	0.20	80	24	90	1.03
B	4	0.33	F	0.30	80	24	89	0.94
C	4	0.33	F	0.30	80	24	91	0.84
D	4	0.33	F	0.30	80	24	91	1.0

^a Solvents: A = methanol, B = dimethylformamide, C = dimethylacetamide, D = *N*-methyl-2-pyrrolidone.

^b E = sodium methoxide, F = triethylamine.

^c Measured in *m*-cresol at 30.0°C.

TABLE II
Polyaddition Reactions of Bis-3,3-ethyleneureas (II) and 1,1,3,3-Diethyleneurea (III)
with Polymethylene Dimercaptans

Reaction conditions				Results					
Poly- (urea sul- fide) ^a	II or III, mole/ l. ^b	Molar ratio of cata- lyst to II or III ^c	Tem- pera- ture, °C.	Time, hr.	Yield, %	Vis- cosity	N, % ^d		Melt- ing point, °C.
							Calcd.	Found	
IVa2	0.50	0.20	80	24	84	0.45 ^e	17.5	17.8	238
IVa3	0.50	0.20	80	24	88	0.58 ^e	16.8	17.9	220
IVa4	0.50	0.20	80	24	90	1.03 ^e	16.1	16.0	f 225
IVa5	0.50	0.20	80	24	90	0.69 ^e	15.5	15.4	207
IVa6	0.50	0.20	80	24	89	0.99 ^e	14.9	15.0	215
IVb2	0.43	0.23	95	24	90	0.49 ^e	14.9	14.8	220
IVb3	0.43	0.23	95	24	93	0.79 ^e	14.4	14.7	177
IVb4	0.43	0.23	95	24	93	0.82 ^e	13.9	13.8	g 194
IVb5	0.50	0.20	95	24	93	1.07 ^e	13.4	13.5	172
IVb6	0.43	0.23	80	24	95	0.46 ^e	13.0	12.7	174
IVc2	0.18	1.7	100	63	83	0.11 ^h	16.5	16.0	245 (dec.)
IVc3	0.18	1.7	100	63	86	0.19 ^h	15.8	15.5	240 (dec.)
IVc4	0.19	1.0	100	63	83	0.10 ^h	15.2	15.3	i 225 (dec.)
IVc5	0.14	1.7	100	63	97	0.15 ^h	14.7	13.9	235 (dec.)
IVc6	0.18	1.7	100	63	94	0.12 ^h	14.1	13.6	235 (dec.)
IVd2	0.33	0.30	80	48	86	0.25 ^h	13.0	12.4	265 (dec.)
IVd3	0.33	0.30	80	48	97	0.18 ^h	12.6	11.6	195 (dec.)
IVd4	0.33	0.30	95	40	85	0.26 ^h	12.2	12.0	j 250 (dec.)
IVd5	0.33	0.30	80	48	88	0.27 ^h	11.9	11.1	220 (dec.)
IVd6	0.33	0.30	80	48	87	0.25 ^h	11.5	10.8	230 (dec.)
V2	0.58	0.71	100	76	80	0.18 ^k	13.6	13.1	185
V3	0.58	0.71	100	76	79	0.27 ^k	12.7	12.4	120
V4	0.71	2.4	100	69	79	0.26 ^k	12.0	11.1	l 105
V5	0.58	0.71	100	76	86	0.27 ^k	11.3	11.1	112
V6	1.2	0.71	100	40	85	0.26 ^k	10.7	10.3	108

^a Code: IVa n , poly(urea sulfide) prepared from IIa; IVb n , from IIb; IVc n , from IIc; IVd n , from II d; and V n , from III, respectively, wherein n is the number of methylene groups in a polymethylene dimercaptan. Thus, IVa2 means poly(urea sulfide) obtained by the reaction of IIa with ethylene dimercaptan.

^b Dimethylformamide solution containing 4-6% LiCl was used as solvent.

^c Triethylamine was used as catalyst.

^d Some of these analyses are somewhat different from theoretical values. This seems to be due to incompleteness of purification; Some polymers gave improved analytical values after being reprecipitated.

^e Intrinsic viscosity measured in *m*-cresol at 30.0°C.

^f Calcd.: C, 48.3%; H, 8.1%. Found: C, 47.0%; H, 8.5%.

^g Calcd.: C, 53.4%; H, 9.0%. Found: C, 53.0%; H, 9.2%.

^h Inherent viscosity measured on a solution of 0.20 g. polymer in 100 ml. of dimethylformamide containing 5% of LiCl at 30.0°C.

ⁱ Calcd.: C, 52.2%; H, 6.6%. Found: C, 51.6%; H, 7.1%.

^j Calcd.: C, 60.3%; H, 6.6%. Found: C, 59.9%; H, 6.8%.

^k Inherent viscosity measured on a solution of 0.20 g. polymer in 100 ml. of *m*-cresol at 30.0°C.

^l Calcd.: C, 46.1%; H, 7.8%. Found: C, 45.6%; H, 8.5%.

poly(urea sulfides) obtained here. Effect of concentration of lithium chloride on the solubility is shown in Figure 1. By the use of dimethylformamide containing lithium chloride as a reaction medium, linear poly(urea sulfide) of high intrinsic viscosity was obtained under mild conditions. Similarly, dimethylacetamide or *N*-methyl-2-pyrrolidone in combination with lithium chloride, was also effective as the solvent. These results are summarized in Table I.

Polyaddition reactions of II and III with polymethylene dimercaptans were then carried out under the conditions mentioned above. Results are collected in Table II. 1,1'-Polymethylenebis(3,3-ethyleneureas) (IIa and IIb) gave products of high molecular weight, whereas aromatic bis-3,3-ethyleneureas (IIc and IIId) and 1,1,3,3-diethyleneurea (III) gave lower molecular weight poly(urea sulfides).

Properties of Poly(urea Sulfides)

The poly(urea sulfides) were stable at room temperatures except those obtained from IIId, which discolored upon a prolonged storage. The poly(urea sulfides) obtained had higher melting points than the corresponding poly(urethane sulfides).² However, the poly(urea sulfides) were unstable on heating; aliphatic ones melted to decompose gradually, whereas aromatic ones decomposed without melting (Table II).

TABLE III
Solubilities of Poly(urea Sulfides)

Solvent	Solubility of poly(urea sulfides) ^{a,b,c}				
	IVa4	IVb4	IVd4	IVd4	V4
Acetic acid anhydride	0	0	0	0	2
<i>m</i> -Cresol	4	4	2	2	4
Dichloroacetic acid	4	4	4	4	4
Dimethylacetamide	3	3	2	3	3
Dimethylformamide	2	2	3	3	3
Dimethylformamide containing LiCl	4	4	4	4	4
Dimethyl sulfoxide	3	3	3	3	3
Dioxane	0	0	0	0	3
Formic acid	3	3	0	0	3
Pyridine	0	0	0	0	3
Tetrachloroethane	1	1	0	0	1

^a Code: See footnote a in Table II.

^b None soluble in carbon tetrachloride, chloroform, ethyl acetate, or methylene chloride.

^c Code: 0 = insoluble; 1 = swollen; 2 = soluble at boiling temperature; 3 = soluble with mild heating; 4 = soluble at room temperatures.

Solubilities of the poly(urea sulfides) are listed in Table III. All the poly(urea sulfides) obtained were soluble in dichloroacetic acid and in dimethylformamide containing lithium chloride. Aliphatic poly(urea sulfides) were soluble also in *m*-cresol, whereas aromatic ones were insoluble in the solvent

at room temperatures. The aliphatic poly(urea sulfides) (IVa, IVb) could be cast from *m*-cresol solutions.

Data on the characteristic bands of the infrared absorption of the monomers and the polymers are given in Table IV with those of 1-phenyl-3,3-ethyleneurea and its derivative for comparison. The C=O stretching vibration bands shifted slightly to the lower numbers when ethylenimine rings were cleaved. It has been reported that an absorption band of ethylenimine at 838 cm^{-1} is assigned to the ring deformation.¹⁰ The absorption bands of monomers at 880–810 cm^{-1} region were not seen in the spectra of the polymers. A N—H stretching vibration band at 3350 cm^{-1} and an amide II band at 1570 cm^{-1} were not observed in III, but in V4.

TABLE IV
Infrared Absorption Bands of Poly(urea Sulfides) and their Monomers

3,3-Ethylene- urea	C=O		Poly(urea sulfide) ^a	C=O stretching vibration, cm^{-1}
	stretching vibration, cm^{-1}	Absorption bands at 880–810 cm^{-1} region, cm^{-1}		
IIa	1650(s)	836(w), 816(w)	IVa4	1622(s)
IIb	1647(s)	841(w), 823(w)	IVb4	1621(s)
IIc	1665(s)	876(w) ^b	IVc4	1639(s)
IId	1663(s)	873(w) ^b	IVd4	1643(s)
III	1695(s)	851(w), 836(w), 813(w)	V4	1626(s)
1-Phenyl- 3,3-ethyleneurea	1672(s)	868(w) ^b	1-Phenyl- 3- β -butylthioethyl- urea	1630(s)

^a Code: See footnote a in Table II.

^b The absorption bands at 860–810 cm^{-1} region could not be detected because of the overlap of the C—H out-of-plane bending bands of phenyl or phenylene group.

References

1. Iwakura, Y., and K. Hayashi, *Kobunshi Jikkengaku Koza*, Vol. 11, Kyo'oritsu Shuppan, Tokyo, 1958, p. 327.
2. Iwakura, Y., and M. Sakamoto, *J. Polymer Sci.*, **47**, 277 (1960).
3. Iwakura, Y., M. Sakamoto, and Y. Awata, *J. Polymer Sci.*, **A2**, 881 (1964).
4. Sakamoto, M., *Bull. Tokyo Inst. Technol.*, **No. 57**, 101 (1964).
5. Bestian, H., *Ann.*, **566**, 210 (1950).
6. Iwakura, Y., and K. Naraba, *Kobunshi Kagaku*, **8**, 400 (1951).
7. Iwakura, Y., M. Sakamoto, and H. Yasuda, *Nippon Kagaku Zasshi*, **82**, 606 (1961).
8. Iwakura, Y., and A. Nabeya, *Bull. Tokyo Inst. Technol.*, **No. 42**, 69 (1961).
9. Brit. Pat. 871,580 (1961).
10. Hoffman, H. T., Jr., G. E. Evans, and G. Glockler, *J. Am. Chem. Soc.*, **73**, 3028 (1951).

Résumé

On a étudié les réactions de polyaddition de polyméthylène dimercaptans avec le 1,1'-tétraméthylène-bis(3-3-éthylène-urée) (IIa), le 1,1'-octaméthylène-bis(3,3-éthylène-urée) (IIb) le 1,1'-*p*-phénylène-bis(3,3-éthylène-urée) (IIc), la 1,1'-(4,4-diphénylméthane)bis(3,3-éthylène-urée) (IId) et le 1,1,3,3-diéthylène-urée. Le 1,1'-polyméthyl-

ène-bis(3,3-éthylène-urée) et les polyméthylène-dimercaptans réagissent à 80–95°C. en présence de triéthylamine et donnent des sulfures de polyurée avec des viscosités intrinsèques de 1,1 avec environ 90% de rendement lorsqu'on utilise comme solvant le diméthylformamide, le diméthylacétamide ou la *N*-méthyl-2-pyrrolidone contenant du chlorure de lithium. Toutefois les autres éthylène-urées n'ont pas fourni de polymères de haut poids moléculaire.

Zusammenfassung

Die Polyadditionsreaktionen von 1,1'-Tetramethylen-bis(3,3-äthylenharnstoff) (IIa), 1,1'-Octamethylen-bis(3,3-äthylenharnstoff) (IIb), 1,1'-*p*-Phenylen-bis(3,3-äthylenharnstoff) (IIc), 1,1'-(4,4'-Diphenylmethan)bis(3,3-äthylenharnstoff) (IIId) und 1,1,3,3-Diäthylenharnstoff (III) mit Polymethylen-dimercaptanen wurden untersucht. Bei Verwendung von Dimethylformamid, Dimethylacetamid oder *N*-Methyl-2-pyrrolidon mit einem Gehalt an Lithiumchlorid als Lösungsmittel reagierten 1,1'-Polymethylen-bis(3,3-äthylenharnstoffe) und Polymethylen-dimercaptane in Gegenwart von Triäthylamin bei 80–95°C. erfolgreich unter Bildung von Polyharnstoffsulfiden mit Viskositätszahlen bis zu 1,1 mit etwa 90% igem Umsatz. Die anderen Äthylenharnstoffe lieferten jedoch keine hochmolekularen Polymeren.

Received November 17, 1964

Revised July 23, 1965

Prod. No. 4816A

Gel Permeation Chromatography. III. Molecular Shape versus Elution

J. G. HENDRICKSON and J. C. MOORE, *Texas Basic Research,
The Dow Chemical Company, Freeport, Texas*

Synopsis

Rules were evolved to predict elution of linear, branched, and polar compounds in GPC, based on testing of 130 compounds. With these rules and in tetrahydrofuran solvent, data for all but a few compounds correlated onto a single calibration line. With small molecules, elution often changed, due to hydrogen bonding to the solvent; this occurred with alcohols, acids, and some chlorinated compounds, but not with mercaptans. Branched and linear isomers usually eluted at about the same point. One may conclude that structural elements were additive in their effect on elution volume in this study.

Introduction

Gel permeation chromatography (GPC) is a new and basic analytical tool that measures the size of molecules and polymers.¹⁻⁴ It is based on elution of the solute through a bed of crosslinked polymer gel, which presents a gradation of size barriers to the molecules. Hence, the smaller molecules penetrate the furthest into the gel, so that they elute last. With polymers, a close approach to the true molecular weight distribution is obtained by using long columns having appropriate permeability and high plate count.

Tetrahydrofuran (THF) is a preferred solvent for many GPC separations, because of its low refractive index and viscosity and its high swelling of the gel. Also, it will dissolve a wide range of polymers; these include polystyrene, poly(vinyl chloride), and poly(propylene oxide). With these products, the correlation of elution with molecular chain length shows that chain substituents sometimes cause deviations. The chain length calculations also depart from the observed results with some small molecules, i.e., chain substituents appear to add differently to molecular bulk in different series. Hence, rules were sought that would explain these phenomena and show the effective dimensions of molecules.

There are five basic forces that one would expect to modify the elution volume of a compound in GPC. These are as follows:

(1) Changes in the width of the network openings in the beads. With the same solvent this remains constant, but it changes with the solvent as a function of gel swelling.⁵

(2) Solvent-solute association. For example, the hydrogen bonding of OH compounds to ethers is well known.⁶⁻⁹ The complete bonding of the solvent and solute often occurs, and then the size of a solute molecule is increased by an amount equal to the size of the solvent.

(3) Dimerization, etc. For example, acetic acid and other organic acids in CCl_4 do form the dimer, as judged by NMR and other measurements.^{6b,9a} In contrast, the dimer is not formed in water, where the hydrogen bonding of the acid's OH to the oxygen of the water predominates. An aggregation of molecules would look two or more times as long as their normal chain length in GPC.

(4) Intramolecular bonding. This is the formation of a ring structure when the groups that one might expect to form a solvent-solute association are located within the same molecule. Reportedly, an ether solvent such as dioxane will break up intermolecular bonding but not intramolecular bonding.¹⁰

(5) Adsorption onto the gel surface or into it. Solute-solvent interaction should be strong enough to suppress any tendency for the solute to be adsorbed to the gel. Since the gels used did not exhibit any strong electron-accepting or -donating groups, any active hydrogen, or any strong dipoles, this should be easy to achieve. If it occurs, adsorption is detected by tailing and/or elution later than would normally occur.

Becker⁸ showed that the equilibrium constant for ROH complexed to dioxane was about 1.0 at 25°C. At 15*M* dioxane, only $1/15$ of the ROH molecules would be in the uncomplexed form. This would support the concept that alcohols are more than 90% complexed with THF as the solvent. At least 25 different physical and spectral tests are useful to detect and measure hydrogen bonding.^{9b} In general, the various methods give good agreement as to the heat of hydrogen bonding, the types of groups that participate, etc. However, there are few if any techniques that measure the aggregate size of molecules that are loosely bonded together in the liquid state.

It is generally agreed that a volume measurement governs elution of large molecules in water-swelling gels;¹¹ however, the most effective measure of this factor is in doubt.¹² This report offers a useful correlation of the elution volumes of a wide variety of small molecules. The additivity of equivalent structural elements is demonstrated, and a basis is provided for comparing their relative sizes in the gel-permeation context. To accomplish this, compounds were compared to the *n*-alkane series, to determine an equivalent chain length. Then these equivalent lengths were added and subtracted to observe the effect of the component parts.

Experimental

A crosslinked styrene gel (Sx8) prepared by the suspension polymerization of a 92% styrene-8% divinyl benzene mixture was obtained from The Dow Chemical Company, Midland, Michigan. It was the same type of bead used to make ion exchange resins, just prior to sulfonation. The

gel was further size-separated, and a 25–50 μ diameter bead fraction was selected.

The GPC runs were made by using a Waters Associates machine with a 16-ft. column consisting of four 4-ft. \times $3/8$ -in. sections packed with the Sx8 gel. The column feed pressure was about 70 lb./sq. in., temperature 25°C., and the flow was THF at 1 ml./min. Samples were injected every 20 min. with the use of sequences designed to avoid misinterpretation. Either homologs were studied in succession of descending order of number of carbon atoms, or compounds of about the same size were injected so as to alternate a compound having a refractive index (RI) higher than THF with one whose RI was lower. The compounds eluted from the column over a rather small number of milliliters (called milliliters base in the tables). The position of the highest point of the peak-shaped curve was called the

TABLE I
Values Used As Effective Chain Length of Various Atoms

Atom	Radius, A.		Group	Bond angle ^a	Chain length	
	Covalent	van der Waal			#C Basis	A.
C	0.77	—		109.5°	1.0	1.25
O	0.66	—		105°	0.67	0.84
N	0.70	—		109.5°	0.91	1.14
S	1.04	—		104°	1.00	1.25
F	0.60	1.35		—	0.27	1.84
Cl	0.99	1.80A		—	1.09	2.60
Br	1.14	1.95		—	1.32	2.88
I	1.36	2.05		—	1.54	3.15
H	0.30	1.00A		—	0.0	1.25
O	0.51	1.60		120°	0.61	2.00

^a Based on Godfrey models.

elution volume. The milliliter base value was used to calculate the theoretical plates per foot (TPF) as previously done.²

Before polar compounds could be studied, a basis was needed for computing their equivalent chain lengths. Since the C—C bond distance is convenient and fairly accurate, this basis was used in this report. Calculations were needed to measure the chain length contribution of the heteroatom on both the angstrom length and the equivalent C—C bond length basis. The chain length per carbon atom in a normal alkane was the C—C bond (1.54 Å.) times the sine of half the C—C—C angle (109.5°) or 1.25 Å. To the number of carbon atoms present (#C), one must add the length of hydrogen on the methyl groups at the ends of the chain. For each end, this value is the sum of the van der Waal's radius for hydrogen (1.0 Å. and the contribution of the covalent radius of hydrogen (0.30 Å. \times sine (109.5°/2) = 0.25 Å.). Therefore, the two measures of chain length are related by the equation

$$\text{Angstrom chain length} = 2.5 + 1.25 (\#C) \quad (1)$$

In the same manner, the corresponding lengths of other groups were calculated, and they are given in Table I.

Discussion

The Sx8 gels were calibrated by using a series of *n*-alkanes, *n*-alkenes, and di-*n*-alkyl ethers. They gave the elution times given in Table II and

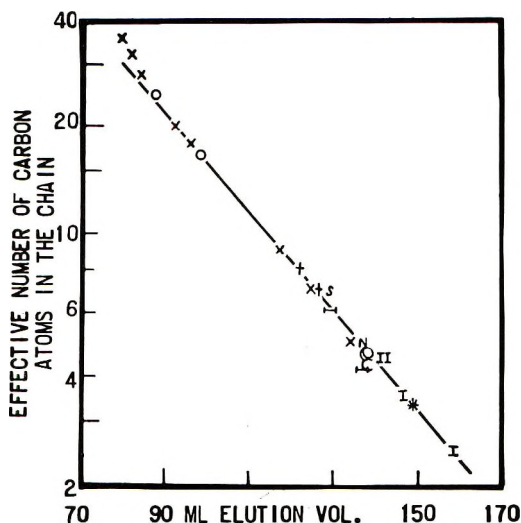


Fig. 1. GPC of straight-chain compounds. (X) *n*-alkanes; †, *n*-alkenes; (O) di-*n*-alkyl ethers, O = 0.67 C; (I) *n*-alkyl iodide, I = 1.54 C; (t-t) *n*-alkyl chlorides, Cl = 1.09 C; (*) *n*-alkyl bromides, Br = 1.32 C; (S) di-*n*-alkyl sulfides, S = 1.0 C; (N) di-*n*-alkyl amines, N = 0.91 C; (C) carbonyl compounds, O = 0.61 C.

plotted in Figure 1. The data looked sufficiently linear to permit an equation to be derived for the line, and this took the form

$$\text{elution volume} = 187 - 73 \log (\#C) \quad (2)$$

where 187 is the elution volume extrapolated to $\#C = 1$ and $(187 - 73)$ is the volume at $\#C = 10$. This equation was tested again by using the observed volumes to calculate the number of carbon atoms expected from the experimental results. These are then compared under the column headed by D_1 in Table II. The agreement up to C_{27} was within 0.5 carbon atoms in all cases, and the average deviation was 0.18 carbon atoms.

After about 130 compounds were studied, another several dozen pure compounds were studied with another Sx8 packed column. The purpose was to prepare another calibration curve, to test reproducibility, and to measure other examples of solvent-solute associations. Unfortunately, the plate count of the 16-ft. Sx8 research column had been ruined, but an 8-ft. column having a lower plate count per foot was available and it was used. The calibration compounds gave a curve from which was derived the equation

$$\text{elution volume} = 94.5 - 35.8 \log (\#C) \quad (3)$$

When this equation was applied to the observed results, all the calculated $\#C$ atoms of these compounds agreed with the theory within 0.5 carbon atoms, and the average deviation was 0.2 units. These and subsequent results with the 8-ft. column are listed under Elution in parenthesis in Tables II-XII.

Many polar, straight-chain compounds were compared to their straight-chain hydrocarbon analogs, by using eq. (2) and the equivalent bond lengths given in Table I. These compounds contained organic sulfides, halides, dihalides, carbonyl compounds, and others. The results are shown in Table III; there was good agreement between the theoretical and calculated values, as summarized in Table XIII. In these and other cases, the results were predicted with an average deviation of 0.25 carbon atoms.

The apparent length of a phenyl group was explored. A benzene molecule should have a diameter equal in length to 3.55 $\#C$ units, and this was the effective length of benzene in our work. However, a phenyl group in other compounds had an effective length that was less than this; so, the elution of simple compounds was used to calibrate the effect of such a group. The results showed that a phenyl group equaled a 2.85 carbon atom chain length, or a 0.70 $\#C$ unit correction. Similarly, 2.4 $\#C$ units appeared to be the effective chain length of a phenylene group. The observed fact that benzene, pyridine, and cyclohexane eluted close to each other and to the predicted times showed that partition is not a major factor in this process.

With a fused ring compound, like naphthalene, the effective length was only about four carbon atoms. Equivalent chain lengths of the polynuclear aromatics are being studied further.

TABLE II
 GPC with Sx8 Gel of Normal Alkanes, Alkenes, and Ethers^a

Run	Compound	Source		Elution, ml. ^d		(TPF)	Compared chain length, #C units ^e		Error (Obs - C), D _i
		Co. ^b	Grade ^c	To peak	At base		Calc.	Obs.	
1	<i>n</i> -C ₃₆ H ₇₄	D	W	79.1	3.92	408	36.0	30.08	-5.92
2	<i>n</i> -C ₃₂ H ₆₆	E	W	80.8	3.87	436	32.0	28.50	-4.50
3	<i>n</i> -C ₂₈ H ₅₈	E	W	83.2	4.38	360	28.0	26.42	-1.58
4	<i>n</i> -C ₃₀ H ₆₂	E	W	91.8	5.23	308	20.0	20.14	+0.14
5	<i>n</i> -C ₁₈ H ₃₈	E	P	94.5	5.37	310	18.0	18.50	+0.50
6	<i>n</i> -Nonane	Ph	99%	117.0	5.28	496	9.0	9.10	+0.10
7	<i>n</i> -Heptane	E	W	124.6	6.49	369	7.0	7.14	+0.14
8	<i>n</i> -Pentane	E	T	133.8	5.38	617	5.0	5.36	+0.36
9	(<i>n</i> -C ₁₂ H ₂₆) ₂ O	HW	—	86.9	4.98	303	23.66	23.50	-0.16
10	(<i>n</i> -C ₁₄ H ₂₈) ₂ O	HW	—	98.0	5.16	361	16.66	16.59	-0.07
11	Octene-1	M	W	121.4	6.73	325	8.0	7.92	-0.08
12	Heptene-1	M	95%	126.2	5.82	470	7.0	6.81	-0.19
13	Diethyl ether	—	C	138.5	5.44	647	4.66	4.62	-0.04

14	Diethyl ether	HW	—	(50.7)	(3.93)	(332)	16.67	16.51	-0.16
15	Dodecane	HW	—	(55.3)	(3.74)	(438)	12.0	12.44	+0.44
16	<i>n</i> -Nonane	+	—	(60.2)	—	—	9.0	9.08	+0.08
17	Octene-1	+	—	(63.0)	—	(350)	8.0	7.95	-0.05
18	<i>n</i> -Heptane	+	—	(63.8)	(4.68)	(372)	7.0	7.21	+0.21
19	Heptene-1	+	—	(64.8)	(4.95)	(342)	7.0	6.77	-0.22
20	<i>n</i> -Pentane	+	—	(68.2)	(4.35)	(492)	5.0	5.47	+0.47
21	Diethyl ether	+	—	(70.5)	(4.31)	(535)	4.67	4.73	+0.06

^a Run conditions: 40 A. limit gel, THF solvent at 1 ml./min. 25°C., 16 ft. column.

^b Source of compounds studied: A = Aldrich Chemical Company; API = American Petroleum Institute Standard; B = Baker Chemical Company; B & A = Baker and Adamson (Allied Chemical Company); D = Dow Chemical Company; E = Eastman Chemical Company; F = Fisher Scientific Company; GA = General Aniline; HW = Humphrey-Wilkinson Company; K = K and K Chemical Company; M = Mallinckrodt Chemical Works; MCB = Matheson, Coleman and Bell; NBS = National Bureau of Standards; Ph = Phillips Chemical Company; U = Union Carbide and Carbon; Z = Crown Zellerbach Corporation; + = mentioned previously; — = not specified.

^c Grades of chemicals used: C = commercial; P = pure, purified; R = reagent grade; S = spectral grade; T = technical; W = white label; X = practical; — = not specified.

^d Elution data in parentheses are from an 8-ft. column.

^e Chain length: calculated values are derived from bond lengths in the longest chain (except where noted); observed values are derived from eqs. (2) and (3). Chain length values in parentheses are based on theories discussed in the text.

TABLE III
 GPC with Sx8 Gel of Polar Straight-Chain Compounds^a

Run	Compound	Source ^b		Elution, ml.		(TPF)	Compared chain length, #C units ^c		Error (Ob - C) D ₁
		Co.	Grade	To peak	At base		Calc.	Obs.	
1	Di- <i>n</i> -propyl sulfide	E	W	129.3	5.52	548	7.0	6.17	-0.83
2	1,4-Dichlorobutane	E	W	129.5	6.00	465	6.18	6.13	-0.05
3	Ethylene dichloride	D	—	137.0	5.67	583	4.18	4.84	+0.66
4	Butyraldehyde	E	W	137.2	5.71	577	4.61	4.81	+0.20
5	Diethyl amine	E	W	137.4	5.49	628	4.91	4.78	-0.13
6	Ethyl formate	E	W	138.0	5.71	585	4.33	4.69	+0.36
7	Allyl bromide	E	W	141.1	6.09	537	4.32	4.25	-0.07
8	Allyl iodide	E	W	141.9	6.30	507	4.54	4.12	-0.42
9	Acetonitrile	E	S	142.5	4.97	810	—	4.07	—
10	<i>n</i> -Propyl iodide	E	W	143.6	6.23	532	4.54	3.93	-0.61
11	Ethyl iodide	F	R	146.3	6.36	529	3.54	3.61	+0.07
12	Ethyl bromide	F	R	149.2	6.32	577	3.32	3.29	-0.03
13	Methyl iodide	F	R	153.5	6.67	565	2.54	2.45	-0.09

^a Run conditions: see Table II.

^b Source and grade: see Table II.

^c Chain length: see Table II.

TABLE IV
GPC with Sx8 Gel of Aromatic Hydrocarbons^a

Run	Compound	Source ^b		Elution, ml.		(TPP)	Compared chain length, #C units ^c		Error (Ob - C), D _i
		Co.	Grade	To peak	At base		Calc.	Obs.	
1	Pyridine	—	R	149.0	6.40	542	3.55	3.29	-0.24
2	Benzene	—	R	147.0	6.16	568	3.55	3.52	-0.03
3	Biphenyl	E	W	133.3	6.87	376	5.70	5.44	-0.26
4	Terphenyl	E	W	121.0	6.88	310	8.10	8.02	-0.08
5	Naphthalene	—	R	141.6	6.72	445	5.10	4.19	+0.01
6	Phenanthrene	E	P	132.1	7.29	328	5.70	5.66	-0.04
7	Anthracene	E	R	132.0	7.21	336	7.10	5.67	-1.43
8	Anthraquinone	E	W	132.6	—	—	7.10	5.56	-1.52
9	2-Ethyl anthraquinone	D	—	125.4	—	—	9.05	6.97	-1.08
10	2-Benzanthracene	A	—	116.0	7.90	146	9.19	9.39	+0.20
11	Toluene	—	R	142.4	6.26	517	3.85	4.08	+0.23
12	<i>p</i> -Xylene	—	C	138.6	—	—	4.40	4.60	+0.20
13	Ethylbenzene	E	W	137.0	6.72	415	4.85	4.84	+0.01
14	<i>n</i> -Propylbenzene	—	—	130.7	6.18	448	5.85	5.91	+0.06
15	Tetralin	E	—	143.2	6.97	422	4.28	3.98	-0.30
16	1,2-Diphenoxyethane	E	W	115.8	5.77	403	9.03	9.41	+0.38

^a Run conditions: see Table II

^b Source and grade: see Table II.

^c Chain length: see Table II.

TABLE V
 GPC with SxS Gel of Compounds Having Pendant Methyl Groups^a

Run	Compound	Source ^b		Elution, ml. ^c		(TPF)	Compared chain length, #C units		Error (Ob - C)	
		Co.	Grade	To peak	At base		Calc.	Ob.	D ₁	D ₂
1	2,2,4-Trimethylpentane	—	C	119.0	—	—	5.0	8.54	3.54	+0.54
2	2,2,4-Trimethylpentene-1	Ph	99%	123	—	—	5.0	7.53	2.53	-0.47
3	2,3-Dimethylpentane	Ph	99%	120.0	5.80	471	5.0	6.85	1.85	-0.15
4	2-Methylpentane	Ph	95%	128.0	5.69	507	5.0	6.43	1.43	+0.43
5	4-Methylpentene-1	A	—	129.2	5.91	477	5.0	6.18	1.18	+0.18
6	3-Methylpentane	M	X	129.5	6.10	451	5.0	6.13	1.13	+0.13
7	2-Methylpentene-1	A	—	131.4	5.91	593	5.0	5.77	0.77	-0.23
8	Cumene	E	W	130.8	5.88	493	4.85	5.89	1.04	+0.04
9	<i>m</i> -Xylene	—	C	138.7	6.11	515	3.85	4.59	0.74	(+0.19)
10	<i>o</i> -Xylene	—	C	139.8	6.29	493	3.85	4.43	0.42	(+0.03)

^a Run conditions: see Table II.

^b Source and grade: see Table II.

^c Chain length: see Table II.

TABLE VI
GPC with Sx8 Gel of Compounds with Pendant Oxygen Groups^a

Run	Compound	Source ^b		Elution, ml. ^c		Compared chain length, #C units ^d			Error (Ob - C)		
		Co.	Grade	To peak	At base	(TPF)	Calc.	Obs.	D ₁	D ₂	D ₃
1	Diphenyl acetone	E	X	115.4	5.83	385	8.70	9.57	+0.87	0.26	+0.07
2	2,5-Hexane dione	E	W	128.4	5.73	502	6.00	6.35	+0.35	(-0.87)	(-1.25)
3	Acetic acid-THF	—	R	129.0	5.64	523	5.21	6.22	+1.01	0.40	+0.21
4	Nitrobenzene	B	T	133.2	6.00	493	4.37	5.46	+1.09	0.48	+0.29
5	Nitroethane	E	W	136.0	5.63	583	3.52	4.99	+1.47	0.86	0.67
6	2-Butanone	—	—	(70.4)	(4.37)	(518)	4.0	4.76	+0.76	+0.15	-0.04
7	Dimethyl sulfoxide	Z	C	(72.4)	(4.70)	(475)	3.0	4.20	+1.20	-0.02	-0.40
8	Acetone	—	C	142	5.69	623	3.0	4.13	+1.13	0.52	+0.33

^a Run conditions: see Table II.

^b Source and grade: see Table II.

^c Elution data in parentheses are from an 8-ft. column.

^d Chain length: see Table II.

TABLE VII
GPC with Sx8 Gel of Cyclic Compounds^a

Run	Compound	Source ^b		Elution, ml.		(TPF)	Compared chain length #C units ^c		Error (Ob - C) Revised	
		Co.	Grade	To peak	At base		Calc.	Obs.	D ₁	D ₂
1	Cycloheptane	NS	99+	141.7	6.66	453	4.20	4.17	-0.03	—
2	Butyrolactone	—	—	143.4	6.02	567	3.74	3.95	+0.21	—
3	Cyclohexanone	B	P	143.7	6.38	507	3.97	3.92	-0.05	—
4	Cyclohexane	—	C	143.7	6.38	507	3.39	3.92	+0.53	—
5	Propylene sulfide	D	—	142.8	6.57	473	(3.0)	4.03	1.0	0.0
6	Epichlorohydrin	D	C	140.5	6.15	522	(4.08)	4.33	+0.25	+0.25
7	Propylene oxide	D	C	151.8	6.30	580	(3.0)	3.02	0.00±	+0

^a Run conditions: see Table II.

^b Source and grade: see Table II.

^c Chain length: see Table II.

TABLE VIII
 GPC with Sx8 Gel of Alcohols^a

Run	Compound	Source ^b		Elution, ml.		Compared chain length, #C units ^c			Error (Ob - C)		
		Co.	Grade	To peak	At base (TPF)	Calc. ^d	Obs.	D ₁	D ₂	D ₃	
1	<i>n</i> -Decyl Alcohol	E	W	104.4	560	10.67	13.54	2.86	+0.32	+0.01	
2	Butyl cellosolve	D	C	109.8	419	10.0	11.42	1.42	-1.12	-0.23	
3	1-Heptanol	E	W	113.1	483	7.67	10.20	2.61	+0.07	-0.24	
4	Trimethylene glycol	D	—	116.5	407	4.33	9.24	4.91	+0.19	—	
5	Methyl cellosolve	D	C	121.7	565	7.0	7.84	0.84	-1.30	—	
6	Ethylene glycol	D	C	120.3	517	3.33	8.20	4.86	-0.22	—	
7	<i>n</i> -Propyl alcohol	—	C	127.3	—	3.67	6.57	2.90	+0.36	+0.05	
8	Ethanol	—	C	131.4	522	2.67	5.78	3.11	+0.57	+0.26	
9	Methanol	—	C	132.5	657	1.67	5.58	3.91	1.37	(+1.06)	
10	Water	—	C	129.2	588	0.67	6.19	5.52	+0.45	—	
11	Tripropylene glycol	D	C	101.8	264	11.67	14.69	3.02	-2.06	-0.28	
12	Dipropylene glycol	D	C	109.2	350	8.00	11.63	3.63	-1.45	+0.33	
13	2,4,4-Trimethylpentanol-1	E	C	109.8	506	8.67	11.42	2.75	+0.21	-0.19	
14	3-Heptanol	E	P	113.5	423	7.67	10.16	2.40	-0.05	-0.26	
15	Propylene glycol	D	C	121.2	404	4.33	7.97	3.64	-1.48	+0.34	
16	Isopropyl alcohol	—	C	125.8	555	3.67	6.89	2.22	-0.32	—	
17	Cyclohexanol	—	C	125.8	438	4.26	6.89	2.63	+0.09	—	

^a Run conditions: see Table II.^b Source and grade: see Table II.^c Chain length: see Table II.^d Branched compounds are compared to their straight chain analogues.

TABLE IX
 GPC with SxS Gel of Polar Aromatic Compounds^a

Run	Compound	Source ^b		Elution, ml. ^c		(TPP)	Compared chain length, #C units ^d		Error (Ob - C) <i>D_i</i>
		Co.	Grade	To peak	At base		Calc.	Obs.	
1	Hydroquinone	B&A	W	118.5	5.48	467	8.53	8.61	+0.08
2	2-Naphthylamine	E	W	120.4	5.86	422	7.80	8.11	+0.31
3	Aniline	—	R	126.6	5.90	461	6.47	6.68	+0.21
4	Nitrobenzene	B&A	T	133.2	6.00	493	5.15	5.46	+0.31
5	α -Iodotoluene	E	W	(70.5)	(4.84)	(484)	5.33	4.73	-0.40
6	Chlorobenzene	E	W	139.7	5.87	566	4.05	4.44	+0.39
7	Iodobenzene	E	W	139.8	7.11	387	4.53	4.43	-0.10
8	Bromobenzene	E	W	140.9	6.53	465	4.27	4.28	+0.01

^a Run conditions: see Table II.

^b Source and grade: see Table II.

^c Elution data in parentheses are from 8-ft. column.

^d Chain length: see Table II.

TABLE X
 GPC with SXS Gel of Compounds with Pendant Halide Groups^a

Run	Compound	Source ^b		Elution, ml. ^c		Compared chain length, #C units ^d				Error (Ob - C)	
		Co.	Grade	To peak	To base	(TPF)	Calc.	Obs.	D ₁	D ₂	
1	HCCL ₂ CCl ₃ H·THF	E	—	(60.7)	—	—	7.08	8.76	+1.68	-0.11	
2	C ₂ Cl ₄ H·THF	D	—	124.7	6.41	379	5.67	7.09	+1.42	-0.38	
3	Cl ₃ H·THF	E	W	126.0	6.41	397	5.08	6.81	+1.73	+0.47	
4	Cl ₃ CCO ₂ Et	—	—	(65.4)	—	—	6.03	6.52	+0.49	-0.41	
5	Hexachlorobutadiene	D	—	128.0	6.75	360	4.87	6.43	+1.52	+0.20	
6	CCl ₃ H·THF	D	—	130.5	5.67	528	4.63	5.91	+1.28	+0.48	
7	CBr ₃ ·THF	D	—	132.8	6.18	462	4.86	5.49	+0.37	(0.71)	
8	C ₂ Cl ₆	D	—	133.9	6.64	407	4.18	5.32	+1.16	-0.64	
9A	CCl ₂ =CH ₂ ·THF	D	—	135.9	6.38	454	4.92	5.01	(+0.09)	(+0.36)	
9B	CCl ₂ =CH ₂	D	—	135.9	6.38	454	3.22	5.01	(+1.79)	(+0.79)	
10A	CHCl=CHCl·THF	D	—	136.9	—	—	4.02	4.86	(+0.81)	(+0.33)	
10B	CHCl=CHCl	D	—	136.9	—	—	3.31	4.86	(+1.52)	(+1.52)	
11	CCl ₄	D	—	139.0	6.58	450	3.16	4.47	1.31	+0.41	

^a Run conditions: see Table II.

^b Source and grade: see Table II.

^c Elution data in parentheses are from 8-ft. column.

^d Chain length: see Table II.

TABLE XI
GPC with Sxs Gel of Compounds with Hydrogen Bonding^a

Run	Compound	Source ^b		Elution, ml. ^c		Compared chain length #C units ^d		Antici- pated (Ob - C)	(Ob - C)	THF bonded, %	
		Co.	Grade	To peak	At base (TPF)	Calc.	Obs.				
1	Oleamide	—	—	(47.3)	(4.25)	(247)	19.0	20.82	2.85	1.82	65
2	Acetamide	—	R	(67.5)	(4.08)	(547)	3.54	5.68	2.85	2.14	75
3	<i>n</i> -Dodecanethiol	E	—	(56.6)	(3.89)	(423)	13	11.44	2.85	—	—
4	1,2-Ethanedithiol	E	—	(70.8)	(4.17)	(577)	4.0	4.59	5.7	0.59	10
5	Adiponitrile	—	—	(60.3)	(4.31)	(392)	8.0	9.0	5.7	1.0	17
6	Acetonitrile	—	R	(72.3)	(4.25)	(580)	3.0	4.17	2.85	1.17	41
7	Phenylacetylene	—	—	(68.2)	(4.54)	(452)	5.0	5.43	2.85	0.43	15
8	Propargyl bromide	—	—	(68.9)	(4.27)	(520)	3.3	5.19	2.85	1.9	67
9	Salicylaldehyde	—	—	(69.2)	(5.14)	(362)	4.9	5.09	2.54	0.19	7
10	β -Chloroethanol	D	—	(64.8)	(4.48)	(418)	3.75	6.75	2.85	3.00	106
11	β -Phenoxyethanol	D	—	(62.2)	(4.13)	(454)	6.18	7.98	1.65	1.80	109
12	Dichloromethane	D	—	(70.6)	(4.25)	(552)	3.16	4.65	2.85	1.49	52
13	Dimethoxymethane	E	—	134.5	5.83	532	4.33	5.24	2.85	0.89	31
14	Dibromomethane	D	—	(74.4)	(5.02)	(437)	3.56	3.64	2.85	0.08	3
15	Dibenzylamine	E	W	(60.7)	(5.04)	(290)	8.70	8.79	2.85	0.09	3
16	Diphenylamine	—	—	123.3	6.48	362	6.61	7.46	2.85	0.85	—

^a Run conditions: see Table II.

^b Source and grade: see Table II.

^c Elution data in parentheses from 8-ft. column.

^d Chain length: see Table II.

TABLE XII
GPC with Sx8 Gel of Other Compounds^a

Run	Compound	Source ^b		Elution, ml. ^c			Compared chain length, #C units ^d		New theory	Error D_1
		Co.	Grade	To peak	At base	(TPF)	Calc.	Obs.		
1	<i>p</i> -Chlorophenol-2THF	E	W	116.8	5.64	427	9.14	9.15		+0.01
2	<i>o</i> -Chlorophenol-2THF	E	X	120.6	6.24	374	8.15	8.12	Adds 2 THF	-0.03
3	Phenol-2THF	-	C	123.0	5.68	469	8.15	7.53		-0.62
4	Triphenylcarbinol-THF	E	W	107.5	7.65	197	12.07	12.27		+0.20
5	Benzophenone	E	W	127.3	6.04	367	6.52	6.56	Add all the pendant groups to get chain length	+0.04
6	Phenolphthalein-2THF	E	W	90.7	7.65	144	20.90	20.85		-0.05
7	Ionol-THF	-	C	109.2	6.63	270	12.15	11.63		-0.52
8	1,2,6-Hexanetriol-3THF	U	-	(52.7)	(4.45)	(280)	14.10	14.7		+0.6
9	2,4,6-Trichlorophenol	-	-	(61.0)	(4.73)	(332)	-	8.62		-0.52
10	Pentachlorophenol	-	-	(61.0)	(5.39)	(261)	-	8.62	Consider only the basic chain length	-0.52
11	Hexachlorobenzene	-	-	(73.0)	(6.05)	(291)	4.48	3.99		-0.49
12	Hexaethylbenzene	E	W	128.0	-	-	6.4	6.43		+0.03

^a Run conditions: see Table II.

^b Source and grade: see Table II.

^c Elution data in parentheses from 8-ft. column.

^d Chain length: see Table II.

TABLE XIII
 Deviation of Predicted GPC Elutions

Table no.	Compound type	Correction	Deviation, #C units ^a		No. compounds	
			Maximum	Average	Studied	Misfits
II	Straight chain	None	0.53	0.20	13	0
	Straight chain ^b	None	0.44	0.20	(7)	0
III	Polar linear	None	0.66	0.28	13	0
IV	Aromatics	C ₆ H ₃ = 2.85 #C	0.50	0.16	16	0
V	Methylated	CH ₃ = 1.0 #C	0.54	0.21	10	0
VI	Carbonyl	C=O = 0.8 #C	0.49	0.27	8	1
VII	Cyclic	—	0.53	0.17	7	0
VIII	Alcohols	H bonding	0.41	0.30	17	2
IX	Polar aromatics	"	0.45	0.26	10	0
X	Chlorinated	H bonding and Cl = 0.44 #C	0.55	0.40	11	0

^a Omits the values in parenthesis in the tables which reflect a doubtful degree of hydrogen bonding or cyclization; these are listed as misfits.

^b Data for 8-ft. column.

Elution times for a series of carbocyclic compounds were also studied; they have good agreement with the values predicted from the theoretical chain length (see Table VII).

The effect of methyl group branching on GPC elution volume was studied with a series of 16 branched chain compounds. Then the elution volumes were compared to the straight chain analogs. For example, isooctane eluted at about the same time as octene-1, a typical C₈ straight chain compound; further, 2,3-dimethylpentane came out very closely to the time observed with both heptene-1 and *n*-heptane. Also, with the xylenes, *p*-xylene served quite well as a model for predicting elution for the other two isomers. From these and the rest of the data, one may conclude that elution volume is probably controlled by the effective volume of the molecule, and our correlations are simply a relative measure of this. With all 10 branched compounds listed in Table V, the maximum deviation was 0.54 carbon atoms, and the average deviation was 0.2 #C units.

The current study includes results with eight carbonyl compounds in which the C=O group was not present at the end of a chain. The object was to be able to predict the change in elution due to this change in structure. The C=O group appeared to have the same effect on elution without regard to position on the chain, but the magnitude of this change would appear open to question. The length contribution of oxygen in the C=O group is equal to 0.61 #C units, and this was used as a correction to obtain the revised differences (*D*₂) listed in Table VI. However, the correction factor of 0.80 #C units gave a better correlation of the data, and this was used to obtain the new data given under the column headed by *D*₃ in Table VI.

Data with the ROH compounds did not conform to the simple chain length picture as observed in prior work. The differences (D_1) between the theory and observed apparent chain lengths were consistently around 2.5 #C units (3.1 A.); also, glycols having two OH groups per molecule differed from the calibration line by about five carbon atoms. Further thought lead to the theory that this corresponded to one THF per OH, and it was due to hydrogen bonding of the OH to the solvent. The differences (D_1) in the observed values for a wide group of straight chain OH compounds were compiled in Table VIII. The D_1 values were added and then divided by the total number of OH groups involved. This technique yields the value of 2.54 carbon atoms (3.18 A.) for the average apparent increase in length due to the hydrogen bonding of THF to each OH group of the solute. The D_1 values were then corrected by the 2.54 #C value, and the revised results are listed in Table VIII under column D_2 .

On much deliberation, it appeared that the OH compounds fell into two distinct groups, depending on the presence or absence of a β or γ ether group (which could yield a cyclic structure).^{13,14} With the latter structure, a value of 1.65 #C units is proposed for the apparent chain length increase per OH; for *n*-alkyl alcohols and related compounds, a value of 2.85 #C (3.54 A.) gave the best correlation. It is significant that 2.85 #C is also the value proposed above in this report to represent the apparent length of a phenyl group. With these new correction values, the new differences are listed in the last (D_3) column of Table VIII.

Further comment is needed as to the possibility that dimers and higher order products account for the apparent size increase of the alcohols studied. To explain the results observed with methanol, one would have to postulate an average aggregate size bigger than a trimer, and there appears to be no literature justification for this to occur in a base-type hydrogen-bonding solvent. Then, of necessity, one would assume the presence of significant amounts of dimer, trimer, tetramer, pentamer, etc. Such a mixture would give a greatly broadened or smeared curve, or the individual species would be separated. This was not observed. The constancy of the increased length (a 2.85 carbon atom increase) also is evidence for saying that the ROH compounds of this study have a high percentage of hydrogen bonding to the solvent. This is independent of polarity and solubility parameter, being applicable even to water. Also, diols are measured as having THF bonded to each OH group. The apparent hydrogen-bonding of chlorinated compounds to the THF gives additional support to this point; if they hydrogen bond to this solvent, why should not an alcohol exert an even stronger bonding to THF.

Results were collected for a series of aromatic compounds that contained polar groups, and these are listed in Table IX. In general, the agreement of the calculated and observed values was good, as tabulated in Table XIII. With a few compounds (such as phenol), further clarification was needed.

Chlorine atoms cause bulk in such compounds as CCl_4 , C_2Cl_6 , $\text{C}_2\text{Cl}_4\text{H}_2$,

and others; but less obviously, groups of chlorine atoms aid in hydrogen bonding in compounds such as CCl_3H .¹⁵ Hence, in a large portion of the chlorine compounds it will be hard to separate the effects of these two interactions—bulk and bonding—both acting in the same direction upon the elution, but differing in magnitudes. Since CCl_3H emerged much earlier than CCl_4 in GPC, it acts like a larger molecule than the CCl_4 by about 1.5 carbon atoms of length. This supports the concept that chloroform forms a hydrogen bond to the THF solvent, and further calculations support the opinion that almost 100% bonding of CCl_3H to the THF occurred. Other compounds with related structures possess an increased apparent chain length that can also be best explained by a high degree of hydrogen bonding. These include $\text{CCl}_3\text{CCl}_2\text{H}$, $\text{HCCl}_2\text{CCl}_2\text{H}$, CBr_3H , and CI_3H . Indeed, the THF appears to attach to both ends of $\text{HCCl}_2\text{CCl}_2\text{H}$, as judged by the apparent chain length equal to 8.79 carbon atoms (compared to 4.16 #C units for $\text{Cl}-\text{C}-\text{C}-\text{Cl}$). This is hard to explain on any basis other than bonding to the solvent.

In spite of the above factors, elution was studied with compounds having pendant chlorine atoms to find a rule that would apply to these compounds. Thus CCl_4 would be rated as having two pendant chlorine atoms. C_2Cl_6 has four, etc.; these results are summarized in Table X. On this basis, the average Cl group appears 40% effective to increase the chain length, compared to a chlorine group at the end of a chain. Data with bromine and iodine compounds appear too incomplete for such a correlation. An attempt was made to run some compounds that contained mostly bromine as substituents, but they appeared impure by GPC.

The usual process was reversed, and the GPC results were used to measure the apparent sizes of molecules. With propylene oxide and epichlorohydrin, the size of the epoxide ring was measured. GPC detected an average chain length increase of 0.1 #C units, which is close to no increase at all. GPC data for propylene sulfide indicated that this compound was four carbon atoms long, which would give full value to the sulfur atom (Table VII). This is an apparent inconsistency.

GPC is proposed as a basic tool with which to measure hydrogen bonding. This is based on finding that most alcohols exhibit almost 100% hydrogen bonding to the solvent in THF. Hence, the 2.85 #C atoms increase due to this bonding (or a modification of this length) has been used to measure per cent hydrogen bonding with some doubtful cases, such as mercaptans,^{9a} nitriles,¹⁶ and acetylenes.¹⁷ From the results in Table XI, one may deduce that about 100% hydrogen bonding occurred with chloroethanol and β -phenoxyethanol. In contrast, less than 10% bonding to the solvent was detected with the SH groups of either dodecanethiol or 1,2-ethanedithiol. Association to the 1:1 complex was observed with acetamide, and to a lesser extent with oleamide. Several compounds having a triple bond ap-

peared to complex to the solvent; this occurred with such diverse species as acetonitrile, adiponitrile, propargyl bromide, and phenylacetylene. However, the number of compounds of this type that were tested appears to be too small to result in any generalizations.

Intermolecular association was tested with salicylaldehyde. This compound showed an apparent chain length slightly larger than benzaldehyde would; this indicates the presence of a cyclic ring that contained the OH group. If hydrogen bonding had occurred, the length would be $>6.5 \#C$ units.

A group of working hypotheses are proposed to explain the elution of some of the larger molecules in GPC. For example, phenol eluted much earlier than can be predicted by the above concepts. The data support the conclusion that two THF groups are bonded to phenol, and such would be the case if the *para* hydrogen of this compound is bonded to the solvent. The literature indicates that it can do this.¹⁸ There appears to be a maximum size above which further substitution on an aromatic ring will not increase the apparent GPC size of a compound. In many cases, the data agree that this happens when the substituents are chlorine or ethyl groups. Some of this effect may be due to adsorption. In contrast, many big bulky compounds act as if all of their substituents should be counted, and these are listed as examples in Table XII. These groups include phenyl, ketone, *tert*-butyl, and THF bonded to an OH. For example, triphenylmethanol eluted at a place that corresponded to adding the chain length of the three phenyl groups, the carbon and oxygen in the center of the molecule and also a THF bonded to the OH group. Ionol gives a chain length that requires the addition of all the *tert*-butyl groups it contains, but no THF group need be added, in keeping with the concept of a sterically hindered OH. With the 1,2,6-hexanetriol, the correct answer is obtained if one assumes three THF molecules contribute to the chain length.

The theoretical plates/foot (TPF) values unexpectedly changed from compound to compound over a wide range in the current runs. This is of special concern, since these values are required to compute the theoretical plates needed for a desired separation and to obtain consistent and optimum correlations between GPC operators. Typical values include: dodecyl carbonate (100), triphenyl carbinol (197), phenolphthalein (144), ionol (270), *o*-dichlorobenzene (485), bromobenzene (465), toluene (517), benzene (568), pyridine (542), cyclohexane (507), *n*-nonane (496), isooctane (344), *n*-pentane (617), 3-methylpentane (451), acetone (623), and acetonitrile (798). This series of compounds would indicate that a lowered TPF value correlates with bulky and rigid molecules. Hence, perhaps the more flexible, smaller molecules have a more rapid rate of penetration through the constrictions of the gel. These aspects are still being studied. In any event, it is hoped that a table that contains these values will better allow a TPF value to be estimated by analogy for an unknown compound.

References

1. Moore J. C., *J. Polymer Sci.*, **A2**, 835 (1964).
2. Moore, J. C., and J. G. Hendrickson, *J. Polymer Sci.*, **C8**, 233 (1965).
3. Maley, L. E., *J. Polymer Sci.*, **C8**, 253 (1965).
4. Harmon, D. J., *J. Polymer Sci.*, **C8**, 243 (1965).
5. Boundy, R. H., and R. F. Boyer, *Styrene, Its Polymers, Copolymers and Derivatives*, Reinhold, New York, 1952, p. 426.
6. Glasstone, T. S., *Textbook of Physical Chemistry*, Van Nostrand, New York, 1940, (a) pp. 111-14; (b) p. 500.
7. Pauling, L., *The Nature of the Chemical Bond*, Cornell Univ. Press, Ithaca, N. Y., 1940.
8. Becker, E. D., *Spectrochem. Acta*, **17**, 436 (1961).
9. Pimentel, G. C., and A. L. McClellan, *The Hydrogen Bond*, W. H. Freeman and Co., San Francisco, 1960, (a) p. 150; (b) pp. 1-189; (c) pp. 193-201.
10. Ackermack, B., *Acta Chem. Scand.*, **15**, 985 (1961).
11. Determan, H., *Angew. Chem.*, **76**, 638 (1964).
12. Ackers, G. K., *Biochem.*, **3**, 723 (1964).
13. Buc, H., *Ann. Chim. (Paris)*, **8**, 409 (1963).
14. Trubnikov, I. S., and Y. A. Tentin, *Zh. Obshch. Khim.*, **32**, 3590 (1962).
15. Denisov, G. S., *Optika i Spektroskopiya*, **11**, 428 (1961).
16. Kosomer, W., and T. S. Sorensen, *J. Am. Chem. Soc.*, **83**, 3142 (1961).
17. Cook, D., *J. Am. Chem. Soc.*, **80**, 49 (1958).
18. Jakkur, S. K., and V. K. Phansalker, *J. Univ. Poona Sci. Technol.*, **22**, 27 (1962).

Résumé

On a élaboré des lois afin de prévoir l'élution de composés linéaires, ramifiés et polaires dans la G.P.C., sur la base d'essais sur 130 composés. Selon ces lois et dans le tétrahydrofurane comme solvant quelques composés seulement se trouvent sur une seule courbe d'étalonnage. L'élution de petites molécules varie parfois; ce qui est dû aux liens hydrogènes avec le solvant. En effet, ces variations se produisent avec les alcools, les acides et quelques composés chlorés, mais pas avec les mercaptans. Les isomères ramifiés et linéaires sont habituellement élevés jusqu'au même point. On peut conclure de cette étude que les éléments de structure sont additifs en ce qui concerne leur influence sur le volume d'élution.

Zusammenfassung

Gesetzmässigkeiten zur Voraussage des Eluierungsverhaltens linearer, verzweigter und polarer Verbindungen in GPC wurden auf der Grundlage von Testen an 130 Verbindungen abgeleitet. Mit diesen Gesetzmässigkeiten lagen für Tetrahydrofuran als Lösungsmittel alle mit Ausnahme einiger weniger Verbindungen auf einer einzigen Kalibrierungslinie. Bei kleinen Molekülen ändert sich die Eluierung wegen der Wasserstoffbindung zum Lösungsmittel oft; dies traf bei Alkoholen, Säuren und einigen chlorierten Verbindungen, nicht aber bei Mercaptanen zu. Verzweigte und lineare Isomere wurden bei etwa dem gleichen Punkt eluiert. Man kann daraus schliessen, dass sich die Strukturelemente in ihrem Einfluss auf das Eluierungsvolumen additiv verhalten.

Received June 7, 1965

Revised August 2, 1965

Prod. No. 4817A

Characterization of Ethylene-Propylene Block Copolymers by Proton Magnetic Resonance

ROGER S. PORTER, *Chevron Research Company, Richmond, California*

Synopsis

A high-resolution proton magnetic resonance compositional analysis has been developed for propylene polymers containing 0-40 wt.-% ethylene as either homopolymer or copolymer blocks. The test is independent of tacticity and provides qualitative information on copolymer sequencing and propylene chain structure. The analysis was developed using a series of standard reference polymers synthesized to contain various ratios of C^{14} -tagged ethylene and propylene. The compositional standards were established by radiotracer analysis for C^{14} and by preparing weighed physical mixtures of homopolymers. Spectra were obtained at $200 \pm 10^\circ C$. by placing externally heated polymer solutions into a conventional probe of a Varian A-60 proton spectrometer. All measurements were made on $\leq 10\%$ polymer solutions in diphenyl ether. Analyses are accurate to about $\pm 10\%$ at higher ethylene concentrations. The method is sensitive, with less precision, to below 1% for ethylene either as blocks or homopolymer.

High resolution PMR has been revealed as an excellent technique for polymer and copolymer analysis.¹⁻⁴ Additional information can also be gleaned from PMR analyses, such as tacticity and comonomer sequencing.

In this study, attention has been directed to the high resolution PMR studies of block copolymers and homopolymer physical mixtures of 0-40 wt.-% ethylene in propylene.

There seems to have been no previous report of an ethylene-propylene block copolymer analysis by high resolution PMR. A compositional analysis by PMR for ethylene-propylene rubbers has been suggested.²

Experimental

All polymers were tested in $\leq 10\%$ concentration and at $200 \pm 10^\circ C$. Resolution improves with increasing temperature and with decreasing polymer concentration. The solvent used throughout was diphenyl ether, Eastman White Label No. 104. In resolving power for these polymers it was better than other solvents, such as tetrachlorobenzene and 2-chlorothiophene; the latter tested at its boiling point near $120^\circ C$. PMR spectra obtained at ambient temperature on solutions of soluble (atactic) polypropylene were inadequately resolved for analysis, although spectra obtained with benzene as the solvent were distinctly better than those with chloroform and carbon tetrachloride. The technique used for preparing and rapidly analyzing the hot diphenyl ether polymer solutions

has been previously described.^{4,5} A Varian A-60 proton spectrometer was used at 100-sec. sweep time, 500 cycles/sec. sweep width, and near 10 amplitude. The spectrometer was zeroed at ambient temperature with 5% tetramethylsilane in carbon tetrachloride. The tests on hot polymer in diphenyl ether caused all peak positions to be shifted by about 0.5 ppm. The scale is therefore listed in arbitrary units. The polymer solvent may be used as an internal reference.

Results

Figure 1a shows the PMR spectrum of a polypropylene, commonly called atactic, which is soluble in boiling *n*-heptane. By origin and spectrum, this polymer likely contains up to about 40% syndiotactic placement, and by Natta definition may be called stereoblock.⁶ The spectrum is inherently complex, as a first-order theoretical calculation indicates the possibility of at least 15 peaks with considerable overlap between peaks because differences in chemical shifts are about the same magnitude as the splitting due to spin-spin coupling. Limited peak assignment is possible, however, because of partial resolution and published spectra for deuterated polypropylenes.⁷

The largest peak, at high field in Figure 1a, represents pendant methyls in propylene units. It is characteristically split by the tertiary hydrogen.

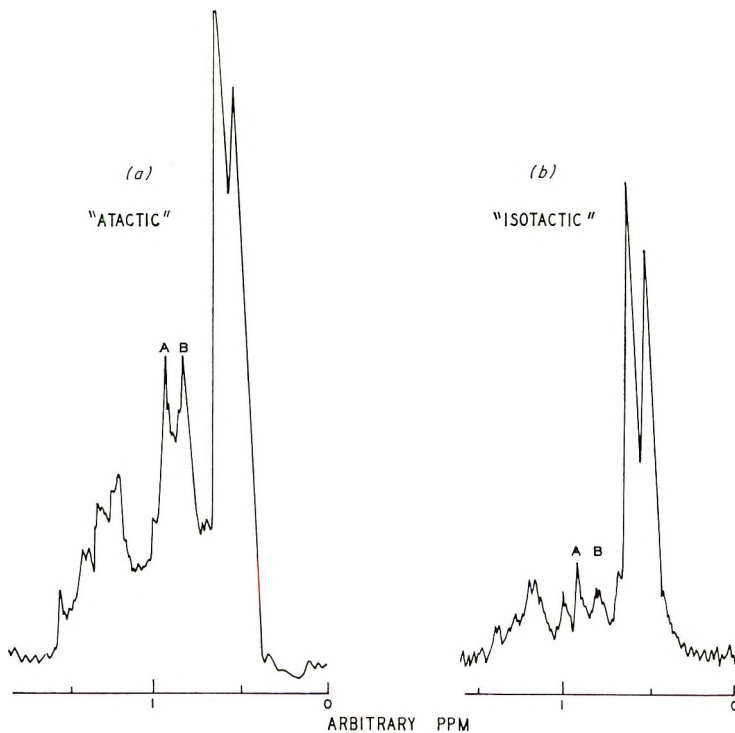


Fig. 1. PMR spectra for polypropylenes.

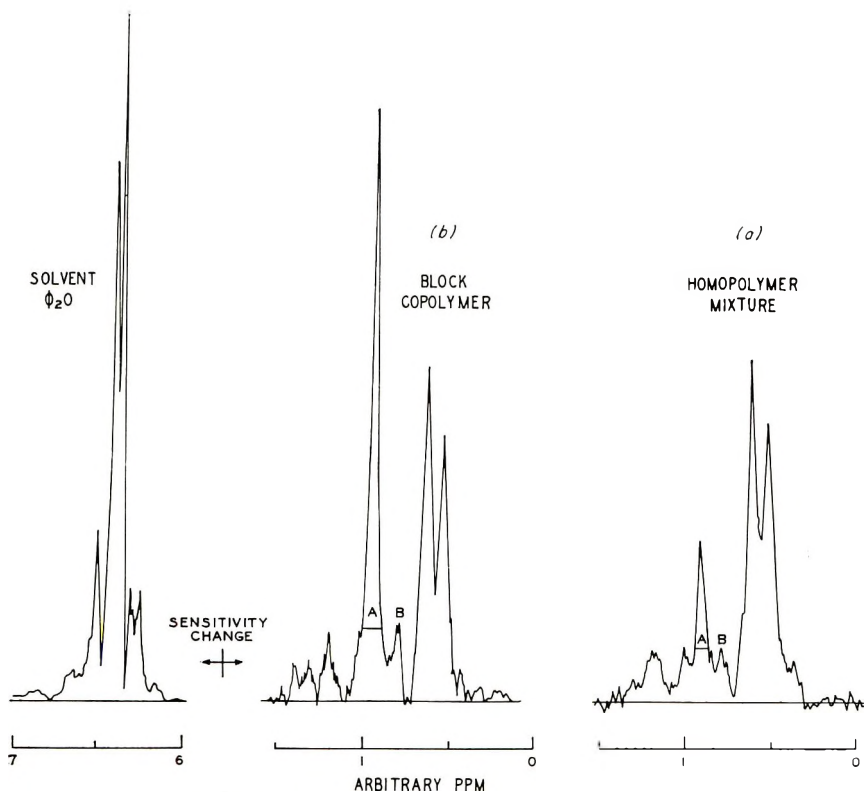


Fig. 2. PMR spectra for polymers of ethylene and propylene.

By area integration, about 20% of the nominal methyl proton peak is due to overlap of absorption from chain methylenes. This overlap is consistent with a reported syndiotactic triplet, two peaks of which are close to A and B in Figure 1a and a third peak which falls with the low field branch of the methyl split.⁷ The absence of a strong singlet peak in the methylene range indicates the virtual absence of "amorphous" polymer in the atactic polypropylene shown in Figure 1a^{6,7} which could possibly be due to head-to-head and tail-to-tail units. The low field peak represents the partial resolution of tertiary protons which are opposite the methyls on the hydrocarbon chain.

Figure 1b shows a spectrum for an isotactic polypropylene, $\geq 95\%$ isotactic by solubility ($\leq 5\%$ soluble in boiling heptane). This spectrum has the same general character as the atactic polypropylene. The important difference is a marked decrease of peak intensity in the chain methylene region. This decrease is caused by extensive splitting and the difference in chemical shifts for the nonequivalent methylene hydrogens in isotactic environments. This is in accord with the study of Stehling on deuterated polypropylenes, which indicates that much of isotactic methylene absorption is "buried" beneath the methyl and tertiary hydrogen peaks.⁷ The fractional area in the nominal methylene region of the spectrum is thus

sensitive to the number of isotactic and syndiotactic dyads and, therefore, may be used as a measure of polypropylene tacticity.^{3,6} A separate PMR study of tacticity in homopolypropylene has been presented elsewhere.⁵

The low field absorption in Figure 2, characteristic of aromatic hydrogens, is due to the polymer solvent, diphenyl ether, which was used throughout. Polymer concentrations in solution can be readily calculated from the ratios of peak areas adjusted to the same sensitivity.

Figure 2*a* shows the spectrum of a physical mixture of a polypropylene and a linear polyethylene. The superpositions of spectra that were obtained separately on the homopolymers show the same pattern, with different intensities, as spectra on physical mixtures. The polyethylene absorption falls on the peak marked A of the chain methylene complex in polypropylene. Peak B, also due to chain methylenes in polypropylene, is resolved in both spectra in Figure 2. Figure 2*b* gives the spectrum for an ethylene-propylene block copolymer. The ethylene contribution again falls on peak A, just as in separate results on homopolymers and on physical mixtures of the two homopolymers.

Analyses for physical mixtures and block copolymers have been developed based on the ratio of the incremental methylene area to the total polymer proton absorption. This concept has been tested by PMR analyses on an extensive series of physical mixtures and block copolymers synthesized with C¹⁴-labeled propylene and others with C¹⁴-labeled ethylene, as described in related papers.⁸ A most important feature of this analysis is that the methylene peaks A and B have virtually the same relative heights in polypropylenes with a variety of tacticities (note Fig. 1). This is also true for PMR spectra given by Satoh and others for a tactic series of polypropylenes.⁶ This suggests that PMR analyses for ethylene are independent of tacticity since the area increment of peak A above peak B has been used for analysis.

Qualitative polypropylene tacticities can be estimated by PMR not only for homopolymers (Fig. 1), but also in the presence of polyethylene and ethylene copolymer blocks. The relative heights of the peaks for secondary and for tertiary hydrogen in Figure 2 indicates that the polypropylene in the copolymer and the physical mixture is dominantly isotactic.

Table I gives analyses for a series of physical mixtures made up with tagged polypropylene. These intimate mixtures were prepared by weight from fine homopolymer powders and then analyzed by radiocount and PMR tests. The three sets of values are in good accord. The area ratio of incremental ethylene to the total PMR absorption is multiplied by a calibration factor of 1.30. This empirical factor apparently results from the regular increase in the height of reference peak B with ethylene content. This increase is the logical result of the small and reproducible spread of the chain ethylene peak and complicates but does not vitiate propylene tacticity estimations in the presence of ethylene. The empirical calibration factor for analysis was established from data on many known

TABLE I
Analyses of Linear Polyethylene-Polypropylene Physical Mixtures

Sample	Polyethylene, wt.-%		
	Made up	PMR	Tracer
6	5.0	4.6	4.2
7	9.0	8.6	7.6
5	17.0	16.7	16.3
8	34.0	31.1	31.0

TABLE II
Analyses of Linear Polyethylene-Polypropylene Physical Mixtures

Sample	Polyethylene, wt.-%	
	Made up	PMR
A	5.0	5.5
B	9.35	8.1
C	10.0	10.6
D	20.0	23.4
E	26.0	23.9

TABLE III
Analyses of Ethylene-Propylene Block Copolymers

Sample	Ethylene, wt.-%	
	PMR	Tracer ^a
3-30	2.9	6.0
3-31	6.3	9.1
3-32	12.7	14.9
3-40	12.2	18.1
3-41	15.5	18.6
3-35	24.2	25.3
3-34	36.2	36.0

^a C¹⁴ tagged ethylene.

physical mixtures and block copolymers. Tables I and II present most of the data used to establish the empirical calibration factor for block copolymer analysis. Each PMR result represents the average of two or more spectral analyses on the same sample.

Tables III and IV present sets of tracer analyses on ethylene-propylene copolymers and compare them with analyses developed using the PMR procedure described above. The analyses are in reasonable accord, though not in as close agreement as are the tracer and PMR analyses on physical mixtures. The PMR procedure analyzes only ethylene in blocks, whereas tracer techniques count all, irrespective of environment. Tables III and IV reveal that PMR analyses indicate generally lower ethylene concentrations than tracer analyses. This implies that a fraction of the ethylene is not in true blocks, although the difference may, in part,

TABLE IV
Analysis of Ethylene-Propylene Multisegment Block Copolymers

Sample	Ethylene, wt.-%	
	PMR	Tracer ^a
3-14 ^b	0.1	0
3-2	2.6	3
3-3	6.0	7
3-6	16.6	18

^a C¹⁴-tagged propylene.

^b Homopolypropylene.

be due to other causes. Random copolymerization units in appreciable concentrations are readily indicated by the broadening of the chain methylene absorption peak.

PMR analyses are accurate to about $\pm 10\%$ relative at higher (10-40 wt.-%) concentrations of chain ethylene in propylene. The analysis is insensitive to spectral resolution. With less precision, area measurements indicate that the method is sensitive to below 1% for ethylene either in blocks or homopolymer. Differences between PMR analyses for blocks and total ethylene content provide a measure of randomness in ethylene-propylene copolymerization.

References

1. Bovey, F. A., *J. Polymer Sci.*, **62**, 197 (1962).
2. Dudek, T. J., and F. Bueche, *J. Polymer Sci.*, **A2**, 811 (1964).
3. *Polymer Division Preprints*, **3**, No. 2, Appendix pages; Symposium on the Spectroscopy of Polymers, 142nd Natl. Meeting, American Chemical Society, Atlantic City, September 1962.
4. Porter, R. S., S. W. Nicksic, and J. F. Johnson, *Anal. Chem.*, **35**, 1948 (1963).
5. Porter, R. S., M. J. R. Cantow, and J. F. Johnson, paper presented to Division of Organic Coatings and Plastics Chemistry, 149th Natl. Meeting, American Chemical Society, Detroit, April 1965; *Preprints*, **25**, No. 1, 162 (1965); *Makromol. Chem.*, in press.
6. Satoh, S., R. Chûjô, T. Ozeki, and E. Nagai, *J. Polymer Sci.*, **62**, S101 (1962).
7. Stehling, F. C., *J. Polymer Sci.*, **A2**, 1815 (1964).
8. Barrall, E. M., II, R. S. Porter, and J. F. Johnson, paper presented to Division of Polymer Chemistry, 148th Natl. Meeting, American Chemical Society, Chicago, September 1964; *Preprints*, **5**, No. 2, 816 (1964); *J. Appl. Polymer Sci.*, **9**, 3061 (1965).

Résumé

On a mis au point un procédé d'analyse basé sur la résonance magnétique nucléaire à haute résolution de polymères de propylène contenant de l'éthylène de 0 à 40% en poids, aussi bien sous forme d'homopolymère que de blocs copolymériques. La mesure est indépendante de la tacticité et fournit des données qualitatives quant à l'ordonnance des séquences dans le copolymère et à la structure caténaire de l'homopolymère. La méthode a été étalonnée en synthétisant une série d'échantillons standards de polymères de référence contenant des rapports variables d'éthylène marqué au C¹⁴ et de propylène. La composition des échantillons a été établie par analyse de ratiotraceurs au C¹⁴ et en préparant par pesée des mélanges physiques d'homopolymères. Les spectres ont été

relevés à l'aide d'un spectromètre Varian A-60 à $200^{\circ}\text{C} \pm 10^{\circ}\text{C}$. Toutes les mesures ont été effectuées sur des solutions à $\leq 10\%$ du polymère dans l'éther diphenylique. La précision d'analyse est de $\pm 10\%$ aux plus hautes teneurs en éthylène, tandis qu'elle est sensible, avec une précision moindre, jusqu'au-dessous de 1% d'éthylène, présent tant sous forme de blocs que d'homopolymère.

Zusammenfassung

Eine hochauflösende protonmagnetische Resonanzzusammensetzungsanalyse wurde für Propylenpolymere mit 0–40 Gewichts% Äthylen als Homo- oder Copolymerblock entwickelt. Der Test ist von der Taktizität unabhängig und liefert eine qualitative Information über die Copolymersequenzen und die Struktur der Propylenkette. Die Analyse wurde an einer Reihe von Standardreferenzpolymeren entwickelt, welche mit einem variierten Verhältnis von C^{14} -markiertem Äthylen und Propylen synthetisiert worden waren. Die Zusammensetzungsstandards wurden durch Radiotraceranalyse auf C^{14} und durch Herstellung gewogener physikalischer Mischungen der Homopolymeren erhalten. Die Spektren wurden bei $200^{\circ} \pm 10^{\circ}\text{C}$ an von aussen geheizten Polymerlösungen im konventionellen Probenraum eines Varian A-60 Protonspektrometers gemessen. Sämtliche Messungen wurden an Lösungen mit einem Polymergehalt $\leq 10\%$ in Diphenyläther ausgeführt. Die Analysen besitzen bei hohen Äthylenkonzentrationen eine Genauigkeit von etwa $\pm 10\%$. Die Methode ist mit geringerer Genauigkeit brauchbar für Gehalte an Äthylen als Block- oder Homopolymeres unterhalb 1% .

Received May 20, 1965

Revised August 2, 1965

Prod. No. 4826A

Radiation-Induced Graft Polymerization of Styrene to Poly(vinyl Chloride)

TOSHIAKI TAKAMATSU and KENICHI SHINOHARA,

The Institute of Physical and Chemical Research, Bunkyo-ku, Tokyo, Japan

Synopsis

The radiation-induced graft polymerization of styrene to poly(vinyl chloride) (PVC) was investigated. Relations between the rate of grafting and the dose rate when the polymer is irradiated in liquid monomer or in monomer vapor, and between the rate of grafting and monomer concentration absorbed in the polymer have been investigated. The rate of grafting in monomer vapor was found to be far larger than that in liquid monomer. A high rate of grafting in monomer vapor was thought to result from a lower concentration of monomer in PVC during irradiation. An experiment carried out on PVC containing the monomer at various concentrations showed that the rate is largest at a monomer concentration of about 3.5 mole/l. and is smaller for higher and lower concentrations. On the assumption that the theory of homogeneous homopolymerization can be applied to this grafting reaction, the value of k_p^2/k_t has been obtained, where k_p and k_t are propagation constant and termination constant, respectively. The value of k_t greatly increases when the monomer concentration exceeds 3.5 mole/l. This increase of k_t can be accounted for if it is assumed that the monomer absorbed in the polymer works as a plasticizer and increases the molecular motion of the polymer. A measurement of the elastic modulus of PVC containing the monomer at various concentrations showed that this is, in fact, the case.

INTRODUCTION

There exist several methods of carrying out radiation-initiated graft polymerization. Among those, the method of grafting in monomer vapor¹⁻⁵ has several unique features, i.e., the amount of homopolymer produced is small, the separation and purification of graft copolymer is easy, and also the expenditure of monomer is small. In many cases it is also possible to get a larger degree of graft compared with other methods for the same absorbed dose. Vapor-phase grafting to polyethylene, poly(vinyl chloride), polytetrafluoroethylene, and some other polymers have previously been studied in our laboratory. Monomers used were styrene, acrylic esters, acrylonitrile, 4-vinylpyridine, and others.^{1,2}

The mechanism of other methods of grafting has been studied by a number of investigators.⁶⁻¹⁰ Only a few studies have been published, however, on the reaction mechanism of vapor-phase grafting. It is the purpose of the present work to obtain more information on vapor-phase grafting and to compare this process with liquid-phase grafting. Poly-

(vinyl chloride) (PVC) was chosen as the polymer and styrene as the monomer, since PVC is an amorphous polymer having a low degree of crystallinity and it can be swollen easily in styrene.

In the present paper, measurements were carried out on the relation between the rate of grafting and the dose rate when the polymer is irradiated in liquid monomer and in monomer vapor, and also on the relation between the rate of grafting and the concentration of monomer absorbed in the polymer. Some discussions of the mechanism of graft polymerization is presented.

EXPERIMENTAL

Poly(vinyl chloride) films, about 0.06 mm. thick (supplied by Kureha Chemical Co. Ltd.), were used. The films were washed by exhaustive extraction with hot benzene in a Soxhlet extractor to remove plasticizers. After extraction, the films were placed between two glass plates, dried in a thermostat at 60°C. for 24 hr., and evacuated in a high vacuum vessel for 3-4 days. Commercial styrene monomer was purified, before use, by distillation at a reduced pressure.

γ -Rays were from a 1000-curie Co^{60} source. The dose rate ranged from 4.2×10^2 to 1.7×10^5 r/hr. Electrons accelerated by a Van de Graaff generator giving 1.5 M.e.v. were also used. The dose rate was estimated to be about 1.0×10^5 rad/sec.

The arrangement for the irradiation by γ -rays in the monomer vapor is shown in Figure 1. A suitable amount of monomer was placed in the lower part of a glass ampule and poly(vinyl chloride) film in its upper part. The ampule was thoroughly degassed by a freezing-thawing cycle and was then sealed. The polymer film in the ampule was then irradiated while the lower part of the ampule containing the monomer was shielded

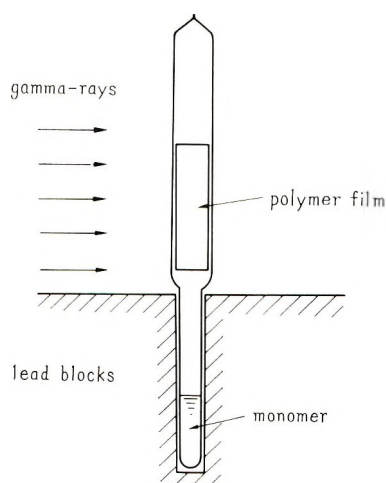


Fig. 1. Arrangement for irradiation in monomer vapor.

by lead blocks. After irradiation to various doses, the film was taken out and washed with benzene to remove homopolymer that may have been formed.

The degree of grafting g (in per cent) was defined, as usual, by the equation,

$$g = 100 (W - W_0)/W_0 \quad (1)$$

where W_0 and W are the weight of the film before and after grafting.

When the amount of the monomer grafted per liter of the graft polymer expressed in moles is required instead of the degree of grafting, the eq. (2) was used:

$$\frac{1000\Delta W}{m} = \frac{1000 (W - W_0)}{m\{(W_0/d_0) + [(W - W_0)/d]\}} \quad (2)$$

where d_0 and d are the density of the polymer and grafted monomer, respectively, ΔW is the weight of the monomer grafted per cubic centimeter

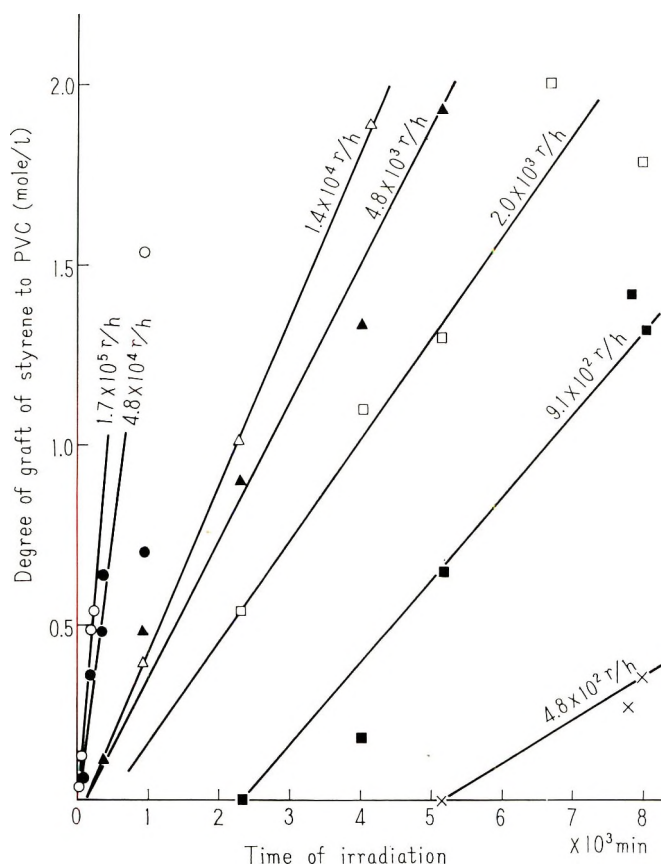


Fig. 2. Relation between the degree of grafting of styrene to PVC and the time of irradiation. Polymer irradiated in liquid monomer at room temperature.

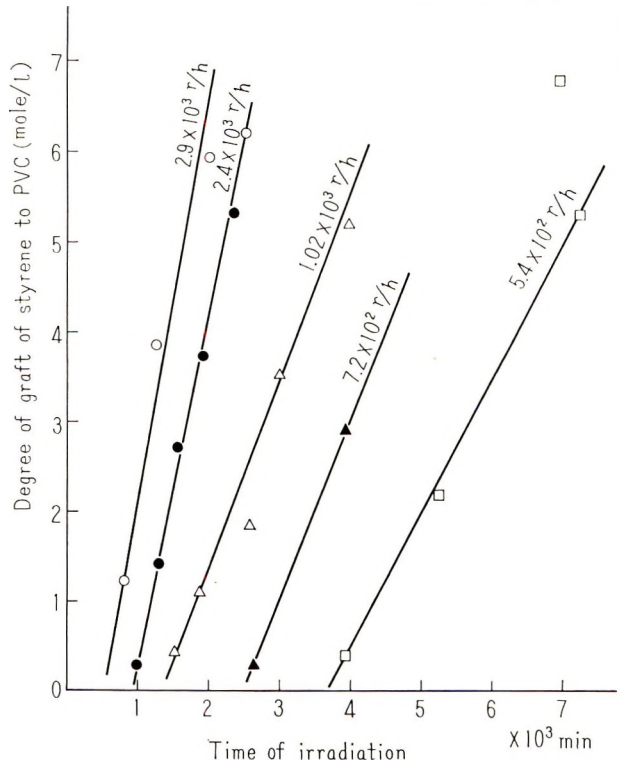
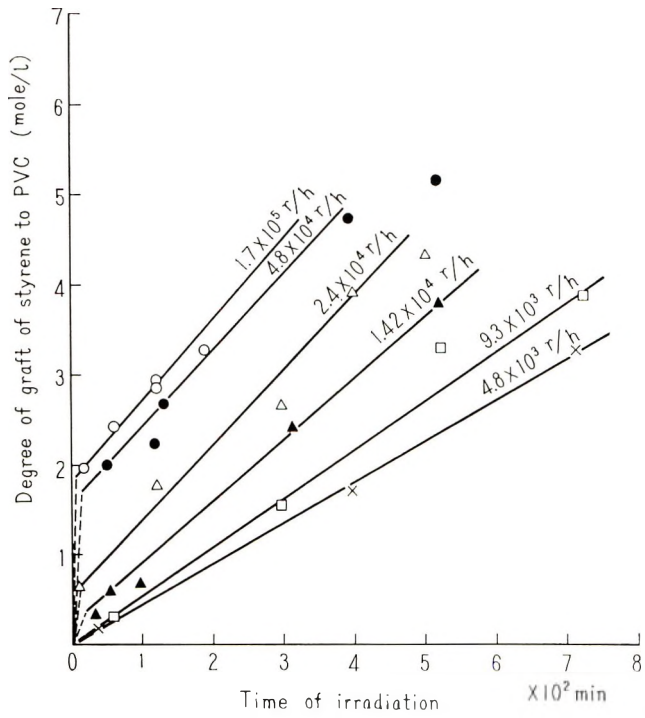


Fig. 3. Relation between the degree of grafting of styrene to PVC and the time of irradiation. Polymer irradiated in monomer vapor at room temperature.

of graft polymer, and m is the molecular weight of the monomer. Equation (2) is based on the assumption that the volume of graft polymer is always additive, without contraction or expansion of individual volume of grafted styrene and PVC.

The value of monomer concentration which is absorbed in the polymer can also be calculated by using a similar equation in which the monomer content is replaced by the absorbed monomer.

RESULTS

Effect of Dose Rate on the Rate of Grafting by γ -Irradiation

Figure 2 shows some of the results obtained for the relation between the degree of grafting of styrene to PVC and the time of γ -irradiation when the polymer is irradiated while immersed in liquid monomer. The degree of grafting, in most cases, increases linearly with the time of irradiation.

Figure 3 shows the same relation for irradiation of the polymer in monomer vapor. The degree of grafting increases with increasing time of irradiation in a similar way as in the case of liquid monomer. The efficiency of grafting is seen to be far larger when the polymer is irradiated in the vapor than in liquid.

From the slope of each curve, the rate of grafting defined as the increase of the degree of grafting per unit time was calculated. Figure 4a shows the

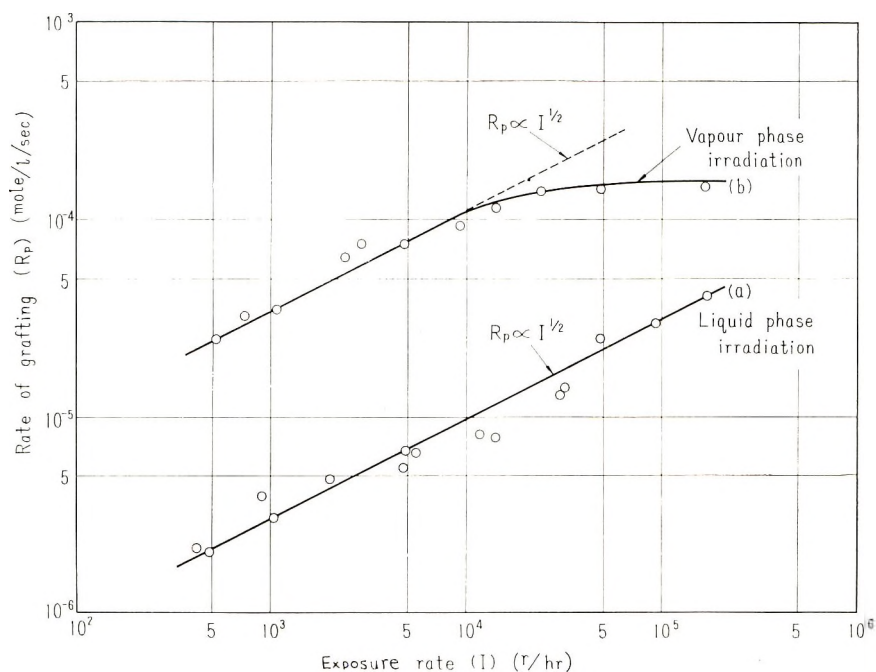


Fig. 4. Relation between the rate of grafting and exposure rate. Polymer irradiated in liquid monomer or monomer vapor at room temperature.

relation between the rate of grafting and the dose rate when the polymer is irradiated in monomer liquid. The rate of grafting R_P is seen to be proportional to the square root of dose rate within the range of 4.2×10^2 – 1.7×10^5 r/hr., the whole range of dose rate used.

Figure 4b shows the relation between the rate of grafting and the dose rate, obtained as the slope of solid curves in Figure 3. The rate of grafting is proportional to the square root of dose rate only in the range below 10^4 r/hr. At higher dose rates, the increase of the rate of grafting lessens and becomes almost independent of dose rate above 2×10^4 r/hr.

Graft Polymerization by Electron Irradiation

Figure 5 shows the relation between the degree of grafting and the absorbed dose when the polymer is irradiated in monomer vapor by electrons.

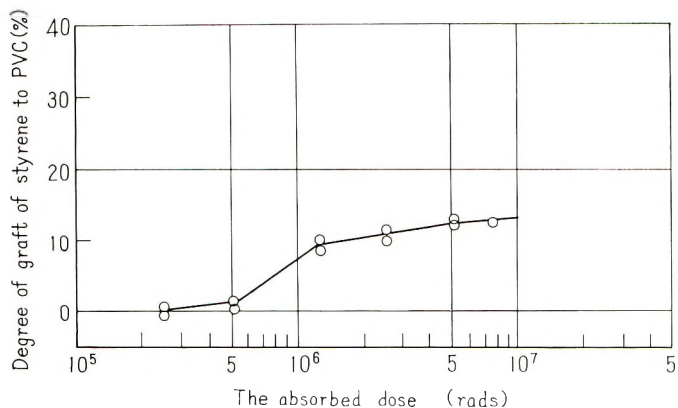


Fig. 5. Relation between the degree of grafting of styrene to PVC and the absorbed dose. Polymer irradiated in monomer vapor by electrons.

The dose rate is estimated to be about 1×10^5 rad/sec. In the range of absorbed dose below 1×10^7 rads, the grafting reaction occurs only to a small extent, and the efficiency of grafting is much smaller than that of γ -ray irradiation.

Concentration of Monomer Absorbed in PVC

When PVC is kept in styrene vapor or immersed in liquid styrene, the monomer gradually diffuses into the polymer. Figure 6a shows the relation between the concentration of styrene absorbed in the polymer and the time the polymer is kept in liquid styrene. The concentration of monomer in the polymer quickly attains its equilibrium value, which is about 5.2 mole/l. at 20°C . Figure 6b shows the increase of the concentration of the monomer absorbed in the polymer with time for polymer kept in the monomer vapor. The concentration increases only slowly with time and does not readily reach its equilibrium value.

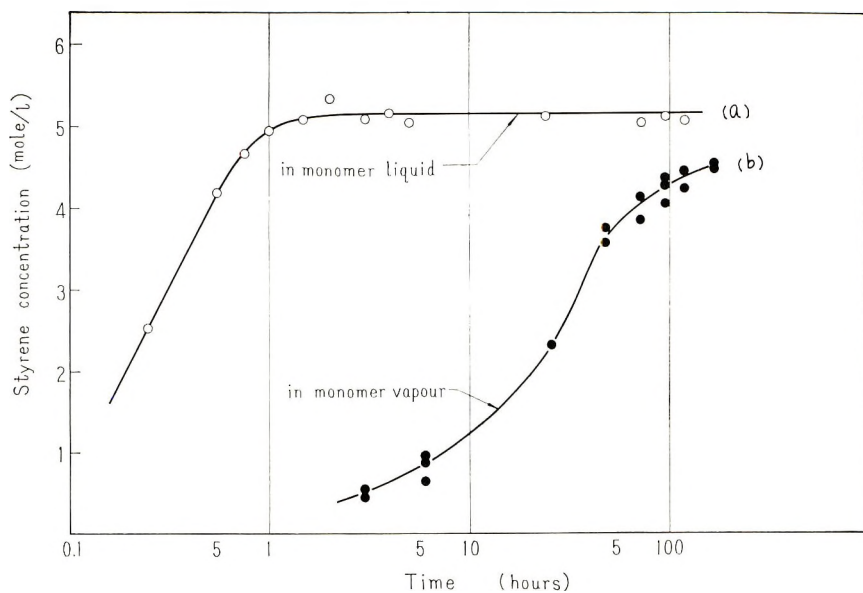


Fig. 6. Relation between the styrene concentration absorbed and the time of polymer-monomer contact for polymer kept in monomer vapor or immersed in liquid monomer.

Rate of Grafting and Monomer Concentration

PVC films were kept in oxygen-free styrene vapor at room temperature to absorb the vapor to a certain concentration in the polymer. PVC films containing styrene at various concentrations were thus prepared. Irradiation was carried out in the same styrene vapor with γ -rays from a Co^{60}

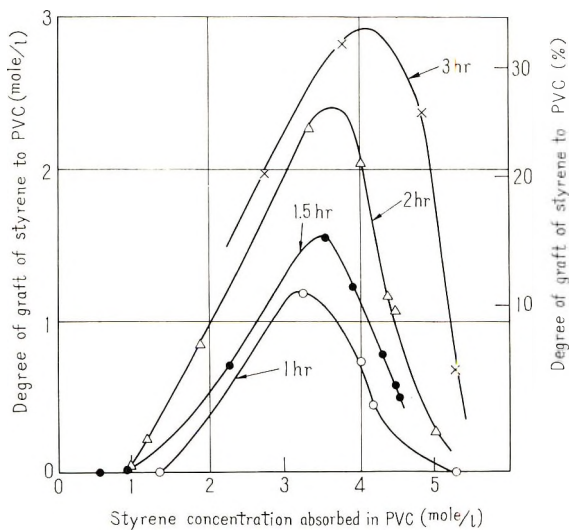


Fig. 7. Relation between the degree of grafting and styrene concentration absorbed in PVC for various irradiation times. Exposure rate: 4.8×10^4 r/hr.

source. The dose rate was 4.8×10^4 r/hr. Figure 7 shows the relation between the concentration of styrene at the beginning of irradiation and the degree of grafting for various irradiation times. The rate of grafting is small at low concentration, becomes larger as the concentration increases, and again becomes small at higher concentrations.

DISCUSSION

Liquid-Phase Grafting

In the liquid-phase grafting, irradiation of the polymer begins at high concentration of the monomer, since the time required to prepare the sample and to begin irradiation is long enough for the polymer to absorb the monomer to saturation of 5.2 mole/l. (Fig. 6a). During the course of the irradiation, the monomer in the polymer will be consumed in grafting, but fresh monomer will diffuse into the polymer to compensate the loss. The rate of diffusion and the degree of swelling were found experimentally to become greater as the degree of grafting increases.

The monomer can diffuse into the polymer at a rate of 1.4×10^{-4} mole/l.-sec. as is calculated from the initial slope of the curve in Figure 6a. The rate of expenditure due to grafting at the dose rate of 5×10^4 r/hr., for example, is estimated to be about 2.5×10^{-5} mole/l.-sec. from Figure 4a. Therefore, the monomer can diffuse into the polymer at a rate much larger than the rate of expenditure due to grafting. The graft polymerization will progress under the condition that the monomer concentration in the polymer is kept essentially constant and at a very high value.

Vapor-Phase Grafting

The situation under which vapor-phase grafting proceeds is more complicated. The irradiation usually starts about 20 hr. after the polymer is placed in the vapor. There is, therefore, some uncertainty in the concentration of the monomer when the irradiation starts, but it is probably in the range of 1.5–2.5 mole/l., as seen from Figure 6b. Moreover, the concentration will vary during irradiation.

At a very low exposure rate of $5\text{--}10 \times 10^2$ r/hr., the rate of consumption of the monomer will be $3\text{--}4 \times 10^{-5}$ mole/l.-sec. (Fig. 4b). The rate of diffusion of monomer into the polymer, on the other hand, is estimated from the initial slope of the curve in Figure 6b to be about 2.2×10^{-5} mole/l.-sec. The supply of the monomer by diffusion will, therefore, be nearly equal to the rate of consumption of the monomer into the polymer and the monomer concentration in the polymer will be kept nearly constant during graft polymerization at this low dose rate.

When the dose rate is more than 10^3 r/hr., the rate of diffusion of the monomer into the polymer will be smaller than the rate of monomer consumption by grafting, and the monomer concentration in the polymer should gradually decrease.

When the dose rate is more than 10^4 r/hr., the rate of consumption of the monomer will be more than 10^{-4} mole/l.-sec. The concentration of the monomer will decrease rather quickly during the course of grafting.

Since the degree of grafting should increase from zero, its increase in the early stage of irradiation should be as those given by the dotted curves. Figure 4b was plotted on the basis of the slope of the solid lines in Figure 3. Therefore, it gives, for dose rates higher than 10^4 r/hr., the relation between the rate of grafting and the dose rate, after the concentration has decreased considerably. If it were possible to estimate the rate of grafting from the dotted curves in Figure 3, the values at the starting concentration of the monomer would have been obtained. The result would, then, probably be that shown by the dotted line in Figure 4. We may, therefore, conclude that at the concentration of the monomer at which the irradiation was begun, the rate of grafting is proportional to the square root of the dose rate, also in the vapor-phase grafting.

On comparing the grafting in monomer liquid with that in monomer vapor, it is evident that the grafting in monomer vapor proceeds, at any dose rate, at a lower concentration of the monomer. It seems probable that the high rate of grafting in monomer vapor is due to the lower concentration during irradiation.

Rate of Grafting and Monomer Concentration

The data of Figure 7 were replotted in the form shown in Figure 8 for convenience; this latter figure shows the relation between the time of irradiation and the degree of grafting, taking the starting concentration of styrene as the parameter. The rate of grafting was then obtained as

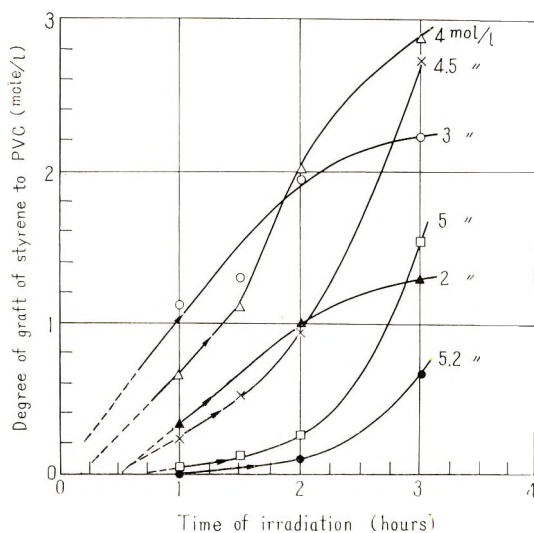


Fig. 8. Relation between the degree of grafting and the time of irradiation for various initial concentrations of monomer.

the slope of each curve in Figure 8, at the early stage of irradiation, and these values are plotted in Figure 9a against the concentration. A value of 5.2 mole/l. was obtained from the result of liquid-phase grafting obtained in Figure 5a, rather than from Figure 8, since liquid-phase grafting is supposed to proceed at this concentration and since it gave a more definite value. Since the concentration of the monomer was kept practically constant during the short time covered by this slope, this curve shows the relation between the rate of grafting and the concentration. The rate of grafting is seen to be largest at a concentration of about 3.2 mole/l. and is smaller for both lower and higher concentrations.

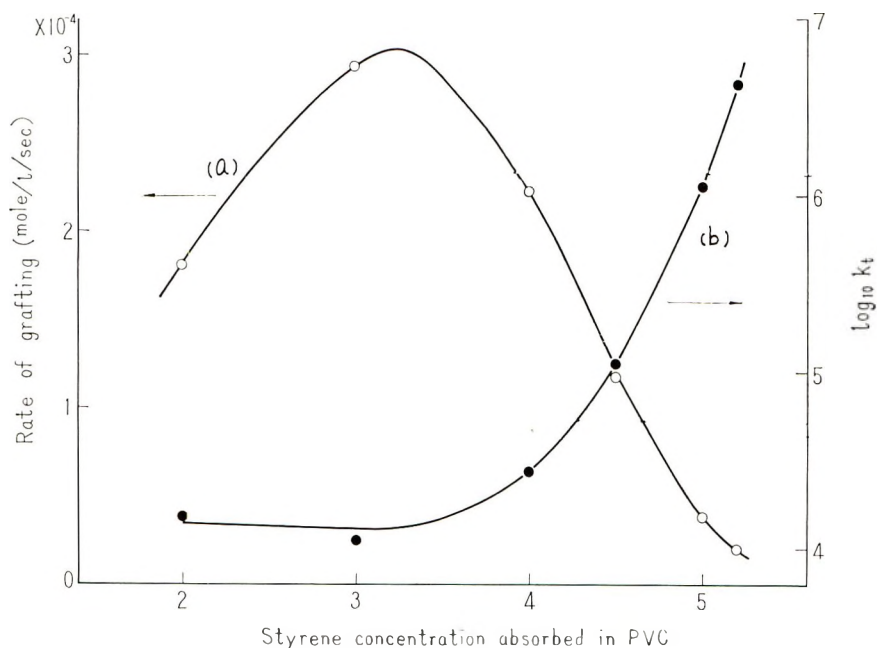


Fig. 9. Plots of (a) rate of grafting R_p and (b) k_t as functions of monomer concentration $[M]$.

A qualitative explanation can now be given for the behavior of the curves in Figure 8. As the consumption of the monomer will be more than the supply by diffusion at this high dose rate of 4.8×10^4 r/hr., the concentration will decrease gradually as the grafting reaction proceeds. At a starting concentration below 3 mole/l., the rate of grafting will become smaller as the concentration decreases and the rate of the increase of the degree of grafting with time decreases. At a starting concentration above 4.5 mole/l., the decrease of the concentration leads to a larger rate of grafting. At a concentration of 4 mole/l., the decrease of the concentration at first leads to a larger rate of grafting, but after the concentration decreases below the value corresponding to the peak of the curve *a* in Figure 9, the rate of grafting begins to decrease.

Consideration of Kinetics of Graft Polymerization

In order to understand the reaction mechanism in graft polymerization, it will be important to analyze the results in terms of reaction kinetics. It was, therefore, attempted to apply the theory of homogeneous homopolymerization to the graft polymerization reaction on the basis of the following assumptions: (1) the monomer is uniformly absorbed in the polymer, (2) the grafting reaction homogeneously takes place in the matrix, (3) the monomer concentration in the polymer is kept constant, (4) the rates of production and disappearance of the free radicals produced by irradiation are always kept at equilibrium values, and (5) chain transfer reactions from the grafted polystyrene radicals to the styrene monomer or PVC polymer can be neglected. Moreover, it was assumed that the number of free radicals contributing to the grafting reaction does not differ for different concentrations of the monomer. The applicability of these assumptions will be examined in detail later. The initiation of polymerization is the production of free radicals in the polymer. The G value for the production of the free radicals in PVC has been measured by many authors by means of electron spin resonance absorption methods.¹¹⁻¹⁶ The reported values ranged from 1.6 to 17 *in vacuo* at room temperature. This value is larger than that of radical production in styrene, which is about 0.5.¹⁷ The contribution of the radicals produced in styrene will, therefore, be neglected. It is assumed that all the radicals produced in PVC contribute to grafting. According to the theory for the stationary state reaction kinetics,^{17,18}

$$R_p = k_p[M](R_i/k_t)^{1/2} \quad (3)$$

where R_p is the amount in moles of styrene grafted per second per liter of PVC film containing styrene, $[M]$ is the concentration of styrene in moles per liter of PVC-styrene, k_p is the rate constant for propagation, k_t is the rate constant for termination by bimolecular combination or disproportionation, and R_i is the rate of initiation of the graft polymerization. R_i is given by

$$R_i = G\phi\rho_p/(6.023 \times 10^{25}) \quad (4)$$

where G is the G value of production of free radicals in PVC, ϕ is the rate of absorption of γ -ray energy by PVC in PVC-styrene film, expressed in electron volts per gram per second, and ρ_p is the mass of one liter of PVC-styrene in grams.

If the dose rate I is given in roentgens per second, ϕ may be obtained from

$$\phi = I \times 5.69 \times 10^{13} (n_{\text{PVC}}/n_{\text{PVC-st}})$$

where n_{PVC} and $n_{\text{PVC-st}}$ are the number of extranuclear electrons in PVC and the total number of extranuclear electrons in PVC-styrene, respectively.

Equation (3) can be written as

$$k_p^2/k_t = R_p^2/[M]^2R_t \quad (5)$$

This equation can be used in calculating k_p^2/k_t from the measured values of R_p , $[M]$, and R_t .

Table I gives the value of R_p obtained experimentally and the value of k_p^2/k_t calculated by using eq. (5). A G value of 3.2 obtained by Nitta et al.¹⁵ was used in the present calculation.

TABLE I
Values of k_p^2/k_t and k_t for Graft Polymerization^a

[M], mole/l.	R_t , mole/l.-sec.	R_p , mole/l.-sec.	k_p^2/k_t l./mole-sec.	k_t l./mole-sec.
2	4.08×10^{-8}	1.80×10^{-4}	1.99×10^{-1}	1.52×10^4
3	3.46×10^{-8}	2.92×10^{-4}	2.73×10^{-1}	1.11×10^4
4	2.84×10^{-8}	2.22×10^{-4}	1.08×10^{-1}	2.8×10^4
4.5	2.52×10^{-8}	1.17×10^{-4}	2.69×10^{-2}	1.12×10^5
5	2.22×10^{-8}	3.83×10^{-5}	2.64×10^{-3}	1.15×10^6
5.2	2.09×10^{-8}	2.0×10^{-5}	7.09×10^{-4}	4.27×10^6

^a Dose rate $I = 4.8 \times 10^4$ r/hr. = 7.55×10^{14} e.v./g.-sec. for poly(vinyl chloride).¹⁷

The value of k_p^2/k_t given in Table I may be compared with the value of k_p^2/k_t , obtained by various authors for the radiation-induced homopolymerization of styrene.¹⁹⁻²² The latter values are given in Table II. Our value of 7.1×10^{-4} l./mole-sec. obtained for the concentration of 5.2 mole/l. is slightly larger than the literature values. This fact may indicate that at this high concentration of monomer, graft polymerization reaction takes place in a similar way as the polymerization reaction in pure styrene.

TABLE II
Value of k_p^2/k_t for Homopolymerization of Styrene at 19°C.

k_p^2/k_t , l./mole-sec.	Reference
0.95×10^{-4}	Matheson et al. ¹⁹
1.14×10^{-4}	Tobolsky and Baysal ²⁰
1.66×10^{-4}	Tobolsky and Offenbach ²¹
0.87×10^{-4}	Chapiro and Wahl ²²

The value of k_p for graft polymerization is not known, but if it is allowed to assume, tentatively, that the value is the same as for homopolymerization of styrene, k_t can be calculated from the value of k_p^2/k_t .

The value of 55 l./mole-sec. was assumed,²¹ therefore, for k_p , and k_t was calculated. The result is given in the last column of Table I, and is also plotted against the concentration in Figure 9b. The value of k_t and hence the rate of recombination decreases rapidly as the concentration decreases from the value of 5.2 mole/l.

Now the assumptions made above should be examined. Assumptions (1)–(3) will be accepted in view of the facts that the thickness of the films used are thin, and the polymer can be easily swollen in the monomer. The monomer concentration in the polymer is kept constant and can be considered as constant in the vapor also, so long as the initial stage of irradiation is considered.

As to the assumption (4), it can be shown that the concentration of free radicals quickly attains an equilibrium value as soon as the irradiation starts, and the reaction takes place, practically, at its equilibrium state.

The growth of the concentration r of free radicals will be governed by

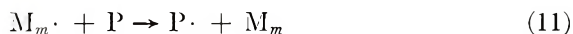
$$dr/dt = R_i - k_t r^2 \quad (6)$$

Since $r = 0$ at $t = 0$, we have, from this equation,

$$r = (R_i/k_t)^{1/2} \tanh (t/\tau) \quad (7)$$

where $\tau = (k_t R_i)^{-1/2}$ is the time constant for the concentration of free radicals to reach equilibrium. The value of τ can be calculated by using the value of k_t given in Table I. Even for the lowest concentration of the monomer, the value obtained was only 40 sec. Therefore, the concentration of free radicals attains its equilibrium value in quite a short time in all cases.

Concerning the assumption (5), following chain transfer reactions may deserve consideration:



where P represents the polymer (PVC), M the monomer (styrene), $M\cdot$ the styrene radicals, $M_m\cdot$ the styrene homopolymer radicals, $P\cdot$ the PVC radicals and $PM_m\cdot$ the grafted polymer radicals.

The extent to which chain transfer reactions (8) and (9) occur may be estimated from a consideration of the pertinent chain transfer constants. Chain transfer from PVC and the graft copolymer radicals to styrene monomer, i.e., reactions (8) and (9), would be expected to be negligible because of the reported value²³ of 6×10^{-5} for the self-transfer constant of styrene at 60°C. Chain transfer constants for reactions (10) and (11) are not known. The chain transfer from styrene homopolymer radicals to PVC, reaction (11), can be neglected because the G value of radical production of styrene homopolymer is much less than that of PVC, and also, because reactions (8) and (9) can be neglected. The only chain transfer reaction which must be considered would be reaction (10). At present we have no approach to the determination of rate constants for this chain reaction. The degree of polymerization of grafted polystyrene

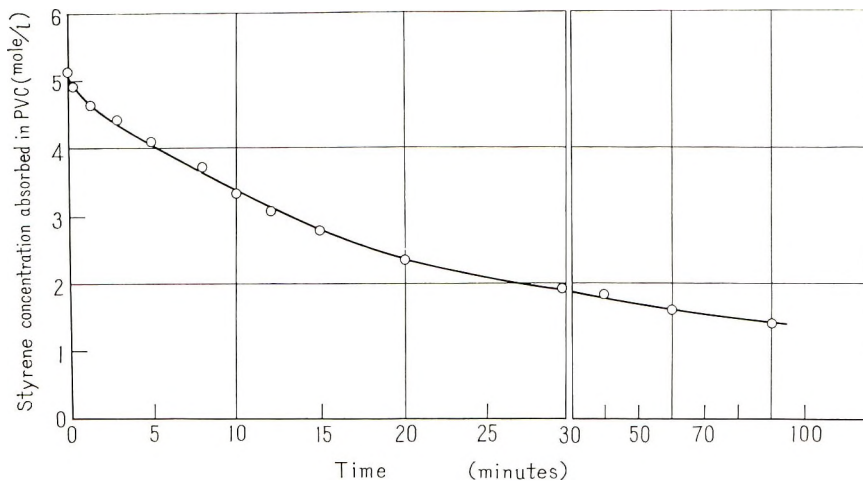


Fig. 10. Relation between the monomer concentration in the polymer and the time allowed to stand in air.

would be largely modified by this reaction. However, the rate of grafting R_p is only concerned with the increase of polystyrene grafted per unit time and independent of the distribution of the length of grafted branches. Therefore the conclusion derived above from R_p experimentally determined will not be much affected by the chain transfer reactions.

Molecular Motion of the Polymer and the Rate of Grafting

The treatment given above has shown that the value of k_t changes greatly as the concentration of the monomer is varied. Since k_t is a measure of recombination of active centers at the end of the growing chain, its value will be easily affected by the molecular motion of the chain. In the case of graft polymerization, this motion of grafted branches will, in turn, be influenced by the molecular motion of the polymer. The fact that the value of k_t changes with the concentration suggests that the concentration has a large effect on the molecular motion of the polymer.

The glass transition temperature of PVC is about 82°C .²⁴ Below this temperature the polymer is in a glassy state and the molecular motion is frozen. When the temperature rises above the transition temperature, the polymer changes from a high-viscosity glass to a low-viscosity state of a more or less viscous liquid. The changes of glass transition temperature on mixing the polymer with other compounds has already been observed by several authors. For example, a measurement of dielectric dispersion and loss carried out by Fuoss,²⁵ on a mixture of PVC and diphenyl showed that the glass transition temperature gradually decreased as the amount of diphenyl increased. It was also observed that low molecular esters added to various derivatives of cellulose,²⁶ butyl esters added to GR-S rubber,²⁵ water absorbed in poly(vinyl alcohol) all worked as plasticizers and lowered the glass transition temperatures of the respective polymers.

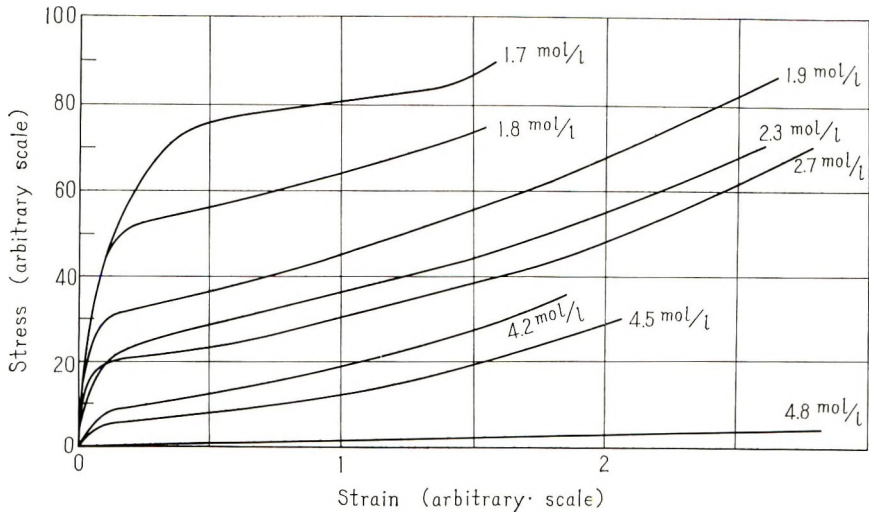


Fig. 11. Stress-strain curves of PVC films containing various amounts of styrene.

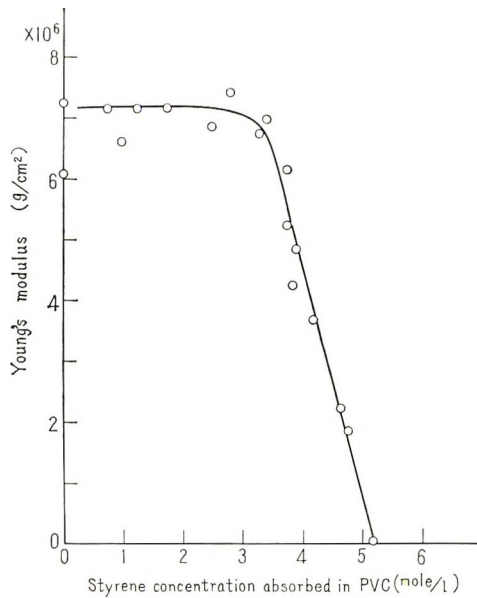


Fig. 12. Relation between styrene concentration in PVC and the modulus of elasticity.

As styrene used as monomer in our experiment is similar in molecular structure to diphenyl, it was thought that styrene worked as a plasticizer and promoted the molecular motion of the polymer. The following experiment was, therefore, carried out.

A piece of PVC film was immersed in styrene and left in the liquid for a time sufficient for styrene to reach saturation concentration. It was then taken out and left in the air at room temperature. The monomer evaporated and the concentration decreased with time as shown in Figure 10.

This experiment provided us with PVC films of various concentrations. In this way PVC films of various styrene concentration having a dimension of 2 mm. \times 25 mm. were prepared and Young's modulus was measured on them.

Figure 11 shows the relation between the stress and strain for various concentrations of the monomer. The film which was measured immediately after removal from the liquid and which therefore contains monomer at saturation concentration, does not show elastic property but plastic deformation. When the monomer concentration decreases below 4 mole/l., the film begins to show elastic properties of an ordinary polymer.

The relation between the Young's modulus in the elastic region and the concentration of the monomer was obtained from Figure 11, and is shown in Figure 12. It shows that below 3.5 mole/l., Young's modulus does not change appreciably from its original value of PVC by absorption of the monomer, but when the concentration exceeds that value the Young's modulus rapidly decreases and becomes very small at the concentration of 5.2 mole/l.

This result may be explained if we consider that the monomer absorbed in the polymer acts as plasticizer and allows the motion of the polymer molecule which had hitherto been frozen. The glass transition temperature is considered to have dropped below room temperature at a concentration in the neighborhood of 3.5 mole/l.

Figure 12 may be compared with Figure 9, which shows the relation between the value of k_t and the concentration. The concentration at which Young's modulus shows a rapid decrease corresponds to the concentration in Figure 12 at which k_t begins to increase. This result may be taken as the evidence showing that both Young's modulus and k_t are governed by the same molecular motion. It will further indicate that below the concentration of 3.5 mole/l., the molecular motion is not much affected by absorption of the monomer, and above that the glass transition temperature rapidly falls till it becomes lower than room temperature.

The authors wish to thank Dr. E. Fukada of this laboratory for helpful discussion and suggestions and Prof. S. Yoshida of Gakushuin University for his interest in this work.

References

1. Shinohara, K., and T. Takamatsu, *Rika Gaku Kenkyusho Hokoku*, **36**, 562 (1960); *ibid.*, **37**, 285 (1961); *ibid.*, **38**, 1, 409 (1962).
2. Takamatsu, T., *Rika Gaku Kenkyusho Hokoku*, **37**, 1 (1961).
3. Shinohara, Y., M. Kashiwagi, and E. Mukaibo, *Nippon Isotope Kaigi Hobunshu*, **2**, 137 (1958).
4. Kadonaga, M., A. Furuhashi, and M. Ono, *Nippon Isotope Kaigi Hobunshu*, **4**, 100 (1963).
5. Kadonaga, M., F. Ueda, and K. Kimura, *Nippon Isotope Kaigi Hobunshu*, **4**, 103 (1963).
6. Restaino, A. J., and W. Reed, *J. Polymer Sci.*, **36**, 499 (1959).
7. Odian, G., M. Sobel, A. Rossi, and R. Klein, *J. Polymer Sci.*, **55**, 663 (1961).
8. Chandler, H. W., E. J. Henley, and E. N. Trachtenberg, *Int. J. Appl. Radiation Isotope*, **13**, 239 (1962).

9. Mock, R. A., and W. N. Vanderkooi, *J. Polymer Sci.*, **56**, 69 (1962).
10. Odian, G., M. Sobel, A. Rossi, R. Klein, and T. Acker, *J. Polymer Sci.*, **A1**, 639 (1963).
11. Lawton, E. T., and J. S. Balwit, *J. Phys. Chem.*, **65**, 815 (1961).
12. Kuri, Z., H. Ueda, and S. Shida, *J. Chem. Phys.*, **32**, 371 (1960).
13. Atchison, G. J., *J. Appl. Polymer Sci.*, **7**, 1471 (1963).
14. Kuri, Z., H. Ueda, and S. Shida, *Doitai To Hashasen*, **2**, 495 (1959).
15. Ohnishi, S., Y. Ikeda, M. Kashiwagi, and I. Nitta, *Polymer*, **2**, 119 (1961).
16. Nitta, I., Y. Ikeda, S. Ohnishi, R. Kashiwagi, and S. Sugimoto, *Rept. Japan Assoc. Radiation Res. Polymer*, **1**, 183 (1959); *ibid.*, **2**, 219 (1960).
17. Chapiro, A., *Radiation Chemistry of Polymeric Systems*, Interscience, New York, 1962, p. 173.
18. Walling, C., *Free Radicals in Solution*, Wiley, New York, 1957, p. 54.
19. Matheson, M. S., E. E. Auer, E. B. Bevilacqua, and E. J. Hart, *J. Am. Chem. Soc.*, **73**, 1700 (1951).
20. Tobolsky, A. V., and B. Baysal, *J. Polymer Sci.*, **11**, 471 (1953).
21. Tobolsky, A. V., and J. Offenbach, *J. Polymer Sci.*, **16**, 311 (1955).
22. Chapiro, A., and P. Wahl, *Compt. Rend.*, **238**, 1803 (1954).
23. Mayo, F. R., R. A. Gregg, and M. S. Matheson, *J. Am. Chem. Soc.*, **73**, 1691 (1951).
24. Wood, L. A., *J. Polymer Sci.*, **28**, 318 (1958).
25. Fuoss, R. M., *J. Am. Chem. Soc.*, **61**, 2334 (1939); *ibid.*, **63**, 369, 378 (1941).
26. Mandelkern, L., and P. J. Flory, *J. Am. Chem. Soc.*, **73**, 3206 (1951).
27. Brietman, L., *J. Appl. Phys.*, **26**, 1092 (1955).
28. Sone, Y., and I. Sakurada, *Kobunshi Kagaku*, **14**, 151 (1957).

Résumé

La polymérisation greffée par irradiation du styrène au chlorure de polyvinyle (PVC) a été étudiée. Des relations entre la vitesse de greffage et la vitesse d'exposition, quand le polymère est irradié dans le monomère en phase liquide et en phase gazeuse, et entre la vitesse de greffage et la concentration en monomère absorbé dans le polymère ont été étudiées. La vitesse de greffage dans le monomère en phase vapeur est beaucoup plus grande que celle dans le monomère liquide. On croit que la vitesse élevée de greffage dans le monomère en phase vapeur résulte du fait de la présence d'une plus petite concentration en monomère dans le PVC durant l'irradiation. Une expérience, faite sur du PVC contenant du monomère à différentes concentrations, montre que la vitesse est la plus grande pour une concentration en monomère d'environ 3,5 mole/l et plus petite pour des concentrations plus élevées et plus basses. En admettant que la théorie de l'homopolymérisation en phase homogène peut être appliquée à cette réaction de greffage, la valeur kp^2/kt a été déterminée, kp et kt étant respectivement les constantes de propagation et de terminaison. La valeur de kt augmente considérablement quand la concentration en monomère dépasse les 3,5 mole/l. Cette augmentation peut être expliquée par le fait que le monomère absorbé dans le polymère agit comme plastifiant et augmente la mobilité moléculaire du polymère. Une mesure du module d'élasticité du PVC contenant du monomère en différentes concentrations montre que ceci est en effet le cas.

Zusammenfassung

Die strahlungsinduzierte Pfropfpolymerisation von Styrol auf Polyvinylchlorid (PVC) wurde untersucht. Die Beziehungen zwischen der Aufpfropfgeschwindigkeit und der Bestrahlungsintensität bei Bestrahlung des Polymeren im flüssigen Monomeren und in seinem Dampf sowie zwischen der Aufpfropfgeschwindigkeit und der Konzentration des im Polymeren absorbierten Monomeren wurden untersucht. Die Aufpfropfgeschwindigkeit im Monomerdampf war weitaus grösser als diejenige im flüssigen Monomeren. Es wurde angenommen, dass die hohe Aufpfropfgeschwindigkeit im Monomerdampf durch eine niedrigere Monomerkonzentration im PVC während der Bestrahlung bedingt ist.

Ein Versuch mit PVC, das Monomeres in verschiedener Konzentration enthielt, zeigte, dass die Geschwindigkeit bei einer Monomerkonzentration von etwa 3,5 Mol/l am grössten und für höhere und niedrigere Konzentrationen kleiner ist. Mit der Annahme, dass die Theorie der homogenen Homopolymerisation auf diese Pfropfreaktion angewendet werden kann, wurde ein Wert für k_p^2/k_t erhalten, wo k_p und k_t die Wachstums- bzw. die Abbruchskonstante sind. Der Wert von k_t nimmt bei Monomerkonzentrationen oberhalb 3,5 Mol/l stark zu. Diese Zunahme von k_t kann man verstehen, wenn man annimmt, dass das im Polymeren absorbierte Monomere als Weichmacher wirkt und die Molekülbewegung des Polymeren erhöht. Eine Messung des Elastizitätsmoduls von PVC mit verschiedenen Monomerkonzentrationen zeigte, dass dies tatsächlich der Fall ist.

Received November 17, 1964

Revised May 28, 1965

Prod. No. 4827A

Relationship between the Ionic Nature of Some Organoaluminum-Transition Metal Catalysts and the Rate of Polymerization

R. D. BUSHICK and R. S. STEARNS, *Research and Development, Sun Oil Company, Marcus Hook, Pennsylvania*

Synopsis

The electrical conductivity of several trialkylaluminum and alkyl-aluminum halides was investigated in dry benzene at 25°C. within the concentration range of 10^{-1} – $10^{-3}M$. The equivalent conductance of the trialkylaluminum systems decreased in the following order: $Al(n-C_6H_{13})_3 > Al(n-C_{10}H_{19})_3 > Al(n-C_4H_9)_3 > Al(i-C_4H_9)_3 > Al(n-C_3H_7)_3 > Al(C_2H_5)_3$. The conductance ($1/R$) of a given series was also examined and found to decrease as each alkyl group was successively replaced by a chlorine atom, thus: $Al(C_2H_5)_3 > Al(C_2H_5)_2Cl > Al(C_2H_5)_{1.5}Cl_{1.5} > Al(C_2H_5)Cl_2$ and $Al(i-C_4H_9)_3 > Al(i-C_4H_9)_2Cl > Al(i-C_4H_9)Cl_2$. The ion pair dissociation constants K were calculated and show in a qualitative manner the difference between various organoaluminum systems. The relative rate of olefin polymerization was related to the conductivity of various organoaluminum-transition metal catalyst systems used. The effect of Lewis bases such as monoglyme, diglyme, triglyme, and tetraglyme on triethylaluminum indicated that the first-mentioned base forms a 1:1 type of complex as ordinary ethers do, whereas the remaining three bases utilize only two of their available oxygen atoms to coordinate with triethylaluminum. The effect of $TiCl_3$ (in the presence of an ether) on the conductance was also determined.

INTRODUCTION

Although the use of organoaluminum compounds in connection with olefin polymerization is well known, relatively little has been published concerning the nature of the ionic species present in various polymerization systems. The study of ionic species in solvents of low dielectric constant in particular has received little attention even though the literature contains a vast amount of information on polymerization in such solvents. One of the most obvious ways of attempting to gain information concerning the behavior of ionic systems is by examining their electrical conductivity, although we are well aware that quantitative data are often difficult to obtain. Kraus¹ and more recently Day, Barnes, and Cox² have studied alkali metal picrates and substituted thiocyanates in benzene and sodium aluminum alkyls in toluene and diethyl ether, respectively. Nicolescu and Angelescu³ investigated the relationship between catalytic activity and electric conductivity of the soluble catalyst system $Al(C_2H_5)_3-Ti(OC_4H_9)_4$.

The complexes formed between certain aluminum alkyls and Lewis bases have been studied potentiometrically,⁴ conductometrically,⁵ calorimetrically,^{5,6} and more recently by infrared⁷⁻⁹ and NMR.^{10,11} The addition of electron-donor molecules to Lewis acid systems are known to have tremendous effects on the rate of polymerization as well as on the nature of the polymer formed.¹²⁻¹⁷

We have studied the electrical conductivity of several trialkylaluminum compounds and some alkylaluminum halides in addition to the effect of added Lewis bases and TiCl_3 on the conductivity and have attempted to correlate the ionic nature of the species involved in some qualitative way with various polymerization systems such as the relative rate of polymerization of ethylene and propylene and the copolymerization of these monomers. We have also shown a correlation between the relative rate of ethylene polymerization in solvents of varying dielectric strength and the conductance of the catalyst system in these solvents.

EXPERIMENTAL

Materials

Reagent-grade benzene was dried over anhydrous calcium sulfate. The benzene was subsequently distilled from metallic sodium in an inert atmosphere of nitrogen at atmospheric pressure. The center cut was collected and stored in quart crown-cap bottles over sodium ribbon under nitrogen pressure. The organoaluminum compounds, ethers, vanadates, and titanium chlorides were obtained from commercial sources.

The organoaluminum compounds were used without further purification. The 1M solutions of these compounds in benzene were made up by weight in a dry box under an atmosphere of dry nitrogen.

The ethers (monoglyme, diglyme, triglyme, and tetraglyme) were freed of peroxides by chromatography on an alumina (Woelm-basic) column and then distilled from calcium hydride under reduced pressure. The 1M ether solutions in dry benzene were stored in pint crown-cap bottles over calcium hydride under nitrogen.

The vanadium compounds were distilled *in vacuo* and stored under nitrogen pressure in a dry box. The 1M solutions in dry benzene were stored under nitrogen pressure.

Pyridine was purified by treatment with potassium hydroxide, fractionally distilled, and stored in a crown-cap bottle under nitrogen pressure.

The titanium (III) chloride and titanium (IV) chloride were used as received to make 1M solutions in heptane, benzene, or mixtures of these solvents. The titanium (III) chloride was ground *in situ* in the desired solvent to keep it in suspension.

In the preparation of all stock solutions, precautions were taken to exclude contamination by air or moisture.

Apparatus

A constant direct source of 45 v. was supplied by dry cell batteries.

The voltage was constantly monitored by means of a precision voltmeter. The current was read from a precision electrometer which was equipped with a decade shunt. Minimum full scale of this particular instrument was 2×10^{-12} amp. and minimum measurable current was 5×10^{-14} amp. Leads to the electrometer and the conductivity cell were fully shielded. A diagram of the apparatus is shown in Fig. 1.

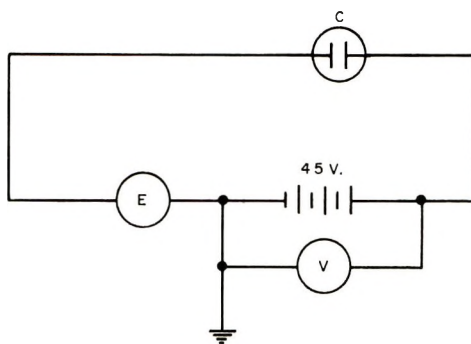


Fig. 1. Conductivity apparatus: (C) conductivity cell; (E) electrometer; (V) voltmeter. R_x is calculated by $R_x = R_s(E_1 - E_2)/E_2$, where R_x is the unknown resistance, R_s is the current range, E_1 is the constant voltage supply, and E_2 is the electrometer reading.

The conductivity cell was a 100-ml. bottle with a 14/20 ground glass taper. A nitrogen inlet located near the neck was used to maintain a blanket of dry nitrogen within the cell at all times. The electrodes were platinum, and the geometry of the cell was such that the cell constant was found to be 0.94 by using standardized potassium chloride solutions. This cell was used for all of the organoaluminum studies with and without added Lewis bases. Another similar cell having a cell constant of 0.89 was used for the vanadium-organoaluminum studies. The top of the cell was fitted with a male 14/20 stem that was inserted into a Teflon sleeve which in turn contained a silicone septum at the end. The thermostat was an oil bath, large enough to contain the cell, a motor-driven stirrer, and a coil through which water was circulated from a large water bath maintained at $25.00 \pm 0.02^\circ\text{C}$.

A hypodermic syringe with a Teflon plunger was used in connection with a spring-loaded three-way stopcock, located between the end of the syringe and the needle, so as to obtain a constant nitrogen purge during transfer of material to the cell.

Measurements

The conductance cell was thoroughly dried prior to each run by baking in an oven at 110°C . overnight. Usually, enough solvent (35 ml.) was

charged to the cell, using a hypodermic syringe, to bring the liquid level slightly above the electrodes. An atmosphere of dry nitrogen was maintained within the cell at all times. A small sample of the particular compound to be studied was added and the current change was noted and recorded after equilibration. The conductivity ($1/R$) of the dry benzene was observed to be about 10^{-11} mho. All measurements were done while agitating the solution by means of Teflon-coated magnetic stirring bar.

Calculation of Dissociation Constant K

A plot of conductance ($1/R$, where R is the measured resistance) versus the square root of concentration in moles per liter gave a rather good reproducible linear correlation for all organoaluminum compounds with the exception of isobutylaluminum dichloride and diisobutylaluminum chloride. From the intercept of such a plot a value of $1/R_0$ was obtained and the conductance measurements were corrected by this value. Conductance values were chosen from the smoothed line drawn through the experimental points since there was little deviation of the experimental points from the straight line. A value of the conductance at zero concentration (λ_0) was obtained from a plot of λ' versus $C^{1/4}$, where

$$[(1/R) - (1/R_0)]/C \equiv \lambda'$$

and C = concentration. The degree of dissociation α was taken to be λ'/λ_0 , and from a plot of $(1 - \alpha)/\alpha^2$ versus C , a value for the dissociation constant (K) was obtained from the slope. The values of the equivalent conductance (Λ) were calculated by multiplying λ' by $1000k$, where k is the cell constant.

RESULTS AND DISCUSSION

Relationship Between Conductance and Ionic Polymerization Systems

The electrical conductivity of triethylaluminum, diethylaluminum chloride, ethylaluminum sesquichloride, ethylaluminum dichloride, tri-*n*-propylaluminum, tri-*n*-butylaluminum, triisobutylaluminum, diisobutylaluminum chloride, isobutylaluminum dichloride, tri-*n*-hexylaluminum, and tri-*n*-decylaluminum was determined in benzene at 25°C. Because of the low dielectric constant of benzene ($\epsilon = 2.27$) and because the Lewis acids examined are such weak electrolytes, one would not expect them to dissociate to a very large extent into discrete solvent-separated species, but rather into ion pairs, triplets, and possibly higher ion aggregates.¹⁸⁻²⁰ Such ion formation may be represented as $[ABA]^+$ and $[BAB]^-$, where the triple ions will be more stable due to the excess potential energy in a solvent of low dielectric constant. Ion aggregates more complex than triple ions may also be expected in such solvents.^{21,22} In benzene the concentration of free ions is exceedingly low, and therefore one may neglect ion atmosphere effects.²³

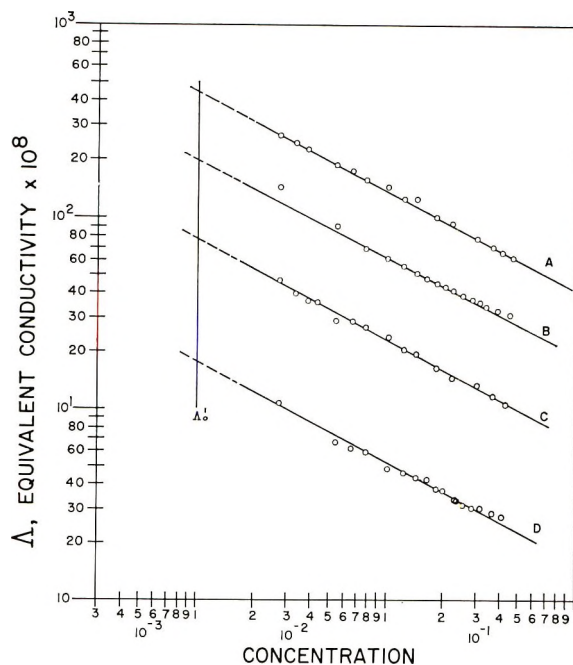


Fig. 2. Equivalent conductivity of the ethylaluminum series at 25°C. as a function of concentration: (A) $\text{Al}(\text{C}_2\text{H}_5)_3$; (B) $\text{Al}(\text{C}_2\text{H}_5)_2\text{Cl}$; (C) $\text{Al}(\text{C}_2\text{H}_5)_{1.5}\text{Cl}_{1.5}$; (D) $\text{Al}(\text{C}_2\text{H}_5)\text{Cl}_2$.

Using our data we found that a plot of the logarithm of equivalent conductance versus the logarithm of concentration for all organoaluminum systems investigated except diisobutylaluminum chloride and isobutylaluminum dichloride was linear with a slope of -0.51 , an example of which is illustrated in Figure 2. This is in good agreement with the theoretical slope of -0.50 (Ostwald dilution law). Behavior of this type is expected when the conductance is determined by an ionization governed by the law of mass action when the principal species is the ion pair and the dissociation constant is small.^{18,24}

The equivalent conductance of the aluminum trialkyls in benzene were found to decrease in the following order: $\text{Al}(n\text{-C}_6\text{H}_{13})_3 > \text{Al}(n\text{-C}_{10}\text{H}_{19})_3 > \text{Al}(n\text{-C}_4\text{H}_9)_3 > \text{Al}(i\text{-C}_4\text{H}_9)_3 > \text{Al}(n\text{-C}_3\text{H}_7)_3 > \text{Al}(\text{C}_2\text{H}_5)_3$. We cannot explain at this time the inverted order of $\text{Al}(n\text{-C}_6\text{H}_{13})_3$ and $\text{Al}(n\text{-C}_{10}\text{H}_{19})_3$. The trialkylaluminum compounds containing long alkyl groups are thought to form smaller, more simple, ion pairs immediately upon dissociation; whereas the compounds with shorter alkyl groups (such as ethyl) exist as dimers to begin with and would have a tendency to first form more complex ion pair aggregates which then would dissociate into smaller ion pairs and would be expected to have lower mobility and carry less current. The ethyl and isobutyl series were investigated further to determine the order of conductivity within a given set as an alkyl group was successively replaced by a chlorine atom. The conductance of these two sets of organo-

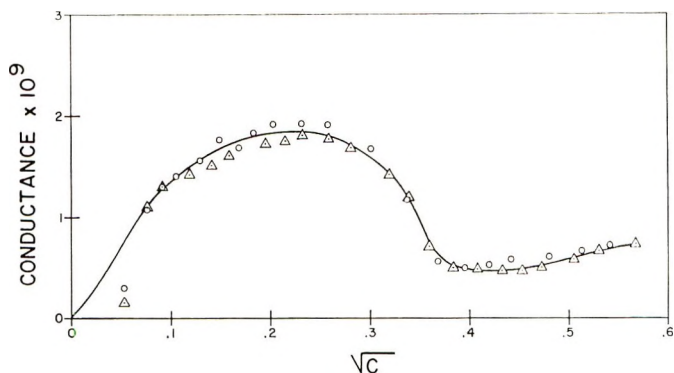
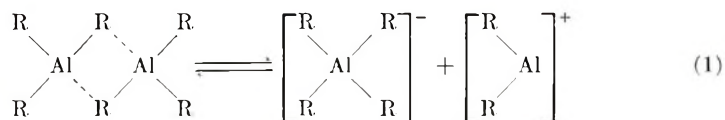


Fig. 3. Conductance of diisobutylaluminum chloride as a function of concentration (in moles per liter) for duplicate experiments.

aluminum compounds was found to decrease as expected in the following order: $\text{Al}(\text{C}_2\text{H}_5)_3 > \text{Al}(\text{C}_2\text{H}_5)_2\text{Cl} > \text{Al}(\text{C}_2\text{H}_5)_{1.5}\text{Cl}_{1.5} > \text{Al}(\text{C}_2\text{H}_5)\text{Cl}_2$ and $\text{Al}(i\text{-C}_4\text{H}_9)_3 > \text{Al}(i\text{-C}_4\text{H}_9)_2\text{Cl} > \text{Al}(i\text{-C}_4\text{H}_9)\text{Cl}_2$. The conductance decrease parallels the increased tendency for halogenated aluminum alkyls to coordinate²⁵ more readily, forming complex ion pair aggregates which must further dissociate into simple ion pairs. The magnitude of the conductance in our work was comparable to that determined for triethylaluminum by Bonitz.⁵

A general scheme for the autodissociation⁵ of aluminum alkyls and related halides can be represented as shown in eq. (1).



This scheme was based for the most part on the reaction between sodium aluminum tetraethyl and dialkylaluminum halide which has been known for many years. One may conceive of other more complex ion pair aggregates such as $(\text{Al}_2\text{R}_5)^+$ and $(\text{AlR}_4)^-$ and so on being involved and contributing to the conductivity.

The conductance behavior of diisobutylaluminum chloride and isobutylaluminum dichloride differed from the typical behavior exhibited by the other organoaluminum compounds studied. Rather than a steady, linear increase in conductance with the square root of the concentration, in moles per liter, as was obtained with the other systems examined, one obtains a curve as is evident from the data plotted in Figure 3. These data were all found to be reproducible, and therefore the trend is assumed to be real. The increase, decrease, and eventual increase in conductance may be looked upon as being due to ion formation and association followed by dissociation along with additional ions being produced as the concentration is increased. The curvature for isobutylaluminum dichloride was

less prominent than for diisobutylaluminum chloride, which is shown in Figure 3.

An idea of the extent of dissociation of complex aggregates already discussed can be obtained from the dissociation constant K for the various alkyl aluminum compounds studied and calculated as described in the experimental section and summarized in Table I. The dissociation constants indicate that for the ethylaluminum series the dissociation is of the order of about 3×10^{-3} attributable to the formation of complex aggregates which tend to dissociate more readily than the smaller ion pairs more logically anticipated for the higher aluminum alkyls. An approximate tenfold difference exists between the ethylaluminum series and the higher alkyl series.

TABLE I
Dissociation Constants for Organoaluminum Compounds Studied at 25°C.

Aluminum compound	K
$\text{Al}(\text{C}_2\text{H}_5)_3$	3.2×10^{-3}
$\text{Al}(\text{C}_2\text{H}_5)_2\text{Cl}$	3.8×10^{-3}
$\text{Al}(\text{C}_2\text{H}_5)_{1.5}\text{Cl}_{1.5}$	2.4×10^{-3}
$\text{Al}(\text{C}_2\text{H}_5)\text{Cl}_2$	2.5×10^{-3}
$\text{Al}(n\text{-C}_3\text{H}_7)_3$	5.7×10^{-4}
$\text{Al}(n\text{-C}_4\text{H}_9)_3$	8.1×10^{-4}
$\text{Al}(i\text{-C}_4\text{H}_9)_3$	8.0×10^{-4}
$\text{Al}(n\text{-C}_6\text{H}_{13})_3$	8.7×10^{-4}
$\text{Al}(n\text{-C}_{10}\text{H}_{19})_3$	8.9×10^{-4}

For convenience the value of Λ'_0 was taken at a concentration of $10^{-2}M$ (Fig. 2) as being indicative of the ionic nature of each system studied. Taking the Λ'_0 values as relative differences between each Lewis acid, one can correlate them with the relative rate of polymerization of propylene, with TiCl_3 as the cocatalyst.²⁶ This is illustrated in Figure 4. All other parameters being held constant, one can readily see that a definite relationship exists between the ionic nature of the organoaluminum compound and the relative rate of propylene polymerization.

More recently, Gippin²⁷ investigated the stereoregular polymerization of butadiene with alkylaluminum chlorides and cobalt octoate in benzene. He varied the solvent ($\epsilon = 2.27\text{--}10.2$) and found the rate of polymerization to be proportionally dependent upon the magnitude of the dielectric constant of the solvent. A mechanism of catalysis based on ion pairs such as $[\text{Et}_2\text{Al}]^+ [\text{EtAlCl}_3]^-$ was postulated. Ion pairs have also been shown to be the major species in the anionic polymerization of styrene.²⁸ We have found a similar correlation involving the maximum conductivity of the catalyst system ethylaluminum sesquichloride-titanium (IV) chloride, as a function of the solvent composition. The solvents used were benzene ($\epsilon = 2.27$), heptane ($\epsilon = 1.92$), and mixtures thereof. The change in the conductivity of the catalyst with time was examined in each solvent for

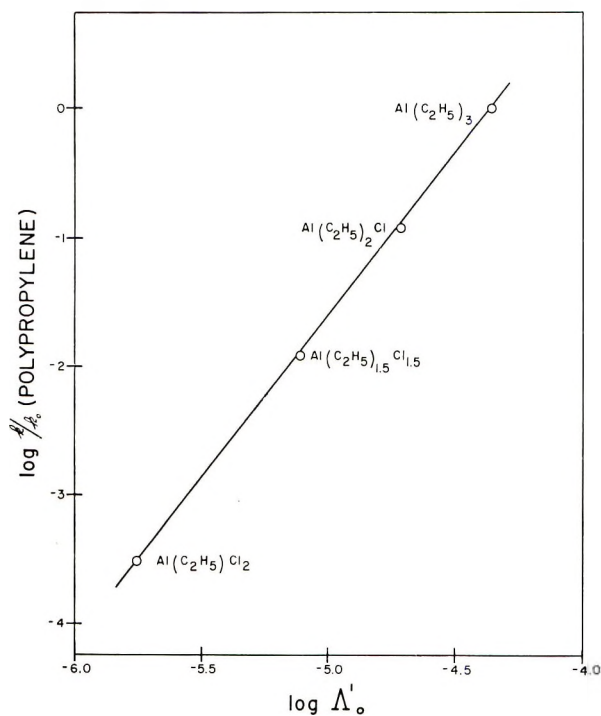


Fig. 4. Relative rate of propylene polymerization as a function of equivalent conductivity at Λ'_0 .

the catalyst system mentioned at an Al/Ti mole ratio equal to 0.5. A typical curve is shown in Figure 5. The maximum conductance ($1/R_{\max}$) was taken as representative of the catalyst system under consideration, and in each case we have taken the ionic species to be $(\text{AlR}_2)^+ (\text{RTiAlCl}_7)^-$ based on our knowledge of the system and the literature.²⁹ The length of time necessary for the maximum conductance to be reached was found to increase from 50 to 175 min. as the solvent system was changed from benzene to heptane. The decrease in conductance is attributed to the reduction of Ti(IV) to Ti(III), accompanied by the formation of less conducting titanium compounds as well as insoluble species. The maximum of the conductivity curve shifts with time as the solvent system is changed. This shift is attributed to the greater stabilization of Ti(IV) in benzene as compared to heptane (Table II), presumably due to the formation of a charge transfer complex³⁰ in the former solvent.

The relative rate of ethylene polymerization,³¹ plotted as a function of the logarithm of the maximum conductivity ($1/R_{\max}$) of the catalyst system in solvents of varying dielectric constant was found to be linear (Fig. 6). This suggests that the rate of polymerization is proportional to some constant times the logarithm of $1/R_{\max}$, where $1/R_{\max}$ is a measure of the concentration of the ionic species present in the catalyst system. Our data indicate a decrease in the relative rate of polymerization of ethyl-

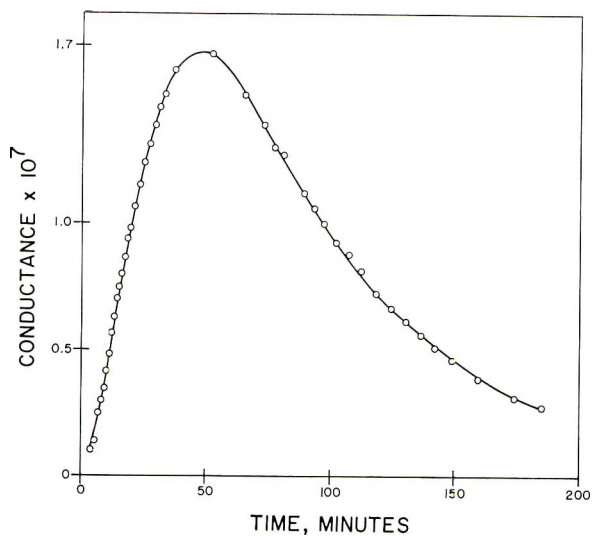


Fig. 5. Conductance of ethylaluminum sesquichloride-titanium(IV) chloride as a function of time in 100% benzene.

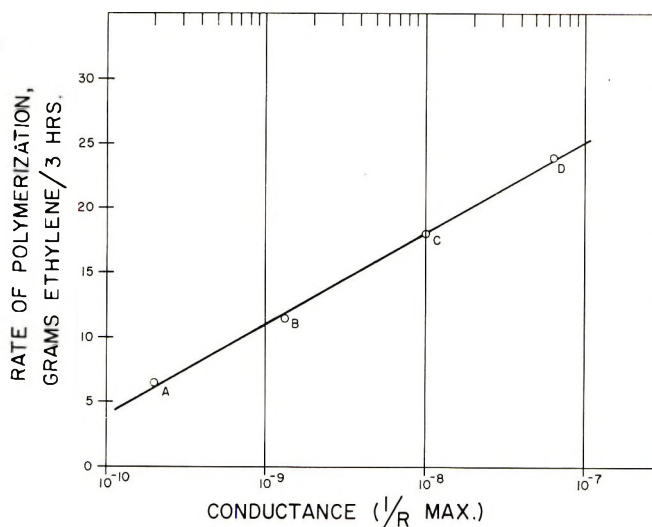


Fig. 6. Rate of ethylene polymerization as a function of maximum conductance of the ionic catalyst species in various solvents for the catalyst system $\text{Al}_2(\text{C}_2\text{H}_5)_3\text{Cl}_3$ - TiCl_4 : (A) heptane (100%); (B) heptane (30%), benzene (70%); (C) heptane (70%), benzene (30%); (D) benzene (100%).

ene as the dielectric constant of the medium is decreased. Others^{27, 32-36} have shown the pronounced effect of the dielectric constant on the polymerization rate for a variety of polymerization systems.

Proceeding still further, we have also investigated the electrical conductivity of several esters of orthovanadic acid in the presence of an aluminum alkyl. The concentration of the vanadium compound was

TABLE II
Conductance-Rate Data for the Catalyst System Ethylaluminum Sesquichloride-Titanium(IV) Chloride in Benzene-Heptane Mixtures

Solvent	Conductance $1/R_{\max}$, mho	Rate, g. $C_2=$ /3 hr. ^a	Time to $1/R_{\max}$, min.
Benzene (100%)	1.67×10^{-7}	23.7	50
Benzene (70%)– heptane (30%)	1.0×10^{-8}	17.5	75
Benzene (30%)– heptane (70%)	1.4×10^{-9}	11.1	140
Heptane (100%)	2.0×10^{-10}	6.2	175

^a Data of Antonsen.³¹

constant while the Al/V ratio varied during the addition of diisobutylaluminum chloride, eventually reaching a value of 15–20. The systems examined were: $VO(O-n-C_4H_9)_3$, $VO(OC_2H_5)_3$, $VO(OC_2H_5)_2Cl$, and $VO(OC_2H_5)Cl_2$, each in the presence of $Al(i-C_4H_9)_2Cl$. The conductance (Table III) decreased in the order: $VOCl(OC_2H_5)_2 > VOCl_2(OC_2H_5) > VO(OC_2H_5)_3 > VO(O-n-C_4H_9)_3$, the maximum conductivity occurring at an Al/V mole ratio in the range of 4–8. If one plots the rate of copolymerization³⁷ of ethylene and propylene against the maximum conductivity for each system, a correlation can be obtained, again indicating a relationship between the ionic character of the catalyst system involved and the polymerization rate (Fig. 7). (It has been assumed that the conductivity characteristics of the organoaluminum component used

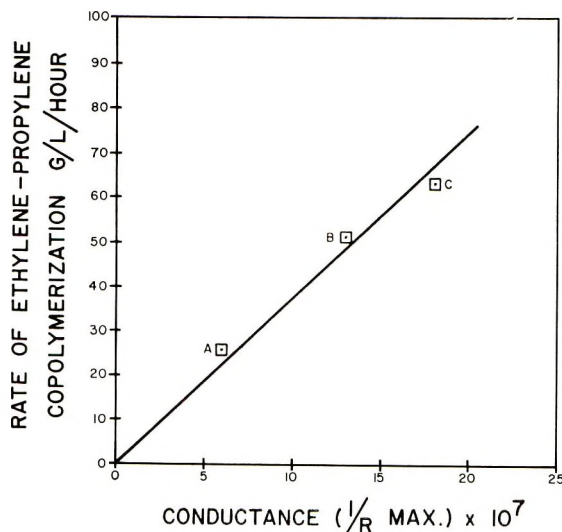


Fig. 7. Rate of ethylene-propylene copolymerization as a function of maximum conductance, each with $Al(i-C_4H_9)_2Cl$: (A) $VO(OC_2H_5)_3$; (B) $VO(OC_2H_5)Cl_2$; (C) $VO(OC_2H_5)_2Cl$.

TABLE III
Conductance-Polymerization Rate Data for Diisobutylaluminum Chloride and Various Vanadium Esters^a

Ester	Conductance $1/R_{\max}$, mho	Rate, g./l.-hr. ^b
$\text{VOCl}(\text{OC}_2\text{H}_5)_2$	18.8×10^{-7}	63
$\text{VOCl}_2(\text{OC}_2\text{H}_5)$	12.8×10^{-7}	51.8
$\text{VO}(\text{OC}_2\text{H}_5)_3$	7.5×10^{-7}	25.2
$\text{VO}(\text{O}-n\text{-C}_4\text{H}_9)_3$	5.7×10^{-7}	35

^a For 1*M* solution of diisobutylaluminum chloride and the vanadium esters in benzene. Conductivity measurements made at 25°C.

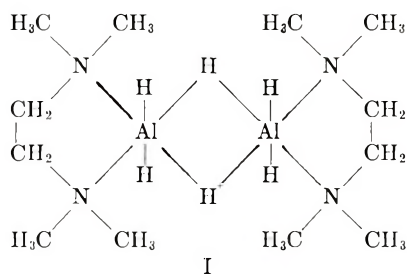
^b Data of Lukach et al.³⁷

in this study are similar to those of the catalyst system cited by Lukach et al.³⁷)

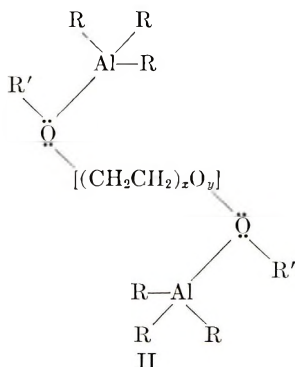
Effect of Electron Donors

The use of an electron-donor molecule as a third component in conjunction with a transition metal compound and an organoaluminum reducing agent has become well established in recent years. The nature of the polymer formed as well as the rate at which the product is formed is known to be greatly dependent upon the amount of the electron donor used. Zambelli and co-workers¹⁵ and Ambrož and Hanřík³⁸ showed that the ratio of donor to reducing agent was very critical. The former group found that the most satisfactory polymerizations occurred when the mole ratio of electron donor to monoalkylaluminum dihalide was equal to about 0.5. Jacober and Kraus³⁹ showed the influence of diethyl ether on the electrical conductivity of CH_3AlBr_2 and $(\text{CH}_3)_2\text{AlBr}$ in methyl bromide at 0°C. In both cases the conductivity increased to a maximum value at approximately 0.7 mole of ether/mole of solute. This maximum was attributed to the bimolecular form of the solutes which dissociate on complexing with the added ether; this dissociation being greater than that of the monomolecular form. In contrast to the AlBr_3 -ether systems, whose conductance rises very sharply beyond a 1:1 mole ratio, the CH_3AlBr -ether and $(\text{CH}_3)_2\text{AlBr}$ -ether systems both reached a conductivity value beyond a 1:1 mole ratio. The triethylaluminum-diethyl ether system⁵ was shown to reach a maximum in conductivity when a 1:1 complex had formed.

We have observed similar behavior when monoglyme (dimethyl ether of ethylene glycol) was added to triethylaluminum. The 1:1 complex formed is thought to be similar to that occurring between triethylaluminum and diethylether. However, it is also known that structures which contain two electron-donor atoms per molecule can coordinate with aluminum, through each of these atoms, forming a chelate-type structure in which case aluminum will possess a coordination number of six. Davidson and Wartick⁴⁰ have postulated such a structure (I) for *N,N,N',N'*-tetramethylethylenediamine and aluminum hydride:



On the other hand, when diglyme, triglyme, and tetraglyme (dimethyl ether of diethylene glycol, triethylene glycol, and tetraethylene glycol, respectively) were each added to triethylaluminum, coordination occurred as evidenced by the maximum in conductance at an ether to triethylaluminum mole ratio of about 0.5, as indicated by the data in Table IV and illustrated in a typical plot (Fig. 8). This would suggest coordination between two triethylaluminum molecules per each ether molecule. Further, our data indicate that only 1.5–2.0 of the available ether oxygens are coordinated with the aluminum compound illustrated in a typical plot (Fig. 8). The ability for coordination to occur with the additional available oxygen atoms would be decreased because of the inductive effect and also because of electrostatic repulsion resulting from charge polarization as a result of coordination with aluminum. We postulate a structure (II) for the coordination of the polyethers with triethylaluminum which could dissociate into an ionic species such as $(2\text{AlR}_2^+ \cdot \text{R}'\text{OR}') (2\text{AlR}_4^-)$.



(In structure II, $x = 2, 3, 4$ when $y = 1, 2, 3$.) Steric requirements would prevent the formation of such a complex when monoglyme or an ordinary ether is used.

The fact that only two of the available oxygen atoms of diglyme coordinate is further substantiated by the work of Merrall and co-workers,⁴¹ who showed that only two molecules of BF_3 will coordinate with diglyme, the second molecule being held only loosely. Recently, Antonsen, Hoffman, and Stearns⁴² demonstrated that only two of the three ether oxygens of diglyme are available for coordination because of steric requirements. They showed the marked effect of the ether structure on both the rate of

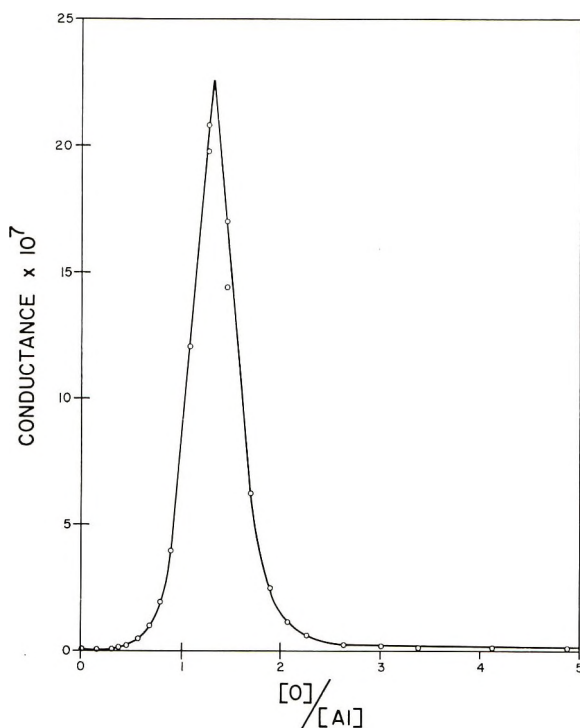
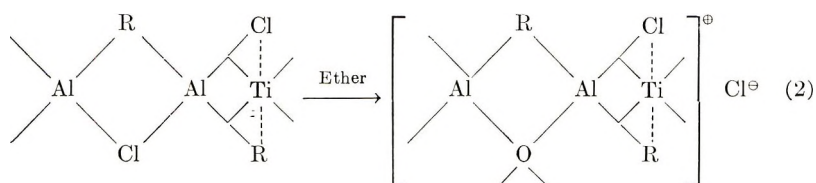


Fig. 8. Conductance as a function of diglyme to triethylaluminum mole ratio at 25°C.

polymerization and the nature of octene-1 oligomers. The effect of ether oxygen was also shown to have a pronounced effect on the yield; the most active catalyst being obtained at an O/Al mole ratio of 0.5. The influence of ether on the catalyst system, $\text{Al}_2\text{Et}_3\text{Cl}_3\text{-TiCl}_4$, was represented by these authors as shown in eq. (2):



where the bonding energy as well as the bulk steric effect of the ether itself was shown to influence the environment of the polymerization site.

The addition of an amine such as pyridine to triethylaluminum (Fig. 9) and diethylaluminum chloride (Fig. 10) in benzene both showed a sharp maximum in conductance at a pyridine to aluminum mole ratio of 1, indicative of a 1:1 type of complex being formed. A similar occurrence was shown by other investigators for AlBr_3 -pyridine,⁴³ diethylaluminum chloride-isoquinoline,⁵ triethylaluminum-quinoline and diethylaluminum bromide-quinoline,⁴⁴ and more recently for trimethylaluminum-diphenylamine.¹¹

Unlike Graevskii and co-workers,⁴⁴ however, we did observe a maximum in conductance when the mole ratio of pyridine to diethylaluminum chloride was equal to 2:1 (Fig. 10). This may be due to complex formation between the amine and dialkyl aluminum hydride, if any is present, since it is known that a 2:1 complex of this type is possible; or this second

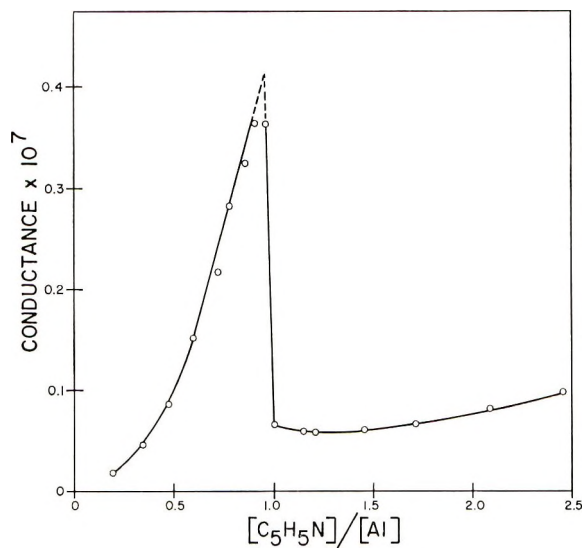


Fig. 9. Conductance as a function of pyridine to triethylaluminum mole ratio at 25°C

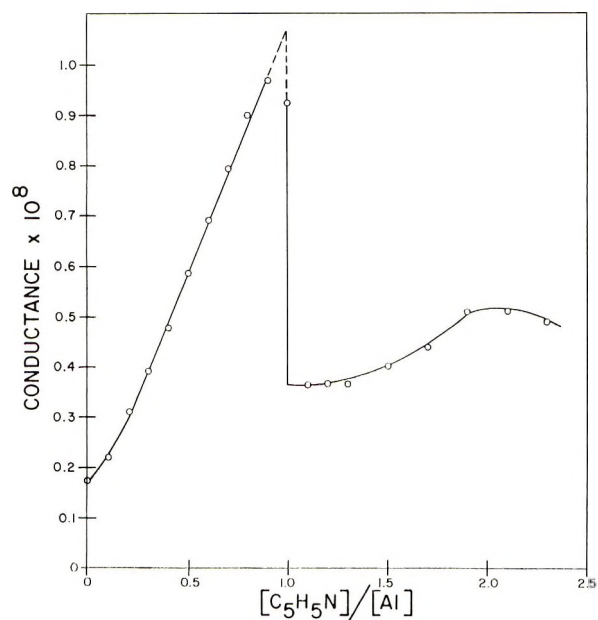


Fig. 10. Conductance as a function of pyridine to diethylaluminum chloride mole ratio at 25°C.

TABLE IV
Conductance of Triethylaluminum in Benzene in the Presence of Various Ethers at 25°C.^a

Compound	Ether/alkyl	Ether oxygen/alkyl	Conductance $1/R_{\max}$, mho
$\text{CH}_3\text{CH}_2\text{OCH}_2\text{CH}_3$	1.0	1.0	0.18×10^{-7}
$\text{CH}_3\text{OCH}_2\text{CH}_2\text{OCH}_3^{\text{b}}$	0.87	1.75	0.068×10^{-7}
$\text{CH}_3\text{O}(\text{CH}_2\text{CH}_2\text{O})_2\text{CH}_3^{\text{c}}$	0.49	1.47	22.7×10^{-7}
$\text{CH}_3\text{O}(\text{CH}_2\text{CH}_2\text{O})_3\text{CH}_3^{\text{d}}$	0.46	1.82	11.6×10^{-7}
$\text{CH}_3\text{O}(\text{CH}_2\text{CH}_2\text{O})_4\text{CH}_3^{\text{e}}$	0.42	2.11	17.5×10^{-7}

^a For 1M solution of the ethers and triethylaluminum in benzene. Measurements were made at 25°C.

^b Monoglyme.

^c Diglyme.

^d Triglyme.

^e Tetraglyme.

maximum at a lower conductance may well be due to further reaction between the 1:1 complex and additional amine to form a 2:1 complex of amine to organoaluminum compound. Similar behavior was reported by Pease and Luder⁴³ for the system $(\text{C}_2\text{H}_5\text{N})-\text{AlBr}_3$. On the other hand, Hoeg and Liebman⁶ discussed the possibility of a 2:1 complex between two molecules of acid per molecule of base; however, conductometric titrations indicated a maximum at a 1:1 mole ratio further substantiating what we observed.

The use of electron donors as polymerization promoters is attributed, by some workers, to ion-pair formation which is thought to be facilitated by the absorption of the donor group on the catalyst surface. We believe that Figure 11 illustrates such a process. Initially, as $\text{Al}(\text{C}_2\text{H}_5)_2\text{Cl}$ is added to benzene, the conductivity rises to a constant level. However, when TiCl_3

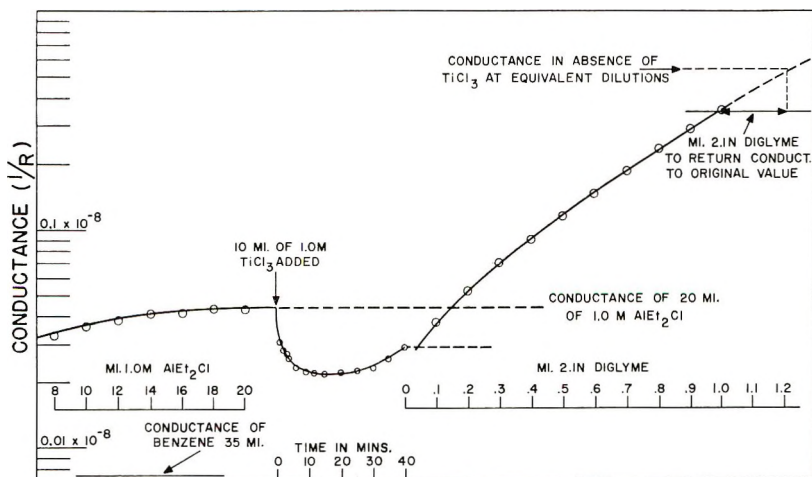


Fig. 11. Conductance of an $\text{Al}(\text{C}_2\text{H}_5)_2\text{Cl}-\text{TiCl}_3$ (ARA)-diglyme system as a function of concentration and time.

is added to the mixture there is an abrupt decrease in the conductance, presumably due to complex formation or coordination accompanied by absorption of ionic species by the solid together with a kinetic phenomenon involved in the desorption of some other ionic species, which may well be RTiCl_3 type compounds, eventually approaching a value close to the original conductivity of the diethylaluminum chloride itself. Upon the addition of diglyme to the diethylaluminum chloride-titanium (III) system, the specific conductivity increases rapidly and continues to increase steadily with further addition of the ethereal compound, indicating the formation of highly conducting ionic species.

Although the data presented are highly qualitative in nature, it nevertheless is evident that the conductivity level measured in all of the systems examined did correlate very well with the rate of polymerization. This is at least another piece of albeit circumstantial evidence that these coordination catalysts are highly ionic in nature and that it is an ionic species which is actively involved in the ultimate moiety responsible for polymerization.

The authors wish to express thanks to Mr. Martin Ackermann (University of California, Berkeley) for obtaining some of the experimental results and to Dr. W. L. Butte for his helpful comments.

References

1. Kraus, C. A., *J. Phys. Chem.*, **58**, 673 (1954); *ibid.*, **60**, 129 (1956).
2. Day, M. C., H. M. Barnes, and A. J. Cox, *J. Phys. Chem.*, **68**, 2595 (1964).
3. Nicolescu, I. V., and E. M. Angelescu, *J. Polymer Sci.*, **A3**, 1227 (1965).
4. Farina, M., M. Donati, and M. Ragazzini, *Ann. Chim. (Rome)*, **48**, 501 (1958).
5. Bonitz, E., *Chem. Ber.*, **88**, 742 (1955).
6. Hoeg, D. F., and S. Liebman, *J. Org. Chem.*, **28**, 1554 (1963).
7. Kissin, I. V., E. V. Kolstykh, and N. M. Chirkov, *Dokl. Akad. Nauk SSSR*, **145**, 104 (1962).
8. Geddes, A. L., paper presented at 137th National Meeting, American Chemical Society, Cleveland, Ohio, April 1960; *Abstracts*, p. 15R.
9. Gray, A. P., A. B. Callear, and F. H. C. Edgecombe, *Can. J. Chem.*, **41**, 1502 (1963).
10. Swift, H. E., C. P. Poole, Jr., and J. F. Ttzel, Jr., *J. Phys. Chem.*, **68**, 2509 (1964).
11. Kawai, M., T. Ozawa, and K. Hirota, *Bull. Chem. Soc. Japan*, **37**, 1302 (1964).
12. Geiseler, G., and W. Knothe, *Chem. Ber.*, **91**, 2446 (1958).
13. McConnell, R. L., H. W. Coover, Jr., and F. B. Joyner, paper presented at 145th National Meeting, American Chemical Society, New York, September 1963; *Abstracts*, p. 20M.
14. Joyner, F. B., and H. W. Coover, Jr., paper presented at the 145th National Meeting, American Chemical Society, New York, September 1963.
15. Zambelli, A., J. Dipietro, and G. Gatti, *J. Polymer Sci.*, **A1**, 403 (1963).
16. Milouskoya, E. B., and P. I. Dolyopolskoya, *Vysokomol. Soedin.*, **4**, 1049 (1962).
17. Solomon, O. F., P. Glineschi, and E. Mihailescu, *Dokl. Akad. Nauk SSSR*, **152**, 117 (1963).
18. Fuoss, R. M., and F. Accascina, *Electrolytic Conductance*, Interscience, New York, 1959, Chap. 18.
19. Robinson, R. A., and R. H. Stokes, *Electrolyte Solutions*, Academic Press, New York, 1959, Chap. 14.
20. Strong, L. E., and C. A. Kraus, *J. Am. Chem. Soc.*, **72**, 166 (1950).
21. Luder, W. F., and C. A. Kraus, *J. Am. Chem. Soc.*, **58**, 255 (1936).

22. Kraus, C. A., *J. Phys. Chem.*, **60**, 129 (1956).
23. Kraus, C. A., *J. Chem. Educ.*, **35**, 324 (1958).
24. Fuoss, R. M., and C. A. Kraus, *J. Am. Chem. Soc.*, **55**, 2387 (1933).
25. Lehmkuhl, H., *Angew. Chem. Intern. Ed.*, **3**, 107 (1964).
26. Jezl, J., *et al.*, unpublished results.
27. Gippin, M., paper presented at 148th National Meeting, American Chemical Society, Chicago, Illinois, September 1964; *Abstracts*, p. 2X.
28. Worsfeld, J., and S. Bywater, *J. Chem. Soc.*, **1960**, 5234.
29. Uelzmann, H., *J. Polymer Sci.*, **32**, 457 (1958).
30. Dijkgraaf, C., *J. Phys. Chem.*, **69**, 660 (1965).
31. Antonsen, D. H., unpublished results.
32. Eley, D. D., and A. W. Richards, *Trans. Faraday Soc.*, **45**, 425 (1949).
33. Pepper, G. G., *Trans. Faraday Soc.*, **45**, 397 (1949).
34. Brown, C. P., and A. R. Mathieson, *J. Chem. Soc.*, **1958**, 3445.
35. Coombes, J. D., and D. D. Eley, *J. Chem. Soc.*, **1957**, 3700.
36. George, J., and H. Wechsler, *J. Polymer Sci.*, **6**, 725 (1951).
37. Lukach, C. A., H. M. Spurlin, and S. G. Olsen (to Hercules Powder Company), South African Patent 60/839 (February 29, 1960).
38. Ambrož, J., and O. Hamřík, *Collection Czech. Chem. Commun.*, **28**, 2550 (1963).
39. Jacober, W. J., and C. A. Kraus, *J. Am. Chem. Soc.*, **71**, 2409 (1949).
40. Davidson, J. M., and T. Wartick, *J. Am. Chem. Soc.*, **82**, 5506 (1960).
41. Merrall, G. T., G. A. Latremoville, and A. M. Eastham, *Can. J. Chem.*, **38**, 1967 (1960).
42. Antonsen, D. H., P. S. Hoffman, and R. S. Stearns, *Ind. Eng. Chem., Prod. Res. Develop.*, **2**, 224 (1963).
43. Pease, L. E. D., and W. F. Luder, *J. Am. Chem. Soc.*, **75**, 5195 (1953).
44. Graevskii, A. I., Sh. S. Shchegol, and Z. S. Smolyan, *Dokl. Akad. Nauk SSSR*, **119**, 101 (1958).

Résumé

La conductivité électrique de plusieurs halogénures de trialkyl-aluminium et d'alkylaluminium a été étudiée dans du benzène sec, à 25°C, dans un domaine de concentration 10^{-1} à 10^{-3} molaire. La conductance équivalente des systèmes trialkylaluminium décroît dans l'ordre suivant: $\text{Al}(n\text{-C}_6\text{H}_{13})_3 > \text{Al}(n\text{-C}_{10}\text{H}_{19})_3 > \text{Al}(n\text{-C}_4\text{H}_9)_3 > \text{Al}(i\text{-C}_4\text{H}_9)_3 > \text{Al}(n\text{-C}_3\text{H}_7)_3 > \text{Al}(\text{C}_2\text{H}_5)_3$. La conductance (I/R) de séries données a été également examinée elle diminue par remplacement successif d'un groupe alkyle par un atome de chlore. Donc: $\text{Al}(\text{C}_2\text{H}_5)_3 > \text{Al}(\text{C}_2\text{H}_5)_2\text{Cl} > \text{Al}(\text{C}_2\text{H}_5)_{1.5}\text{Cl}_{1.5} > \text{Al}(\text{C}_2\text{H}_5)\text{Cl}_2$ et $\text{Al}(i\text{-C}_4\text{H}_9)_3 > \text{Al}(i\text{-C}_4\text{H}_9)_2\text{Cl} > \text{Al}(i\text{-C}_4\text{H}_9)\text{Cl}_2$. Les constantes de dissociation de la paire d'ions ont été calculées et montrent d'une façon qualitative la différence entre plusieurs système d'organoaluminium. La vitesse relative de polymérisation oléfinique a été reliée à la conductivité de plusieurs systèmes d'organoaluminium-métal de transition employés en catalyse. L'effet des bases de Lewis telles que le monoglyme, le diglyme, le triglyme et le tétraglyme indique que la première base citée forme un type de complexe 1:1, comme ordinairement les éthers le font, tandis que les trois autres bases utilisent seulement 2 de leurs atomes d'oxygène pour coordonner avec triéthylaluminium. L'influence de TiCl_3 (en présence d'un éther) sur la conductance a été également établie.

Zusammenfassung

Die elektrische Leitfähigkeit einiger Trialkylaluminium- und Alkylaluminiumhalogenide wurde in trockenem Benzol bei 25°C im Konzentrationsbereich von 10^{-1} bis 10^{-3} molar untersucht. Die Äquivalentleitfähigkeit der Trialkylaluminiumsysteme nahm in folgender Reihe ab: $\text{Al}(n\text{-C}_6\text{H}_{13})_3 > \text{Al}(n\text{-C}_{10}\text{H}_{19})_3 > \text{Al}(n\text{-C}_4\text{H}_9)_3 > \text{Al}(i\text{-C}_4\text{H}_9)_3 >$

$\text{Al}(n\text{-C}_3\text{H}_7)_3 > \text{Al}(\text{C}_2\text{H}_5)_3$. Die Leitfähigkeit ($1/R$) einer gegebenen Reihe wurde ebenfalls untersucht und nahm bei sukzessivem Ersatz der Alkylgruppe durch Chloratome in folgender Reihe ab: $\text{Al}(\text{C}_2\text{H}_5)_3 > \text{Al}(\text{C}_2\text{H}_5)_2\text{Cl} > \text{Al}(\text{C}_2\text{H}_5)_{1,6}\text{Cl}_{1,6} > \text{Al}(\text{C}_2\text{H}_5)\text{Cl}_2$ und $\text{Al}(i\text{-C}_4\text{H}_9)_3 > \text{Al}(i\text{-C}_4\text{H}_9)_2\text{Cl} > \text{Al}(i\text{-C}_4\text{H}_9)\text{Cl}_2$. Die Dissoziationskonstante (K) der Ionenpaare wurde berechnet; sie zeigt qualitativ den Unterschied zwischen verschiedenen aluminium-organischen Systemen. Die Relativgeschwindigkeit der Olefinpolymerisation stand in Beziehung zur Leitfähigkeit der verschiedenen verwendeten Organometall-Übergangsmetall-Katalysatorsysteme. Der Einfluss von Lewisbasen wie Monoglyme, Diglyme, Triglyme und Tetraglyme auf Triäthylaluminium zeigte, dass die erstgenannte Base einen 1:1-Komplextyp sowie gewöhnliche Äther liefert, während die übrigen drei Basen nur zwei ihrer Sauerstoffatome zur Koordination mit Triäthylaluminium benützen. Schliesslich wurde der Einfluss von TiCl_3 (in Gegenwart eines Äthers) auf die Leitfähigkeit bestimmt.

Received July 8, 1965

Prod. No. 4828A

Investigation by Infrared Absorption of the By-Products of the Cyanoethylation of Cotton Cellulose*

PRONoy K. CHATTERJEE† and CARL M. CONRAD, *Plant Fibers Pioneering Research Laboratory, Southern Utilization Research and Development Division, Agricultural Research Service, U. S. Department of Agriculture, New Orleans, Louisiana*

Synopsis

The soluble cyanoethyl ether of cellulose, prepared by reaction in the presence of NaOH catalyst to high degrees of substitution ($DS = 2.95$), can be precipitated by various organic media and contains more nitrogen than can be accounted for by simple addition of acrylonitrile at each cellulose hydroxyl group. Infrared absorption spectra of such samples and of the reacted residues show various types of vibrational absorption bands, characteristic of amino groups. At advanced stages of the reaction the characteristic broad unresolved band of cellulose extending from $1200\text{--}950\text{ cm.}^{-1}$ largely disappears, leaving only a few weaker bands which likely overlap those due to C-N stretching. Comparison is made of the spectra of the partially cyanoethylated cellulose and the polyacrylonitrile which forms in the stock acrylonitrile, to characterize the products. It is inferred that the highly cyanoethylated cellulose, partly dissolved in the acrylonitrile, further degrades and changes under a complex mechanism to various forms of amines. The yellow to orange color of the samples is assumed to be due to these by-products. The thermogravimetric analysis reveals that these products are more heat-resistant than the cyanoethylated cellulose.

INTRODUCTION

During a study of the kinetics of cyanoethylation of cellulose¹ it was noticed that the main reaction is always accompanied at the latter stages by side reactions which makes an estimation of the degree of substitution erroneous. The reactions at higher degrees of substitution invariably give a strong orange color to the cellulose ether, and the reacted fiber becomes brittle and contains more nitrogen than can be accounted for by simple addition of acrylonitrile molecules to each hydroxyl group of the cellulose (i.e., more than $DS = 3$). This effect is more pronounced at higher temperatures and when the catalyst concentration is greater. A substantial amount of acrylonitrile may be consumed during cyanoethylation, to form β,β' -oxydipropionitrile as has been suggested by Gruber, Bikales,² and others.³ But it is quite unlikely that β,β' -oxydipropionitrile has any direct action towards changing the fiber properties.

* Paper presented at the 149th National Meeting of the American Chemical Society, Detroit, Michigan, April 4-9, 1965.

† Postdoctoral Resident Research Associate, 1963-65.

The conditions for formation of any considerable amount of pure polyacrylonitrile are considered unfavorable under the present circumstances, although the formation of small amounts of polymer in acrylonitrile cannot be ruled out altogether. Again, this effect is too insignificant to account for a noticeable change of the product.

Attempts have been made, without success, to remove the colored component by extracting it with different solvents. However, it was found that if reaction continues to an advanced degree of cyanoethylation, the product becomes somewhat soluble in acrylonitrile. Infrared absorption spectra of these soluble products and the residue have been studied and compared with the partially cyanoethylated fibers in order to throw light on the nature of the by-products which accompany the cyanoethyl ether during the advanced stages of reaction.

EXPERIMENTAL METHODS

Cyanoethylation of Fibers

The cellulosic material used in the present study was in the form of cheesecloth, supplied by Kendall Company, Grinsville, Massachusetts.

About 1 g. of sample in each case was treated with 6% and in some cases with 20% sodium hydroxide solution for 30 min. at room temperature. After squeezing out the excess sodium hydroxide solution, the fiber was treated with liquid acrylonitrile in a constant temperature bath at 50°C. as described in our earlier paper.¹ After the required time of reaction, the undissolved portion was taken out and immersed in a 5% acetic acid solution and washed successively with water, ethanol, and ether. The product was finally dried at 50°C.

It was found that the dissolved product could be precipitated by a number of solvents such as benzene, toluene, chloroform, etc. During the present investigation chloroform was used as the precipitant. The liquid portion was treated with chloroform and filtered; the precipitate was washed with chloroform and dried at 50°C. It was observed in a series of samples, reacted at 50°C. and with chloroform as the precipitant, that no dissolved product was found below $DS = 2.5$. The product dissolves somewhat at $DS = 2.95$. After a more extended reaction, the precipitated product lost its fibrous appearance and turned yellow to orange color. The precipitated product is soluble in acetone.

The control cheesecloth sample was prepared with 6% sodium hydroxide and heated in toluene at 50°C. for 300 min. The sample was then treated with 5% acetic acid solution, washed, and dried like the other samples. The nitrogen value was determined by the Kjeldahl method.

Reaction between Acrylonitrile and Sodium Hydroxide

A 52 ml. portion of acrylonitrile and 10 ml. of a 6% sodium hydroxide solution were heated in a flask fitted with an air condenser at 50°C. under

continuous shaking for 10 hr. The acrylonitrile portion was then separated and treated with chloroform, but no precipitate was observed. The experiment was repeated with 20% sodium hydroxide solution and also by increasing the time and the reaction temperature, but no polymer was found which could be precipitated by chloroform.

Polymer Extracted from the Acrylonitrile Stock

The commercial acrylonitrile stock was distilled and the fraction, collected at the boiling point of acrylonitrile (77–78°C.), was kept in a stoppered bottle at room temperature for 2 months. One liter of this liquid was evaporated to about 50 ml. and then treated with chloroform. A very small amount of white precipitate formed; this was then filtered and washed with chloroform a number of times and finally dried at 50°C.

Infrared Spectroscopy

The Infracord Model 237B grating spectrophotometer supplied by Perkin-Elmer was used. Infrared spectra were obtained by the potassium bromide pellet technique. Fibers were cut to pass a 20-mesh screen in a Wiley mill, and in the case of a hard mass the product was powdered with a mortar and pestle. The potassium bromide disc was prepared with 2

TABLE I

Sample	Description of the sample	N, %
A	Cheesecloth (control)	
B	Partially cyanoethylated fibers (DS = 0.76)	5.25
C	Trisubstituted cyanoethylated fibers (DS = 2.85)	12.72
D	Soluble product obtained on reacting 6% NaOH-treated fibers with acrylonitrile for 225 min.	14.54
E	Soluble product obtained on reacting 6% NaOH-treated fibers with acrylonitrile for 300 min.	23.03
F	Soluble product obtained on reacting 20% NaOH-treated fibers with acrylonitrile for 36 hr.	25.53
G	Sample F washed with water and dried at 105°C.	25.48
H	Insoluble portion obtained on reacting a 20% NaOH-treated fibers with acrylonitrile for 36 hr. (a hard, glue-like mass)	23.16
I	Residue obtained on extracting sample H with hot acetone (washed with alcohol and ether)	19.13
J	Acetone-soluble product from H (dried from acetone solution)	24.75
K	Polymer (polyacrylonitrile) recovered from acrylonitrile stock	25.63

mg. of the sample by following the technique outlined by O'Connor et al.⁴

Thermogravimetry

A continuous recording thermobalance, supplied by the Robert L. Stone Co., was employed for studying the thermal stability of the sample. About 100 mg. of the sample was weighed in a porous base crucible and mixed with tabular alumina to make the total weight of the contents 2 g. The sample was heated in helium (0.35 standard cubic feet per hour) from room temperature to 800°C. The increase in furnace temperature was maintained at 3°C./min.

Sample

A brief description of the samples studied is given in Table I.

RESULTS AND DISCUSSION

Sample D (Fig. 1) which is the acrylonitrile soluble product, obtained on reacting for 225 min. at 50°C., gives an infrared spectrum closely resembling that of the cyanoethylated insoluble (sample C) fibers, except for the band of N-H deformation at a frequency of 1587 cm.⁻¹, which is well developed in the present case. There are many significant changes, however, in the

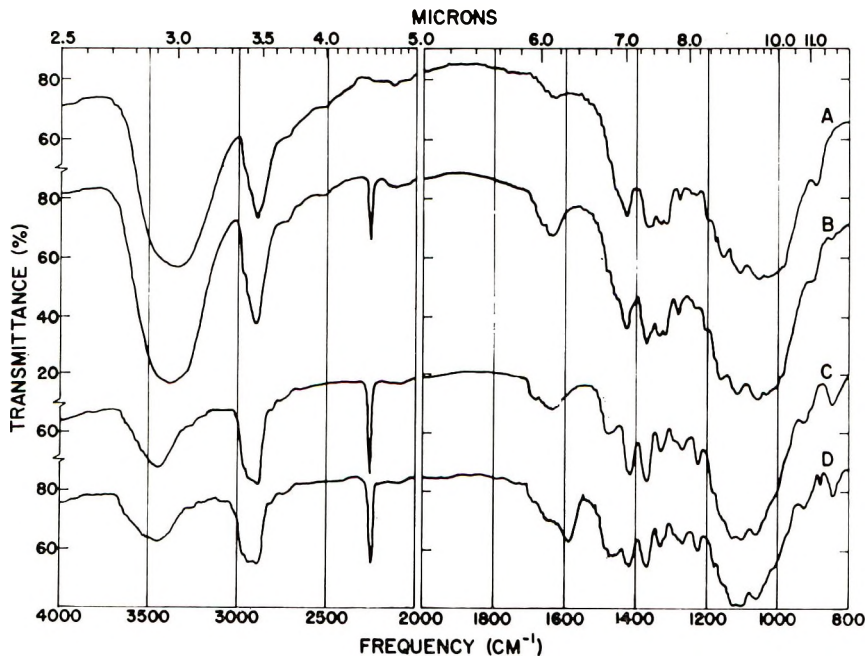


Fig. 1. Infrared spectra of: (A) cellulose fibers (control), (B) partially cyanoethylated (DS = 0.76), (C) highly cyanoethylated (DS = 2.85), and (D) cyanoethylated soluble product. (N = 14.54%.)

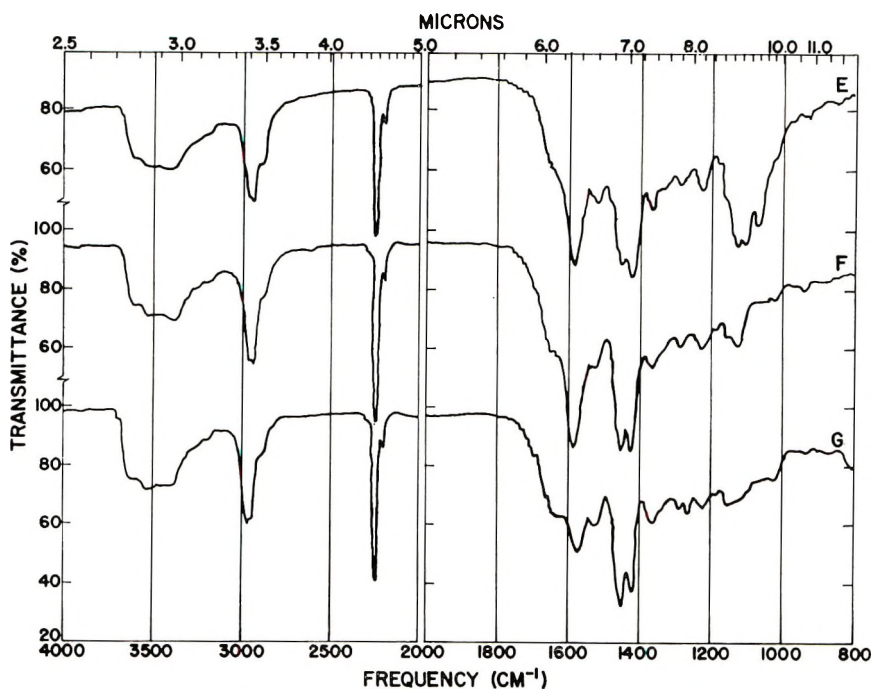


Fig. 2. Infrared spectra of the cyanoethylated soluble product obtained after reaction for (E) 300 min. with 6% NaOH catalyst ($N = 23.03\%$); (F) 36 hr. with 20% NaOH catalyst ($N = 25.53\%$); (G) sample F washed with water.

spectrum of the product (sample E, Fig. 2) obtained on reacting the fibers for 300 min.

The soluble product obtained by reacting material treated with 20% sodium hydroxide for 36 hr., (sample F) shows a spectrum similar to that of sample E and some of the bands are found to be more prominent. It seems that a part of the highly substituted cyanoethylated product becomes soluble in acrylonitrile and this soluble product is converted into other products on extensive reaction with the reagent. These transformed products are colored yellow or orange.

The spectra of the control fibers (sample A, Fig. 1), partially cyanoethylated fibers (sample B), and highly cyanoethylated products (sample C) all show a single broad absorption band near the O-H stretching region; the intensity of absorption decreases on substitution. The spectrum of sample C shows the band maxima at 3450 cm^{-1} , whereas in the case of the original fiber the band maxima is at 3350 cm^{-1} . An almost similar O-H stretching band has been observed with the spectrum of sample D, but the spectra of samples E and F show a broadening of this band and splitting into three parts. The location of these bands are: 3600 , $3520\text{--}3450$, and 3375 cm^{-1} . In the spectra of samples E and F, other bands are probably developed from N-H stretching vibrations of NH_2 groups, which are formed as a result of the secondary reaction of the cyanoethylated product. A

good deal of overlapping between O-H and N-H stretching bands always occurs in this region, making differentiation difficult. However, the spectra of unsubstituted fibers and ordinary cyanoethylated fibers having a low nitrogen content, where presumably the NH_2 group is absent, showed one broad band in this region. Since the soluble products give two more bands and the absorption region is widely spread, the bands could be assumed to be due to a N-H stretching vibration.

Furthermore, it is seen that the N-H deformation band (at 1587 cm.^{-1}) is developed in these cases.

In the C-H stretching region, a new band between 2825 and 2875 cm.^{-1} , has been found to develop, with the progress of cyanoethylation and is more prominent in the soluble products. All other types of C-H vibration in this region shift slightly towards the higher frequency range. Substitution always affects the location of the bands in the C-H stretching region and therefore the shifting is possibly due to the effect of the substitution of the cyanoethyl group. Again, since there is no methyl group present (which absorbs at 2872 cm.^{-1}),^{5a} it is assumed that the weak band at 2725 cm.^{-1} , already present in the spectrum of the original fibers, has been shifted gradually to 2875 cm.^{-1} and further developed due to substitution.

Along with the $\text{C}\equiv\text{N}$ stretching band, a small shoulder band which was not present in the spectrum of the cyanoethylated fibers (up to $\text{DS}\equiv 2.9$) has been found in the spectra of samples E and F at 2200 cm.^{-1} . The literature⁶ shows that the range 2200 - 2000 cm.^{-1} covers all the various forms in which the $\text{C}\equiv\text{N}$ grouping occurs in inorganic compounds. Therefore, this band probably indicates the formation of a small amount of inorganic cyanide possibly sodium cyanide which might result from a side reaction. These cyanides could not be removed simply by washing the sample with water, however, (see spectrum of sample G).

A couple of new bands have been observed in the spectra of samples E and F at 1587 and 1520 cm.^{-1} . Both bands are due to N-H bending vibrations. This N-H bending vibration arises particularly from the secondary amine^{5b} and amide group. The expected transformation of the cyanoethyl group in the presence of sodium hydroxide and water is to the amide group⁷ ($-\text{CONH}_2$). In the case of amide, the spectrum should always show a strong amide I and a weak amide II band.⁷ In the present case, however, strong bands are located in the position of amide II, which is also the position of the band due to the deformation of N-H in amino groups, but no distinct amide I band ($\text{C}=\text{O}$ stretching), as was expected, has been found in any of the samples. The present set of observations, of course, cannot disprove the possibility of formation of a small amount of amide, since the broad band due to moisture (at 1623 cm.^{-1}) may overlap the amide I band near 1650 cm.^{-1} , but it can be concluded that the soluble reaction products are mostly amines and not amides.

An entire change of the spectrum has been observed between 1500 cm.^{-1} and the lower frequency region. The strong and broad band extending from 1200 to 950 cm.^{-1} consisting of several close bands which is typical

of all cellulosic fibers⁸ has been found to change to a relatively transparent region having only a few individual weaker bands. In the spectrum of sample D the bands in this region still characterize the cellulosic structure. In the spectrum of sample E the broadness of the band has been much reduced, and in the spectra of samples F and G this changes almost completely. All of these are soluble products obtained during cyanoethylation, differing in the extent of reaction only. Since sample F is the product obtained under the most excessive reaction conditions it has been assumed to represent the final transformed product. Further comparison of the spectrum obtained from sample F may be made with that obtained from the unsubstituted material (sample A) and the trisubstituted fibers (sample B).

In the region of $\begin{array}{c} \diagup \\ \text{CH}_2 \\ \diagdown \end{array}$ scissoring, wagging, and twisting vibrations, a new band has been observed at 1450 cm.^{-1} for $\begin{array}{c} \diagup \\ \text{CH}_2 \\ \diagdown \end{array}$ scissoring vibration which either characterizes some sort of cyclization or may be due to a C-H bending vibration from the cellulose-acrylonitrile graft polymer. The $\begin{array}{c} \diagup \\ \text{CH}_2 \\ \diagdown \end{array}$ twisting and wagging vibration at 1312 cm.^{-1} which occurs in the spectrum of the original cellulose fibers has been found to be absent in that of sample F. Similarly, the fact that the C-OH stretching vibrations at 1205 cm.^{-1} are absent, might be due to the complete substitution of the hydroxyl groups. The region, where a number of close bands makes the appearance of a strong and broad band with cellulosic fibers⁸ and also with cellobiose⁹ ($1200\text{--}950 \text{ cm.}^{-1}$), is replaced in the spectrum of this sample by a transparent region except for a few discrete bands at 1280, 1225, 1150, and 1120 cm.^{-1} . But these are the absorption regions of various types of amines also where the band appears due to C-N stretching vibrations.^{5a} Therefore, C-N stretching vibration of various forms of amines are, quite likely, overlapping in these regions, contributing to the intensities of the individual bands.

A comparison of the spectra from samples H, I, and J (Fig. 3) indicates that the O-H stretching band from sample I resembles that of the cyanoethylated cellulose. The spectrum of sample J fairly corresponds to that of sample H, except in the region $1200\text{--}950 \text{ cm.}^{-1}$. The spectrum thus suggests that sample H contains a very small amount of ether in the cellulosic form. Therefore, only after removing the acetone-soluble portion do the characteristic absorption bands of cellulose appear distinctly. There is an indication of a carbonyl stretching band in the spectrum of sample J at 1712 cm.^{-1} which was not found in the spectrum of sample H or in any other. This was assumed to be due to traces of trapped acetone.

A spectrum of sample K, the polymer (polyacrylonitrile) found on storing acrylonitrile stock, has been included in Figure 3 in order to complete the series and permit comparison with the spectra of the cyanoethylated products. The absorption pattern of this polymer is obviously quite different from that obtained from the products discussed above.

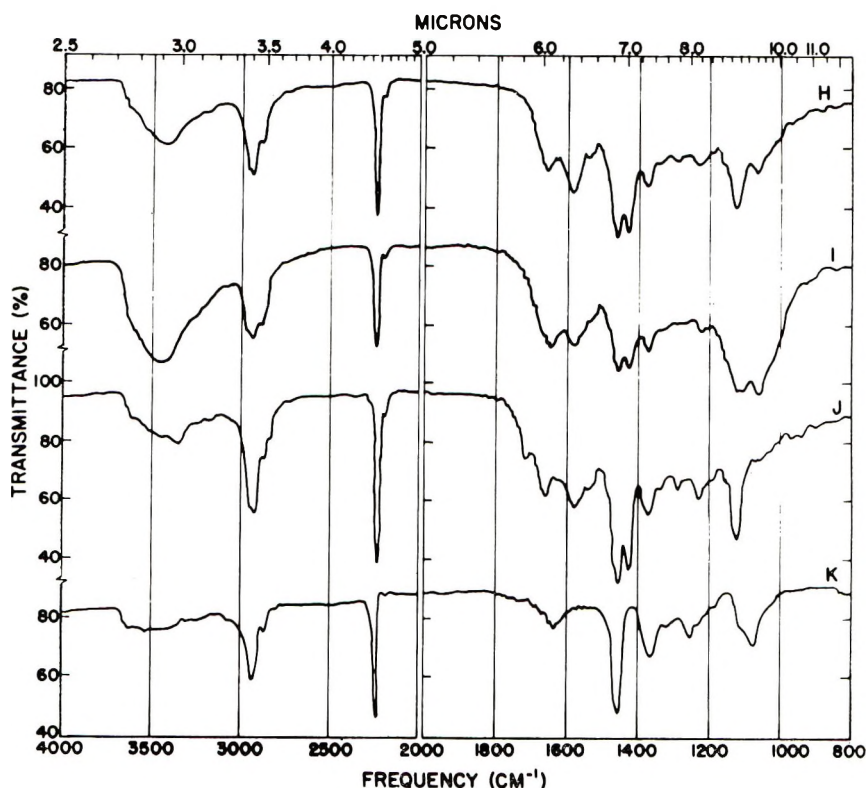
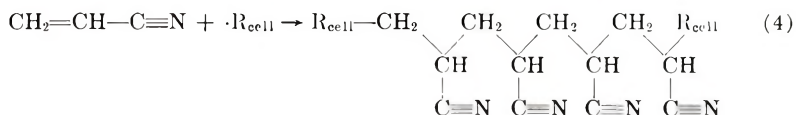
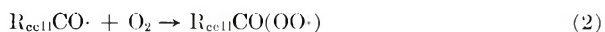
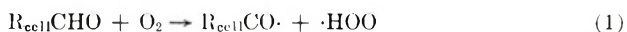


Fig. 3. Infrared spectra of the samples: (*H*) cyanoethylated insoluble product after 36 hr. of reaction with 20% NaOH catalyst ($N = 23.16\%$); (*I*) acetone-insoluble portion from sample *H*; (*J*) acetone-soluble portion from sample *H*; (*K*) polymer recovered from acrylonitrile stock.

Due to the presence of sodium hydroxide and molecular oxygen, an auto-catalytic degradation of cyanoethyl cellulose, resulting in the production of radicals is quite likely. These radicals could start the graft polymerization of acrylonitrile onto the cellulose according to the mechanism shown in eqs. (1)–(4).



where R_{cell} represents cyanoethylated cellulose.

This mechanism can account for the high value of nitrogen, but does not allow for the presence of amino groups or the intense color.

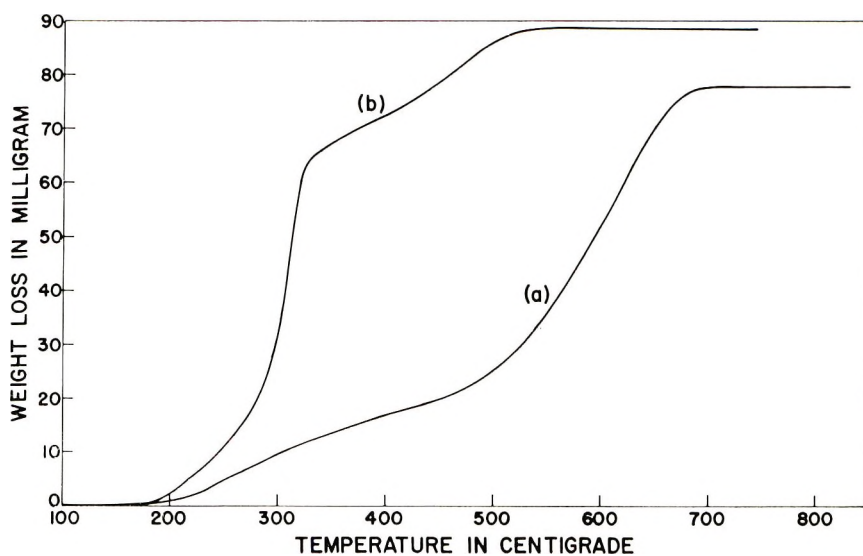
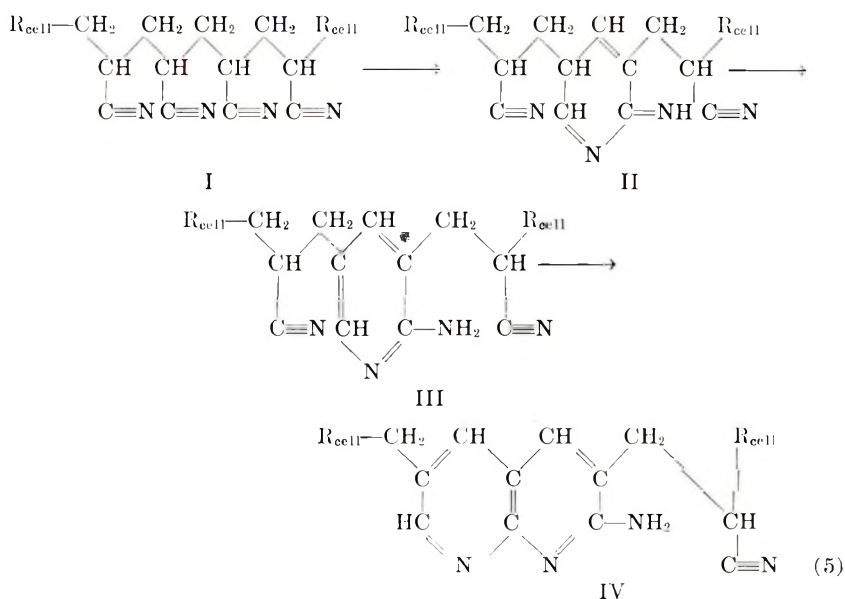


Fig. 4. Thermogravimetric chart of (a) sample E; (b) cyanoethylated cellulose (DS = 2.38).

Houtz¹⁰ suggested a probable mechanism for the transformation from polyacrylonitrile to condensed aromatic ring systems on heating. There is as yet no chemical evidence to support this mechanism. If his hypothesis is correct, a reaction might occur on heating in this case also, as shown in eq. (5).



Such a condensed aromatic ring structure is supposed to be highly heat-resistant. Figure 4 shows the thermogravimetric curve of the sample E

and of the cyanoethylated cellulose, $DS = 2.38$. It is evident from the figure that only about 21% of the product decomposed at about 470°C . at which point the cyanoethylated cellulose ($DS = 2.38$) almost completely decomposed. The remainder of the sample decomposed between 470 and 690°C .

The structure of sample E might be of the type I, II, or III if the transformation takes place during the cyanoethylation. And, on heating, it might finally have changed to IV, which is very stable. There may be many other factors and other types of reaction involved. At this stage, no reaction mechanism can be suggested.

It could be inferred from the above investigation that highly substituted cyanoethylated cellulose, partly soluble in acrylonitrile, on further reaction partially degrades and changes into various amines. The color of the product (cyanoethylated cellulose) is that of these by-products and is not due to pure polyacrylonitrile. The high nitrogen content of the products indicates that the reaction is not simply from nitrile to amines but that several other types of complex reaction are taking place in the fully substituted cyanoethylated products.

Appreciation is expressed to Mr. J. S. Mason for nitrogen determination and to Mr. G. I. Pittman for construction of the charts. Special appreciation is also expressed to Dr. Robert H. Barker for suggestions and advice.

Use of a company and/or product name by the Department does not imply approval or recommendation to the exclusion of others which also may be suitable.

References

1. Chatterjee, P. K., and C. M. Conrad, paper presented at the 149th National Meeting of the American Chemical Society, Detroit, Mich., April 4-9, 1965; *J. Polymer Sci.*, in press.
2. Gruber, A. H., and N. M. Bikales, *Textile Res. J.*, **26**, 67 (1956).
3. Weaver, J. W., E. Klein, B. G. Webre, and E. F. DuPre, *Textile Res. J.*, **26**, 518 (1956).
4. O'Connor, R. T., E. F. DuPre, and E. R. McCall, *Anal. Chem.*, **29**, 998 (1957).
5. Weissberger, A., *Chemical Applications of Spectroscopy*, Interscience, New York, 1956, (a) p. 339; (b) pp. 520, 521, 527; (c) p. 530.
6. Bellamy, L. J., *The Infra-red Spectra of Complex Molecules*, Wiley, New York, 1958, p. 347.
7. MacGregor, J. H., *J. Soc. Dyers Colourists*, **67**, 66 (1951).
8. O'Connor, R. T., E. F. DuPre, and D. Mitcham, *Textile Res. J.*, **28**, 382 (1958).
9. Hall, D. M., and P. E. Robbins, *Textile Res. J.*, **32**, 860 (1962).
10. Houtz, R. C., *Textile Res. J.*, **20**, 786 (1950).

Résumé

L'éther soluble cyanoéthylénique de la cellulose, préparé en présence de NaOH en quantité catalytiques, à un degré élevé de substitution ($DS = 2.95$) peut être précipité par divers milieux organiques et contient plus d'azote que l'on ne peut s'y attendre sur la base d'une simple addition d'acrylonitrile à chaque groupement hydroxylique de la cellulose. Les spectres d'absorption infra-rouge de ces échantillons ainsi que des résidus de réaction révèlent l'existence des divers types de bandes d'absorption vibrationnelles caractéristiques de groupements aminés. À des stades avancés de la réaction la bande

d'absorption large et non résolue de la cellulose s'étendant de 1200 à 950 cm^{-1} disparaît fortement, laissant subsister seulement quelques bandes plus faibles qui recouvrent probablement celles des vibrations C—N. En vue de caractériser les produits, on a comparé les spectres des celluloses partiellement cyanoéthylées au polyacrylonitrile qui se forme dans l'acrylonitrile durant sa conservation; on admet que la cellulose hautement cyanoéthylée, partiellement dissoute dans l'acrylonitrile, se dégrade ensuite et se transforme par un mécanisme complexe en divers types d'amines. La couleurjaune-orange des échantillons est attribuée à la présence de ces produits secondaires. L'analyse thermogravimétrique montre que ces produits sont plus thermostables que la cellulose cyanoéthylée.

Zusammenfassung

Der lösliche, durch Reaktion in Gegenwart von NaOH als Katalysator mit hohem Substitutionsgrad ($DS = 2,95$) dargestellte Zellulosecyanoäthyläther kann durch verschiedene organische Medien gefällt werden und enthält mehr Stickstoff, als einer einfachen Addition von Acrylnitril an jede Zellulosehydroxylgruppe entspricht. Die Infrarotabsorptionsspektren solcher Proben und des Reaktionsrückstandes zeigen verschiedene für Aminogruppen charakteristische Typen von Schwingungsbanden. Bei fortschreitendem Stadium der Reaktion verschwinden die charakteristischen breiten, nicht aufgelösten Zellulosebanden im Gebiet von 1200–950 cm^{-1} weitgehend, und es bleiben nur einige schwächere Banden zurück, welche sich wahrscheinlich mit denjenigen der C—N-Valenzschwingung überlagern. Zur Charakterisierung der Produkte wird ein Vergleich der Spektren der partiell cyanoäthylierten Zellulose und des im Acrylnitril gebildeten Polyacrylnitrils durchgeführt. Es wird angenommen, dass die hochgradig cyanoäthylierte, zum Teil im Acrylnitril gelöste Zellulose abgebaut wird und sich über einen komplexen Mechanismus in verschiedene Amiformalen unwandelt. Die gelbe bis orange Farbe der Proben wird auf diese Nebenprodukte zurückgeführt. Die thermogravimetrische Analyse zeigt, dass diese Produkte hitzebeständiger sind als die cyanoäthylierte Zellulose.

Received May 10, 1965

Revised July 27, 1965

Prod. No. 4836A

NOTES

NMR Spectra of Propylene-Styrene Copolymers

In connection with our study on propylene-styrene copolymerization,¹ the high resolution nuclear magnetic resonance (NMR) technique was applied to elucidate the structure of polymers obtained. The copolymers were prepared with $\text{AlEt}_3\text{-TiCl}_3$ (Natta) catalyst (Table I), and then extracted successively by acetone, ethyl ether, chloroform, and *n*-heptane.

TABLE I
Copolymerization by $\text{AlEt}_3\text{-TiCl}_3$ System^a

No.	Initial styrene, mole-%	Styrene, mole-% ^b in copolymer
1	73.6	3.1
2	83.0	27.1

^a Al/Ti = 3.0; temp., 70°C.; total monomers, 0.3 mole; solvent, *n*-heptane 250 cc.

^b Determined by elementary analysis.

NMR spectra of these fractions in 5–10% CDCl_3 or tetrachloroethylene solutions were observed at 25 and/or 120°C. with Mullard SL44-MK2 and Varian V-4300C spectrometers at 40 and 56.4 Mc./sec. respectively. Typical examples of the spectra of these soluble fractions are shown in Figure 1. The signals at the lowest field ($\tau = 2.9$

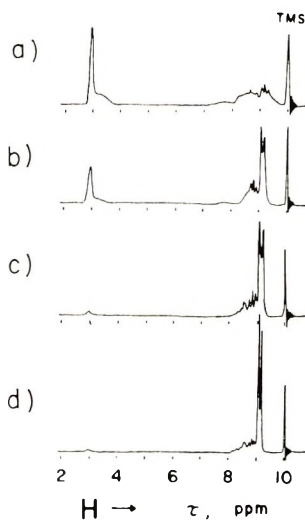


Fig. 1. NMR spectra of the soluble fractions of copolymer No. 1 in CDCl_3 at 25°C. and 56.4 Mc. Styrene mole-%: (a) acetone extract, 22; (b) ether extract, 10.5; (c) *n*-heptane extract, 3.1.

ppm) are due to the aromatic protons of the styrene monomeric unit, whereas the higher field part ($\tau = 3.5$ ppm) in the aromatic proton region, which appears in a spectrum of polystyrene,² is absent in the spectra of these soluble fractions. Bovey et al.² has also reported a case of aromatic peak as singlet in extremely low molecular weight poly-

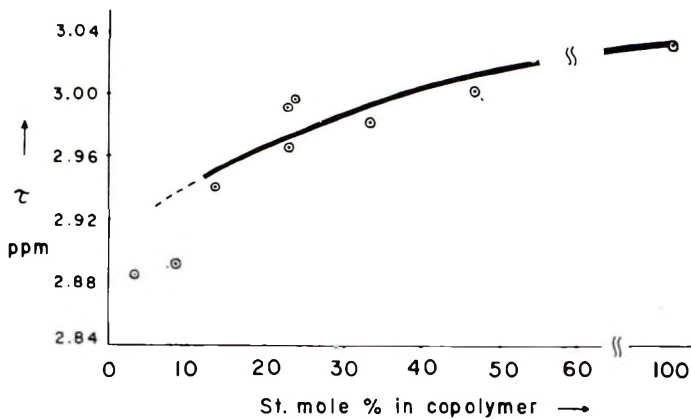


Fig. 2. Chemical shifts of aromatic protons vs. styrene content in CDCl_3 at 25°C . and 40 Mc. Styrene mole-% in copolymers was determined by elementary analysis.

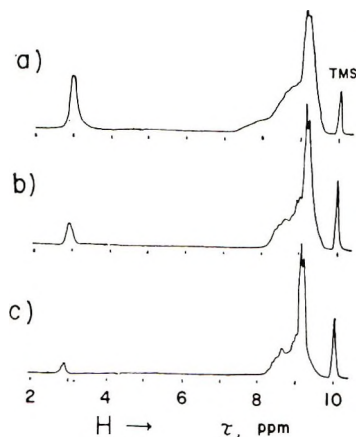


Fig. 3. NMR spectra of copolymer no. 2 in C_2Cl_4 at 120°C . and 56.4 Mc. Styrene mole-%: (a) acetone extract, 49.6; (b) ether extract, 30.2; (c) *n*-heptane extract, 6.5; (d) residue, 2.9.

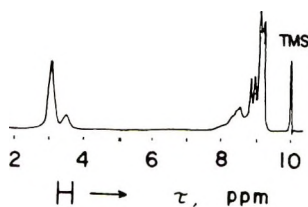


Fig. 4. NMR spectrum of a mixture of Natta polypropylene ether extract (70%) and atactic polystyrene (30%) in C_2Cl_4 at 120°C . and 56.4 Mc.

styrene ($P_n = 5$). As our soluble fractions were prepared by precipitation into methanol, such low molecular weight polystyrene would be dissolved out in methanol. Therefore these spectra may suggest that these soluble fractions are not mixtures of both homopolymers, but are copolymers.

In Figure 2 peak positions of aromatic protons are plotted as a function of the mole fraction of styrene in the soluble copolymers. When the contents of the styrene monomeric unit are low, the aromatic proton peak is broader, so the error of the peak position is relatively large, but as the proportion of styrene in the copolymer increases, the error becomes small. The aromatic proton peaks shift to higher field with increasing styrene content in the copolymer. As suggested by Bovey et al.,² this shielding effect is due to the magnetic anisotropy arising from the phenyl groups of the neighboring styrene monomeric units and becomes particularly marked when most of the styrene units are sandwiched between styrene units. It is apparent from the above discussions that the polymers obtained are random copolymers, in which the styrene sequences are very short, probably no longer than about 5 units.

Other examples of the spectra at 120°C. of the copolymer with higher content of styrene are shown in Figure 3. As shown in Figures 3a and b, the spectra of phenyl protons are slightly different, i.e., shoulders appear at 3.0–3.5 τ . Because this copolymer contains a large amount of the styrene unit, it may be plausible to suppose that the fractions with higher styrene content, such as acetone or ether extracts, would contain longer sequences of the styrene unit in the molecular chain than those of the copolymer No. 1. Then, they would give shoulders at the phenyl proton signals.

Spectrum 3b differs markedly from that of a mixture of Natta polypropylene ether extract (70%) and atactic polystyrene (30%) (Fig. 4). Figures 3c and d are very similar in the higher field region to the spectra of the corresponding fractions of polypropylene, prepared with the same catalyst system as was used to prepare copolymer No. 2. This suggests that the stereoregularity of the segments of propylene in the copolymer is not as affected by the localized styrene units, as when the styrene content is low.

References

1. Ashikari, N., T. Kanemitsu, K. Yanagisawa, K. Nakagawa, H. Okamoto, S. Kobayashi, and A. Nishioka, *J. Polymer Sci.*, **A2**, 3009 (1964).
2. Bovey, F. A., and G. V. D. Tiers, *J. Polymer Sci.*, **38**, 73 (1959).

S. KOBAYASHI
Y. KATO
H. WATANABE
A. NISHIOKA

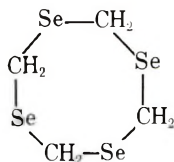
Electrical Communication Laboratory,
Nippon Telegraph and Telephone Public Corporation, Musashino, Tokyo, Japan.

Received December 16, 1964

Revised June 28, 1965

**New Crystalline Modification of Polyselenomethylene by
Polymerization of 1,3,5,7-Tetraselenocane**

The cyclic *symmetrical*-formals, *symmetrical*-thioformals, and their polymers have been largely investigated in recent years. In contrast *symmetrical*-selenoformals¹ and their polymers^{2,3} have received comparatively little study. This paper, which will be a *contribution* to this field, deals with a new preparative method of 1,3,5-triselenane and of hexagonal polyselenomethylene and the isolation of a new oligomer, the cyclic tetramer of selenoformaldehyde, 1,3,5,7-tetraselenocane I, previously unknown in the literature.



I

The preparation of tetraselenocane, has now made possible the preparation of several cyclic oligomers of formaldehyde, thioformaldehyde, and selenoformaldehyde; their characteristics are shown in Table I.

Tetraselenocane has been obtained, with little yield, by reaction of Na_2Se and CH_2Cl_2 , together with 1,3,5-triselenane and hexagonal polyselenomethylene. Tetraselenocane* is a stable crystalline solid with a melting point of 80–81°C. It is soluble in organic solvents such as C_6H_6 , CH_2Cl_2 , and in CHCl_3 and insoluble in water. With cationic initiators (e.g., BF_3) tetraselenocane polymerizes in bulk, probably by the same mechanism reported for the polymerization of oligomers listed in Table I.³⁻⁷

We have ascertained that the polyselenomethylene, obtained by cationic polymerization of 1,3,5,7-tetraselenocane, does not present the known hexagonal crystalline structure,² but shows the same orthorhombic crystalline structure of polyselenomethylene obtained by γ -radiation of triselenane.⁸ The two crystalline forms of polyselenomethylene give rise to a dimorphic system with orthorhombic-hexagonal transition temperature of about 185°C,⁸ near to the melting range of hexagonal polyselenomethylene.

Figure 1 shows the powder spectra of hexagonal (A) and of orthorhombic (B) polyselenomethylene.

EXPERIMENTAL

1,3,5,7-Tetraselenocane Preparation

The preparation has been carried in a four-necked flask provided with a mechanical stirrer, a reflux condenser, a dropping funnel, and a N_2 gas-inlet capillary.

All reagents used in this preparation have been previously deaerated and all reactions have been carried out under a nitrogen stream to avoid oxidation of Na_2Se by air. Na_2Se has been prepared by bubbling H_2Se (167 g.) into a solution of NaOH (165 g.) in H_2O (600 ml.) and CH_3OH (2800 ml.). The mixture so obtained was heated at 55°C. and CH_2Cl_2 (173 g.) added. The mixture was refluxed for 5 hr. with stirring, and a yellow solid separated.

The mixture was cooled at room temperature and the product (tetraselenocane, triselenane, and polyselenomethylene) was separated from the solution. The recovered solid was washed with water, dried (yield calculated as CH_2Se , 41%), and extracted in a

* The detailed crystal structure determinations by x-ray analysis have been carried out in this Institute.

TABLE I
 Characteristics of Cyclic *Symmetrical-Formals*, *Symmetrical-Thioformals*, *Symmetrical-Selenoformals*

	<i>n</i> = 3			<i>n</i> = 4			<i>n</i> = 5		
	X = O	X = S	X = Se	X = O	X = S	X = Se	X = O	X = S	X = Se
Melting point, °C.	62-64	215-218	226-228	112	49-50	80-81	—	120-121	—
Crystalline system	Trigonal	Orthorhombic	Orthorhombic	Monoclinic	Monoclinic	Orthorhombic	—	Monoclinic	—
Solubility	Solubility	Insolubility	Insolubility	Solubility	Insolubility	Insolubility	—	Insolubility	—
at room temperature	Solubility	Insolubility	Insolubility	Solubility	Solubility	Solubility	—	Solubility	—

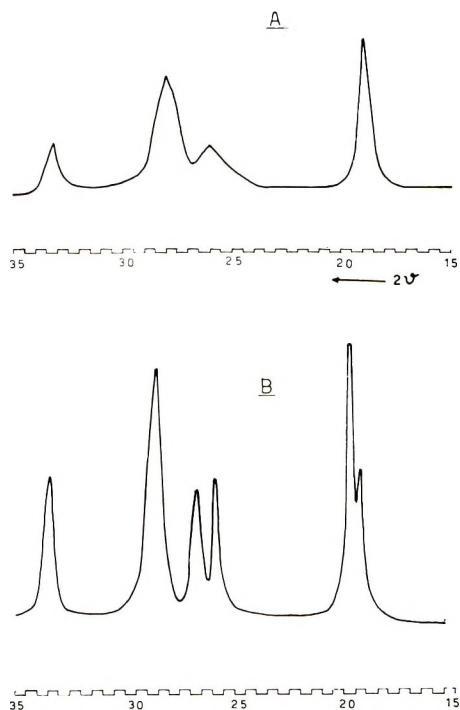


Fig. 1. X-ray powder patterns obtained by a high angle spectrometer using $\text{CuK}\alpha$ radiation: *A*, hexagonal polyselenomethylene; *B*, orthorhombic polyselenomethylene.

Soxhlet apparatus with benzene for 48 hr. The unextracted product (yield CH_2Cl_2 , 7%) shows the x-ray pattern of hexagonal polyselenomethylene, melting point 110–130°C., partially decomposed. This sample shows an increase of its melting point, when melted under vacuum. After several treatments its melting range rises to 150–165°C. At this temperature (under vacuum) the sample is stable indefinitely. The benzene solution was concentrated to about 1/5 of the original volume by distillation of the solvent and a first solid, composed essentially by triselenane, was recovered. By removing the last part of the solvent a waxy product (yield CH_2Cl_2 , 4%) separated. After several crystallizations by light petroleum, I has been obtained as white crystals with a melting point of 80–81°C.

ANAL. Calcd. for $\text{C}_4\text{H}_8\text{Se}_4$: C, 12.90; H, 2.15; Se 85.00. Found: C, 12.75; H, 2.20; Se, 84.8. Molecular weight: found,* 369; theoretical, 372.

1,3,5,7-Tetraselenocane Polymerization

The bulk polymerization was carried out with BF_3 -etherate as initiator. Into a dry glass polymerization tube, fitted with a sidearm and a N_2 gas-inlet capillary, 1.0 g. tetraselenocane was introduced. The tube was heated at $100 \pm 0.1^\circ\text{C}$., under a nitrogen stream. When the tetraselenocane is completely melted, 0.005 g. BF_3 -etherate was added with stirring; the mixture rapidly became viscous. The polymerization was stopped after 1 hr. and the white solid was removed from the tube, washed with benzene, to remove unreacted tetraselenocane, and vacuum dried. The polymerization yield was 53% (melting range: 187–195°C.).

* The molecular weight was determined with Mechrolab V.P.O. model 301 A, in CH_2Cl_2 , at 25°C.

ANAL. Calcd. for $(\text{CH}_2\text{Se})_n$: C, 12.9; H, 2.15; Se, 85.0. Found: C, 13.0; H, 2.18; Se, 84.7.

X-ray analysis shows that the product obtained by bulk polymerization of tetraselenocane is orthorhombic polyselenomethylene.

Owing to the insolubility of orthorhombic polyselenomethylene, like hexagonal polyselenomethylene, in usual organic solvents,³ it was not possible to measure viscosity.

The authors wish to thank Dr. G. Carazzolo of C.R.R. Soc. Montecatini, Castellanza (Varese) for his private communications.

References

1. Mortillaro, L., L. Credali, M. Mammi, and G. Valle, *J. Chem. Soc.*, **1965**, 807.
2. Carazzolo, G., L. Mortillaro, L. Credali, and S. Bezzi, *J. Polymer Sci.*, **B3**, 997 (1965).
3. Mortillaro, L., L. Credali, M. Russo, and C. De Checchi, *J. Polymer Sci.*, **B3**, 581 (1965).
4. Kern, V., and V. Jaacks, *J. Polymer Sci.*, **48**, 399 (1960).
5. Gipstein, E., E. Wellisch, and O. J. Sweeting, *J. Polymer Sci.*, **B1**, 239 (1963).
6. Russo, M., L. Mortillaro, C. De Checchi, G. Valle, and M. Mammi, *J. Polymer Sci.*, **B3**, 501 (1965).
7. Russo, M., L. Mortillaro, L. Credali, and C. De Checchi, *J. Polymer Sci.*, **B3**, 455 (1965).
8. Carazzolo, G., private communication.

MARIO RUSSO
LUIGI MORTILLARO
LINO CREDALI
CARLO DE CHECCHI

Istituto di Chimica Organica dell'Università, Centro Nazionale di Chimica delle Macromolecole, Soc. Montecatini Istituto Unificato per le Ricerche di Base Guido Donegani Padua, Italy

Received June 23, 1965

Revised September 7, 1965

Influence of Dose Rate on Radiation-Induced Network Formation in Polyethylene Terephthalate

It has been reported that exposure *in vacuo* of polyethylene terephthalate (PET) to high energy electrons (1–4 M.e.v.), at dose rates of the order 1–10 Mrad/min., results in network formation, the gel point being reached after a dose in the range 100–1000 Mrad.^{1,2,3} By contrast, exposure *in vacuo* to γ -rays at a dose rate of 2.5×10^{-2} Mrad/min. did not effect network formation even after a dose as high as 5000 Mrad.⁴ Another difference is that carboxyl group formation is the predominant chemical change at 2.5×10^{-2} Mrad/min. with, initially, $G(-COOH) = 0.8$,⁴ whereas the formation of such groups was not reported in the earlier rather comprehensive studies at much higher dose rates. The present note presents further experimental data on the influence of dose rate on such changes and suggests types of chemical reactions which could account for them.

Biaxially oriented PET ($M_n \sim 15,000$) of some 50% crystallinity (Mylar C film of thickness 0.0025 cm.: DuPont) was degassed *in vacuo* for 72 hr. at 50°C. and then rolled up and sealed in glass tubes at ca. 10^{-6} torr. The tubes were exposed to either γ -rays or electrons generally at ambient temperature or with water cooling. In one set of experiments the tubes were maintained at temperatures in the range 47–240°C. during exposure to Co^{60} γ -rays at a dose rate of 2.5×10^{-2} Mrad/min. Polymer samples were dissolved in *ortho*-chlorophenol by heating at 90°C. for 16 hr. and limiting viscosity numbers, $[\eta]$, determined at 25°C. by extrapolation of three or more values of η_{sp}/C to zero concentration. Carboxyl groups were determined, following dissolution of the polymer in hot benzyl alcohol, by titration with sodium hydroxide.⁵

Limiting viscosity numbers obtained at various dose rates are plotted against dose in Figure 1a. It is important to note that the irradiated samples were completely soluble in *ortho*-chlorophenol and, also, dissolved within a few minutes at room temperature in trifluoroacetic acid. Therefore, there was no gel fraction. Data for the concentration of carboxyl groups in the same or in similar samples are shown in Figure 1b. The relatively

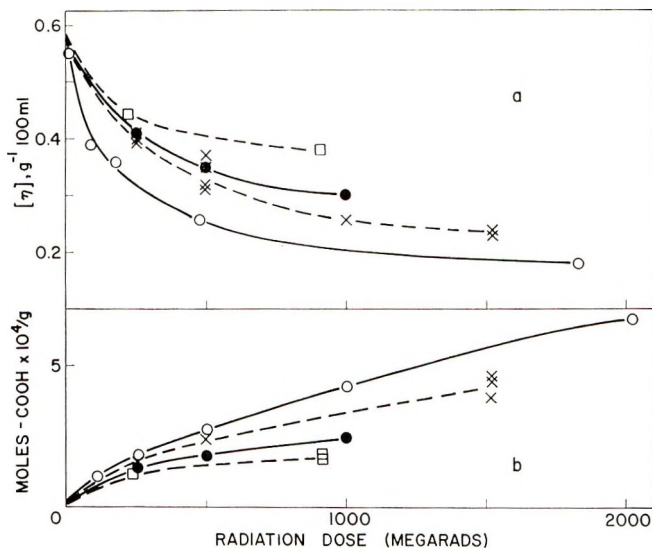


Fig. 1. Influence of dose rate on values of $[\eta]$ (a) and yields of carboxyl groups (b). Dose rates in Mrad/min.: \square , 1.4 (electrons); \bullet , 0.17 (electrons); \times , 0.15 (γ); \circ , 0.025 (γ).

few carboxyl groups in the unirradiated polymer are believed to be located at the ends of the macromolecules.⁶

The influence of temperature, between the glass transition and melting points of the polymer (ca. 80–250°), during γ -irradiation at one dose rate is shown in Figure 2. Values of $[\eta]$ were not obtained for 240°C. the highest temperature investigated, because of insolubility of both irradiated and unirradiated control samples in *ortho*-chlorophenol caused by prolonged heating *in vacuo*. As these samples remained easily soluble in trifluoroacetic acid it is believed that this insolubility in *ortho*-chlorophenol is due to some physical change. For example, it has been shown that such a heat treatment results in further crystallization of the polymer.⁶

The following conclusions are drawn from Figures 1a and 1b: First, the ratio of crosslinks to fractures, as judged qualitatively from the value of $[\eta]$, increases with dose rate. Second, the yield of fractures, as diagnosed on the reasonable assumption that the —COOH groups are endgroups, decreases with dose rate. Third, there is relatively little difference between the effects of γ -rays and electrons. From Figure 2 it is concluded that possibly higher temperatures during irradiation at higher dose rates would

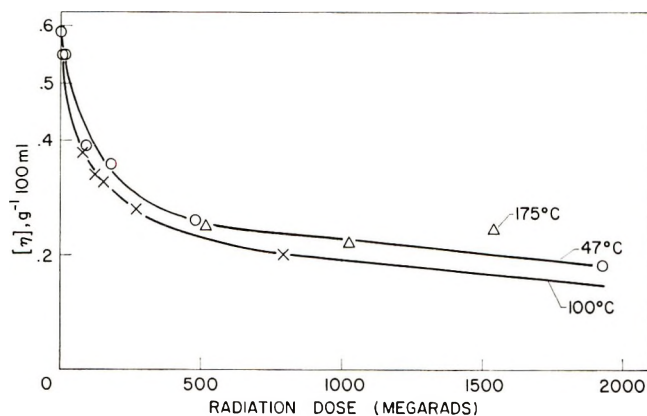


Fig. 2. Influence of temperature on values of $[\eta]$ at a dose rate of 0.025 Mrad/min. (γ).

not account for a higher ratio of crosslinks to fractures. Moreover, the above conclusions could be extended to include previous reports concerning the chemistry of PET at much higher dose rates than investigated in the present work. Under such conditions it may be presumed that the ratio of crosslinks to fractures is sufficiently high for a network to be formed while the yield of carboxyl groups might be so low as to explain why they were not detected in the course of infrared studies.^{1,2}

Previously, an increase in network formation in a polymer with dose rate has only been observed in aqueous solutions of various cellulose derivatives (1–4%).^{9,10} No similar dose rate effect has been observed in any "solid" polymer (cf. polyethylene¹¹ and natural rubber¹²). Therefore, in a "solid" polymer crosslink formation previously has been supposed to originate from reactions within isolated spurs or clusters of radicals. From the present results it appears necessary to postulate reactions between radicals formed in separate spurs in the "solid" state. It seems unlikely that "microbrownian motion" of chain segments of the polymer studied here could provide sufficient mobility and it seems more plausible to invoke the concept of radical migration by intermolecular reactions which was first suggested by Dole to account for certain features of the radiation chemistry of polyethylene (cf. ref. 13). However, in order to avoid speculation, detailed discussion of this possibility is deferred until more information about the types of radicals formed in PET is obtained from ESR studies.

We are grateful to Mrs. S. D. Burow and Mrs. B. Dauterman for analyses of carboxyl groups.

This work was sponsored by the Langley Research Center of the National Aeronautics and Space Administration under NASA Contract NAS1-3183.

References

1. Sobue, H., and A. Kajiura, *Kogyo Kagaku Zasshi*, **62**, 1771 (1959).
2. Slovokhotova, N. A., G. K. Sadovskaya, and V. A. Karbin, *J. Polymer Sci.*, **58**, 1293 (1962).
3. Hellwege, K. H., U. Johnsen, and W. Seufert, *Kolloid-Z.*, **188**, 11 (1963).
4. Burow, S. D., G. F. Pezdirtz, G. D. Sands, and D. T. Turner, *Polymer Preprints* (Chicago) **396** (1964).
5. Pohl, H. A., *Anal. Chem.*, **26**, 1964 (1954).
6. Sobue, H., and A. Kajiura, *Kogyo Kagaku Zasshi*, **62**, 1766 (1959).
7. Wall, L. A., *J. Polymer Sci.*, **17**, 141 (1955).
8. Sobue, H., Y. Tabata, and M. Hiraka, *Kogyo Kagaku Zasshi*, **64**, 372 (1961).
9. Leavitt, F. C., *J. Polymer Sci.*, **51**, 349 (1961).
10. Hillend, W. J., and H. A. Swensen, *J. Polymer Sci.*, **24**, 4921 (1964).
11. Atchinson, G. J., *J. Polymer Sci.*, **35**, 557 (1959).
12. Turner, D. T., *Polymer*, **1**, 27 (1960).
13. Dole, M., C. D. Keeling, and D. G. Rose, *J. Am. Chem. Soc.*, **76**, 4304 (1954).

D. T. TURNER

Camille Dreyfus Laboratory
Research Triangle Institute
Durham, North Carolina

GEORGE F. PEZDIRTZ
GEORGE D. SANDS

Applied Materials and Physics Division
Langley Research Center
National Aeronautics and Space Administration
Hampton, Virginia

Received August 3, 1965

Revised September 24, 1965

Relationship between Orientation Parameters in Biaxially Oriented Polymers

A second-order parameter, found useful in characterizing orientation of a crystallographic or molecular direction in polymers, is of the form $\langle \cos^2\phi \rangle$, where ϕ is the angle that such a direction makes with a reference direction in the sample, and the angular brackets denote a weight averaging over all the crystals or molecules under consideration.^{1,2} For biaxial orientation, (a type commonly found in polymer film, sheet, and fiber) it can be shown that $\langle \cos^2\phi \rangle$ in any direction is expressible in terms of $\langle \cos^2\phi \rangle$ in the principal directions. Let the principal directions coincide with the x , y , and z axes of a cartesian coordinate system. Then the orientation parameter in a reference direction, Q , can be expressed in the form³

$$\langle \cos^2\phi \rangle = \alpha^2 \langle \cos^2\phi_x \rangle + \beta^2 \langle \cos^2\phi_y \rangle + \gamma^2 \langle \cos^2\phi_z \rangle \quad (1)$$

where α , β , and γ are the direction cosines of Q along the x , y , and z axes, respectively, and the orientation parameters on the right are in the directions of the coordinate axes indicated by the subscripts.

Because of the orthogonality relationship

$$\langle \cos^2\phi_x \rangle + \langle \cos^2\phi_y \rangle + \langle \cos^2\phi_z \rangle = 1 \quad (2)$$

measurements for only two of the parameters, at most in the principle directions need be carried out. Uniaxial symmetry may be considered as a special case of biaxial symmetry for which two of the parameters in eq. (2) are equal to each other. In this case the value of the orientation parameter in only one of the principal directions is sufficient.

In the following example, the application of eq. (1) is demonstrated for a polyethylene film which showed a biaxial type of orientation. The principal directions were the machine direction (x), transverse direction (y), and the direction normal to the film surface (z). Measurements of orientation parameters in the plane of the film were made by a method previously described³ which does not require the determination of a complete pole figure. In this method, the samples examined are formed from strips of film rolled into cylindrical rods about 1 mm. in diameter, with the cylinder axis parallel to the reference direction, Q . In the present experiment, however, the specimen consisted of a sheet of these rods parallel to each other, rather than a single rod. With this modification, a slit collimated beam irradiated a constant area of the specimen during the measurements.

Measurements of $\langle \cos^2\phi \rangle$ were carried out for the (100) and (110) crystallographic directions. Corrections of the intensities for background level were made; however, with the present arrangement, corrections for geometric factors were considered negligible. Values of $\langle \cos^2\phi \rangle$, determined in the x and y directions, were used in eq. (1) to calculate $\langle \cos^2\phi \rangle$ in other directions in the xy plane. Experimental values of $\langle \cos^2\phi \rangle$ were also obtained in the Q directions making angles of 30, 45, and 60° with the x axis. A comparison

TABLE I
Experimental and Calculated Orientation Parameters in xy Plane

Angle between Q and x axis, degrees	$\langle \cos^2\theta \rangle_{100}$		$\langle \cos^2\theta \rangle_{110}$	
	Exp.	Calc.	Exp.	Calc.
0	0.61	—	0.26	—
30	0.49	0.51	0.27	0.28
45	0.41	0.41	0.29	0.30
60	0.31	0.30	0.32	0.33
90	0.20	—	0.35	—

of the experimental and calculated values listed in Table I shows a satisfactory agreement within the experimental accuracy.

The favorable results obtained demonstrate the feasibility of using eq. (1). This relationship may be quite useful for obtaining $\langle \cos^2\phi \rangle$ in cases where values are required in a large number of directions, or in directions for which direct experimental measurements are difficult to make.

References

1. Stein, R. S., and F. H. Norris, *J. Polymer Sci.*, **21**, 381 (1956).
2. Wilchinsky, Z. W., *J. Appl. Phys.*, **31**, 1969 (1960).
3. Wilchinsky, Z. W., *J. Appl. Polymer Sci.*, **7**, 923 (1963).

ZIGMOND W. WILCHINSKY

Esso Research and Engineering Company
Linden, New Jersey

Received August 12, 1965
Revised October 15, 1965